



HAL
open science

Study of pretreatments of cellulose for the production of microfibrillated cellulose MFC

Ahlem Mnasri

► **To cite this version:**

Ahlem Mnasri. Study of pretreatments of cellulose for the production of microfibrillated cellulose MFC. Organic chemistry. Université Grenoble Alpes [2020-..]; Université de Monastir (Tunisie), 2022. English. NNT : 2022GRALI054 . tel-03853597

HAL Id: tel-03853597

<https://theses.hal.science/tel-03853597v1>

Submitted on 15 Nov 2022

HAL is a multi-disciplinary open access archive for the deposit and dissemination of scientific research documents, whether they are published or not. The documents may come from teaching and research institutions in France or abroad, or from public or private research centers.

L'archive ouverte pluridisciplinaire **HAL**, est destinée au dépôt et à la diffusion de documents scientifiques de niveau recherche, publiés ou non, émanant des établissements d'enseignement et de recherche français ou étrangers, des laboratoires publics ou privés.

THÈSE

Pour obtenir le grade de

DOCTEUR DE L'UNIVERSITE GRENOBLE ALPES

**préparée dans le cadre d'une cotutelle entre
l'Université Grenoble Alpes et l'Université de
Monastir**

Spécialité : **Mécanique des fluides, Energétique, Procédés
(IMEP2) & Chimie (EDMDM)**

Arrêté ministériel : le 25 mai 2016

Présentée par

Ahlem MNASRI

Thèse dirigée par **Evelyne MAURET** et **Hatem DHAOUADI**
codirigée par **Ramzi KHIARI** et **Sami HALILA**

préparée au sein des **Laboratoire de Génie des Procédés pour la
Bioraffinerie, les Matériaux Bio-sourcés et l'Électronique Imprimée –
LGP2 et Laboratoire de Chimie de l'Environnement et des Procédés
Propres (LCE2P – LR21ES04)**

dans les **Écoles Doctorales Ingénierie – Matériaux, Mécanique,
Environnement, Energétique, Procédés, Production (IMEP2) et
Matériaux, Dispositifs et Microsystèmes (EDMDM)**

Etude et optimisation de prétraitements de la cellulose pour la production de microfibrilles de cellulose (MFC)

Thèse soutenue publiquement le **18 juillet 2022**,
devant le jury composé de :

M. Mohamed Naceur BELGACEM

Professeur à Grenoble INP, Président

M. Fleury ETIENNE

Professeur à INSA Lyon, Rapporteur

M. Sami BOUFI

Professeur à l'université de Sfax, Rapporteur

M. Hatem MAJDOUB

Professeur à la faculté des sciences de Monastir, Examineur

M. Hatem DHAOUADI

Professeur à la faculté des sciences de Monastir, Directeur de thèse

Mme. Evelyne MAURET

Professeure à Grenoble INP, Directrice de thèse

M. Sami HALILA

Chercheur CERMAV-CNRS, Co-directeur de thèse, Invité

M. Ramzi KHIARI

Maitre de conférences à l'université de Monastir, Co-directeur de thèse, Invité



Dédicaces

C'est avec une joie immense et le cœur ému que je dédie cette thèse :

A la mémoire de mon père Mohamed El Hedi qui nous a quitté très tôt, qui m'a toujours encouragé et soutenu dans mes études. Je t'aime infiniment et tu resteras toujours dans le cœur de ta fille. Que Dieu le tout puissant lui accorde son infinie miséricorde et l'accueille dans son éternel paradis.

A ma mère Jamila, mes sœurs Emna, Hanen, Bouthayna, Abir et mes frères Nabih et Ahmed merci pour vos encouragements tout au long de mes études. Merci d'être toujours à mes côtés par votre amour dévoué et votre soutien. Je vous aime infiniment.

Remerciements

Je tiens tout d'abord à remercier les membres du jury : Prof. Naceur Belgacem d'avoir accepté présider le jury, Prof. Etienne Fleury et Prof. Sami Boufi qui ont accepté d'être rapporteurs de cette thèse. Je remercie également Prof. Hatem Majdoub d'avoir accepté examiner ce travail.

Je remercie profondément mes directeurs de thèse Prof. Evelyne Mauret et Prof. Hatem Dhaouadi de m'avoir fait confiance pour mener à bien ce projet. Evelyne merci pour ta gentillesse, ton soutien, tes conseils et ta disponibilité. Merci pour nos discussions et le temps partagé ensemble (balade, restaurants...). Merci pour tout ce que tu as fait pour moi. Ces trois années de thèse à tes côtés ont été très enrichissantes professionnellement et personnellement. Monsieur Hatem merci pour vos encouragements, vos conseils et votre disponibilité. Merci pour vos aides toujours précieuses. Je remercie également mes deux encadrants de thèse, Dr. Sami Halila et Dr. Ramzi Khiari. Sami merci d'avoir participé à ce travail de thèse. C'est grâce à toi que j'ai pu trouver le bon chemin pour réussir la thèse. Merci de m'avoir donné la chance de travailler au CERMAV et rencontrer des gens sympathiques. Merci pour ta disponibilité et tes remarques pertinentes. Ramzi merci de m'avoir impliqué dans le projet CMCU et d'avoir participé à ce travail.

Ensuite je remercie Prof. Gérard Mortha de m'avoir beaucoup aidé dans la partie de chromatographie d'exclusion stérique. Gérard merci pour ta grande disponibilité, tes explications et ton aide précieuse. Merci pour ta gentillesse et tes encouragements.

Un grand merci aux membres du comité de suivi individuel : Prof. Gérard Mortha, Dr. Isabelle Baussanne et Dr. Bruno Jean. Merci pour vos conseils et vos suggestions qui ont beaucoup contribué à l'amélioration de cette thèse.

Tout travail de recherche en thèse nécessite la contribution scientifique de personnes du laboratoire ou extérieures. Je remercie toutes les personnes du LGP2 et CERMAV qui ont contribué à la réussite de cette thèse. Je tiens tout d'abord à remercier Cécile Sillard. Cécile merci beaucoup pour ton aide, ta disponibilité et tes conseils. Ensuite je remercie Stéphane Dufresne pour sa disponibilité et son aide. Je remercie également Denis Curtil pour sa gentillesse et sa grande disponibilité. Je remercie Bertine Khelifi pour le MEB, Killian Barry pour les analyses chromatographique, Isabelle Jacomine pour les analyses RMN, Christine Lacelon-Pin pour le TEM et Thierry Encinas pour le Drx. Merci également au personnel du service informatique et technique du LGP2.

J'adresse également mes remerciements à tous les doctorants et postdoc du LGP2 que j'ai eu la chance de pouvoir connaître : Marlène, Lorette, Lorelei, Joao, Saad, Clémentine, Khaoula, Ahmed, Andrea, Florian, Arnaud, Fanny, Amélie, Gloria, Maxime et Mathieu.

Merci énormément à mes ami(e)s pour leur soutien : Malek, Olfa, Hanen et Mourad. Merci d'être toujours à mes côtés.

Finalement je tiens à remercier particulièrement toute ma famille que j'adore. Merci pour votre confiance et votre soutien. Merci de m'avoir soutenu dans les moments difficiles.

Table of contents

Scientific contributions	5
General introduction	9
References	15
Chapter I. Literature review	19
Introduction	23
I.1 From natural plant to cellulose	24
I.1.1 Lignocellulosic biomass structure	24
I.1.2 Cellulose generalities	26
I.1.3 Cellulose structure	29
I.2 Cellulose fibres dissolution and chemical modification	30
I.2.1 Cellulose dissolution	30
I.2.2 Cellulose chemical modification	33
I.3 From cellulose to nanocellulose	36
I.3.1 Cellulose nanocrystals CNC	37
I.3.2 Microfibrillated cellulose MFC	38
I.3.3 Mechanical processes used for MFC production	41
I.4 Cellulose pre-treatments for MFC production	46
I.4.1 Enzymatic hydrolysis	47
I.4.2 TEMPO oxidation	49
I.4.3 Quaternisation	52
I.4.4 Phosphorylation	53
I.4.5 Deep Eutectic Solvents DES	55
I.5 Focus on Deep Eutectic Solvents	55
I.5.1 DES preparation and classification	58
I.5.2 DES physicochemical properties	60

I.5.3 Lignocellulosic biomass treatment: selective extraction of lignin and hemicelluloses	65
I.5.4 Cellulose treatment	69
I.5.5 Cellulose microfibrillation using DES	73
Conclusion and challenges	79
References	81
Chapter II. Study of DES pre-treatment effects on cellulose structure	109
Introduction	115
II.1 Study of DES pre-treatment effects on cellulose fibres and paper properties	116
II.1.1 Introduction	117
II.1.2 Materials and Methods	120
II.1.3 Results and discussions	125
II.1.4 Conclusion	142
II.2 High-Performance Size Exclusion chromatography HPSEC to study DES effects on cellulose structure	145
II.2.1 Introduction	146
II.2.2 Materials and Methods	148
II.2.3 Results and discussion	150
II.2.4 Conclusion	166
Appendix II.2	168
References	169
Chapter III. Microfibrillated cellulose MFC production from DES pre-treatment	179
Introduction	185
III.1 MFC production from Deep Eutectic Solvents pre-treatment using ultra-fine friction grinder	186
III.1.1 Introduction	186
III.1.2 Materials and Methods	188
III.1.3 Results and discussions	193

III.1.4 Conclusion.....	208
III.2 High content MFC suspensions produced from DES-treated fibres using twin-screw extruder	210
III.2.1 Introduction	210
III.2.2 Materials and Methods.....	212
III.2.3 Results and discussions	217
III.2.4 Conclusion.....	225
References.....	227
General conclusions and perspectives	237
Extended French abstract – Résumé étendu en français.....	243
Appendix.....	275
References.....	289

Scientific contributions

Publications in scientific journals

- 1) **Mnasri, A.**, Dhaouadi, H., Khiari, R., Halila, S., Mauret, E., 2022. Effects of Deep Eutectic Solvents on cellulosic fibres and paper properties: Green “chemical” refining. *Carbohydrate Polymers* 119606. <https://doi.org/10.1016/j.carbpol.2022.119606>
- 2) **Mnasri, A.**, Khiari, R., Dhaouadi, H., Halila, S., Mauret, E., 2022. Acidic and alkaline Deep Eutectic Solvents pre-treatment to produce high aspect ratio microfibrillated cellulose MFC. *Under revision in Bioresource Technology*.
- 3) **Mnasri, A.** Khiari, R., Dhaouadi, H., Halila, S., Mortha, G., Mauret, E., 2022. High-Performance Size Exclusion Chromatography HPSEC to study Deep Eutectic Solvents effects on cellulose structure. *Submitted to be published in Polymer*.
- 4) **Mnasri, A.** Khiari, R., Dhaouadi, H., Halila, S., Mauret, E., 2022. Combination of Deep Eutectic Solvents and twin-screw extruder to produce microfibrillated cellulose at high solid contents. *Accepted to be published in Chemistry Africa*.

Oral presentations in international conferences

- 1) **Mnasri, A.**, Halila, S., Dhaouadi, H., Khiari, R. & Mauret, E. Acidic and alkaline Deep Eutectic Solvents pre-treatment to produce high quality microfibrillated cellulose (MFC) in *EPNOE international polysaccharide conference (2021)*.
- 2) **Mnasri, A.**, Dhaouadi, H., Khiari, R., Halila, S. & Mauret, E. Size Exclusion Chromatography SEC to study Deep Eutectic Solvents effects on cellulose fibres in *ICACE-3 international conference on applied chemistry and environment (2022)*.

Poster presentation

Mnasri, A., Halila, S., Khiari, R., Dhaouadi, H. & Mauret, E. Microwave assisted methoxycarbonylation of cellulose using dimethyl carbonate in *Winter School nanocellulose Glycoalpes (2019)*.

List of abbreviations

Chemicals and materials

AGU: Anhydroglucose unit

AMIMCl: 1-allyl-3-methylimidazolium chloride

BHCl: Betaine hydrochloride

BMIMCl: 1-butyl-3-methylimidazolium chloride

CC: Choline chloride

CED: Cupri-ethylene diamine

CF: Cotton fibres

CMC: Carboxymethyl cellulose

CMF: Cellulose microfibrils

CNC: Cellulose nanocrystals

CNF: Cellulose nanofibrils

CTC: Cellulose tricarbanilated

DES: Deep eutectic solvents

DMA: N, N-dimethylacetamide

DMC: Dimethyl carbonate

DMSO: dimethyl sulfoxide

EF: eucalyptus fibres

EMIMCl: 1-N-ethyl-3-methylimidazolium chloride

HBA: Hydrogen bond acceptors

HBD: Hydrogen bond donors

IL: Ionic liquids

LCMF: Lignin cellulose microfibrils

M: Monoethanolamine

MCC: Microcrystalline cellulose

MeP: Methylphosphonate

MFC: Microfibrillated cellulose

MG: Methyl-alpha-glucopyranoside

NFC: Nanofibrillated cellulose
NMMO: N-methylmorphine-Noxide
TBAF: Tetrabutylammonium fluoride trihydrate
TEMPO: (2,2,6,6-tetramethylpiperidin-1-yl)oxyl
THF: tetrahydrofuran
U: Urea

Methods

AFM: Atomic force microscopy
CrI: Crystallinity index
DP: Degree of polymerisation
DP-CED: Degree of polymerisation measured from cupri-ethylene diamine method
DP_n: Degree of polymerisation in number
DP_p: Degree of polymerisation of the pic
DP_w: Degree of polymerisation in weight
DS: Degree of substitution
FTIR: Fourier transform infrared spectroscopy
HPLC: High-performance liquid chromatography
HPSEC: High-performance size exclusion chromatography
IV: Intrinsic viscosity
LALS/RALS: Light and right-angle light scattering
MHS: Mark-Houwink-Sakurada
MMD: Molecular mass distribution
M_n: Molecular mass in number
M_p: Molecular mass of the pic
M_w: Molecular mass in weight
NF: Nanosized fraction
NMR: Nuclear magnetic resonance
QI*: Simplified quality index
R_g: Radius of gyration

R_h: Hydrodynamic radius

SEM: Scanning electron microscopy

TEM: Transmission electron microscopy

TGA: Thermogravimetric analysis

TSE: Twin-screw extruder

WRV: Water retention value

XrD: X-ray diffraction

General introduction

General introduction

Today, there is a strong requirement for replacing synthetic polymers produced from petrol with biodegradable and bio-based polymers. This need stems from the extensive use of these petro-sourced polymers which led to many problems, including, oil resources depletion, plastic pollution...

To overcome these issues, cellulose polymer is proposed to replace in part synthetic ones. The main advantages of using cellulose are the facts that: i) it is the most abundant polymer on earth with a production around 200 Gt per year (Delmer and Amor, 1995); ii) cellulose is characterised by its biodegradability, sustainability and renewability and iii) it can be extracted from different lignocellulosic biomass including, hardwood, softwood, cotton, flax... Despite its interesting properties, cellulose as a raw material presents some limitations because of its affinity with water (hygroscopic material) and fibres network (papers present low mechanical and low barrier properties).

Few decades ago, researches have been oriented towards nanocellulose which is extracted from cellulose fibres. Nanocellulose presents very interesting chemical and physical (thermal and mechanical) properties. Two kinds of nanocellulose can be identified: cellulose microfibrils (CMF) or microfibrillated cellulose (MFC) and cellulose nanocrystals (CNC). MFC are produced mainly by disintegrating the cellulosic suspension through a mechanical treatment (Turbak et al., 1983), while CNC are obtained by a severe acid treatment (Habibi et al., 2010).

The production of MFC is very costly, due to the energy consumption of the mechanical processes such as grinding, homogenisation... (Abdul Khalil et al., 2014). The need to reduce this energy consumption has led researchers to find pre-treatments including chemical or biological ones. Many pre-treatments are available in the literature such as TEMPO-oxidation (Isogai et al., 2011; Nooy et al., 1994; Saito et al., 2009), enzymatic hydrolysis (Henriksson et al., 2007; Hu et al., 2011; Nie et al., 2018; Pääkkö et al., 2007) to name but a few. TEMPO-oxidation is the most effective pre-treatment that allows producing high quality MFC with low energy cost. Despite the effectiveness of this pre-treatment, it presents some limitations such as toxicity and the use of catalyst (generally based on bromide ion), which is not always appropriate depending on the targeted applications.

Recently, a new emerging pre-treatment, namely, Deep Eutectic Solvents (DES) were investigated. DES are defined as the mixture of hydrogen bond donors and hydrogen bond

acceptors which together present lower melting point compared to their individual melting temperature (Abbott et al., 2003). DES are suggested as green and designer solvents and reagents with interesting properties including biodegradability, non or low toxicity, recyclability and selectivity. The first system used for MFC production is a mixture of choline chloride-urea by Sirviö et al. (2015). Other systems were then proposed and the results demonstrated the effectiveness of this pre-treatment to produce MFC (Hong et al., 2020; Laitinen et al., 2017; Sirviö et al., 2020; Suopajarvi et al., 2017; Yu et al., 2021). However, research in this area is still recent and the small amount of published work indicates that further work is needed.

For many years, one of the main topics of our group has been related to the reduction of the energy costs associated with cellulose microfibrillation. This was done by investigating various mechanical, chemical or/and enzymatic processes (Khiari et al., 2019; Nechyporchuk et al., 2016; Rol et al., 2019). In the light of promising results with DES pre-treatment, this thesis work aims at contributing to this field and investigating the influence of DES on physical-chemical properties of cellulose fibres. Finally, this project must provide reinforced enlightening on the study of DES pre-treatment for ease the microfibrillation process.

This PhD thesis is a joint supervision between the Laboratory of Process Engineering for Biorefinery, Bio-based Materials and Functional Printing LGP2 (University of Grenoble Alpes, France) and the Laboratory of Chemical environment and Clean Process LCE2P- LR21ES04 (Faculty of Science of Monastir-university of Monastir, Tunisia) and in collaboration with CERMAV (UPR CNRS 5301, Grenoble, France). This work was financially supported by the “PHC Utique” program of the French Ministry of Foreign Affairs and Ministry of higher education, research and innovation and the Tunisian Ministry of higher education and scientific research in the CMCU project number TN 18G1132// FR 39316VF.

The manuscript is divided into three main chapters as described in Figure 1.

The **first chapter** is a literature review: the first section is about cellulose, its structure, properties, dissolution and modification. The second section is dedicated to nanocellulose (cellulose microfibrils and cellulose nanocrystals) extraction and their properties. Then, cellulose microfibrils production, properties and the used pre-treatments are discussed. The last section focuses on Deep Eutectic Solvents properties, applications and their use for cellulosic biomass treatment.

Chapter II is dedicated to the effects of DES on cellulose structure. In this section, the morphological, chemical, structural and mechanical properties of cellulose fibres and papers are studied, before and after DES treatment. In the second part, DES effects on cellulose fibres are studied using high-performance size exclusion chromatography (HPSEC) to deeply understand their effects at the molecular scale.

Chapter III describes the effectiveness of DES pre-treatment in producing MFC. In the first section, the microfibrillation of DES-treated fibres using ultra-fine friction grinder is studied. Then, twin-screw extruder TSE is used as mechanical treatment to investigate the production of MFC at high solid contents.

Finally, a general conclusion highlights the main results of this work and presents some perspectives.

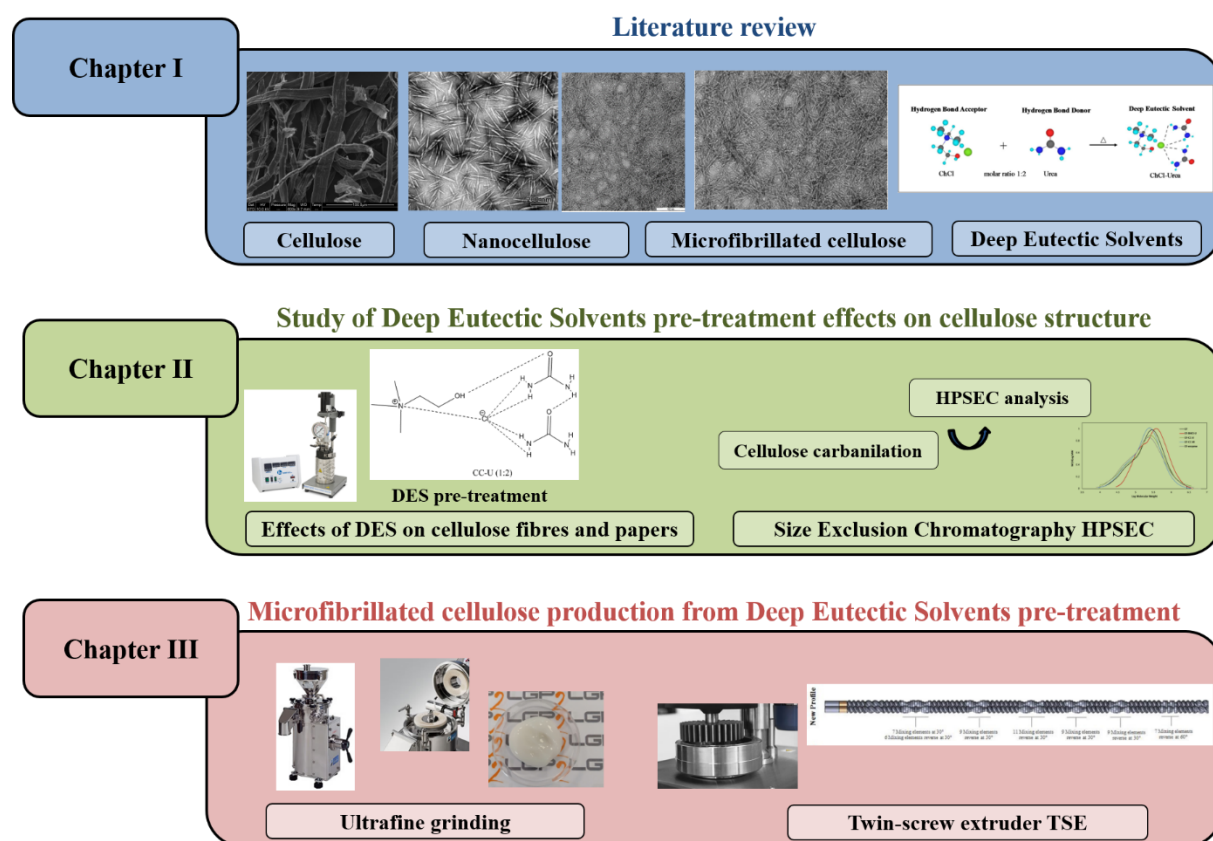


Figure 1. General scheme of the manuscript organisation

References

- Abbott, A.P., Capper, G., Davies, D.L., Rasheed, R.K., Tambyrajah, V., 2003. Novel solvent properties of choline chloride/urea mixtures. *Chemical Communications* 0, 70–71. <https://doi.org/10.1039/B210714G>
- Abdul Khalil, H.P.S., Davoudpour, Y., Islam, Md.N., Mustapha, A., Sudesh, K., Dungani, R., Jawaid, M., 2014. Production and modification of nanofibrillated cellulose using various mechanical processes: A review. *Carbohydrate Polymers* 99, 649–665. <https://doi.org/10.1016/j.carbpol.2013.08.069>
- Delmer, D.P., Amor, Y., 1995. Cellulose biosynthesis. *Plant Cell* 7, 987–1000.
- Habibi, Y., Lucia, L.A., Rojas, O.J., 2010. Cellulose Nanocrystals: Chemistry, Self-Assembly, and Applications. *Chemical Reviews*. 110, 3479–3500. <https://doi.org/10.1021/cr900339w>
- Henriksson, M., Henriksson, G., Berglund, L.A., Lindström, T., 2007. An environmentally friendly method for enzyme-assisted preparation of microfibrillated cellulose (MFC) nanofibers. *European Polymer Journal* 43, 3434–3441. <https://doi.org/10.1016/j.eurpolymj.2007.05.038>
- Hong, S., Yuan, Y., Li, P., Zhang, K., Lian, H., Liimatainen, H., 2020. Enhancement of the nanofibrillation of birch cellulose pretreated with natural deep eutectic solvent. *Industrial Crops and Products* 154, 112677. <https://doi.org/10.1016/j.indcrop.2020.112677>
- Hu, J., Arantes, V., Saddler, J.N., 2011. The enhancement of enzymatic hydrolysis of lignocellulosic substrates by the addition of accessory enzymes such as xylanase: is it an additive or synergistic effect? *Biotechnol Biofuels* 4, 36. <https://doi.org/10.1186/1754-6834-4-36>
- Isogai, A., Saito, T., Fukuzumi, H., 2011. TEMPO-oxidized cellulose nanofibers. *Nanoscale* 3, 71–85. <https://doi.org/10.1039/C0NR00583E>
- Khiari, R., Rol, F., Brochier Salon, M.-C., Bras, J., Belgacem, M.N., 2019. Efficiency of Cellulose Carbonates to Produce Cellulose Nanofibers. *ACS Sustainable Chem. Eng.* 7, 8155–8167. <https://doi.org/10.1021/acssuschemeng.8b06039>
- Laitinen, O., Suopajarvi, T., Österberg, M., Liimatainen, H., 2017. Hydrophobic, Superabsorbing Aerogels from Choline Chloride-Based Deep Eutectic Solvent Pretreated and

- Silylated Cellulose Nanofibrils for Selective Oil Removal. *ACS Applied Materials & Interfaces*, 9, 25029–25037. <https://doi.org/10.1021/acsami.7b06304>
- Nechporchuk, O., Belgacem, M.N., Bras, J., 2016. Production of cellulose nanofibrils: A review of recent advances. *Industrial Crops and Products* 93, 2–25. <https://doi.org/10.1016/j.indcrop.2016.02.016>
- Nie, S., Zhang, K., Lin, X., Zhang, C., Yan, D., Liang, H., Wang, S., 2018. Enzymatic pretreatment for the improvement of dispersion and film properties of cellulose nanofibrils. *Carbohydrate Polymers* 181, 1136–1142. <https://doi.org/10.1016/j.carbpol.2017.11.020>
- Nooy, A.E.J. de, Besemer, A.C., Bekkum, H. van, 1994. Highly selective tempo mediated oxidation of primary alcohol groups in polysaccharides. *Recueil des Travaux Chimiques des Pays-Bas* 113, 165–166. <https://doi.org/10.1002/recl.19941130307>
- Pääkkö, M., Ankerfors, M., Kosonen, H., Nykänen, A., Ahola, S., Österberg, M., Ruokolainen, J., Laine, J., Larsson, P.T., Ikkala, O., Lindström, T., 2007. Enzymatic Hydrolysis Combined with Mechanical Shearing and High-Pressure Homogenization for Nanoscale Cellulose Fibrils and Strong Gels. *Biomacromolecules* 8, 1934–1941. <https://doi.org/10.1021/bm061215p>
- Rol, F., Belgacem, M.N., Gandini, A., Bras, J., 2019. Recent advances in surface-modified cellulose nanofibrils. *Progress in Polymer Science* 88, 241–264. <https://doi.org/10.1016/j.progpolymsci.2018.09.002>
- Saito, T., Hirota, M., Tamura, N., Kimura, S., Fukuzumi, H., Heux, L., Isogai, A., 2009. Individualization of Nano-Sized Plant Cellulose Fibrils by Direct Surface Carboxylation Using TEMPO Catalyst under Neutral Conditions. *Biomacromolecules* 10, 1992–1996. <https://doi.org/10.1021/bm900414t>
- Sirviö, J.A., Hyypiö, K., Asaadi, S., Junka, K., Liimatainen, H., 2020. High-strength cellulose nanofibers produced via swelling pretreatment based on a choline chloride–imidazole deep eutectic solvent. *Green Chemistry* 22, 1763–1775. <https://doi.org/10.1039/C9GC04119B>
- Sirviö, J.A., Visanko, M., Liimatainen, H., 2015. Deep eutectic solvent system based on choline chloride-urea as a pre-treatment for nanofibrillation of wood cellulose. *Green Chemistry* 17, 3401–3406. <https://doi.org/10.1039/C5GC00398A>

REFERENCES

- Suopajarvi, T., Sirviö, J.A., Liimatainen, H., 2017. Nanofibrillation of deep eutectic solvent-treated paper and board cellulose pulps. *Carbohydrate Polymers* 169, 167–175. <https://doi.org/10.1016/j.carbpol.2017.04.009>
- Turbak, A.F., Snyder, F.W., Sandberg, K.R., 1983. Microfibrillated cellulose, a new cellulose product: properties, uses, and commercial potential. *Journal of Applied Polymer Science: Applied Polymer Symposium; (United States)* 37.
- Yu, W., Wang, C., Yi, Y., Wang, H., Yang, Y., Zeng, L., Tan, Z., 2021. Direct pretreatment of raw ramie fibers using an acidic deep eutectic solvent to produce cellulose nanofibrils in high purity. *Cellulose* 28, 175–188. <https://doi.org/10.1007/s10570-020-03538-3>

Chapter I. Literature review

Table of contents

Chapter I. Literature review	19
Introduction.....	23
I.1 From natural plant to cellulose.....	24
I.1.1 Lignocellulosic biomass structure.....	24
I.1.2 Cellulose generalities.....	26
I.1.3 Cellulose structure.....	29
I.2 Cellulose fibres dissolution and chemical modification.....	30
I.2.1 Cellulose dissolution.....	30
I.2.2 Cellulose chemical modification.....	33
I.2.2.1 Esterification.....	33
I.2.2.2 Etherification.....	34
I.3 From cellulose to nanocellulose.....	36
I.3.1 Cellulose nanocrystals CNC.....	37
I.3.2 Microfibrillated cellulose MFC.....	38
I.3.2.1 MFC properties.....	38
I.3.2.2 MFC applications.....	40
I.3.3 Mechanical processes used for MFC production.....	41
I.3.3.1 Conventional processes.....	42
I.3.3.2 Non-conventional processes.....	44
I.4 Cellulose pre-treatments for MFC production.....	46
I.4.1 Enzymatic hydrolysis.....	47
I.4.2 TEMPO oxidation.....	49
I.4.3 Quaternisation.....	52
I.4.4 Phosphorylation.....	53

I.4.5 Deep Eutectic Solvents DES	55
I.5 Focus on Deep Eutectic Solvents	55
I.5.1 DES preparation and classification	58
I.5.2 DES physicochemical properties	60
I.5.3 Lignocellulosic biomass treatment: selective extraction of lignin and hemicelluloses	65
I.5.4 Cellulose treatment	69
I.5.5 Cellulose microfibrillation using DES	73
Conclusion and challenges.....	79
References.....	81

Introduction

The present chapter aims at introducing the basic knowledge of this PhD project and is intended for both expert and non-expert readers.

In grey and italic are comments in relation with this PhD thesis.

This chapter is divided into five main parts. The first part gives an overview of cellulose and how it could be extracted from natural plants. The chemical composition of lignocellulose biomass is described with a focus on cellulose structure, biosynthesis, its different allomorphs and how to obtain them.

The second section is devoted to cellulose dissolution and chemical modification in conventional and greener solvents.

The third part focuses on nanocellulose as a bio-based material. The two types of nanocellulose namely cellulose nanocrystals CNC and microfibrillated cellulose MFC, are presented. Their preparation, structure and properties are discussed. Then, the production of MFC using conventional processes (homogenisation...) and non-conventional processes (extrusion...) are presented.

The fourth section is dedicated to cellulose pre-treatments for MFC production. Pre-treatments (TEMPO-oxidation, enzymatic hydrolysis...) are first described with an emphasis on new emerging ones. Deep Eutectic Solvents (DES), studied in this project and considered as an emerging pre-treatment, is briefly described.

The last section aims at describing DES, their chemical properties, preparation and applications. The treatment of lignocellulosic biomass and cellulose is discussed with a focus on cellulose microfibrillation.

I.1 From natural plant to cellulose

I.1.1 Lignocellulosic biomass structure

Cellulose can be extracted from several varieties of sources (Nechyporchuk et al., 2016), including wood (hardwood and softwood), seed fibres (cotton...), grasses (bamboo...), waste marine biomass (*Posidonia oceanica*), fungi and bacteria. Industrially, wood is the most dominant source of cellulose (Siró and Plackett, 2010).

Contrary to cotton and/or kapok that is made of pure cellulose fibres, the extraction of cellulose fibres from wood or non-wood plants requires some chemical and/or mechanical processes depending on the used biomass. They are defined as pulping process (cooking, bleaching...) to obtain cellulose fibres with low lignin content. It can be done via kraft or sulphite process. Kraft process is the most often used and is based on the use of sodium hydroxide and sodium sulphide (Santos et al., 2011). Sulphite process uses sodium carbonate and sodium sulphite (Hemmasi, 2012; López et al., 2000). *In this PhD project, cotton fibres and bleached kraft pulp (extracted from hardwood) are used as feedstocks.*

In the fibres, cellulose is found in the form of macrofibrils composed from microfibrils which are themselves constituted from elementary fibrils. Cellulose is a linear homopolymer defined as the most important element in plants and other cellulosic sources because it allows maintaining their structure. In lignocellulosic biomass, cellulose is not the only component of the fibres as reported in Figure I. 1. It is linked to hemicelluloses and to lignin through hydrogen and covalent bonding. Hemicelluloses are identified as a strongly branched polymer in comparison to cellulose. Lignin is a hydrocarbon polymer, composed of aromatic and aliphatic components. It is described as a very irregular and as a three-dimensional polymer.

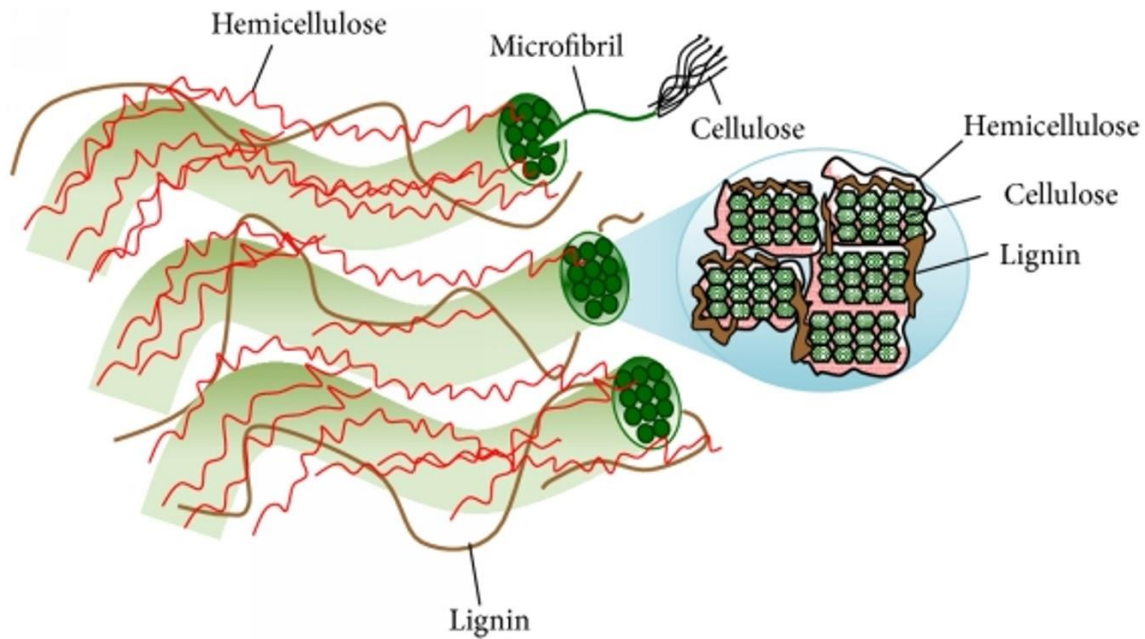


Figure I. 1. Lignocellulosic biomass structure (Lee et al., 2014).

Hemicelluloses are constituted from heteropolysaccharides, that are mainly composed from xylans (β -1,4-linked D-xylose units), mannans (β -1,4-linked D-mannose units), arabinans (α -1,5-linked L-arabinose units) and galactans (β -1,3-linked D-galactose units). As given in Table I. 1, hardwood hemicelluloses are mainly constituted from 80-90% of methylglucuronoxylan, while for softwood, the major constituent is galactoglucomannan (about 60-70%).

Table I. 1 Hemicelluloses in wood (Spiridon and Popa, 2008).

	Hardwood	Softwood
Methylglucuronoxylan, %	80–90	5-15
Arabinomethylglucuronoxylan, %	0.1–1	15-30
Glucomannan, %	1–5	1-5
Galactoglucomannan, %	0.1–1	60-70
Arabinogalactan, %	0.1–1	1–15
Other galactans, %	0.1–1	0.1-1
Pectin, %	1–5	1–5

Hemicelluloses represent a complex group of polysaccharides that are characterised by a relatively low molecular weight and their solubility in alkaline solutions (Spiridon and Popa, 2008).

I.1.2 Cellulose generalities

Cellulose was first established by Anselme Payen in 1838 (Payen, 1838). It is defined as the most abundant polymer on earth. The repeating unit of cellulose polymer is the glucose unit which is 1-4 β -D-glucopyranose unit (French, 2017). The linkage between two glucopyranose units via glycosidic bonds forms the cellobiose unit (4-O-(β -D-glucopyranosyl)- β -D-glucopyranose). The structure of cellulose monomer (glucose) contains three hydroxyl groups in the carbon atom 2, 3 and 6 as described in Figure I. 2. These hydroxyl groups are available for reaction due to their hydrogen bonding ability. Cellulose is characterised by two different chain ends. One end has a spare secondary hydroxyl function on C4 and it is called non-reducing end. The other end is formed by cyclic hemiacetal function (on C1), which is in equilibrium in a small proportion with an aldehyde. The presence of the aldehyde function in the chain-end gives rise to reducing properties: it reduces Cu^{2+} ion into Cu^+ in a Fehling's solution. Therefore, cellulose chains are chemically polarized (Dufresne, 2017).

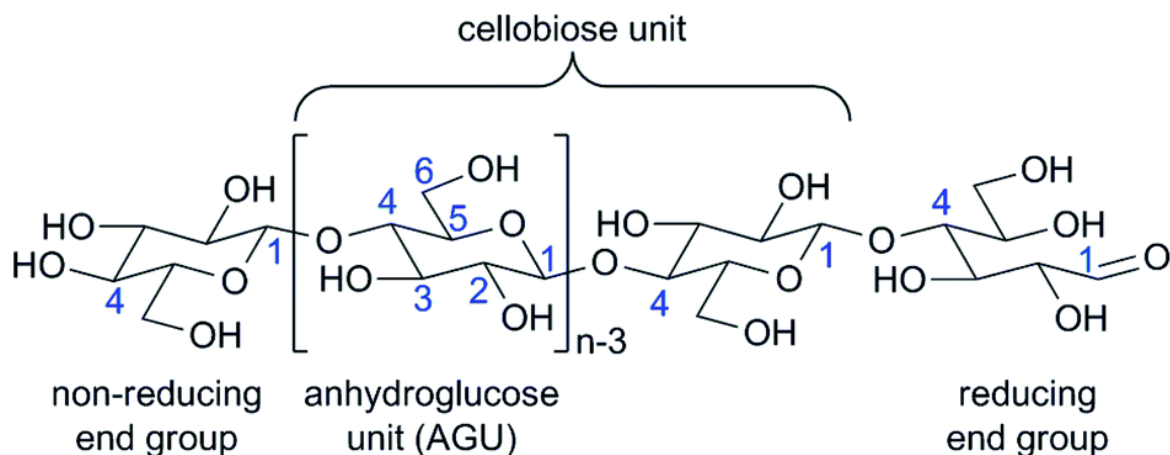


Figure I. 2. Cellulose structure (Credou and Berthelot, 2014).

Cellulose is produced by biosynthesis in two steps. The first one consists of glucose polymerisation to produce β -1,4-D-glucopyranose chains. The second step is the arrangement

of fibrillar supramolecular architecture followed by the creation of crystalline structure called elementary fibrils. These later are defined as a collection of highly oriented cellulose chains. The formation of elementary fibrils has been studied by Cousins and Brown (1995). They proposed a model composed of four steps (Figure I. 3). The first step is the enzymatic polymerisation of glucose to create glucan chains. The second one consists of glucan chains association via Van der Waals forces giving rise to mini-sheets. The third step is mini-crystals formation called also elementary fibrils that results from mini-sheets association via hydrogen bonds. The last step is the assembly of elementary fibrils to create microfibrils (Cousins and Brown, 1995).

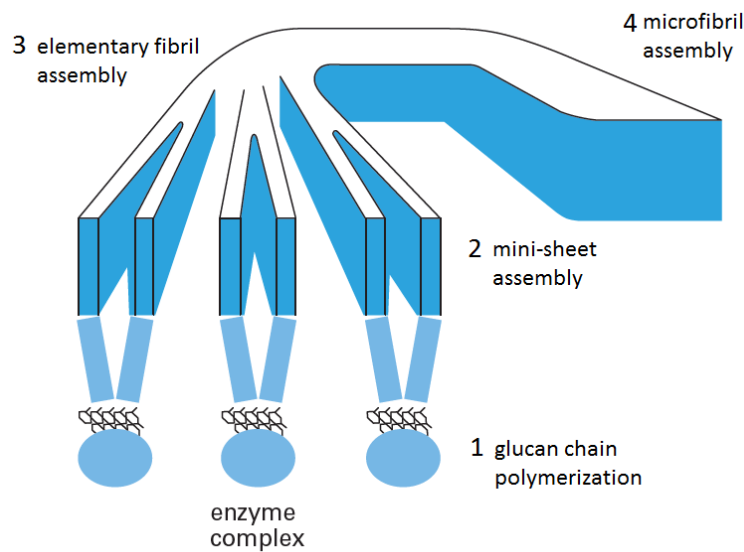


Figure I. 3. A general proposed model for microfibrils formation (Cousins and Brown, 1995).

At the supramolecular level, glucose chains that are linked together through hydrogen bonding, give rise to the metastable form of cellulose namely cellulose I. This architecture is present in the most common lignocellulosic biomass. Cellulose has a various ordered crystalline organisation called polymorphs. This polymorphism is the result of the intra and inter hydrogen bonds, that lead to different arrangements of crystalline regions. Different transitions between cellulose polymorphs are possible, as described in Figure I. 4.

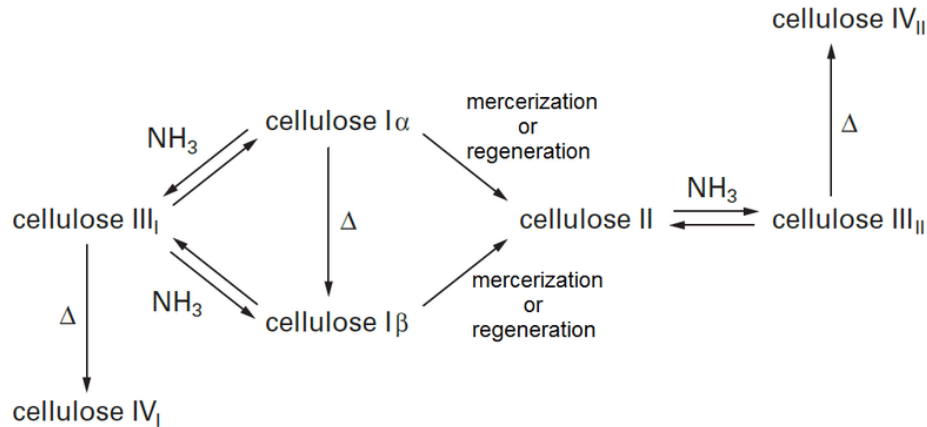


Figure I. 4. Possible interconversions of cellulose polymorphs (Dufresne, 2017).

Cellulose I refers to the native cellulose. It consists of the mixture of two crystalline forms: cellulose I α and I β . The I α form is a triclinic phase, while cellulose I β is a monoclinic phase. The ratio of these two crystalline forms depends mainly on the biomass. I α is basically present in cellulose obtained from primitive organisms (bacteria, algae), while I β phase is mainly found in plants (wood, cotton, ...) and animals (marine animals). Therefore, cellulose reactivity may be affected by the presence of these two polymorphs as I α is metastable and more reactive than I β (Dufresne, 2017).

Cellulose II is known as the most thermodynamically stable polymorph because it results from irreversible transformation of cellulose I. It is obtained by two methods, mercerization (caustification) or regeneration of the cellulose I. Mercerization consists of the swelling of native cellulose in concentrated aqueous solutions of sodium hydroxide with 17 to 20% (wt/vol). This technique is used to activate the polymer by swelling without dissolution. During mercerization, cellulosic chain structure changes from parallel to antiparallel structure. Regeneration is based on cellulose solubilisation in a suitable solvent with subsequent precipitation to obtain regenerated cellulosic fibres. Many techniques of regeneration are used at the industrial scale such as viscose and copper ammonium treatments. The chain structure of cellulose II is a monoclinic chain like cellulose I β , but it differs in chain arrangement, which is antiparallel. Cellulose II can be produced naturally by some bacteria and algae.

Cellulose III is produced from cellulose I and also from cellulose II by treatment with liquid ammonium or some organic amines, such as ethylene diamine. Two forms of cellulose III are available, cellulose III_I obtained from cellulose I and cellulose III_{II} from cellulose II. It has an

hexagonal unit cell. During the transformation from cellulose I to III, which is reversible, an extended decrystallisation and fragmentation of cellulose crystals were detected and a considerable decrease of the lateral dimensions of the crystallites was observed. During the reverse transformation (from cellulose III to cellulose I), partial recrystallisation was observed, while crystal fragmentations are irreversible (Sarko et al., 1976).

Cellulose IV is prepared from cellulose III by treatment at high temperature in glycerol. Two types are obtained, cellulose IV_I (from cellulose III_I) and cellulose IV_{II} (from cellulose III_{II}). It was shown that these transformations are difficult due to the partial conversion of cellulose III. IV_I is a disorganised form of cellulose I, which is confirmed by the presence of this polymorph in various plants (primary walls of cotton and some fungi) (Chanzy et al., 1979, 1978).

I.1.3 Cellulose structure

Cellulose is characterised by a highly crystalline structure, due to the existence of numerous hydroxyl groups. These hydroxyl functions give rise to a network of intra- and intermolecular hydrogen bonding. Van der Waals forces are also involved between the layers of the chains. The presence of these two interactions maintains the ordered crystalline structure of cellulose. As described in Figure I. 5, intramolecular hydrogen bonds occur between the hydrogen of the hydroxyl group of the C3 or C6 carbon cycle and oxygen from adjacent ring O5 or O2, respectively. The intermolecular bonds are established between hydrogen of the hydroxyl group (HO-6) and oxygen (O3) in the cycle of another unit.

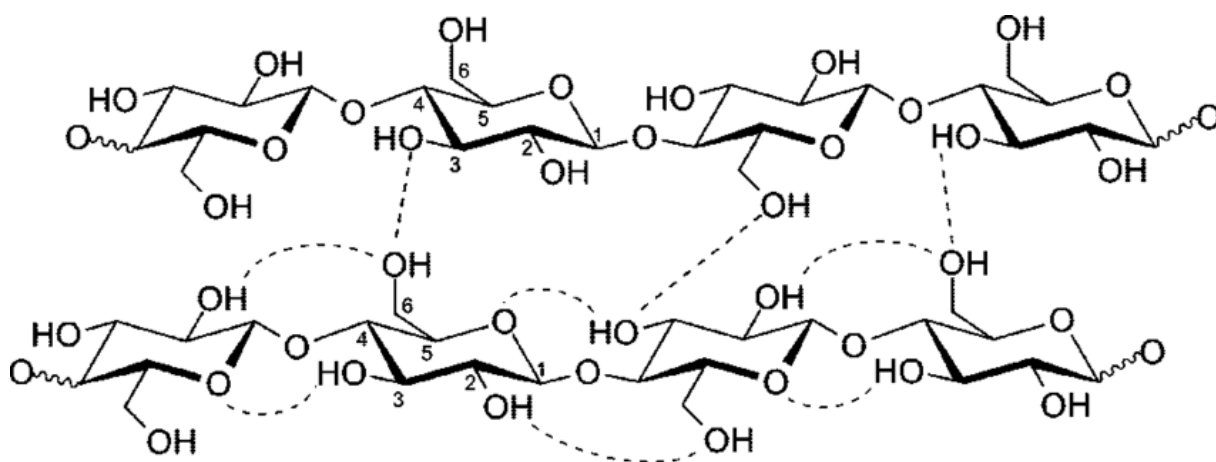


Figure I. 5. Intra- and intermolecular hydrogen bonds between cellulose chains (Pinkert et al., 2009).

Cellulosic chains, which are ordered and parallel to each other, present the basic crystal structure namely, elementary fibrils. During their biosynthesis, the crystalline arrangement may be destroyed by twists being formed along the chain. These disordered parts are called amorphous regions. Elementary fibrils structure can thus be described as a chain of cellulose crystallites, connected by amorphous zones along the chain axis as reported in Figure I. 6. From these elementary fibrils, two kinds of nanocellulose can be obtained depending on the isolation process: cellulose microfibrils CMF and cellulose nanocrystals CNC. From these elementary fibrils, two kinds of nanocellulose can be obtained depending on the isolation process: cellulose microfibrils CMF and cellulose nanocrystals CNC.

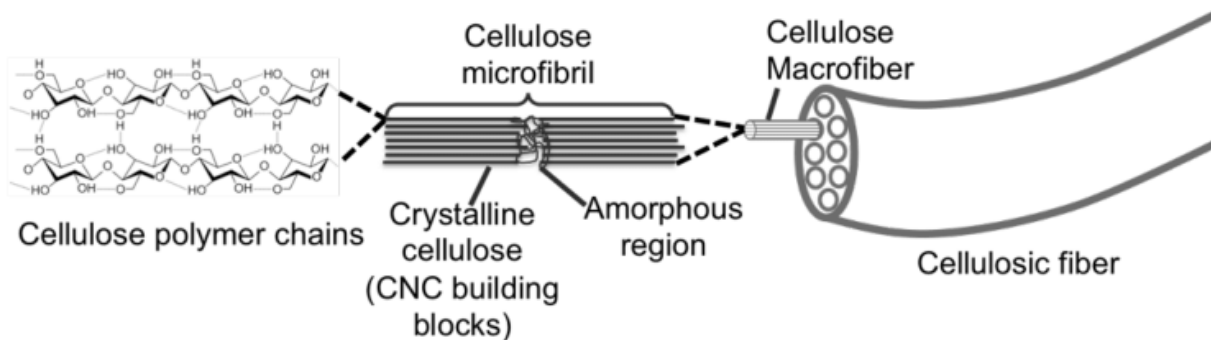


Figure I. 6. Hierarchical structure of cellulose fibres (Parry, 2016).

I.2 Cellulose fibres dissolution and chemical modification

Owing to its high crystalline structure and the presence of hydrogen bonding within and between chains, cellulose dissolution in common organic solvents and water is quite difficult which limits its application. To deal with this drawback, cellulose should be modified. Cellulose dissolution and chemical modification will be outlined in the following parts.

I.2.1 Cellulose dissolution

Cellulose solvents are divided into two categories: (i) derivatising solvents such as CS_2/NaOH and (ii) non-derivatising solvents including N,N-dimethylacetamide/lithium chloride (DMAc/LiCl), N-methylmorpholine-N-oxide (NMMO) and tetrabutylammonium fluoride trihydrate/DMSO (TBAF/DMSO). They are toxic and present some environmental issues like inefficient recyclability (Ge et al., 2022; Salama and Hesemann, 2020). Recent advances in cellulose processing have been oriented towards replacing conventional solvents by new generation reagents such as greener solvents as recently reviewed by Ge et al. (2022). Novel non-derivatising solvents for cellulose dissolution have been introduced, and they are classified

into two classes: (i) non-aqueous solvents (ionic liquids (IL) and deep eutectic solvents (DES) and (ii) aqueous solvents (alkali/urea solutions, quaternary onium hydroxides). They can be used for both cellulose dissolution and modification.

Ionic liquids (IL) are described as organic molten salts with melting temperature below 100 °C (Wilkes, 2002). They mainly combine a large organic cation (pyridinium, imidazolium, morpholinium, ammonium...) with a smaller inorganic anion (Cl^- , Br^- ...) or organic anion (Feng and Chen, 2008). IL present many attractive properties including low vapor pressure, non-flammability, good thermal and chemical stability. Cellulose dissolution in IL (1-butyl-3-methylimidazolium cations coupled with a range of small or large anions) was first reported by Swatloski et al. (2002). Afterwards, many other IL systems were developed to promote cellulose dissolution such as imidazolium, quaternary onium and pyridinium based IL (Gericke et al., 2012; Isik et al., 2014). The dissolving capacity of these ionic liquids was classified in the following order: imidazolium-based IL > pyridinium-based IL > ammonium-based IL (Li et al., 2018). It was also demonstrated that IL composed of Cl^- , $[\text{OAc}]^-$, $[\text{HCOO}]^-$ or $[(\text{EtO})_2\text{PO}_2]^-$ anions enhance cellulose dissolution better than those formed by non-coordinating anions $[\text{PF}_6]^-$ or $[\text{BF}_4]^-$. In addition, others IL have been investigated for cellulose dissolution without derivation, such as 1-butyl-3-methylimidazolium chloride (BMIMCl) and 1-allyl-3-methylimidazolium chloride (AMIMCl) (Zhu et al., 2006). The dissolution was significantly enhanced using microwave heating.

The use of co-solvent with IL can enhance cellulose dissolution. For instance, Ren et al. (2021) used a mixture of dimethyl sulfoxide (DMSO) and different IL including 1-butyl-3-methylimidazolium acetate, 1-propyl-3-methylimidazolium acetate, and 1-ethyl-3-methylimidazolium acetate. The addition of DMSO with these IL has significantly improved cellulose dissolution. Despite the advantages of these IL and their effectiveness in cellulose dissolution, their industrialisation is limited due to their sensitivity to water, high viscosity and limited recycling (Ren et al., 2021).

Cellulose dissolution in DES, that are considered as a new class of solvents, was also studied. DES are obtained from a mixture of acids and Lewis or Bronsted bases. They are also defined as a combination of hydrogen bond donors (HBD) and hydrogen bond acceptors (HBA) (Abbott et al., 2003). This mixture has a lower melting point (generally below 100 °C) compared to that of individual components. They are often classified as ionic liquids, but in comparison they

exhibit some advantages such as easy preparation, low cost, biodegradability, low toxicity and recyclability. Owing to these interesting properties, DES have been studied for cellulose processing (dissolution, modification...). In particular, for cellulose dissolution, Chen et al. (2019) has used mixtures of choline chloride-urea, choline chloride-resorcinol, choline chloride-phenol, choline chloride- α -naphthol... and has shown that cellulose solubility in DES was low with a maximum solubility (6.10 wt %) obtained with choline chloride-resorcinol system. Afterwards, zwitterion DES were developed, allowing to increase cellulose solubility to i.e 15 wt % (Sharma et al., 2021). To conclude, unlike IL, DES are not able to dissolve cellulose in a great extent and there is a need of more research in this field. *This part will be discussed in detail in section 5.*

Aqueous alkali/urea solutions can also be interesting systems for cellulose dissolution due to their simplicity, eco-friendly, low toxicity and low cost (Ge et al., 2022; Liu et al., 2020). These solvents are based on alkaline water mixture including NaOH/urea, LiOH/urea and NaOH/thiourea. Cai and Zhang (2006) used the mixture of NaOH/urea (7 and 12% w/w, respectively) to solubilise cellulose at low temperature (-10 °C). The dissolution was very fast, resulting in a stable and irreversible gel solution even under cooling to -10°C (temperature of dissolving). Another system composed of 4.6 wt% LiOH and 15 wt % urea was tested to rapidly dissolve cellulose (Cai et al., 2006). In LiOH/urea mixture, the intermolecular hydrogen linkages of cellulose were broken at low temperature giving rise to new compound related to cellulose, LiOH, urea and water cluster. This compound provides an effective distribution of cellulose molecules in the aqueous solution. The obtained cellulose solution was transparent and stable during storage and use. It is important to note that, in these systems, cellulose dissolution occurs at low temperatures which is not the case with other systems. Cai et al. (2018) have studied the dissolution mechanism in NaOH/urea system by using many techniques such as ^{13}C NMR, FT-IR, static and dynamic laser light scattering, wide-angle X-ray diffraction, transmission electron microscopy (TEM), and small angle neutron scattering. The authors shown that the clusters formed with NaOH, urea and water rise with reducing the temperature and NaOH hydrates are linked to cellulose chains by means of hydrogen bonding. The urea hydrates can self-associate onto the cellulose surface that is linked to NaOH hydrates to create an inclusion complex which is quite stable at low temperatures, leading to the formation of a clear cellulose aqueous solution. It is worth noting that the dissolving ability of alkali/urea systems can be affected by the temperature and also the molecular weight M_w of cellulose.

Thus, cellulose with higher M_w ($> 10^5$) cannot be entirely dissolved, resulting in some aggregates (Liu et al., 2020; Qi et al., 2008).

Quaternary onium hydroxide solutions can also dissolve cellulose. Many systems were developed including quaternary ammonium hydroxides [e.g., tetraethylammonium hydroxide (TEAH) (Sirviö and Heiskanen, 2020), tetrabutylammonium hydroxide (TBAH) (Ema et al., 2014), tetramethylammonium hydroxide (TMAH), benzyltrimethylammonium hydroxide (BTMAH) (Swensson et al., 2020)] and quaternary phosphonium hydroxides [e.g., tetraalkylphosphonium hydroxide (TAPH) (Desideria Seiler et al., 2020), tetrabutylphosphonium hydroxide (TBPH) (Nguyen et al., 2019)]. Quaternary ammonium hydroxides offer more dissolving capacity compared to aqueous alkali/urea solutions and are able to solubilise cellulose at a greater concentration under soft conditions.

I.2.2 Cellulose chemical modification

The objectives of cellulose modification are mainly (i) the derivatisation of cellulose fibres and (ii) cellulose pre-treatments. Cellulose fibres derivatisation is achieved by esterification and/or etherification reactions in order to produce cellulose derivatives which are used in many applications. Cellulose pre-treatments aim at facilitating MFC production, by reducing energy consumption and this effect may also result from the grafting of new functions on cellulose. *Cellulose fibre pre-treatments will be detailed in section 4.*

I.2.2.1 Esterification

Cellulose esterification is the reaction between cellulose (hydroxyl groups) and acid, acid anhydride or acyl halide in acidic medium. Several esterification reactions were proposed in the literature. Two kinds of cellulose ester can be produced: organic ester such as cellulose acetate and inorganic ester including cellulose sulphate and cellulose nitrate. Cellulose acetate was first synthesised in 1865 by Paul Schutzenberger from wood pulp using acetic anhydride. Owing to their interesting properties (biocompatibility, non-toxicity...), cellulose acetate was investigated in the biomedical field (tissue regeneration, drug delivery...) and also in electrospinning (Liu et al., 2021).

Cellulose nitrate is the oldest derivative and one of the most significant inorganic cellulose esters. This ester is used in several applications such as coatings, plastics and explosives (Wang

et al., 2018). It is produced industrially from the reaction between cellulose and nitric acid, in the presence of sulfuric acid and water. Cellulose trinitrate can also be produced using the following nitrating systems: nitric acid/phosphoric acid/phosphorus pentoxide or nitric acid/acetic acid/acetic anhydride (Alexander and Mitchell, 1949). A wide range of cellulose derivatives (cellulose ester) is then obtained by reacting cellulose with sulphates and phosphates groups. These new derivatives have quite different characteristics that depend basically on the grafting group and the substitution degree. Commercialised cellulose esters are produced by heterogenous methods which is unable to control the reaction process and thus results in low degree of substitution.

The mixture of lithium chloride/N, N-dimethyl acetamide (LiCl/DMA) is considered as an efficient solvent of cellulose. This system was used to solubilise cellulose and to produce a series of cellulose esters from fatty acid chlorides (Willberg-Keyriläinen and Ropponen, 2019).

Cellulose modification can also be carried out in green solvents such as ionic liquids (IL) and Deep Eutectic Solvents (DES). The esterification and acylation of cellulose in ionic liquids were widely studied and several cellulose esters were produced including cellulose acetate, vinyl esters, methyl esters... For instance, cellulose acetate can be synthesised in 1-allyl-3-methylimidazolium chloride ([AMIM][Cl]) (Wang et al., 2008; Wu et al., 2004), 1-N-butyl-3-methylimidazolium chloride ([BMIM][Cl]) (Barthel and Heinze, 2006; Ferreira et al., 2019), 1-N-ethyl-3-methylimidazolium chloride ([EMIM][Cl]) (Barthel and Heinze, 2006) and 1-ethyl-3-methyl-imidazolium acetate ([EMIM][OAc]) (Kakuchi et al., 2015; Van Nguyen et al., 2017). These solvents offer a good solubilization of the cellulose and an easy acetylation with high degrees of substitution.

Deep Eutectic Solvents (DES) were also studied as green medium for cellulose esterification. For instance, the mixture of choline chloride-ZnCl₂ (CC-ZnCl₂) was used as both solvent and reagent to enhance cellulose acetylation. Acetylated cellulose was obtained with DS ranging from 0.15 to 0.47 (Abbott et al., 2005). *This part will be detailed in section 5.*

I.2.2.2 Etherification

The etherification reaction of cellulose is generally obtained by nucleophilic substitution of SN₂ type in an alkaline medium, the main reaction route using alkyl chlorides, hydroxyalkyls and epoxides as etherification agents. Some cellulose ethers were studied including

carboxymethyl cellulose CMC, ethyl cellulose and methyl cellulose. CMC is obtained by reacting alkali cellulose (treated with sodium hydroxide) with monochloroacetic acid. CMC is considered as a highly reactive cellulose derivative having a great water solubility with excellent gelation capacity. CMC is used in various applications, such as biomedicine (Ogushi et al., 2007), food, textile (Rahman et al., 2021). Ethyl cellulose and methyl cellulose are obtained by mixing alkali cellulose with ethyl chloride or methyl chloride, respectively.

Cellulose etherification can be also carried out in green solvents such as ionic liquid, DES, aqueous alkali/ urea solutions and quaternary onium hydroxides. Some etherification reactions such as carboxymethylation, carboxyethylation (Mikkola et al., 2007) and hydroxyalkylation were performed in imidazolium-based IL (Köhler et al., 2010). For instance, [EMIM][OAc] was investigated to produce a water-soluble hydroxyalkyl cellulose from cellulose and epoxides. Binary IL mixtures such as mixture of 1-ethyl-3-methylimidazolium methylphosphonate ([EMIM][MeP] and Brønsted acidic IL were also shown to be effective solvents and catalyst for cellulose etherification.

DES were also studied for the synthesis of cellulose ether. Many systems were used to produce cationised cellulose including chlorocholine chloride-urea (Abbott et al., 2006). This DES was used as both solvent and reagent. The mixture of boric acid and glycidyl trimethyl ammonium chloride was also used for cellulose cationisation (Vuoti et al., 2018). Modified cellulose was then tested in waste water treatment.

Aqueous alkali/ urea solutions are considered as suitable systems for homogenous reaction between cellulose and etherifying agents (alkyl halide, epoxides...) (Ge et al., 2022). Many cellulose ethers were synthesised by this way: methyl cellulose (Zhou et al., 2004), carboxymethyl cellulose CMC (Qi et al., 2009), hydroxyethyl cellulose (Zhou et al., 2006) and allyl cellulose (Hu et al., 2015).

Zhou et al. (2004) have successfully produced hydroxypropyl cellulose and methyl cellulose using 6 wt % of NaOH and 4 wt % urea. They were obtained by reacting cellulose (solubilized in NaOH/urea) with propylene oxide and dimethyl sulphate, respectively. It was demonstrated that this system offers more advantage than traditional systems (Zhou et al., 2004). In addition, the mixture of 7 wt % NaOH and 12 wt % urea was used to prepare CMC by reacting cellulose with sodium monochloroacetate (Qi et al., 2009).

Quaternary onium hydroxides exhibit strong basicity like aqueous alkali/urea systems, which is suitable for homogenous cellulose etherification. For instance, the mixture of tetraalkylonium hydroxide (47% tetra-n-butylphosphonium hydroxide aqueous solution) was investigated in cellulose benzylation (Abe et al., 2017). The results showed a fast benzylation reaction: benzyl cellulose with high degree of substitution ($DS > 2.5$) was prepared in 10 min at room temperature. No degradation of cellulose for highly substituted BC was observed. This mixture is more adequate for the benzylation of cellulose than that of NaOH/urea (Ge et al., 2022).

I.3 From cellulose to nanocellulose

Nanocellulose has gained great attention from the scientific community which is explained by its fascinating properties such as biodegradability, biocompatibility, high specific surface area and renewability. To obtain nanocellulose from cellulosic biomass, many steps are required as described in Figure I. 7. Nanocellulose is constituted mainly from two families: cellulose nanocrystals (CNC) and cellulose nanofibrils (CNF) with different properties and morphologies. There are several names for cellulose nanofibrils such as nanofibrillated cellulose (NFC), microfibrillated cellulose (MFC) and cellulose microfibrils (CMF). This nanomaterial is widely available and used as a commercial product in industrial applications. For these reasons, CNF are attracting more and more interest in the scientific community. *During our study, microfibrillated cellulose (MFC) has been chosen to refer to cellulose nanofibres.*

To produce cellulose nanocrystals, an acid hydrolysis is performed, that allows to remove amorphous regions of cellulose fibrils as already mentioned. For MFC which contains both amorphous and crystalline regions, cellulose fibres are subjected to chemical or biological pre-treatment followed by a mechanical disintegration. The different morphology of these two nanomaterials will be described in the following sections.

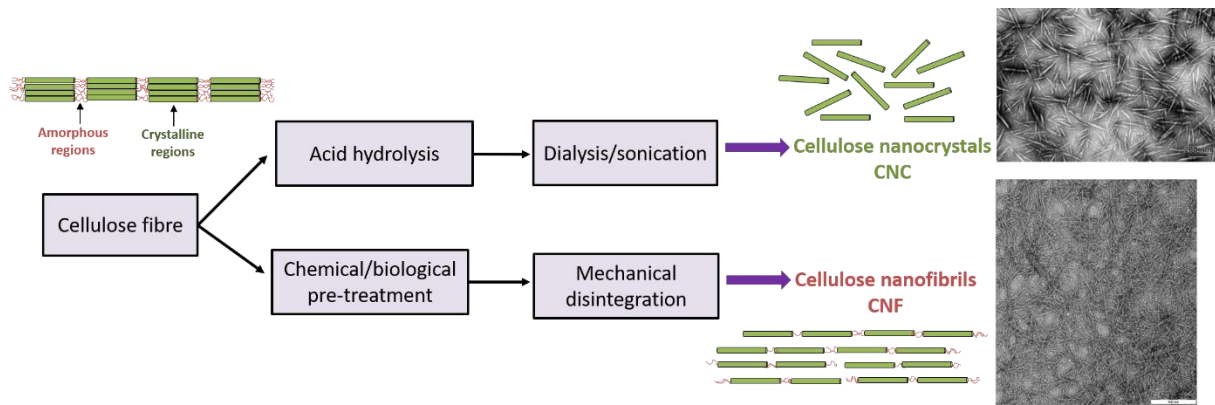


Figure I. 7. Methods for MFC and CNC production from cellulose fibre and their morphologies, TEM images of CNC and MFC extracted from (Habibi et al., 2008) and (Fatah et al., 2014) respectively.

I.3.1 Cellulose nanocrystals CNC

Cellulose nanocrystals, called also whiskers, were first reported by Rånby in 1951 (Rånby, 1951). Whiskers are isolated from cellulose microfibrils using a simple process based on acidic hydrolysis. Several strong acids have been investigated including sulfuric, nitric and hydrochloric acid, but the most effective one is sulfuric acid. Cellulose nanocrystals extraction is based on the penetration of acid into cellulose fibres and leads to the hydrolysis of amorphous regions while crystalline domains remain intact. A transverse cleavage of the microfibrils into nanocrystals occurs due to the disruption of amorphous domains. Cellulose nanocrystals dimensions vary depending on the source of the cellulose and the hydrolysis conditions (acid concentration, hydrolysis time and temperature). Their length and width are of few hundreds of nanometres and few nanometres, respectively as observed in Figure I. 8. Another important parameter is their aspect ratio (ratio of the length to the width) which determines their reinforcement properties (Dufresne, 2012). Recently, Deep Eutectic Solvents (DES) were also used to extract CNC and the most effective one is the mixture of choline chloride-oxalic acid dihydrate. This system was first studied by Sirviö et al. (2016) who obtained CNC with good thermal stability. The same system was used with different molar ratio between their components by Ling et al. (2019). It was then optimised to extract CNC with a good yield (Douard et al., 2021).

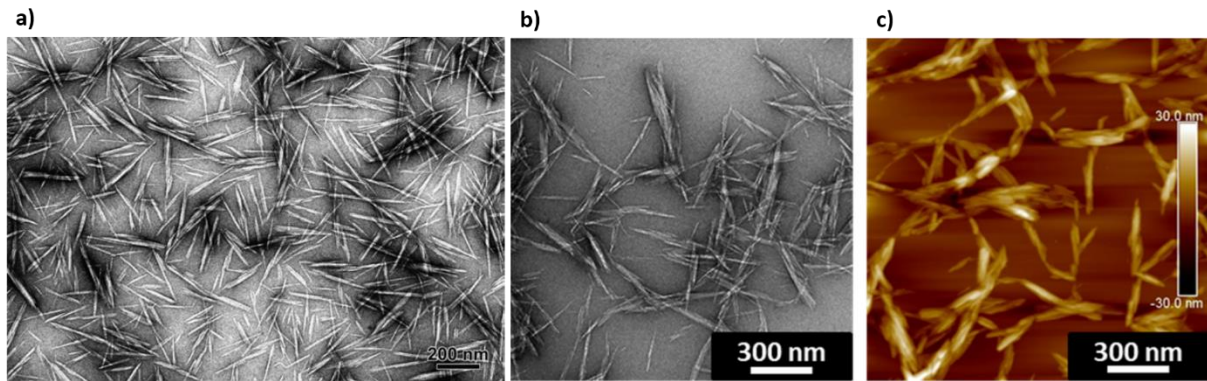


Figure I. 8. TEM and AFM images of CNC produced from acid hydrolysis (a) and DES treatment (b and c) extracted from (Habibi et al., 2008) and (Douard et al., 2021) respectively.

I.3.2 Microfibrillated cellulose MFC

Microfibrillated cellulose (MFC) were introduced by Turbak et al. (1983). They can be prepared from many cellulosic sources (cotton, wood, non-wood, annual plants...) by mechanical disintegration, coupling or not chemical and mechanical pre-treatments of the cellulosic fibres. MFC are usually produced by high shear mechanical treatments applied to cellulose fibres (Dufresne, 2013). Consequently, microfibrils are released by breaking interfibrillar hydrogen bonding of the cellulosic fibre wall.

I.3.2.1 MFC properties

Microfibrillated cellulose were described as microfibrils with nanometric dimensions as reviewed by Xia et al. (2003). This nanomaterial is characterised by its fascinated properties including, low thermal expansion (Fukuzumi et al., 2009; Nogi et al., 2009), high aspect ratio which means the ratio between length and diameter (Moon et al., 2011), high mechanical and optical properties of films produced from them (Abdul Khalil et al., 2014). The availability of hydroxyl groups on their surface facilitates the chemical modification of MFC, which is used to impart new functionalities and propose new applications.

MFC properties depend mainly on cellulose source, the selected pre-treatment and the applied mechanical treatment. In terms of morphology, MFC display similar morphologies but different dimensions. Many techniques are used to characterise MFC, mainly by measuring their diameter, such as transmission electron microscopy (TEM) and atomic force microscopy

(AFM). The specific surface area is a key parameter that characterises the MFC quality because it increases with the fineness of the MFC (Spence et al., 2010). It can be measured by the Brunauer–Emmett–Teller (BET) method. This method is based on the preparation of aerogels in order to avoid aggregation phenomena of MFC. The specific surface area of the MFC is measured and the diameter is then calculated (Sehaqui et al., 2011).

The structural properties of MFC can be studied by measuring the degree of polymerisation DP and crystallinity index CrI. The DP is determined using a viscosity method (ISO 5351) which consists of dissolving MFC in cupri-ethylene diamine (cellulose solvent) (Banvillet et al., 2021b; Rol et al., 2017; Sirviö et al., 2015). The average DP of MFC samples is determined from the Mark-Houwink-Sakurada equation. The DP is an important parameter when characterizing the MFC, but it has a little influence on the properties of obtained MFC.

Crystallinity index CrI gives valuable information on the structure of MFC since they are composed of amorphous and crystalline regions. The CrI can be determined from X-ray diffraction analysis (Boufi and Chaker, 2016; Liu et al., 2021; Suopajarvi et al., 2020a) or solid-state ^{13}C NMR (Banvillet et al., 2021a; Villares et al., 2017). The CrI can be impacted by several parameters. It increases when the amorphous regions are removed after some chemical or biological pre-treatments, while it decreases when the crystalline parts are destructed after mechanical disintegration due to the high shear forces, for instance.

The MFC mechanical properties can be studied by performing mechanical tests on films called also nanopapers (Henriksson et al., 2008). These films are produced from MFC suspension using two methods: solvent casting (solvent evaporation) or filtration and drying under vacuum. The later method can be done using a classic handsheet former (Rapid Köthen former, for instance) and an appropriate sieve to well retain MFC as described in Figure I. 9.

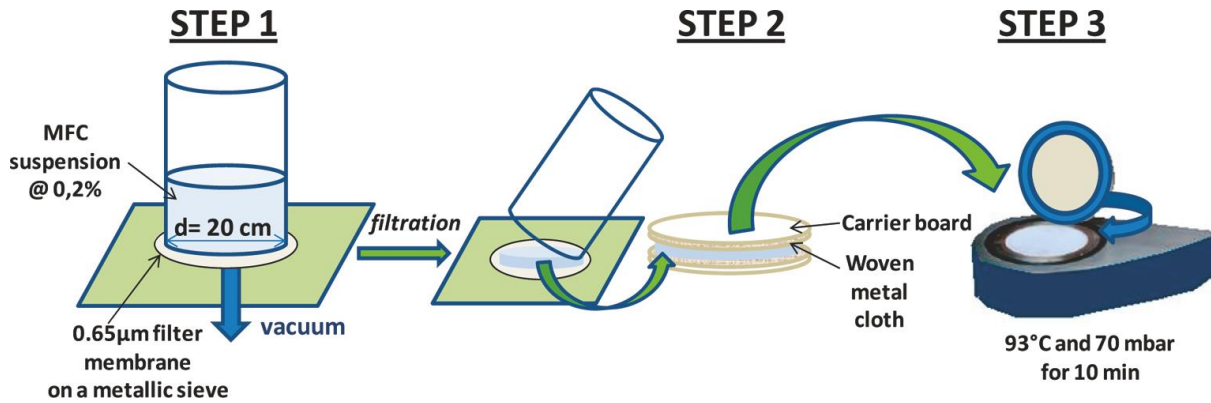


Figure I. 9. Nanopapers preparation using sheet former (Rapid-Köthen) (Sehaqui et al., 2010).

The properties (density, Young's modulus, tensile strength, tear resistance...) of these nanopapers can be analysed. They depend on the pre-treatment and the used microfibrillation process. A tensile strength and Young's modulus of 100-200 MPa and 5-10 GPa, respectively, are usually reported for MFC obtained from enzymatic hydrolysis. However, TEMPO-oxidation pre-treatment allows obtaining higher values between 200-250 MPa and 10-20 GPa, respectively (Benítez and Walther, 2017).

I.3.2.2 MFC applications

MFC are used in various applications due to their interesting properties. For instance, they can be used in papermaking as described in many studies (Adel et al., 2016; Boufi et al., 2016; Gao et al., 2016). In this case, MFC enhance the bond strength between fibres and they also act as a reinforcing agent in paper coatings (Klemm et al., 2011). For instance, Adel et al. (2016) prepared MFC from various sources (bagasse, rice straw and cotton stalk) and demonstrated that MFC enhances the tensile properties of produced papers. However, some crucial issues need to be clarified, at the industrial scale due the high cost for producing MFC (Boufi et al., 2016).

MFC can be also applied in nanocomposite applications as a reinforcing material in the polymer matrix. The incorporation of MFC enhances significantly the thermomechanical properties of produced nanocomposites. There is a need to control morphological and surface properties of MFC to improve the properties of composites. Thus, it is important to understand MFC thermal behaviour during the preparation of nanocomposites to avoid their degradation (MFC have a decomposition temperature about 200-300 °C). Despite the promising results given by the use

of MFC in nanocomposites materials (Dominic et al., 2020; Kulshrestha et al., 2020; Orts et al., 2005), the scaling up of this process is quite difficult and requires more development to decrease the costs (Gan et al., 2020).

Finally, MFC can be used to impart barrier properties (Aulin et al., 2012; Lavoine et al., 2012), in health applications (Jorfi and Foster, 2015; Khoshnevisan et al., 2018) and waste water treatment (Mohammed et al., 2018).

I.3.3 Mechanical processes used for MFC production

Several mechanical processes have been used to produce MFC. They aim at microfibrillating cellulose fibres into small fragments, so they require high energy to break the inter-fibrillar hydrogen bonding (Bharimalla et al., 2015). These processes were classified by Nechyporchuk et al. (2016) into two types as described in Figure I. 10. The first ones are conventional processes such as homogenisation (using homogenizer or microfluidiser) and grinding (ultra-fine friction grinder Masuko). They produce aqueous dispersions of MFC with low solid content ($< 5\%$) (Rol et al., 2019) which is not always desired depending on the targeted applications. Then, the second ones are the non-conventional processes such as twin-screw extruder which leads to high MFC solid content (Rol et al., 2017b), steam explosion, ball milling, refining, blending, etc.

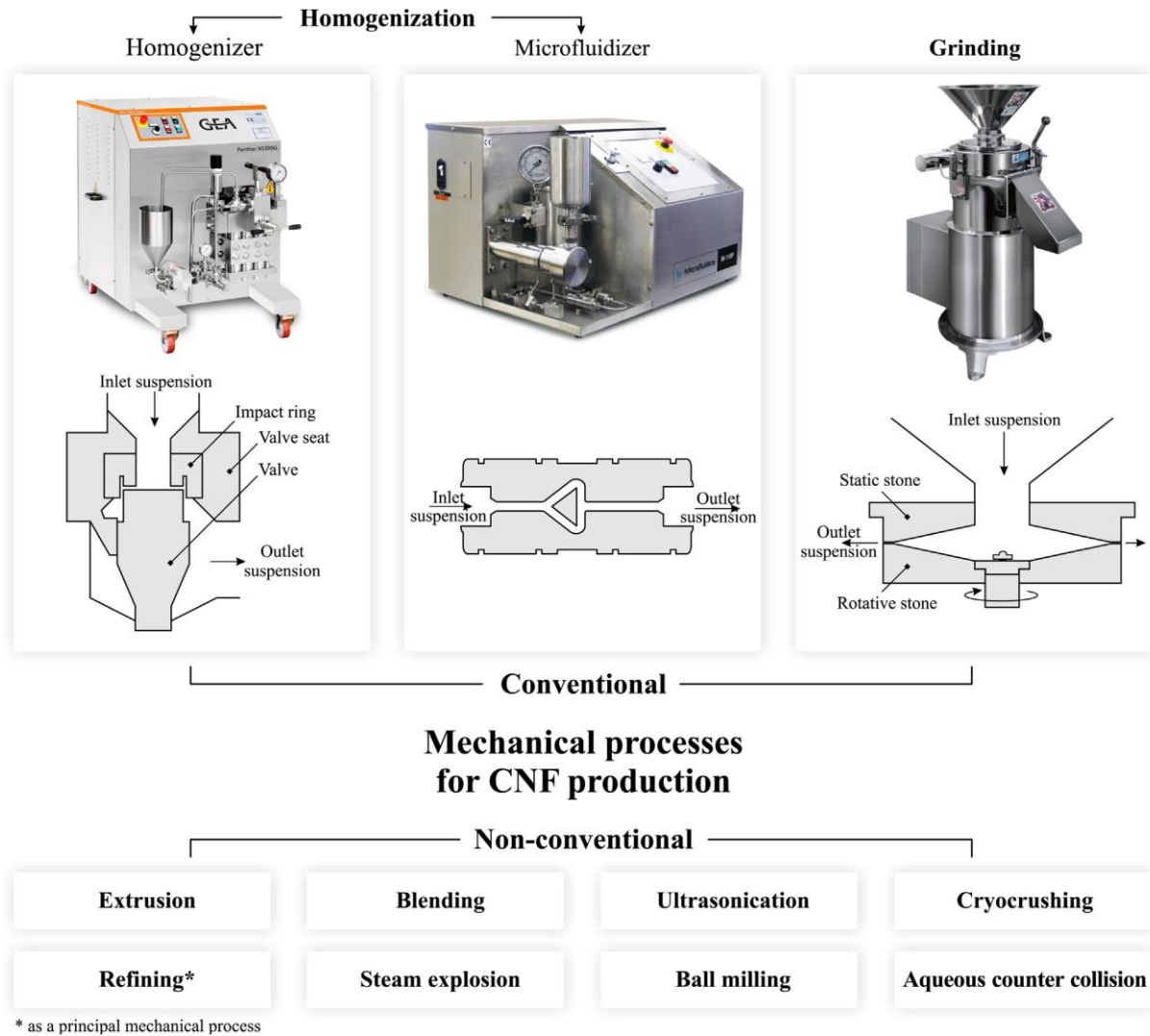


Figure I. 10. Conventional and non-conventional processes to produce MFC (Nechyporchuk et al., 2016).

I.3.3.1 Conventional processes

Homogenisation

Homogenisation was first introduced by Herrick et al. (1983) and Turbak et al. (1983). The disintegration consists of subjecting cellulose suspension (2%) to a high-pressure shear. The obtained product was described as a gel-like material with high viscosity (Herrick et al., 1983).

Two devices are used for homogenisation: the homogeniser and the microfluidiser. The disintegration of cellulose fibres using the homogeniser is based on passing cellulose suspension across a small annular space formed between the valve of the homogeniser and an

impact ring (Rol et al., 2019). As a result, the quick opening and closure of this valve facilitates the microfibrillation process by inducing high shear forces. Cellulose fibres are then microfibrillated and, subsequently, microfibrils are individualised due to internal and external fibrillation of the fibres.

Microfluidisation is a bit different: it is carried out by passing a cellulosic suspension through an intensifier pump (Z or Y shape chamber). Again, microfibrillation is performed thanks high shear forces that make fibres splitting into microfibrils (Ferrer et al., 2012; Wang et al., 2016).

The homogeniser is the most efficient equipment that leads to obtain homogenous suspensions of MFC (Boufi and Gandini, 2015). Several passes are required to obtain smaller and more homogenous MFC (Siró and Plackett, 2010). However, the energy consumption increases with the passes number: it was estimated to be in the range of 20-50 kWh/kg of dry MFC (Boufi and Gandini, 2015; Klemm et al., 2011). Moreover, the clogging of the small orifice of the homogeniser by the fibre suspension is relatively frequent (Abdul Khalil et al., 2014) and a mechanical pre-treatment of the fibres (refining) is necessary to limit this problem. To conclude, the disintegration of cellulose fibres into MFC using homogenisation has two major problems: high energy consumption and clogging. These problems can be avoided using some pre-treatments such as refining, chemical modification or biological pre-treatment.

Grinding

Grinding was described by Taniguchi and Okamura (1998) as an efficient method for producing MFC with a diameter ranging from 20 to 90 nm. This method consists in passing cellulosic suspensions (2-5 wt %) between two disks (stator and rotor), the gap (distance) between the disks can be adjusted to avoid clogging problems (Nechyporchuk et al., 2016; Siró and Plackett, 2010). During grinding, the cellulose fibres are exposed to huge compression, shearing, and rolling friction forces, allowing their later disintegration. A smaller gap between the disks leads to closer contact and, therefore, higher shear forces (Serpa Guerra et al., 2020). It was demonstrated that the gap of the grinder has a significant impact on controlling the microfibrillation (Kang, 2007).

A comparative study between the homogeniser, microfluidiser and ultra-fine friction grinder showed that MFC produced by homogenisation had the highest specific surface area. However, MFC obtained from the microfluidiser and ultra-fine friction grinder exhibited better physical and optical properties than those produced using the homogeniser (Spence et al., 2011).

I.3.3.2 Non-conventional processes

Extrusion is an emerging process that was patented by Heiskanen et al. (2014) and used to produce MFC using a twin-screw extruder TSE. TSE is described in many studies as an effective process which leads to obtain MFC suspensions at high solid contents with low energy requirement compared to homogeniser and ultra-fine friction grinder.

During this procedure, a fibrous suspension at high concentration (15-30% w/w) is disintegrated by two co-rotating screws engaged in a closed cylinder. The fibres are subjected to shear forces and well separated microfibrils are produced with high aspect ratio (Hietala et al., 2011). For instance, MFC suspensions at high solid content (20%) were obtained from a pre-treated hardwood kraft pulp (enzymatic hydrolysis or TEMPO oxidation) after 7 passes through an extruder (Rol et al., 2017b). The results showed that the energy consumption was decreased by 63% compared to grinding. This procedure is thus very promising and could be a solution for industrialisation and transportation problems of MFC. In another study, Rol et al. (2018) showed that producing MFC by TSE coupled with homogenisation reduces the energy consumption compared to MFC produced only by homogenisation. Finally, other studies also used the extruder to produce MFC (Baati et al., 2017; Banvillet et al., 2021b; Ho et al., 2015). However, this mechanical treatment causes a decrease of the cellulose DP and crystallinity more important than that observed with more conventional processes.

Steam explosion is a thermomechanical process used in chemical fractionation and biotechnological conversion. It was also studied to produce MFC by breaking down the structure of cellulosic materials due to the combined actions of steam heat and shear forces. This process allows saturating the material with steam in the reactor where polysaccharide hydrolysis may occur depending on the chosen temperature and the residence time (which does not generally exceed few minutes). Then, this step is followed by a sudden pressure drop and mechanical forces, generated by the water evaporation resulting from the sudden depressurisation, may weaken the fibre wall (Cherian et al., 2010).

Many raw materials have been tested: for instance, Cherian et al. (2010) isolated MFC from pineapple leaf fibres by acidic treatment coupled with steam explosion (Cherian et al., 2010). Tanpichai et al. (2019) extracted MFC from pineapple leaves using steam explosion. During this extraction, the lengths of treated fibres were reduced. Coarse elements with width of 3 μm and length of 93 μm were obtained after 5 cycles. MFC with 10-50 nm of width were also

produced from wheat straw by alkali steam explosion treatment coupled with homogenisation (Kaushik and Singh, 2011) or isolated from sugarcane bagasse waste using steam explosion, alkali treatment and peroxide bleaching followed by homogenisation (Hongrattanavichit and Aht-Ong, 2020). The results indicated that the temperature of the explosion affects significantly the fibres more than the duration of treatment. Recently, the steam explosion combined with TEMPO-oxidation pre-treatment was investigated to produce cellulose microfibrils from waste biomass marine (Khadraoui et al., 2022). It was also implicated in the production of lignin containing cellulose microfibrils from beech wood (Nader et al., 2022).

The steam explosion process seems to be an efficient treatment to produce cellulose microfibrils. However, the main disadvantage of this treatment is that MFC have lower qualities than those produced from other processes.

High intensity ultrasonication is also a mechanical process used to extract microfibrils from different cellulose sources. It is based on high mechanical oscillation power that leads to the fibre's microfibrillation owing to the hydrodynamic forces generated by the ultrasounds. Ultrasound refers to a part of the sound spectrum (around 20 kHz - 10 MHz) produced by converting mechanical or electrical energy into high frequency acoustical energy. This energy is conveyed to cellulose chains by cavitation which is a physical phenomenon based on bubbles gas transformation (expansion, explosion, etc) resulting from the absorption of ultrasonic energy by water molecules. Added to that, ultrasonication has been applied in a wide range of processes such as emulsification, homogenisation and catalysis (Wang and Cheng, 2009). The ultrasonication was investigated to isolate cellulose microfibrils from various cellulose sources. (Cheng et al., 2010). The results showed that a mixture of elements having diameters varying from 30 nm to some micrometres.

MFC with high aspect ratio (long and uniform MFC) and good thermal stability were isolated from homogenisation and ultrasonication process (Dilamian and Noroozi, 2019). The ultrasonication technique is considered as an environmentally method that produce MFC with low cost. However, further research is required to enhance this process.

High speed blending is another mechanical process used to produce microfibrillated cellulose. This technique was used by Uetani and Yano (2011) and they successfully produced MFC with identical diameter of 15-20 nm during 30 min. Surprisingly, they observed many balloons along the fibres, appearing during stirring; these balloons are extended to the borders which leads to

the microfibrils individualisation. Thus, the results obtained are very promising and showed that high speed blender can produce MFC having the same level of fibrillation with much less destruction compared to those produced by the grinder (Uetani and Yano, 2011). The high-speed blender can be involved at industrial scale owing to its simplicity and the possibility to produce MFC using high volume without any clogging problem, as mentioned by Boufi and Chaker (2016) who produced MFC by blending, after TEMPO oxidation pre-treatment. The obtained MFC were incorporated into polymer matrix and they showed high reinforcing potential (Boufi and Chaker, 2016). Other studies also used this technique (Nakagaito et al., 2015; Rahimi Kord Sofla et al., 2019).

Ball milling is an efficient one-step technique for preparing MFC at room temperature and under ambient pressure due to its simplicity in operation and also the use of inexpensive equipment. MFC were produced with an average diameter of 100 nm using mild mechanical milling conditions involving cerium-doped zirconia balls having diameters between 0.4-0.6 mm during 1.5 h without the use of alkaline pre-treatment (Zhang et al., 2015). During milling process, best conditions should be selected such as milling time, mass ratio ball/cellulose and ball dimension in order to obtain microfibrillated cellulose and not particles. The ball milling can be used in combination with ionic liquids at room temperature to produce MFC with high quality (Phanthong et al., 2017). It can be also carried out with only oxidation treatment (Kekäläinen et al., 2015) or coupled with oxidation treatment and PFI refining (Liimatainen et al., 2015). In addition, acetylated MFC were obtained using mechanochemical acylation of cellulose with hexanoyl chloride (Deng et al., 2016). Thus, this technique has become an effective and easy process to produce MFC at high solids contents (≥ 50) (Kekäläinen et al., 2015). However, the homogeneity and quality of produced MFC still remains the principle challenge for this process.

In this PhD project, the ultra-fine grinding and the twin-screw extruder will be used as a principal mechanical treatment to produce microfibrillated cellulose and MFC at high solid contents, respectively.

I.4 Cellulose pre-treatments for MFC production

As discussed in the previous section, the production of MFC is energy consuming. To overcome this problem, many pre-treatments of cellulosic fibres have been developed to facilitate MFC

production, to reduce energy consumption and also to introduce new functions on MFC surfaces. *In this section, cellulose pre-treatments will be discussed in detail because the subject of the thesis is based on the study of cellulose pre-treatments for cellulose microfibrillation.*

Several pre-treatments are available in literature. Biological pre-treatment (enzymatic hydrolysis) induces cellulose hydrolysis, while chemical pre-treatments generally introduce charged groups on cellulose structure. These groups create electrostatic repulsions which improves microfibrillation. The quality of produced MFC is strongly influenced by the used pre-treatment.

In this section we will discuss the following pre-treatments: enzymatic hydrolysis, TEMPO oxidation, quaternization, phosphorylation and DES pre-treatment.

I.4.1 Enzymatic hydrolysis

The enzymatic hydrolysis is considered as an environmentally friendly pre-treatment used at the industrial scale which produces MFC with good quality (Nechyporchuk et al., 2015; Nie et al., 2018). Cellulase enzyme was patented by Walter and Gallatin (1962) as a useful process in papermaking as it improves fibre fibrillation. Cellulase enzyme is divided into three main classes depending on their action (Figure I. 11): (i) endoglucanases, which act on amorphous domains of cellulose (ii) exoglucanases (cellobiohydrolase) that allow the cleavage of the ends of cellulose chains, giving rise to di- and tetrasaccharides, and (iii) cellobiases that hydrolyse cellulose (di and tetra) into glucose (Zhou and Ingram, 2000). Cellulose microfibrillation using enzymatic pre-treatment was first developed by Pääkkö et al. (2007) and Henriksson et al. (2007). They combined homogenisation with enzymatic hydrolysis (endoglucanases). The enzymatic hydrolysis allows producing longer and highly entangled microfibrils with higher aspect ratio. The principal effects of cellulases enzyme on cellulose fibres is a decrease of the degree of polymerisation DP and an enhancement of the crystallinity. The decrease of DP results from the action of exoglucanases on the ends of the cellulose chains, while the increase of crystallinity is due to the hydrolysis of amorphous regions by endoglucanases.

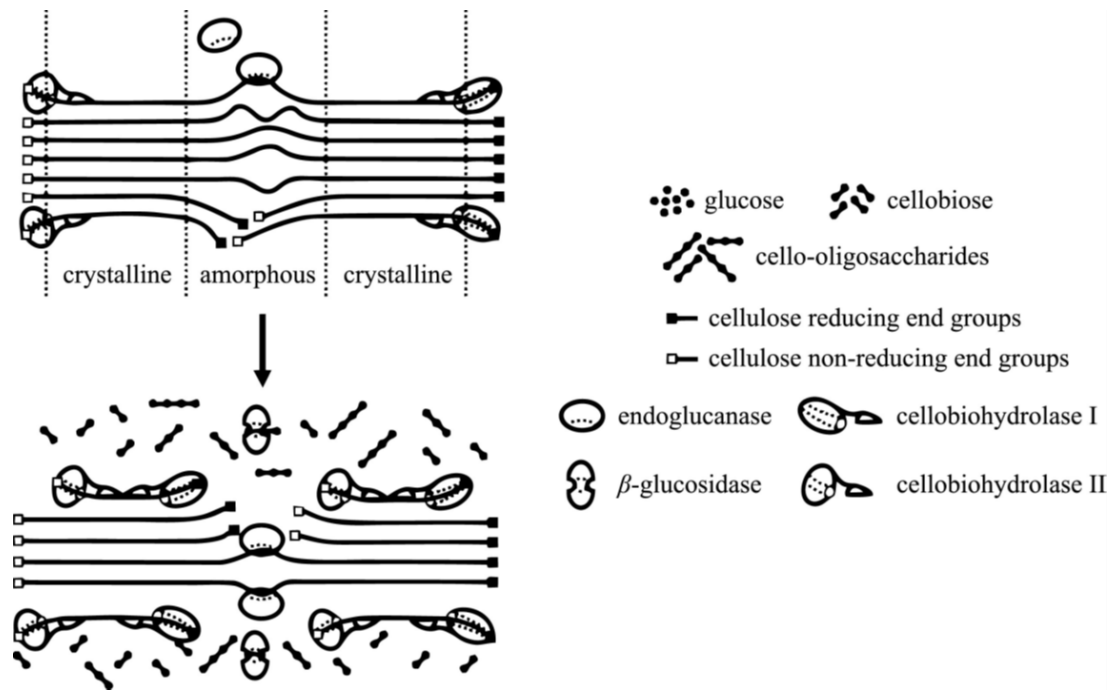


Figure I. 11. Mechanism of enzymatic hydrolysis for different cellulases categories (Nechporchuk et al., 2016).

Many enzymes have been studied as reviewed by Rol et al. (2019), including hemicellulases, lytic polysaccharide monooxygenase and laccases. These enzymes facilitate cellulose accessibility to cellulase without directly acting on hydrolysis. Long et al. (2017) have shown that the activity of endoglucanases can be enhanced by the use of xylanase, which facilitates microfibrillation. The DP was reduced during this treatment while the crystallinity was increased. Xylanase thus allows microfibrillation by opening cellulose fibres without changing their structure.

Enzymatic pre-treatments lead to reduced energy consumption during the further microfibrillation step. High viscosity gels are generally obtained which justifies the presence of MFC with high aspect ratio. Many parameters have been studied (Nechporchuk et al., 2015) including enzyme type and concentration, temperature, pH, reaction time and biomass sources. It was demonstrated that optimal pH of enzymatic treatment is between 5-8, while the optimal temperature is between 20-70 °C.

MFC obtained from enzymatic hydrolysis are not functionalised and thus may require further modification to broaden their applications.

I.4.2 TEMPO oxidation

Cellulose oxidation using TEMPO radical (2,2,6,6-tetramethyl-1-piperidinyloxy) was the first strategy used to introduce negatively charged groups. This approach was initially proposed by Saito and Isogai (2006) as a selective oxidation of cellulose. It consists of the oxidation of cellulose fibres, suspended in water, using sodium chlorite, sodium bromide and catalytic quantities of TEMPO radical at pH = 10.5. The oxidation starts by adding NaClO to the suspension of cellulose in the presence of TEMPO and NaBr. The principle of TEMPO/NaBr/NaClO treatment is described in Figure I. 12. More precisely, it is based on the selective oxidation of cellulose fibres using the nitrosonium ion ($+N=O$) which is produced in situ. As a consequence, the C6 primary hydroxyl functions of cellulose are transformed into aldehydes, that are further converted to carboxylic groups (Saito and Isogai, 2006).

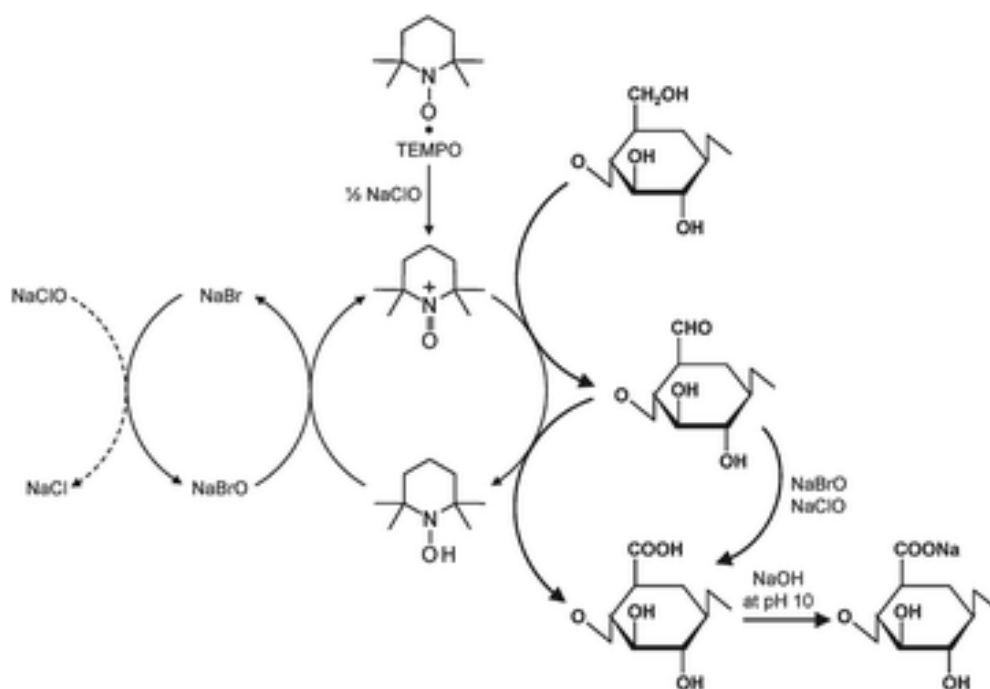


Figure I. 12. Catalytic oxidation mechanism of C6-OH groups of cellulose by TEMPO/NaBr/NaClO at pH=10 (Isogai et al., 2011).

Many protocols of TEMPO-oxidation have been proposed (Besbes et al., 2011; Isogai et al., 2011; Khadraoui et al., 2022; Okita et al., 2010; Saito et al., 2009; Saito and Isogai, 2004). For instance, Saito et al. (2007) have successfully produced individualized MFC with widths of 3-4 nm and lengths of several microns at different carboxylate contents (see Figure I. 13).

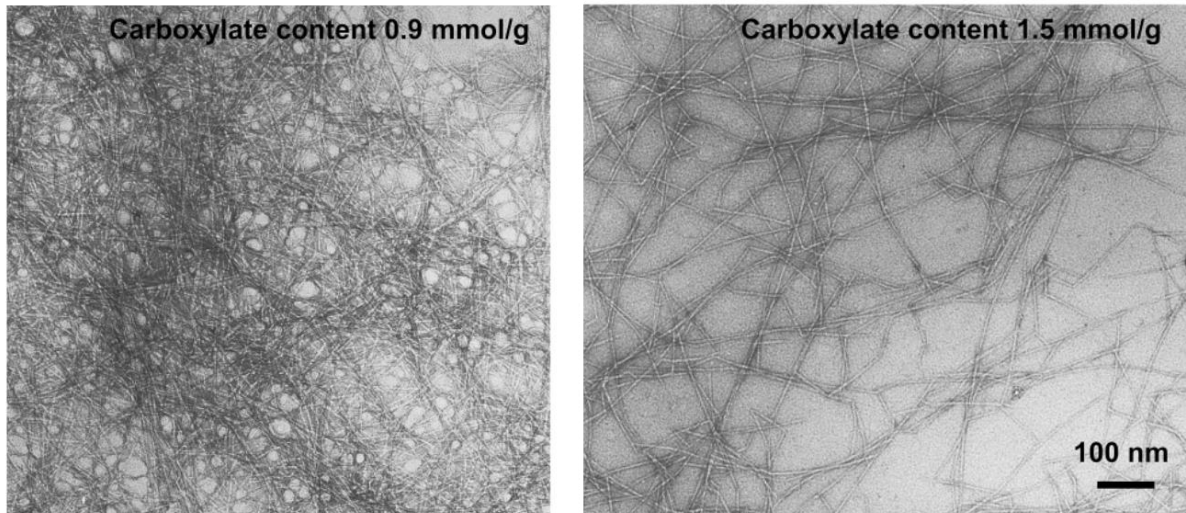


Figure I. 13. TEM images of TEMPO-oxidised CNF extracted from (Saito et al., 2007).

Isogai et al. (2011) demonstrated that, during oxidation process, a remarkable decrease of the degree of polymerisation was observed which was attributed to a depolymerisation caused by some radical species (such as OH radicals). These radicals can penetrate most of the amorphous domains of native cellulose.

To limit depolymerisation, another system was developed which is TEMPO/NaBr/NaClO₂. This system was used in a similar method in neutral or weakly acidic conditions as reported in Figure I. 14 and allows maintaining cellulose DP (Saito et al., 2009, 2007; Zhao et al., 1999).

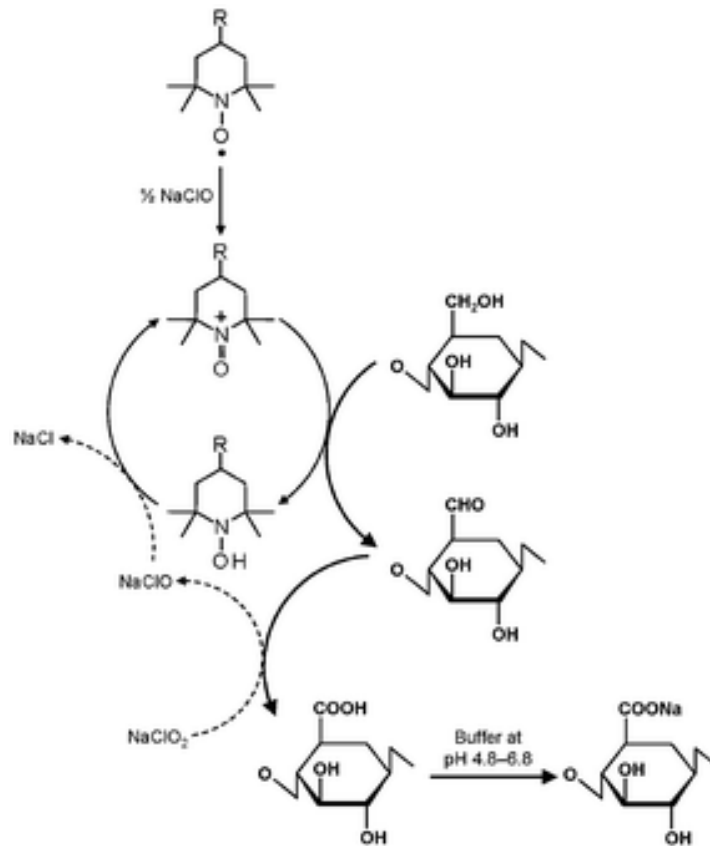


Figure I. 14. Selective oxidation of C6 primary hydroxyls of cellulose to carboxylate groups by TEMPO/NaBr/NaClO₂ oxidation in water at pH 4.8-6.8 (Isogai et al., 2011).

Still now, research works continue to improve TEMPO oxidation for cellulose microfibrillation. For instance, the use of NaBr was replaced by Na₂SO₄, which is cheaper and gives the same carboxylic content (Inamochi et al., 2017).

Other procedures have been also developed for the production of carboxycellulose microfibrils, by using nitric acid and sodium nitrite (Sharma et al., 2017). This treatment leads to a significant decrease of crystallinity (from 62 to 35%) but it allows reducing the use of chemicals with a positive impact on the decrease of energy consumption during ulterior microfibrillation. MFC exhibit length and width of 190-370 and 4-5 nm, respectively. MFC were further used in water purification for the adsorption of heavy metal ions.

TEMPO oxidation is an efficient pre-treatment used industrially to produce MFC. It allows to reduce the energy consumption. The produced MFC exhibit higher qualities compared to enzymatic hydrolysis. However, the main problem with this treatment is the use of corrosive

(TEMPO) and toxic reagent (NaClO) which is not eco-friendly. Moreover, the complexity of the reaction impacts its reproducibility.

I.4.3 Quaternisation

Quaternisation is another chemical pre-treatment used to facilitate the MFC production. It is used to bring cationic charge on cellulosic surface (Aulin et al., 2010; Cai et al., 2003; Abbott et al., 2006; Song et al., 2008). To this end, many reagents have been studied including 2,3-epoxypropyl trimethylammonium chloride (Olszewska et al., 2011), glycidyl trimethylammonium chloride (Pei et al., 2013), (2-chloroethyl) trimethylammonium chloride (chlorocholine chloride) in the presence of dimethyl sulfoxide and sodium hydroxide (Ho et al., 2011) and eutectic mixture of choline derivatives and urea (Abbott et al., 2006). The produced cationic MFC exhibit greater adsorption capacity of anionic dye (Abbott et al., 2006; Pei et al., 2013).

Moreover, Liimatainen et al. (2014) produced cationic MFC by homogenisation. This pre-treatment produced cationic MFC using periodate oxidation and quaternization with (2-hydrazinyl-2-oxoethyl)-trimethylazanium chloride (Girard's reagent T).

Chaker and Boufi (2015) showed that quaternisation facilitates the microfibrillation process (homogenisation) as described in Figure I. 15 and prevents clogging. The obtained MFC were characterised by a strong reinforcing potential and antibacterial activities. It was also demonstrated by Saini et al. (2016) that films produced from cationic MFC displayed promising antibacterial properties without environment concerns.

Cationisation is an emerging pre-treatment resulting in MFC of good quality and antimicrobial properties but it is difficult to reach DS more than 0.5 (Yan et al., 2009). Moreover, this pre-treatment uses CMR (carcinogenic, mutagenic and toxic for reproduction) substances which may limit its industrialisation.

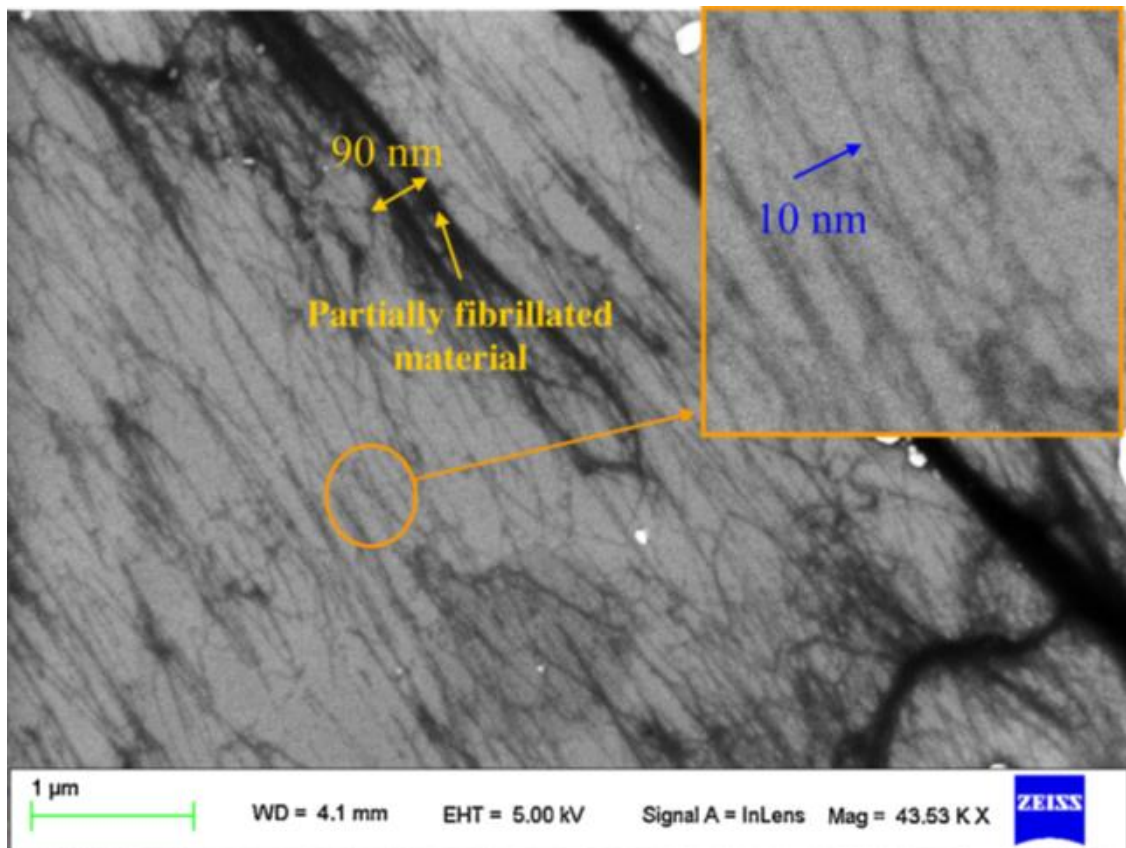


Figure I. 15. SEM image of CNF produced from cellulose quaternisation, extracted from (Chaker and Boufi, 2015).

I.4.4 Phosphorylation

Phosphorylation is another efficient chemical pre-treatment used to introduce negative charges on cellulose fibres. It facilitates the preparation of MFC due to the introduction of anionic phosphate groups on cellulosic fibres. Phosphorylation is achieved using di-ammonium hydrogen phosphate ($(\text{NH}_4)_2\text{HPO}_4$) with urea. During this treatment, the fibres become highly charged due to phosphate and carboxylate groups, which facilitate the release of MFC during homogenisation, as reported by Ghanadpour et al. (2015). In this work, the MFC exhibit good thermal stability with flame-retardant properties. Indeed, the nanopapers produced from them showed self-extinguishing behaviour during flammability tests. In another study, Noguchi et al. (2017) showed that, after phosphorylation, there was no significant decrease in the recovery ratio and the degree of polymerisation remains unchanged. The produced microfibrils exhibited widths around 3-4 nm (see Figure I. 16) and the suspension had high transparency and high viscosity.

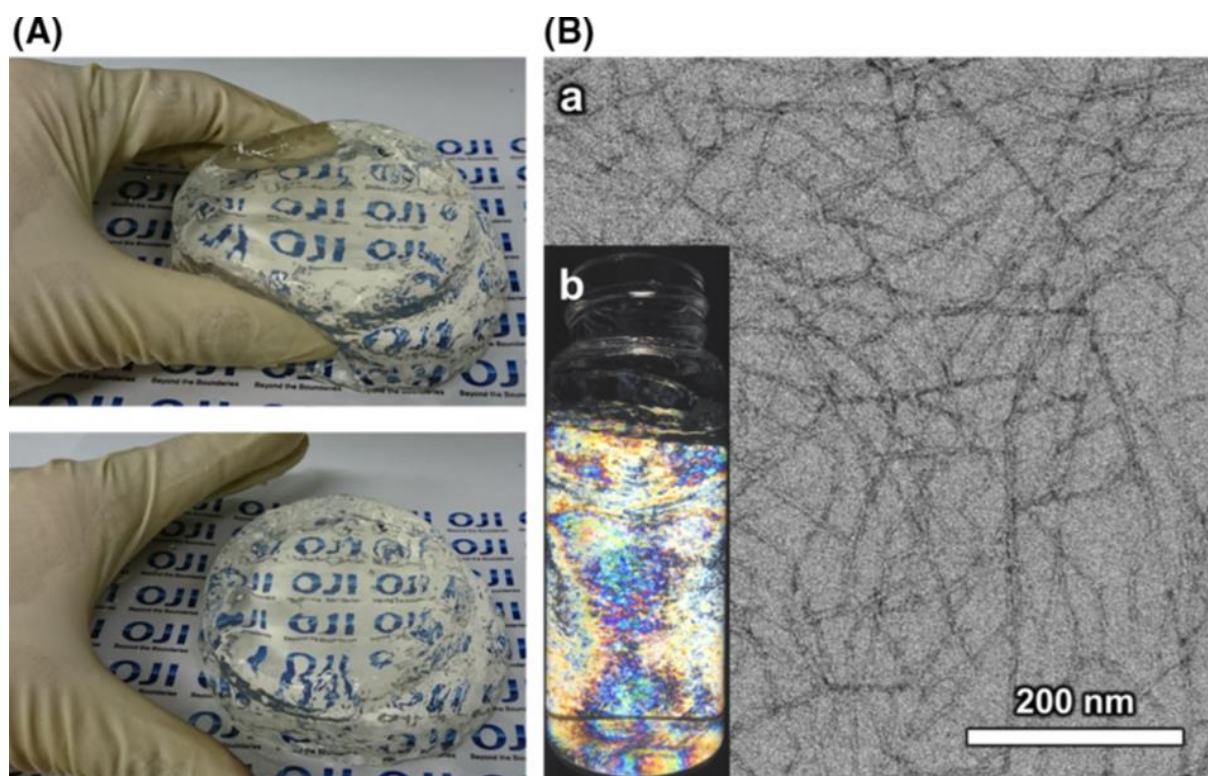


Figure I. 16. Photographs and TEM images of phosphorylated MFC dispersion (A, (B)-a) and phosphorylated MFC dispersion observed between cross polarizers (B)-b) (Noguchi et al., 2017).

More recently, the phosphorylation of cellulose fibres has been studied by Rol et al. (2020) to optimise the charge content and the quality of the obtained materials. Various phosphate salts were tested ($\text{NH}_4\text{H}_2\text{PO}_4$, $(\text{NH}_4)_2\text{HPO}_4$, NaH_2PO_4 and LiH_2PO_4). The authors showed that the elimination of the filtration stage represents an effective solution to improve the charge content. They confirmed that the role of urea during phosphorylation that catalyses the reaction and also prevents cellulose degradation. In the absence of urea, the phosphorylation is achieved with low charge content. They also demonstrated that all the protons of cellulose are implicated and the phosphorylation reaction takes place in amorphous regions of the cellulose fibres.

Phosphorylation pre-treatment seems to be an attractive alternative to TEMPO oxidation, as it is non-toxic and easy to do. On the other hand, the grafting process must be controlled to prevent excessive cellulose depolymerisation (Rol et al., 2020).

I.4.5 Deep Eutectic Solvents DES

DES are considered as a green emerging pre-treatment for MFC production. They were first used as pre-treatment by Sirviö et al. (2015). The first system used for MFC production was choline chloride-urea (CC-U) mixture. Many DES systems were used and tested for cellulose production. DES is an interesting eco-friendly pre-treatment that allows producing good MFC but needs more further research to obtain grades that can compete with TEMPO oxidation, for example.

This pre-treatment will be discussed in detail in section 5. The subject of this thesis is to study cellulose pre-treatment and more specifically, the use of DES as pre-treatment media to produce MFC. Here we have briefly presented the use of some DES to produce MFC without going into details. DES properties, preparation, applications and their use for cellulose treatment, modification and microfibrillation will be detailed with more explanations to understand their interesting properties. DES pre-treatment will be compared to enzymatic hydrolysis which is selected as reference during this PhD project.

I.5 Focus on Deep Eutectic Solvents

The development of green chemistry is one of the promising solutions to deal with environmental problems. This chemistry is particularly based on the use of “green” solvents and reagents. In this context, ionic liquids (IL) have been widely studied. These systems are constituted of large organic cations and inorganic/organic anions (molecular ionic liquids). They exhibit specific properties including non-flammability, low vapor pressure, dissolving capacity, thermal and chemical stability and low melting point. Despite their advantages, ionic liquids are not all regarded as green solvents due to their low biodegradability and their environmental toxicity. In addition, the use of these solvents on an industrial scale is limited for economic reasons related in particular to their preparation and purification which are time consuming (Kudłak et al., 2015).

Deep Eutectic Solvents (DES) were proposed by Abbott et al. (2001) as an alternative to ionic liquids. DES and IL share some similarities such as low volatility, high tunability and capacity of dissolving organic and inorganic compounds. However, they are distinguished in the method of their preparation and the starting materials. DES exhibit more advantages than IL, including low or non-toxicity, easy preparation, the use of cheap and sustainable compounds. Moreover,

the components of DES must not react with each other, while for IL their synthesis requires many synthesis steps using various reagents and organic volatile solvents ((Płotka-Wasyłka et al., 2020).

For these reasons, DES are attracting more and more interest in the scientific community, and this is confirmed by the increasing number of publications in recent years as shown in Figure I. 17.

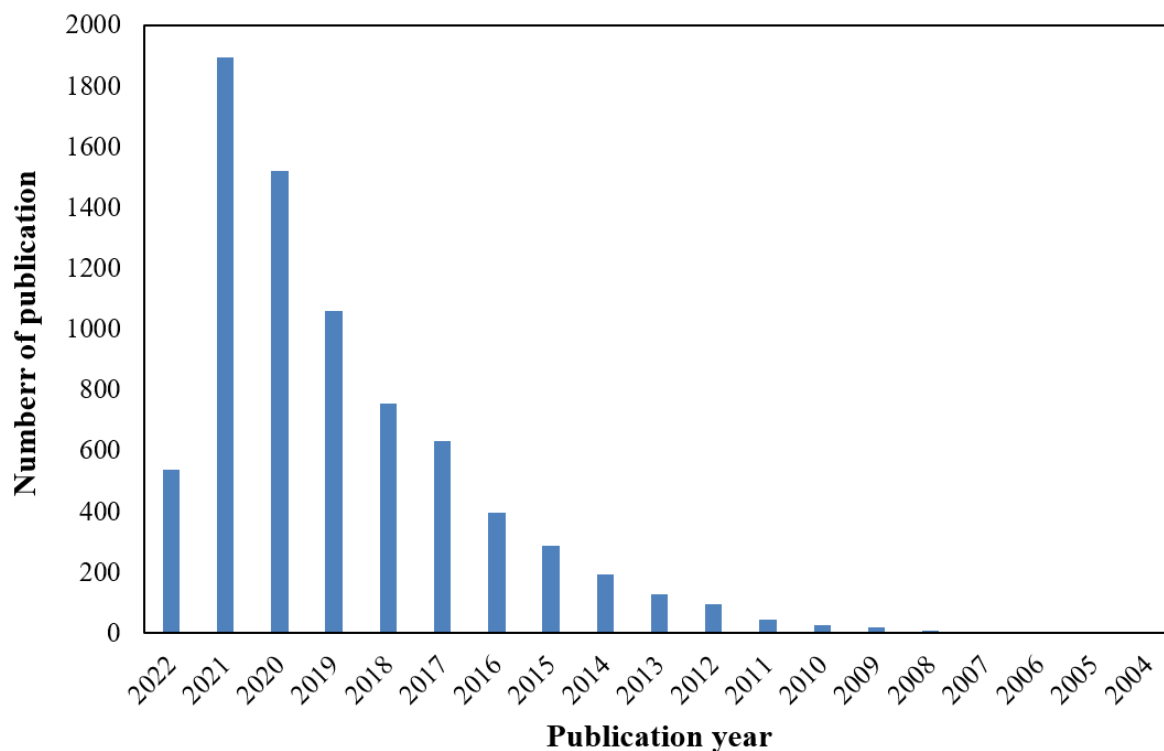


Figure I. 17. Evolution of the number of DES publication between 2004 and 2021 (extracted from Web of science, 17th May 2022).

DES are used in several fields as shown in Figure I. 18 due to their interesting properties. Among these fields, chemistry is the most important one which is confirmed by the high number of publications. These eutectic mixtures are used in organic synthesis (cycloaddition of Diels Alder in particular), extraction and separation of phenolic compounds (Ruesgas-Ramón et al., 2017). Similarly, they are used as selective solvents for some reactions such as the N-alkylation of aromatic primary amines, to avoid multiple N-alkylation.

Polymer science is also a potential field of application of DES (Tomé et al., 2018), especially for the preparation of polymers used in medicine (Liu et al., 2012) and industry (Lionetto et al., 2015). DES are chosen in this case as a simple, fast and green method that avoids the disadvantages of conventional organic solvents (toxicity, low yield, low solubilization capacity of polymers). Eutectic systems have been also studied in electrochemistry (Fernandes et al., 2012; Hosu et al., 2017) mainly in surface treatment to ensure the conductivity of polymer-based electrochemical material, or for the manufacture of functional additives, used as plasticizers for polymers (cellulose, starch ...).

Metals can also be treated by DES. In this case, DES replace the classical water-based electrolytes, which have disadvantages (special reactivity towards some metals, important evolution of the hydrogen bond under special industrial conditions). Eutectic mixtures allow the protection of metals against corrosion and also the preparation of metal-based films. For example, a CC-ethylene glycol mixture was used in the preparation of a Ni-Co film by electrodeposition (You et al., 2012). The manufactured films are characterised by high strength, good corrosion resistance, high value of electrical conductivity and good electro-catalytic activity.

DES are involved in nanomaterial science such as the synthesis of gold nanocrystals (Liao et al., 2008), the dispersion of nanoparticles and their morphological control to obtain the desired product. They are also used in the production of inorganic nanomaterials (calcium phosphate, hydroxyapatite ($\text{Ca}_{10}(\text{PO}_4)_6(\text{OH})_2$) and fluorapatite ($\text{Ca}_{10}(\text{PO}_4)_6\text{F}_2$) which are applied in medicine, dentistry, and orthopedics (Karimi et al., 2016; Mohammad Karimi et al., 2017). In addition, AlOmar et al. (2016) showed that DES can be utilised as a functionalising agent for nanoparticles. For example, carbon nanotubes can be functionalised by DES and then used in heavy metal adsorption in water treatment.

There are other applications of DES. For instance, in food analysis, the use of DES enhances the separation and extraction of inorganic metal and organic compounds (flavonoids, sugars, aromatic amines, etc.) contained in fruits, vegetables and spices (Chen et al., 2019).

Finally, DES can be applied in polysaccharides treatment as described in many reviews (Sattlewal et al., 2018; Zdanowicz et al., 2018). These treatments consist mainly in lignocellulosic biomass delignification, cellulose treatment (modification, microfibrillation, nanocrystals isolation...) or hemicellulose extraction.

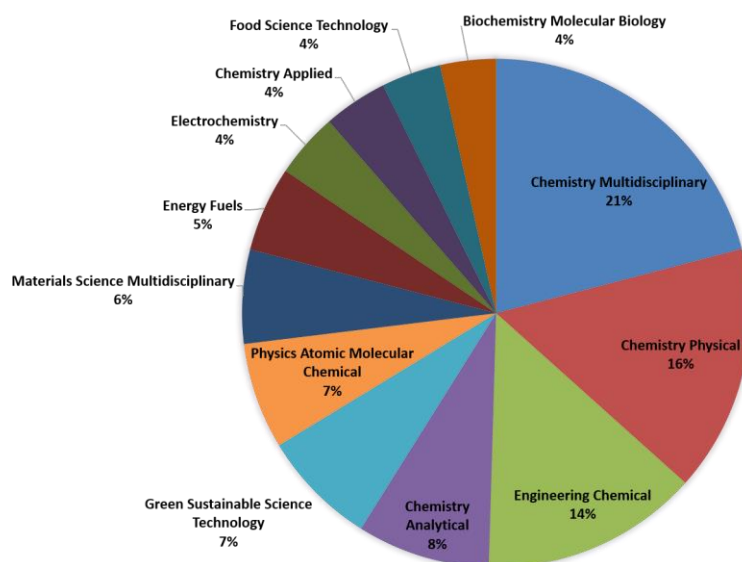


Figure I. 18. Number of DES publications by fields from 2001 to 2021 (extracted from Web of Science, 01 of November 2021).

In the following part, DES properties and their use for cellulosic biomass treatment will be discussed in detail.

I.5.1 DES preparation and classification

DES composed of a quaternary ammonium salt and a metal salt or hydrogen bond donor are the most studied systems. These systems (formed by salts components) are characterised by a low lattice energy which increases the system's stability that leads to charge delocalisation. The occurring charge delocalisation results in a reduction of the melting point of the mixture compared to the that of individual constituents (Smith et al., 2014).

The interaction between DES components has been studied (Zhang et al., 2012) and it was shown that this interaction is mainly based on hydrogen bonding interactions between the HBA and HBD as described in Figure I. 19. Also, some additional forces and van der Waals interactions may be a role. The hydrogen bonding interactions of three CC-based DES were studied by numerical simulation using molecular dynamics (Perkins et al., 2014). In this study, it was shown that hydrogen bonding mainly occurs between the HBD and the halide anion. Thus, the fundamental properties of DES are based on the anion-HBD hydrogen bond network.

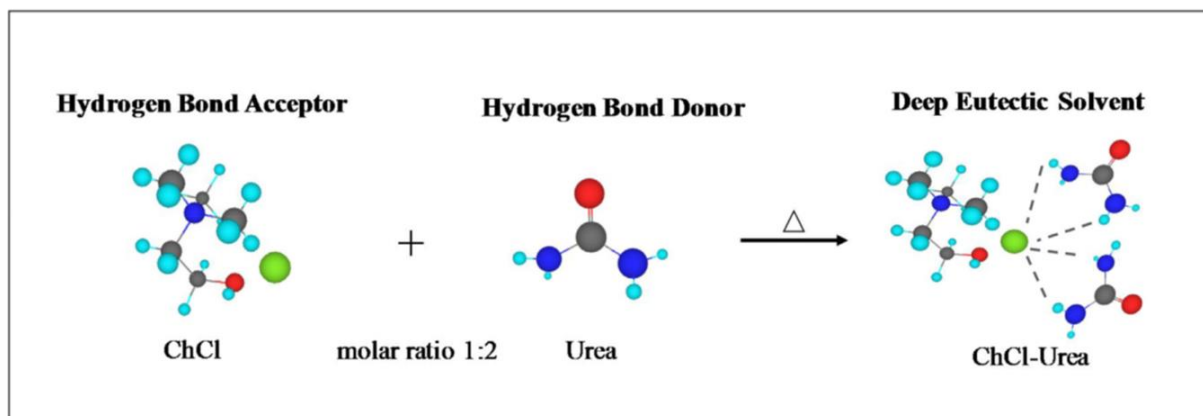


Figure I. 19. Interaction between choline Chloride (HBA) and urea (HBD) (Tomé et al., 2018).

DES are classified into four classes (Smith et al., 2014):

- (i) Mixture of organic and metal salts
- (ii) Mixture of organic salts and metal hydrates
- (iii) Combination of organic salts and hydrogen bonding compounds
- (iv) Combination of metal chlorides and hydrogen bond donor compounds

Many non-cationic DES have also been described in the literature. Therefore, a fifth class (type V) was subsequently proposed (Abranches et al., 2019; Moufawad et al., 2021; Schaeffer et al., 2020), corresponding to the mixture of non-ionic species (HBD, HBA).

Eutectic mixtures are easily prepared by mixing the constituents, while ensuring intimate contact between them. This contact is achieved by different methods, either by stirring (Zahrina et al., 2017), grinding (Florindo et al., 2014) or extrusion (Crawford et al., 2016). It is often necessary to couple mixing to heating, usually in the range of 50 to 100 °C but for, certain systems, more elevated temperatures are needed (Zahrina et al., 2017). For instance, the impact of two different techniques (grinding in a mortar at ambient temperature vs heating at 100 °C) was studied (Florindo et al., 2014), for systems composed of choline chloride (HBD) and several carboxylic acids (HBA). The results have shown that grinding is more efficient than conventional heating since it leads to obtain DES with high purity. Moreover, conventional heating could result in an ester formation between choline chloride and the carboxylic acids used.

I.5.2 DES physicochemical properties

DES are characterised by well-defined physicochemical properties (viscosity, thermal stability, polarity, biodegradability and toxicity) that depend on several factors, such as DES components, their molar ratio and the processing temperature.

Melting point

The eutectic point is the lowest melting point of the system and its related components as described in Figure I. 20. This melting temperature is lower than that of the individual constituents. For instance, the melting temperature of choline chloride-urea (CC-urea) mixture is 80 °C, while those of CC and urea are 302 and 133 °C, respectively. It was shown by Zhang et al. (2012) that there is a relation between melting point and DES components structures. DES composed of HBD with a lower molecular weight result in a greater reduction of the melting point. The significant decrease of the melting temperature can be explained by the interaction between the halide anion and the HBD component via hydrogen bonds that leads to a charge delocalisation (Zhang et al., 2012).

Furthermore, melting point can be decreased by the cation asymmetry due to its lower lattice energy. It can also be increased while increasing electron affinity of the anion, since it leads to a stronger hydrogen bond between DES components (Kovács et al., 2020).

It was shown by Abbott et al. (2004) that the principle behind obtaining a liquid from two solids (CC-urea) is based on the charge delocalisation that results in a liquid with a lower freezing point (12 °C for CC-urea system). The freezing point of the eutectic mixture depends on three parameters: (i) the lattice energies of the DES, (ii) the interaction between the anion-HBD and (iii) the entropy changes resulting from forming a liquid phase (Abbott et al., 2004).

To deeply understand the molecular interactions, thermodynamic changes and charge transfer in DES, three systems (CC-urea, CC-ethylene glycol and CC-malonic acid) were studied (Wagle et al., 2016). Different types of H-bonds (C-H...O and C-H... π) and conventional O-H...Cl or N-H...Cl interactions that contribute to DES stabilisation were characterised. The charge decomposition analysis indicated that the charge is mostly transferred from chloride (Cl⁻) and choline to HBD. It was also shown that the physical properties of DES such as their freezing temperatures can be affected by the choice of the HBD.

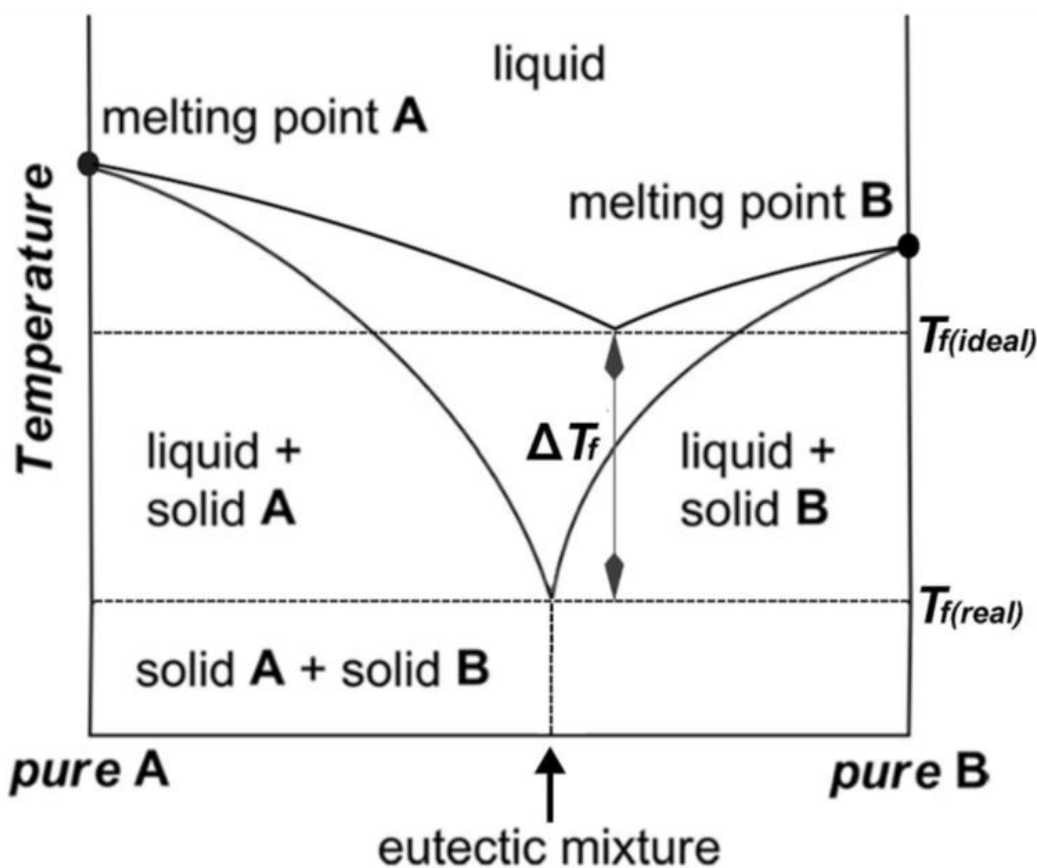


Figure I. 20. Phase diagram of two component mixture representing the eutectic point (Kalhor and Ghandi, 2019)

Surface tension

Surface tension is one of the interfacial properties that allows evaluating cohesive forces between the liquid molecules. Surface tension can be influenced by liquid composition, temperature and salt mole fraction (Mjalli et al., 2014).

For DES, this property depends strongly on the intermolecular force strength occurring between the HBD and the corresponding HBA or salt. Studies related to DES surface tension are still scarce but some systems have been studied (Abbott et al., 2004). The obtained values of surface tension are greater than those of most molecular solvents and similar to those of imidazolium-based ionic liquids and molten salts. They depend on the cation type and alkyl chain length. Cation containing hydroxyl groups provides higher surface tension thanks to their ability of creating hydrogen bonding (García et al., 2015).

Temperature and salt molar ratio effects were studied by Mjalli et al. (2014). It was shown that higher temperatures, by increasing internal energy of the liquid molecules, reduce cohesion forces between molecules because of the molecular vibrations. Oppositely, high salt contents HBA and lower HBD content leads to greater surface tension which is evident in all tested DES.

Density

Density is a very crucial physical property for a solvent that allows identifying the nature of substances. The density of DES can be measured through a specific gravimeter. From the literature, it appears that most of DES exhibit higher density than water (Dai et al., 2013; Zhang et al., 2012).

Many scientific researches have focused on the study of DES density (Dai et al., 2013; Mjalli et al., 2014; Shahbaz et al., 2012; Zhekenov et al., 2017). Mjalli et al. (2014) studied the densities of three DES and their evolution with temperature and DES molar ratio. Density decreases with temperature due to the increase of DES molecules mobility that results in the increase of the thermal expansion of the DES volume. Increasing the molar ratio of DES (HBA/HBD) as well allows reducing the density. Densities of DES type IV (ZnCl_2 -Urea and ZnCl_2 -acetamide) were also studied and the results showed that they are greater than those of the pure components.

It is worth noting that high densities, which might be explained by the decrease of the average hole radius, subsequently reduces the mass transport properties (Abbott et al., 2007).

Viscosity

Viscosity is an important property that needs to be studied for industrial purposes. It was shown that most DES exhibit high viscosities at ambient temperature. It is explained by the presence of the strong interactions between the DES components, that lead to a reduced mobility of free species in the DES. Many parameters can cause the increase of the DES viscosity, especially the large ion size and the small void volume of most DES, as well as electrostatic forces or van der Waals interactions (Zhang et al., 2012).

The viscosity depends mainly on the composition of the DES. For example, DES containing glycerol, phenol or levulinic acid have the lowest viscosities (García et al., 2015), whereas those based on mixtures of choline chloride and sugars or carboxylic acids have the highest viscosities

(Florindo et al., 2014). Table I. 2 presents the viscosity of the most studied DES at different temperatures. It should be noted that CC-based DES viscosity is strongly related to HBD nature.

As expected, viscosity is influenced by temperature and DES with high viscosity must be used at high temperatures. It can be also influenced by the presence of moisture or impurities.

Viscosity is the most crucial factor for the treatment of polysaccharides especially when DES is used as a solvent. This importance is explained by the need to facilitate interactions between the polysaccharide, DES and the reagents present in the reaction medium (in the case of a chemical reaction).

Table I. 2. Viscosity of some DES at different temperatures

Organic salts (HBA)	HBD	Salt: HBD molar ratio	Viscosity (cP)	References
CC	Urea	1:2	750 (25 °C)	(D'Agostino et al., 2011)
CC	Urea	1:2	169 (40 °C)	(Abbott et al., 2006a)
CC	Ethylene glycol	1:2	36 (20 °C)	(Abbott et al., 2007)
CC	Ethylene glycol	1:2	37 (25 °C)	(D'Agostino et al., 2011)
CC	Ethylene glycol	1:3	19 (20 °C)	(Abbott et al., 2007)
CC	Ethylene glycol	1:4	19 (20 °C)	
CC	Glycerol	1:2	376 (20 °C)	(D'Agostino et al., 2011)
CC	Glycerol	1:2	259 (25 °C)	(Abbott et al., 2007)
CC	Glycerol	1:3	450 (20 °C)	
CC	Glycerol	1:4	503 (20 °C)	
CC	Imidazole	3:7	15 (70 °C)	(Hou et al., 2008)
CC	ZnCl ₂	1:2	85000 (25 °C)	(Abbott et al., 2006)
CC	Xylitol	1:1	5230 (30 °C)	

Organic salts (HBA)	HBD	Salt: HBD molar ratio	Viscosity (cP)	References
CC	Sorbitol	1:1	12730 (30 °C)	(Maugeri and Domínguez de María, 2012)
CC	Malonic Acid	1:2	1124 (25 °C)	(D'Agostino et al., 2011)
ZnCl ₂	Urea	1:3.5	11340 (25 °C)	(Abbott et al., 2007)
K ₂ CO ₃	Glycerol	1:4	25.000(25 °C)	(Lim et al., 2019)
K ₂ CO ₃	Glycerol	1:5	17.613 (25 °C)	
K ₂ CO ₃	Glycerol	1:6	7838 (25 °C)	
K ₂ CO ₃	Glycerol	1:7	6638 (25 °C)	

Thermal stability

The thermal stability of DES depends on their composition, the molar ratio between the constituents and the maximum processing time for some DES. For instance, eutectic systems containing imidazole are the less stable. The presence of urea also decreases DES thermal stability. Indeed, a study was carried out on the thermal stability of urea-based DES in the presence of mono-polyalcohols or carbohydrates (Simeonov and Afonso, 2016). This study showed that after 7 hours of heating at 80 °C, there were carbonate and ammonia emissions resulting from DES decomposition.

Thermal stability is also a very important property for the treatment of polysaccharides (dissolution, extraction, modification, etc.) when it is necessary to work at high temperature. The study of thermal stability allows to set the appropriate conditions for the use of DES.

DES recycling

DES recycling is a fundamental issue for industrial applications such as biomass processing. It was shown that DES are more readily recyclable than ionic liquids due to their simple preparation/regeneration which involves the formation of hydrogen bonding interactions between HBD and HBA (Xu et al., 2017).

The recycling and reusability of some DES used for biomass delignification has been already studied (Kim et al., 2018). Recycling was achieved using an easy and simple approach based on the separation of residual lignin from DES after its use for the treatment of the biomass. Evaporating water and ethanol used during the process allows recovering 95% of the DES after each cycle. The reusability tests have shown that the glucose yield is slightly decreased with increasing the number of DES recycling. This decrease can be explained by the increasing presence of impurities in the DES after each recycle (Kim et al., 2018). Li et al. (2018) used a recyclable DES composed from aminoguanidine hydrochloride and glycerol as a solvent and reagent for cationic MFC production. After five recycling steps, no decrease in the efficiency of the reaction was observed. The clear liquid appearance of the DES was maintained, while it changed to yellow colour. Here again, it can be explained by the presence of more impurities in the DES after each cycle. It was also shown that the recovery yield of DES was slightly decreased after several recycles (Li et al., 2018).

Recycled DES (3 times at least) was also used to produce cellulose nanocrystals CNC while maintaining its performance (Wang et al., 2020). In this study, DES was used as catalyst and solvent which constitutes a green (no hazardous waste was produced) and economical process due the high recyclability of DES (85%). The ability of initial DES and that the last recycled DES to dissolve amorphous cellulose were different: the dissolution of cellulose decreased after DES recycling. In the same way, the viscosity of recycled DES slightly decreased compared than that of initial DES which is probably due to the presence of residual humidity.

I.5.3 Lignocellulosic biomass treatment: selective extraction of lignin and hemicelluloses

In this context, DES can be used for the partial removal of lignin or hemicelluloses. The use of DES promotes the hydrolysis of the lignin-carbohydrates complex linkage by breaking the interactions between lignin and carbohydrates and creating new hydrogen bonds between chloride ions of the DES and hydroxyl groups of lignin and carbohydrates (Satlewal et al., 2018). Many DES were applied for lignocellulosic biomass treatment as depicted in Table I. 3. These DES must have a selective solubilisation capacity which depends on the biomass origin. The lignin removal from lignocellulosic biomass using DES was studied on wood and plant fibres. For wood, three mixtures of CC-based DES and alanine-lactic acid were studied for the delignification of hardwood kraft pulp (Majová et al., 2017). The highest lignin extraction rate

(43%) was obtained for the alanine-lactic acid mixture. In addition, aqueous DES solutions (at 50% water content) were used to delignify wood (*eucalyptus globulus* Labill) under mild conditions using different mixtures: propionic acid-urea, CC-lactic acid and CC-p-toluenesulfonic acid with mineral or organic acids (Soares et al., 2021). The results demonstrated that 80 wt % of the lignin can be extracted from wood. Moreover, about 40 wt % of the starting lignin can be recuperated from DES liquor.

In the case of lignin removal from plant fibres, several mixtures were investigated. For instance, CC-lactic acid, betaine-lactic acid mixtures and amino acid-based DES (lactic acid-proline, maleic acid-proline, maleic acid-glycine) were used to delignify wheat straw (Francisco et al., 2012). The results showed that these DES are effective for lignin solubilisation and have a negligible ability to solubilise cellulose, which makes it possible to have a selective action on the biomass. Using the same biomass, Zhao et al. (2018) studied the effectiveness of some DES (strongly and weakly basic DES) for the delignification. The strongly alkaline DES (CC-monoethanolamine CC-M) has a better performance on wheat straw pre-treatment than the weakly alkaline DES (CC-glycerol and CC-urea) and enhances the lignin removal (71.4%). On rice straw biomass, the mixture of CC-urea was tested, but this mixture did not allow an efficient lignin extraction and the crystallinity of the cellulose was reduced (Nor et al., 2015). In addition, switch grass was treated with DES containing lignin-derived phenols as HBD and choline chloride as HBA (Kim et al., 2018). These systems (CC-4-hydroxybenzyl alcohol, CC-catechol, CC-vanillin and CC-p-coumaric acid) were used for delignification and the results showed their effectiveness: the highest delignification of 60.8% was given by CC-p-coumaric acid followed by CC-vanillin (52.5%) and CC-catechol (49%).

Regarding hemicelluloses removal, it was studied on both wood and plant fibres. For wood (pine pulp), CC-urea system was tested (Tenhunen et al., 2018). The authors shown, that the morphological surface of the fibres remained almost the same after DES treatment. The chemical composition of the fibres changed slightly: DES did not allow the dissolution of glucose and galactose but led to the dissolution of a small amount of xylose, mannose and arabinose. In the case of plant fibres, for instance rice straw was treated by strongly acidic DES such as CC or lactic acid-based DES (Hou et al., 2018). They showed that the use of strongly acidic DES allows to hydrolyse 95.8% of hemicelluloses within 3 h at 120 °C. It was demonstrated in the same study that in the case of polyol-based DES, the xylan removal reduced when increasing the hydrophilicity of HBD. The use of HBD with more hydroxyl or amino

groups has negatively influenced the pre-treatment, whereas HBD containing strong electron-withdrawing groups improved the efficiency of this pre-treatment.

The correlation between the xylan elimination and DES properties was determined. It was shown that there is a negative correlation between the removal of xylan with the pKa values of HBD.

Table I. 3. Examples of used DES for the treatment of lignocellulosic biomass.

Biomass	Role of DES	DES	DES molar ratio	References
Hardwood	Delignification	CC-malic acid	1:2	(Majová et al., 2017; Škulcová et al., 2016)
		CC-oxalic acid (dihydrate)	1:1	
		CC-lactic acid	1:9	
		Alanine-lactic acid	1:9	
		Propionic acid-urea	2:1	(Soares et al., 2021)
		CC-urea	1:2	
		CC-lactic acid	1:10	
		CC- <i>p</i> -toluene sulfonic acid	1:1	
Wheat straw	Delignification	Lactic acid-urea	10:1	(Francisco et al., 2012)
		Lactic acid-betaine	2:1	
		Malic acid-proline	1:3	
		CC-urea	1:1	(Liu et al., 2017)
		CC/malic acid		
		CC-lactic acid		
		CC-oxalic acid (dihydrate)		
		CC-monoethanolamine	1:6	(Zhao et al., 2018)
		CC-N-methyldiethanolamine	1:10	
		CC-diethanolamine	1:8	
CC-urea	1:2			
CC-glycerol	1:2			
Rice straw	Pre-treatment	CC-urea	1:1	(Nor et al., 2015)

Biomass	Role of DES	DES	DES molar ratio	References
		CC-lactic acid	1:5	(Kumar et al., 2016)
		CC or lactic acid Based DES	1:1	(Hou et al., 2018)
Switch grass	Delignification	CC-hydroxybenzyl alcohol	1:1	(Kim et al., 2018)
		CC-catechol	1:1	
		CC-vanillin	1:2	
		CC-p-coumaric acid	1:1	
Date palm	Pre-treatment	CC-glycerol	1:2	(Fang et al., 2017)
			1:3	
			1:6	
Oil palm	Pre-treatment	CC-glycerol CC-ethylene glycol Ethyl ammonium chlorite-glycerol	1:2	(Abdulmalek et al., 2017)
Corn straw	Pre-treatment	CC-urea	1:2	(Xu et al., 2016)
		CC-glycerol	1:2	
		CC-formic acid	1:2	
		CC-acetic acid	1:2	
		CC-oxalic acid	1:1	
		CC-malonic acid	1:1	
		CC-citric acid	1:1	
Corn cob residues	Pre-treatment	CC-glycerol	1:2	(Procentese et al., 2015)
		CC-urea	1:2	
		CC-imidazole	3:7	
Corn cob biomass	Delignification	CC with different monocarboxylic, dicarboxylic acids or polyalcohol	Different Molar ratio	(Zhang et al., 2016)
Pine pulp	Pre-treatment	CC-urea	1:2	(Tenhunen et al., 2018)

CC: choline chloride

I.5.4 Cellulose treatment

In this part, the use of DES for cellulose treatment in terms of dissolution, chemical modification or nanocrystals production is also discussed.

The dissolution of cellulose consists in breaking the inter- and intramolecular hydrogen bonds. According to the literature, several ionic liquids are able to solubilise cellulose (María, 2014; Zhang et al., 2017). However, the industrialisation of ionic liquids presents several problems as mentioned above and the use of DES may be an alternative. Many of the used DES for cellulose treatment are listed in Table I. 4 and most of them are based on choline chloride combined with the following compounds: oxalic acid, phenylacetic acid, malonic acid, glycerine, acetamide and formamide.

In this context, Ren et al. (2016a) tested several CC-based systems (CC with one of these donor groups: urea, ammonium thiocyanate, caprolactam and acetamide). To improve cellulose solubility, they activated it with a saturated solution of calcium chlorite using ultrasound which aimed at ensuring the penetration of the DES into the cell wall. From these systems, it was found that CC-urea mixture solubilises 1.43 wt % of cellulose. Then, they replaced urea with imidazole to enhance the solubility which increased to 2.48 wt %. They further improved the solubility (4.57 wt %) by using 5% polyethylene glycol as a co-solvent. The better efficiency of the CC-imidazole mixture compared to the CC-urea mixture for cellulose dissolution can be explained by the basicity of the hydrogen bond and also by the polarity/polarizability effect of the used system.

Another study by Ren et al. (2016b) showed that the solubilisation of cellulose can be improved by using DES with one of the components based on an allyl function. In this case, they synthesised the allyltrimethylammonium chloride-oxalic acid (1:1) system. The solubility of the cellulose increased to 6.48 wt %. However, for the CC-oxalic acid (1:1) mixture, it is less than 1%. This can be explained by the effect of the hydroxyl group of choline chloride which leads to a low dissolution capacity. In conclusion, the solubility of cellulose can be enhanced by using choline derivatives with hydrophobic groups. In these studies, dissolution was monitored by optical microscopy and the structure of the fibres was studied by scanning electron microscopy (SEM). During dissolution, the fibres were swollen and their length was gradually decreased over time which is due to the breaking of hydrogen bonds. The structure of the cellulose fibre changed during dissolution. SEM images showed that the original fibre

structure was organised and condensed. However, after dissolution it becomes more disorganised resulting in more accessible surface to treatments.

Another study was conducted by Malaeke et al. (2018) to compare CC-based DES and the maximum solubility (6.10 wt %) was given by the CC-resorcinol system (1:1).

Until now, all the used DES does not allow a significant solubilisation of cellulose. To improve the dissolution, the hydrogen bond acceptor capacity of DES must be increased (Chen et al., 2019). It is important to classify DES from this point of view. For this purpose, the Kamlet-Abboud-Taft parameter (KAT) can be useful. This classification makes it possible to distinguish DES according to three parameters (i) the acidity of the hydrogen bond (ii) the basicity of the hydrogen bond (iii) the polarity/polarizability properties (π^*) (Eyckens et al., 2016). Indeed, the higher the hydrogen bonding basicity of DES, the more the inter- and intramolecular bonds of the cellulose are weakened while creating hydrogen bonds with the DES components. To simplify, DES containing anions such as Cl^- , OAc^- , HCOO^- , $(\text{MeO}_2)\text{PO}_2^-$ are more effective in dissolving cellulose and in particular imidazole and morphine (Chen et al., 2019).

Recently, Sharma et al. (2021) proposed new DES systems consisting of solid zwitterions and saccharides. The zwitterions were selected as quaternary ammonium salts and the saccharides including glucose, fructose, sucrose, cellobiose were used as hydrogen bond donors HBD. Zwitterion-based DES were prepared by mixing the zwitterions with the HBD at different ratios. Cellulose was gradually added to the DES mixture and heated at 120 °C for 10 min. This procedure was repeated until no more cellulose was soluble. They demonstrated that two DES mixtures among twenty-two combinations of zwitterion/saccharide mixtures have successfully dissolved 10 and 15 wt % of cellulose.

The dissolution of cellulose in DES remains low compared to IL or conventional solvents used for cellulose dissolution. This can be explained by the presence of significant hydrogen bonds in the cellulose structure. Further research is needed to improve the dissolution of cellulose in DES.

Table I. 4. Some DES used for cellulose dissolution (Chen et al., 2019)

Biomass	DES	Molar ratio	Method	Cellulose solubility (wt %)	References
Microcrystalline cellulose AVICEL PH 105	CC-urea	1:2	Treatment at 110 °C	< 0.2	(Zhang et al., 2012)
	CC-ZnCl ₂	1:2		< 0.2	
	Betaine Hydrochloride-urea	1:4	Treatment at 100 °C for 10 h	2.5	(Sharma et al., 2013)
Cellulose (90%, mass fraction purity)	Maleic acid-alanine	1:1	Treatment at 100 °C	0.11	(Francisco et al., 2012)
	Maleic acid-glycine	1:1		0.14	
	Maleic acid-proline	1:2		0.24	
	Oxalic acid dihydrate-histidine	9:1	Treatment at 60 °C	0.25	
	Maleic acid-proline	1:3	Treatment at 100 °C	0.78	
Cotton-ramie pulp (DP = 517)	Acetamide-urea	2:1	Treatment at 50 °C	1.03	(Zhou and Liu, 2014)
	Caprolactam-urea	3:1		2.83	
Cotton linter pulp (DP = 576)	CC-caprolactam	1:1	Activating cellulose by ultrasound-assisted saturated CaCl ₂ solution prior dissolution; treatment at 120 °C	0.16	(Ren et al., 2016a)
	CC-acetamide	1:2		0.22	
	CC-ammonium thiocyanate	1:1		0.85	
	CC-urea	1:2		1.43	
	CC-imidazole	3:7		2.48	
	Triethyl-allyl ammonia-oxalic acid	1:1	Heating at 110 °C	6.48	(Ren et al., 2016b)
	CC-maleic acid	1:1		2.57	

Biomass	DES	Molar ratio	Method	Cellulose solubility (wt %)	References
Cellulose (98% mass fraction purity)	CC-a-naphthol	1:1	Ultrasonicati on (20 Hz) à 90 °C	3.39	(Malaeke et al., 2018)
	CC-phenol	2:1		4.70	
	CC-resorcinol	1:1		6.10	
Avicel pH 101	Polar zwitterion/saccharide-based DES	-	Treatment at 120 °C for 10 min	10 and 15	(Sharma et al., 2021)

In the context of cellulose modification using DES, several systems were used as shown in Table I. 5. For instance, the eutectic mixture CC-ZnCl₂ (1:2) was used as a solvent for the O-acetylation reaction of cellulose (Abbott et al., 2005).

Cellulose cationisation was performed using the mixture of chlorocholine chloride-urea (1:2). The product of this reaction exhibits antibacterial activity and antimicrobial activity against *E. coli* and *B. subtilis* (Wibowo and Lee, 2010).

Afterwards, the dimethylurea-ZnCl₂ system in the presence of dimethyl carbonate yields cellulose methyl carbamate (DS = 0.16). During this reaction, a significant decrease in the degree of polymerisation DP occurs (Sirviö and Heiskanen, 2017). In the same context, Willberg-Keyriläinen et al. (2018) tested three DES for a carbamation reaction: CC-urea, betaine-urea and betaine hydrochloride-urea. The highest derivatisation rate was obtained with the urea-betaine system, where the degree of crystallinity decreased by 20% after the modification.

In the case of nanocrystals production, the CC-oxalic acid dihydrate mixture is the most efficient system (Douard et al., 2021; Sirviö et al., 2016). This mixture allowed the production of cellulose nanocrystals (CNC). The produced CNC exhibited uniform morphology (diameter between 3-25 nm and length between 100-350 nm), high degree of crystallinity (82%) and good thermal stability (> 320 °C) (Liu et al., 2017).

Table I. 5. Some DES used for cellulose treatment (modification and NCC production)

Objectives	Used material	DES	Molar ratio	References
O-acetylation	Microcrystalline cellulose	CC-ZnCl ₂	1:2	(Abbott et al., 2005)
Cationisation	Cotton fibres	Chlorocholine chloride-urea	1:2	(Wibowo and Lee, 2010)
		CC-urea	1:2	(Mehdi Karimi et al., 2017)
Preparation of cellulose methyl carbamate	Bleached softwood kraft pulp	Dimethyl urea-ZnCl ₂	10:3	(Sirviö and Heiskanen, 2017)
Cellulose carbamation	Dissolving hardwood pulp	CC-Betaine CC-Betaine HCl CC-urea	1:2; 1:4	(Willberg-Keyriläinen et al., 2018)
NCC production	Cotton fibres	CC-oxalic acid	1:1	(Liu et al., 2017; Douard et al., 2021)
	Pâte Kraft blanchie de résineux	CC-oxalic acid (anhydrous)	1:2	(Laitinen et al., 2017; Sirviö et al., 2016)
		CC-oxalic acid (dihydrate)	1:1	
		CC-p-toluene sulfonic acid	1:1	
Monohydrate CC-levulinic acid	1:2			
	Recycled fibres	CC-urea	1:2	(Laitinen et al., 2017)

I.5.5 Cellulose microfibrillation using DES

There is very little published data regarding the production of microfibrillated cellulose by DES and the available publications are listed in Table I. 6. These systems have the capacity to swell the fibres and thus break the hydrogen bonds between the cellulose chains but without degrading the polysaccharides. DES can be used as pre-treatment for direct microfibrillation with or without in situ modification. They can be also applied in the direct pre-treatment of

some raw biomasses in order to eliminate the bleaching and delignification steps required before the microfibrillation. In addition, some DES can be implicated in the production of lignin cellulose microfibrils (LCMF).

In the case of cellulose pre-treatment without in situ modification, CC-urea mixture is the most well-known for biomass treatment and it was therefore the first DES tested for microfibrillation (Laitinen et al., 2017; Sirviö et al., 2015). During this treatment, cellulosic fibres were treated with the mixture of CC-urea (molar ratio 1:2) at 100 °C for 2 h. The crystallinity and degree of polymerisation of treated fibres remained unchanged. Then, produced MFC by microfluidisation were characterised by a length between 5 and 20 nm for individual MFC, and between 15 and 200 nm for aggregates or bundles of MFC. During DES pre-treatment, the fibres were swollen. This swelling facilitates the microfibrillation during the subsequent mechanical processing (Sirviö et al., 2015). Using the same DES (CC-urea), MFC were successfully obtained from waste board and paper after DES treatment at 100 °C for 2 h (Suopajarvi et al., 2017).

Another study on microfibrillation showed that urea ammonium thiocyanate or guanidine hydrochloride-based DES can be used for wood pre-treatment (Li et al., 2017). Cellulose microfibrils with widths between 13 and 19.3 nm were produced by microfluidisation. Moreover, films made from MFC suspensions exhibited good thermal and mechanical properties (Young's modulus between 6.4 and 7.7 GPa). The mixture of choline chloride and imidazole was also demonstrated as an efficient system for cellulose microfibrillation (Sirviö et al., 2020). This mixture was used at two different temperatures (60 and 100 °C) for different treatment times (15 min, 2 h and 3 h). DES-treated fibres were analysed and the results indicated that the fibres were swollen, while there is a negligible decrease of the DP. The disintegration of DES-treated fibres results in microfibrils with very good mechanical properties and good oxygen barrier properties. Afterwards, ternary acidic DES (CC-oxalic acid- $\text{AlCl}_3 \cdot 6\text{H}_2\text{O}$ and CC-lactic acid- $\text{AlCl}_3 \cdot 6\text{H}_2\text{O}$) were used for the pre-treatment of sugarcane bagasse (Ji et al., 2021). These systems showed their effectiveness in the cleavage of strong hydrogen bonds in the sugarcane bagasse which facilitates their subsequent microfibrillation.

Cellulose pre-treatment with simultaneous modification was studied. Esterification reaction can be carried out in the presence of DES to produce esterified MFC. Liu et al. (2021) used some carboxylic acid-based DES to pretreat and esterify cellulose at the same time. They showed that

the combination of DES pre-treatment with mechanical treatment results in MFC having widths less than 100 nm. The obtained MFC were used for composites (polylactic acid) reinforcement. Thus, the presence of carboxylic groups in the MFC enhances their dispersity in the polylactic acid matrix, resulting in higher mechanical strength of produced composite. DES treatment provides efficient conversion from wood pulp to MFC with high-added value.

Moreover, cellulose microfibrillation with simultaneous sulfation can be achieved using the mixture of sulfamic acid-glycerol (Li et al., 2021). This DES allows to swell cellulose fibres and promote the sulfation with good degree of substitution ($DS = 0.12$). This pre-treatment enhances the microfibrillation process with reduced energy consumption. The disintegration of DES treated cellulose fibres resulted in MFC having diameters from 10 to 25 nm. It was also demonstrated that initial cellulose allomorph was maintained after DES pre-treatment, while the crystallinity was reduced. Produced MFC were mixed with polyvinyl alcohol to prepare composite films. The obtained composite film displayed good UV resistance ability and mechanical properties.

Cellulose cationisation can be also achieved during DES treatment (Sirviö, 2018). In this study, a mixture of triethylmethylammonium chloride and imidazole was utilised as solvent for cellulose fibres cationization using betaine hydrochloride in the presence of p-Toluenesulfonyl chloride. The reaction was conducted for 4 h at 80 °C and cationised cellulose with cationic charge up to 1.95 mmol/g was produced. The same reaction was performed on softwood dissolving pulp and results in cationic LCMF with high lignin content. Cationised cellulose fibres were mechanically disintegrated using a microfluidiser. Produced cationic MFC and LCMF were individualised with a diameter of 4.7 nm and 3.6 nm respectively, while some larger aggregates were also observed.

In the context of raw biomass direct pre-treatment, the mixture of choline chloride-oxalic acid dihydrate was investigated for the direct pre-treatment of raw ramie fibres for 4 h at 100 °C without further bleaching/purification steps (Yu et al., 2021). Microfibrillation was then performed by ball milling at 1100 rpm for 6 h. The produced microfibrils were characterised by a high purity in glucan (up to 90.31%), high crystallinity (79.2%) and good thermal stability. In addition, Suopajarvi et al. (2020) used some acidic DES including the mixture of choline chloride with lactic acid, levulinic acid, malic acid or glutaric acid, and alkaline DES such as K_2CO_3 -glycerol for both delignification and microfibrillation of agricultural by-products from

wheat straw, corn stalk and rapeseed stem. The pre-treatment was conducted at 100 °C (during 8 or 16 h) or 80 °C for 24 h. All the samples were microfibrillated and their properties were measured. The results indicated that choline chloride-lactic acid and K₂CO₃-glycerol allowed obtaining the highest delignification yields, MFC crystallinity index and viscosity. However, alkaline DES treatment results in nanopapers with better mechanical properties compared to acidic DES. Therefore, these DES are able to delignify and pre-treat in one step the lignocellulosic biomass, which consists a benefit to reduce the steps required for cellulose microfibrillation.

The production of LCMF was carried out using some DES. For instance, the mixture of CC-lactic acid was used to prepare LCMF using microwave assisted DES pre-treatment in combination with ultrasonication (Liu et al., 2020). This results in LCMF with high entanglement network due to the presence of lignin between the microfibrils. These LCMF were used for the reinforcement of UV-absorbing polymer (polyanionic cellulose). Another study (Kwon et al., 2021), investigated the use of choline chloride based-DES (CC with lactic acid, urea or glycerine) for the production of LCMF. The treatment was performed at 140 °C for 6 h and then treated fibres were disintegrated using a high-speed blender and homogeniser. This treatment resulted in LCMF having diameter less than 10 nm. The mixture of CC-lactic acid showed less capacity of microfibrillation, while CC-urea and CC-glycerol allowed efficient microfibrillation.

Table I. 6. Some DES used for cellulose microfibrillation

Objectives	Biomass	DES	Molar ratio	Treatment conditions	References
Microfibrillation	Bleached birch kraft pulp	CC-urea	1:2	t: 2 h T: 100 °C	(Sirviö et al., 2015)
	Waste board	CC-urea	1:2		(Suopajarvi et al., 2017)
	Milk container board				
	bleached birch kraft paper	Ammonium thiocyanate-urea	1:2 1:2	t: 2 h T: 100 °C	(Li et al., 2017)

Objectives	Biomass	DES	Molar ratio	Treatment conditions	References
		Guanidine hydrochloride-urea			
	Poplar wood kraft pulp	CC-oxalic acid dihydrate	1:1	t: 1 h T: 80 °C	(Ma et al., 2019)
	Hardwood kraft pulp	CC-imidazole	3:7	t: 15 min T: 60 °C or 100 °C	(Sirviö et al., 2020)
t: 2 h T: 100 °C					
t: 3 h T: 60 or 100 °C					
	Birch cellulose	Betaine hydrochloride-glycerol	1:2 1:3 1:6 2:3	t: 30 min or 1 h T: 130, 140, or 150 °C	(Hong et al., 2020)
	Sugarcane bagasse	CC-oxalic acid- $\text{AlCl}_3 \cdot 6\text{H}_2\text{O}$ CC-lactic acid- $\text{AlCl}_3 \cdot 6\text{H}_2\text{O}$	1:1:0.2	t: 20 min T: 100 °C	(Ji et al., 2021)
Microfibrillation with simultaneous esterification	Hardwood bleached kraft pulp	CC-formic acid CC-lactic acid CC-acetic acid CC-malonic acid CC-oxalic acid CC-citric acid	1:2 1:9 1:2 1:1 1:1 1:1	t: 3 h T: 50-100 °C	(Liu et al., 2021)
Microfibrillation with simultaneous sulfation	Bleached kraft pulp board	Sulfamic acid-glycerol	1:3	t: 1-1.5 h T: 100 °C	(Li et al., 2021)
	Unbleached spruce	Triethylmethylammonium	1:2	t: 4 h	(Sirviö, 2018)

Objectives	Biomass	DES	Molar ratio	Treatment conditions	References
Production of cationic MFC/LCMF	Softwood dissolving pulp	chloride-imidazole		T: 80 °C	
	Moso bamboo	CC-lactic acid	1:9	t: 2 or 4 h T: 100 or 120 °C	(Liu et al., 2019)
	Soft wood dissolving cellulose pulp	CC-lactic acid CC-levulinic acid	1:2; 1:5 1:2	t: 8, 16 or 24 h T: 80 or 100 °C	(Suopajarvi et al., 2020)
	Wheat straw	CC-malic acid	1:1		
	Rapeseed stem residues	CC-glutaric acid K ₂ CO ₃ -glycerol	1:1 1:5		
	Raw ramie fibres	CC-oxalic acid dihydrate	1:1	t: 4 h T: 100 °C	(Yu et al., 2021)
Production of lignocellulose nanofibrils (LCMF)	Energy cane bagasse	CC-lactic acid	1:8	t: 30 min T: 90, 110, 130 or 150 °C	(Liu et al., 2020)
	Mongolian oak	CC-urea CC-lactic acid CC-glycerol	1:2; 1:6	t: 6 h T: 140 °C	(Kwon et al., 2021)

As discussed in this section, the results obtained with DES pre-treatment are interesting and promising. DES are designer solvents; their properties can be adjusted depending on the purpose of use. Their unique properties and green character make them a good candidate for use as a pre-treatment. DES pre-treatment needs further research to deeply understand their effects on cellulose structure.

During this project, three DES systems at different pH (acidic, neutral and alkaline) were selected as pre-treatment media to promote microfibrillated cellulose production. These DES are respectively, betaine hydrochloride-urea (BHCl-U), choline chloride-urea (CC-U) and

choline chloride-monoethanolamine (CC-M). To the best of our knowledge, BHCl-U and CC-M were never used as pre-treatment media for cellulose microfibrillation. CC-U mixture was selected as reference because of it is a well-known system used for cellulose microfibrillation.

Conclusion and challenges

The first chapter gave a detailed description of cellulose (structure, dissolution, chemical modification...) and microfibrillated cellulose MFC. The MFC production and properties were described and their production from cellulose fibres was also reported. As mentioned before, the main issue with MFC production is the high energy consumption that is why there is a need to use some chemical or biological pre-treatments to reduce this consumption. Many pre-treatments already exist based on our state of the art. The most important pre-treatment is the TEMPO-oxidation, which allows to more reduce the energy consumption and to obtain MFC with high quality. However, this pre-treatment presents some critical issues related to the use of toxic reagents. In addition, this pre-treatment involves the use of catalyst (usually NaBr) which is not appropriate for the application. The use of new emerging pre-treatments such as Deep Eutectic Solvents (DES) could be the solution to reduce the environmental impact. As reported in the literature, some studies reported the use of DES as mild pre-treatment to produce MFC with or without derivatisation.

The goal of this PhD project is to study the use of DES as pre-treatment media to produce MFC. The production will be performed using ultrafine grinding because of its availability in our laboratory and also due to its efficacy to produce MFC. Another mechanical treatment will be used to produce MFC at high content, which is Twin Screw Extruder TSE. DES pre-treatment will be compared to enzymatic hydrolysis as reference.

Studying DES effects on cellulose fibres and understanding how they facilitate MFC liberation are the main challenges today because it is not very well studied in the literature.

Therefore, the following chapters will focus on studying DES effects on cellulose fibres and their potential use for microfibrillation. Two cellulosic fibres were selected; eucalyptus and cotton fibres. Eucalyptus fibres (kraft bleached hardwood) were chosen because this species is widely used both in papermaking and for MFC production. They are composed of cellulose and hemicelluloses which allows to see the effects of DES on both polysaccharides. In addition,

cotton fibres were selected as a model material because they contain only cellulose (almost 100%).

Chapter II is dedicated to study DES effects on cellulosic fibres using many techniques of characterisation. In the second part of this chapter, the use of high-performance size exclusion chromatography HPSEC will be involved in studying DES effects at the molecular scale.

Chapter III is devoted to study the effectiveness of DES pre-treatment to produce MFC with high quality using ultrafine grinding. The second section aims to explore the feasibility of DES pre-treatment to produce MFC at high solid content using TSE.

References

- Abbott, A.P., Bell, J., Handa, T., Stoddart, S.B., 2006. Cationic functionalisation of cellulose using a choline based ionic liquid analogue. *Green Chemistry* 8, 784–786. <https://doi.org/10.1039/B605258D>
- Abbott, A.P., Barron, J.C., Ryder, K.S., Wilson, D., 2007. Eutectic-Based Ionic Liquids with Metal-Containing Anions and Cations. *Chemistry – A European Journal* 13, 6495–6501. <https://doi.org/10.1002/chem.200601738>
- Abbott, A.P., Bell, T.J., Handa, S., Stoddart, B., 2005. O-Acetylation of cellulose and monosaccharides using a zinc based ionic liquid. *Green Chem.* 7, 705. <https://doi.org/10.1039/b511691k>
- Abbott, A.P., Boothby, D., Capper, G., Davies, D.L., Rasheed, R.K., 2004. Deep Eutectic Solvents Formed between Choline Chloride and Carboxylic Acids: Versatile Alternatives to Ionic Liquids. *J. Am. Chem. Soc.* 126, 9142–9147. <https://doi.org/10.1021/ja048266j>
- Abbott, A.P., Capper, G., Davies, D.L., Rasheed, R.K., Tambyrajah, V., 2003. Novel solvent properties of choline chloride/urea mixtures. *Chemical Communications* 0, 70–71. <https://doi.org/10.1039/B210714G>
- Abbott, A.P., Capper, G., Gray, S., 2006. Design of Improved Deep Eutectic Solvents Using Hole Theory. *ChemPhysChem* 7, 803–806. <https://doi.org/10.1002/cphc.200500489>
- Abbott, A.P., Capper, G., L. Davies, D., L. Munro, H., K. Rasheed, R., Tambyrajah, V., 2001. Preparation of novel, moisture-stable, Lewis-acidic ionic liquids containing quaternary ammonium salts with functional side chains. *Chemical Communications* 0, 2010–2011. <https://doi.org/10.1039/B106357J>
- Abbott, A.P., Harris, R.C., Ryder, K.S., 2007. Application of Hole Theory to Define Ionic Liquids by their Transport Properties. *J. Phys. Chem. B* 111, 4910–4913. <https://doi.org/10.1021/jp0671998>
- Abdul Khalil, H.P.S., Davoudpour, Y., Islam, Md.N., Mustapha, A., Sudesh, K., Dungani, R., Jawaid, M., 2014. Production and modification of nanofibrillated cellulose using various mechanical processes: A review. *Carbohydrate Polymers* 99, 649–665. <https://doi.org/10.1016/j.carbpol.2013.08.069>

- Abdulmalek, E., Zulkefli, S., Rahman, M., 2017. Deep eutectic solvent as a media in swelling and dissolution of oil palm trunk. *Malaysian Journal of Analytical Science* 21, 20–26. <https://doi.org/10.17576/mjas-2017-2101-03>
- Abe, M., Sugimura, K., Nishiyama, Y., Nishio, Y., 2017. Rapid Benzoylation of Cellulose in Tetra- n -butylphosphonium Hydroxide Aqueous Solution at Room Temperature. *ACS Sustainable Chem. Eng.* 5, 4505–4510. <https://doi.org/10.1021/acssuschemeng.7b00492>
- Abranches, D.O., Martins, M.A.R., Silva, L.P., Schaeffer, N., Pinho, S.P., Coutinho, J.A.P., 2019. Phenolic hydrogen bond donors in the formation of non-ionic deep eutectic solvents: the quest for type V DES. *Chem. Commun.* 55, 10253–10256. <https://doi.org/10.1039/C9CC04846D>
- Adel, A.M., El-Gendy, A.A., Diab, M.A., Abou-Zeid, R.E., El-Zawawy, W.K., Dufresne, A., 2016. Microfibrillated cellulose from agricultural residues. Part I: Papermaking application. *Industrial Crops and Products* 93, 161–174. <https://doi.org/10.1016/j.indcrop.2016.04.043>
- Alexander, W.J., Mitchell, R.L., 1949. Rapid Measurement of Cellulose Viscosity by Nitration Methods. *Anal. Chem.* 21, 1497–1500. <https://doi.org/10.1021/ac60036a018>
- AlOmar, M.K., Alsaadi, M.A., Hayyan, M., Akib, S., Ibrahim, R.K., Hashim, M.A., 2016. Lead removal from water by choline chloride based deep eutectic solvents functionalized carbon nanotubes. *Journal of Molecular Liquids* 222, 883–894. <https://doi.org/10.1016/j.molliq.2016.07.074>
- Aulin, C., Johansson, E., Wågberg, L., Lindström, T., 2010. Self-Organized Films from Cellulose I Nanofibrils Using the Layer-by-Layer Technique. *Biomacromolecules* 11, 872–882. <https://doi.org/10.1021/bm100075e>
- Aulin, C., Salazar-Alvarez, G., Lindström, T., 2012. High strength, flexible and transparent nanofibrillated cellulose–nanoclay biohybrid films with tunable oxygen and water vapor permeability. *Nanoscale* 4, 6622. <https://doi.org/10.1039/c2nr31726e>
- Baati, R., Magnin, A., Boufi, S., 2017. High Solid Content Production of Nanofibrillar Cellulose via Continuous Extrusion. *ACS Sustainable Chem. Eng.* 5, 2350–2359. <https://doi.org/10.1021/acssuschemeng.6b02673>

- Banvillet, G., Depres, G., Belgacem, N., Bras, J., 2021a. Alkaline treatment combined with enzymatic hydrolysis for efficient cellulose nanofibrils production. *Carbohydrate Polymers* 255, 117383. <https://doi.org/10.1016/j.carbpol.2020.117383>
- Banvillet, G., Gatt, E., Belgacem, N., Bras, J., 2021b. Cellulose fibers deconstruction by twin-screw extrusion with in situ enzymatic hydrolysis via bioextrusion. *Bioresource Technology* 327, 124819. <https://doi.org/10.1016/j.biortech.2021.124819>
- Barthel, S., Heinze, T., 2006. Acylation and carbanilation of cellulose in ionic liquids. *Green Chemistry* 8, 301–306. <https://doi.org/10.1039/B513157J>
- Benítez, A., Walther, A., 2017. Cellulose nanofibril nanopapers and bioinspired nanocomposites: a review to understand the mechanical property space. *Journal of Materials Chemistry A* 5, 16003–16024. <https://doi.org/10.1039/C7TA02006F>
- Besbes, I., Alila, S., Boufi, S., 2011. Nanofibrillated cellulose from TEMPO-oxidized eucalyptus fibres: Effect of the carboxyl content. *Carbohydrate Polymers* 84, 975–983. <https://doi.org/10.1016/j.carbpol.2010.12.052>
- Bharimalla, A.K., Deshmukh, S.P., Patil, P.G., Vigneshwaran, N., 2015. Energy Efficient Manufacturing of Nanocellulose by Chemo- and Bio-Mechanical Processes: A Review. *World Journal of Nano Science and Engineering* 05, 204. <https://doi.org/10.4236/wjnse.2015.54021>
- Boufi, S., Chaker, A., 2016. Easy production of cellulose nanofibrils from corn stalk by a conventional high speed blender. *Industrial Crops and Products* 93, 39–47. <https://doi.org/10.1016/j.indcrop.2016.05.030>
- Boufi, S., Gandini, A., 2015. Triticale crop residue: a cheap material for high performance nanofibrillated cellulose. *RSC Adv.* 5, 3141–3151. <https://doi.org/10.1039/C4RA12918K>
- Boufi, S., González, I., Delgado-Aguilar, M., Tarrès, Q., Pèlach, M.À., Mutjé, P., 2016. Nanofibrillated cellulose as an additive in papermaking process: A review. *Carbohydrate Polymers* 154, 151–166. <https://doi.org/10.1016/j.carbpol.2016.07.117>
- Cai, J., Liu, Y., Zhang, L., 2006. Dilute solution properties of cellulose in LiOH/urea aqueous system. *Journal of Polymer Science Part B: Polymer Physics* 44, 3093–3101. <https://doi.org/10.1002/polb.20938>

- Cai, J., Zhang, L., 2006. Unique Gelation Behavior of Cellulose in NaOH/Urea Aqueous Solution. *Biomacromolecules* 7, 183–189. <https://doi.org/10.1021/bm0505585>
- Cai, X., Riedl, B., Ait-Kadi, A., 2003. Effect of surface-grafted ionic groups on the performance of cellulose-fiber-reinforced thermoplastic composites. *Journal of Polymer Science Part B: Polymer Physics* 41, 2022–2032. <https://doi.org/10.1002/polb.10566>
- Chaker, A., Boufi, S., 2015. Cationic nanofibrillar cellulose with high antibacterial properties. *Carbohydrate Polymers* 131, 224–232. <https://doi.org/10.1016/j.carbpol.2015.06.003>
- Chanzy, H., Imada, K., Mollard, A., Vuong, R., Barnoud, F., 1979. Crystallographic aspects of sub-elementary cellulose fibrils occurring in the wall of rose cells cultured *in vitro*. *Protoplasma* 100, 303–316. <https://doi.org/10.1007/BF01279318>
- Chanzy, H., Imada, K., Vuong, R., 1978. Electron diffraction from the primary wall of cotton fibers. *Protoplasma* 94, 299–306. <https://doi.org/10.1007/BF01276778>
- Chen, J., Li, Y., Wang, X., Liu, W., 2019. Application of Deep Eutectic Solvents in Food Analysis: A Review. *Molecules* 24, 4594. <https://doi.org/10.3390/molecules24244594>
- Chen, Y.-L., Zhang, X., You, T.-T., Xu, F., 2019. Deep eutectic solvents (DESs) for cellulose dissolution: a mini-review. *Cellulose* 26, 205–213. <https://doi.org/10.1007/s10570-018-2130-7>
- Cheng, Q., Wang, S., Han, Q., 2010. Novel process for isolating fibrils from cellulose fibers by high-intensity ultrasonication. II. Fibril characterization. *Journal of Applied Polymer Science* 115, 2756–2762. <https://doi.org/10.1002/app.30160>
- Cherian, B.M., Leão, A.L., de Souza, S.F., Thomas, S., Pothan, L.A., Kottaisamy, M., 2010. Isolation of nanocellulose from pineapple leaf fibres by steam explosion. *Carbohydrate Polymers* 81, 720–725. <https://doi.org/10.1016/j.carbpol.2010.03.046>
- Cousins, S.K., Brown, R.M., 1995. Cellulose I microfibril assembly: computational molecular mechanics energy analysis favours bonding by van der Waals forces as the initial step in crystallization. *Polymer* 36, 3885–3888. [https://doi.org/10.1016/0032-3861\(95\)99782-P](https://doi.org/10.1016/0032-3861(95)99782-P)
- Crawford, D.E., James, L.A., Abbott, A.P., 2016. Efficient continuous synthesis of high purity deep eutectic solvents by twin screw extrusion. *Chemical Communications* 52, 4215–4218. <https://doi.org/10.1039/C5CC09685E>

- Credou, J., & Berthelot, T., 2014. Cellulose: From biocompatible to bioactive material. *Journal of Materials Chemistry B*, 2(30), 4767–4788. <https://doi.org/10.1039/C4TB00431K>
- D’Agostino, C., Harris, R.C., Abbott, A.P., Gladden, L.F., Mantle, M.D., 2011. Molecular motion and ion diffusion in choline chloride based deep eutectic solvents studied by ¹H pulsed field gradient NMR spectroscopy. *Phys. Chem. Chem. Phys.* 13, 21383–21391. <https://doi.org/10.1039/C1CP22554E>
- Dai, Y., van Spronsen, J., Witkamp, G.-J., Verpoorte, R., Choi, Y.H., 2013. Natural deep eutectic solvents as new potential media for green technology. *Analytica Chimica Acta* 766, 61–68. <https://doi.org/10.1016/j.aca.2012.12.019>
- Deng, S., Huang, R., Zhou, M., Chen, F., Fu, Q., 2016. Hydrophobic cellulose films with excellent strength and toughness via ball milling activated acylation of microfibrillated cellulose. *Carbohydrate Polymers* 154, 129–138. <https://doi.org/10.1016/j.carbpol.2016.07.101>
- Desideria Seiler, E.R., Takeoka, Y., Rikukawa, M., Yoshizawa-Fujita, M., 2020. Development of a novel cellulose solvent based on pyrrolidinium hydroxide and reliable solubility analysis. *RSC Advances* 10, 11475–11480. <https://doi.org/10.1039/D0RA01486A>
- Dilamian, M., Noroozi, B., 2019. A combined homogenization-high intensity ultrasonication process for individualizaion of cellulose micro-nano fibers from rice straw. *Cellulose* 26, 5831–5849. <https://doi.org/10.1007/s10570-019-02469-y>
- Dominic, M., Joseph, R., Begum, P.M.S., Joseph, M., Padmanabhan, D., Morris, L.A., Kumar, A.S., Formela, K., 2020. Cellulose Nanofibers Isolated from the *Cuscuta Reflexa* Plant as a Green Reinforcement of Natural Rubber. *Polymers* 12, 814. <https://doi.org/10.3390/polym12040814>
- Douard, L., Bras, J., Encinas, T., Belgacem, M.N., 2021. Natural acidic deep eutectic solvent to obtain cellulose nanocrystals using the design of experience approach. *Carbohydrate Polymers* 252, 117136. <https://doi.org/10.1016/j.carbpol.2020.117136>
- Dufresne, A., 2012. CHAPTER 1. Nanocellulose: Potential Reinforcement in Composites, in: John, M.J., Thomas, S. (Eds.), *Green Chemistry Series*. Royal Society of Chemistry, Cambridge, pp. 1–32. <https://doi.org/10.1039/9781849735315-00001>
- Dufresne, A., 2013. Nanocellulose: a new ageless bionanomaterial. *Materials Today* 16, 220–227. <https://doi.org/10.1016/j.mattod.2013.06.004>

- Dufresne, A., 2017. Nanocellulose: From Nature to High Performance Tailored Materials. Walter de Gruyter GmbH & Co KG.
- Ema, T., Komiyama, T., Sunami, S., Sakai, T., 2014. Synergistic effect of quaternary ammonium hydroxide and crown ether on the rapid and clear dissolution of cellulose at room temperature. *RSC Advances* 4, 2523–2525. <https://doi.org/10.1039/C3RA45888A>
- Eyckens, D.J., Demir, B., Walsh, T.R., Welton, T., Henderson, L.C., 2016. Determination of Kamlet–Taft parameters for selected solvate ionic liquids. *Phys. Chem. Chem. Phys.* 18, 13153–13157. <https://doi.org/10.1039/C6CP01216G>
- Fang, C., Thomsen, M.H., Frankær, C.G., Brudecki, G.P., Schmidt, J.E., AlNashef, I.M., 2017. Reviving Pretreatment Effectiveness of Deep Eutectic Solvents on Lignocellulosic Date Palm Residues by Prior Recalcitrance Reduction. *Ind. Eng. Chem. Res.* 56, 3167–3174. <https://doi.org/10.1021/acs.iecr.6b04733>
- Fatah, I.Y.A., Khalil, H.P.S.A., Hossain, M.S., Aziz, A.A., Davoudpour, Y., Dungani, R., Bhat, A., 2014. Exploration of a Chemo-Mechanical Technique for the Isolation of Nanofibrillated Cellulosic Fiber from Oil Palm Empty Fruit Bunch as a Reinforcing Agent in Composites Materials. *Polymers* 6, 2611–2624. <https://doi.org/10.3390/polym6102611>
- Feng, L., Chen, Z., 2008. Research progress on dissolution and functional modification of cellulose in ionic liquids. *Journal of Molecular Liquids* 142, 1–5. <https://doi.org/10.1016/j.molliq.2008.06.007>
- Fernandes, P.M.V., Campiña, J.M., Pereira, N.M., Pereira, C.M., Silva, F., 2012. Biodegradable deep-eutectic mixtures as electrolytes for the electrochemical synthesis of conducting polymers. *J Appl Electrochem* 42, 997–1003. <https://doi.org/10.1007/s10800-012-0474-5>
- Ferreira, D.C., Oliveira, M.L., Bioni, T.A., Nawaz, H., King, A.W.T., Kilpeläinen, I., Hummel, M., Sixta, H., El Seoud, O.A., 2019. Binary mixtures of ionic liquids-DMSO as solvents for the dissolution and derivatization of cellulose: Effects of alkyl and alkoxy side chains. *Carbohydrate Polymers* 212, 206–214. <https://doi.org/10.1016/j.carbpol.2019.02.024>
- Ferrer, A., Filpponen, I., Rodríguez, A., Laine, J., Rojas, O.J., 2012. Valorization of residual Empty Palm Fruit Bunch Fibers (EPFBF) by microfluidization: Production of nanofibrillated cellulose and EPFBF nanopaper. *Bioresource Technology* 125, 249–255. <https://doi.org/10.1016/j.biortech.2012.08.108>

- Florindo, C., Oliveira, F.S., Rebelo, L.P.N., Fernandes, A.M., Marrucho, I.M., 2014. Insights into the Synthesis and Properties of Deep Eutectic Solvents Based on Cholinium Chloride and Carboxylic Acids. *ACS Sustainable Chem. Eng.* 2, 2416–2425. <https://doi.org/10.1021/sc500439w>
- Francisco, M., Bruinhorst, A. van den, Kroon, M., 2012. New natural and renewable low transition temperature mixtures (LTTMs): screening as solvents for lignocellulosic biomass processing. *Green Chemistry* 14, 2153–2157. <https://doi.org/10.1039/C2GC35660K>
- French, A.D., 2017. Glucose, not cellobiose, is the repeating unit of cellulose and why that is important. *Cellulose* 24, 4605–4609. <https://doi.org/10.1007/s10570-017-1450-3>
- Fukuzumi, H., Saito, T., Iwata, T., Kumamoto, Y., Isogai, A., 2009. Transparent and High Gas Barrier Films of Cellulose Nanofibers Prepared by TEMPO-Mediated Oxidation. *Biomacromolecules* 10, 162–165. <https://doi.org/10.1021/bm801065u>
- Gan, P.G., Sam, S.T., Abdullah, M.F. bin, Omar, M.F., 2020. Thermal properties of nanocellulose-reinforced composites: A review. *Journal of Applied Polymer Science* 137, 48544. <https://doi.org/10.1002/app.48544>
- Gao, Y., Li, Q., Shi, Y., Cha, R., 2016. Preparation and Application of Cationic Modified Cellulose Fibrils as a Papermaking Additive. *International Journal of Polymer Science* 2016, 1–8. <https://doi.org/10.1155/2016/6978434>
- García, G., Aparicio, S., Ullah, R., Atilhan, M., 2015. Deep Eutectic Solvents: Physicochemical Properties and Gas Separation Applications. *Energy Fuels* 29, 2616–2644. <https://doi.org/10.1021/ef5028873>
- Ge, W., Shuai, J., Wang, Y., Zhou, Y., Wang, X., 2022. Progress on chemical modification of cellulose in “green” solvents. *Polymer Chemistry* 13, 359–372. <https://doi.org/10.1039/D1PY00879J>
- Gericke, M., Fardim, P., Heinze, T., 2012. Ionic Liquids — Promising but Challenging Solvents for Homogeneous Derivatization of Cellulose. *Molecules* 17, 7458–7502. <https://doi.org/10.3390/molecules17067458>
- Ghanadpour, M., Carosio, F., Larsson, P.T., Wågberg, L., 2015. Phosphorylated Cellulose Nanofibrils: A Renewable Nanomaterial for the Preparation of Intrinsically Flame-Retardant Materials. *Biomacromolecules* 16, 3399–3410. <https://doi.org/10.1021/acs.biomac.5b01117>

- Habibi, Y., Goffin, A.-L., Schiltz, N., Duquesne, E., Dubois, P., Dufresne, A., 2008. Bionanocomposites based on poly(ϵ -caprolactone)-grafted cellulose nanocrystals by ring-opening polymerization. *Journal of Materials Chemistry* 18, 5002–5010. <https://doi.org/10.1039/B809212E>
- Heiskanen, I., Harlin, A., Backfolk, K., Laitinen, R., 2014. Process for the production of microfibrillated cellulose in an extruder and microfibrillated cellulose produced according to the process. US8747612B2.
- Hemmasi, A.H., 2012. Manufacturing Paper Sheets from Olive Wood by Soda, Sulphite and Kraft Pulping 4.
- Henriksson, M., Berglund, L.A., Isaksson, P., Lindström, T., Nishino, T., 2008. Cellulose Nanopaper Structures of High Toughness. *Biomacromolecules* 9, 1579–1585. <https://doi.org/10.1021/bm800038n>
- Henriksson, M., Henriksson, G., Berglund, L.A., Lindström, T., 2007. An environmentally friendly method for enzyme-assisted preparation of microfibrillated cellulose (MFC) nanofibers. *European Polymer Journal* 43, 3434–3441. <https://doi.org/10.1016/j.eurpolymj.2007.05.038>
- Herrick, F.W., Casebier, R.L., Hamilton, J.K., Sandberg, K.R., 1983. Microfibrillated cellulose: morphology and accessibility. *J. Appl. Polym. Sci.: Appl. Polym. Symp.*; (United States) 37.
- Hietala, M., Niinimäki, J., Niska, K.O., 2011. THE USE OF TWIN-SCREW EXTRUSION IN PROCESSING OF WOOD: THE EFFECT OF PROCESSING PARAMETERS AND PRETREATMENT. *BioResources* 6, 4615–4625.
- Ho Kim, K., Dutta, T., Sun, J., Simmons, B., Singh, S., 2018. Biomass pretreatment using deep eutectic solvents from lignin derived phenols. *Green Chemistry* 20, 809–815. <https://doi.org/10.1039/C7GC03029K>
- Ho, T.T.T., Abe, K., Zimmermann, T., Yano, H., 2015. Nanofibrillation of pulp fibers by twin-screw extrusion. *Cellulose* 22, 421–433. <https://doi.org/10.1007/s10570-014-0518-6>
- Ho, T.T.T., Zimmermann, T., Hauert, R., Caseri, W., 2011. Preparation and characterization of cationic nanofibrillated cellulose from etherification and high-shear disintegration processes. *Cellulose* 18, 1391–1406. <https://doi.org/10.1007/s10570-011-9591-2>

- Hong, S., Yuan, Y., Li, P., Zhang, K., Lian, H., Liimatainen, H., 2020. Enhancement of the nanofibrillation of birch cellulose pretreated with natural deep eutectic solvent. *Industrial Crops and Products* 154, 112677. <https://doi.org/10.1016/j.indcrop.2020.112677>
- Hongrattanaichit, I., Aht-Ong, D., 2020. Nanofibrillation and characterization of sugarcane bagasse agro-waste using water-based steam explosion and high-pressure homogenization. *Journal of Cleaner Production* 277, 123471. <https://doi.org/10.1016/j.jclepro.2020.123471>
- Hosu, O., Bârsan, M.M., Cristea, C., Săndulescu, R., Brett, C.M.A., 2017. Nanostructured electropolymerized poly(methylene blue) films from deep eutectic solvents. Optimization and characterization. *Electrochimica Acta* 232, 285–295. <https://doi.org/10.1016/j.electacta.2017.02.142>
- Hou, X.-D., Li, A.-L., Lin, K.-P., Wang, Y.-Y., Kuang, Z.-Y., Cao, S.-L., 2018. Insight into the structure-function relationships of deep eutectic solvents during rice straw pretreatment. *Bioresource Technology* 249, 261–267. <https://doi.org/10.1016/j.biortech.2017.10.019>
- Hou, Y., Gu, Y., Zhang, S., Yang, F., Ding, H., Shan, Y., 2008. Novel binary eutectic mixtures based on imidazole. *Journal of Molecular Liquids* 143, 154–159. <https://doi.org/10.1016/j.molliq.2008.07.009>
- Hu, H., You, J., Gan, W., Zhou, J., Zhang, L., 2015. Synthesis of allyl cellulose in NaOH/urea aqueous solutions and its thiol–ene click reactions. *Polymer Chemistry* 6, 3543–3548. <https://doi.org/10.1039/C5PY00301F>
- Inamochi, T., Funahashi, R., Nakamura, Y., Saito, T., Isogai, A., 2017. Effect of coexisting salt on TEMPO-mediated oxidation of wood cellulose for preparation of nanocellulose. *Cellulose* 24, 4097–4101. <https://doi.org/10.1007/s10570-017-1402-y>
- Isik, M., Sardon, H., Mecerreyes, D., 2014. Ionic Liquids and Cellulose: Dissolution, Chemical Modification and Preparation of New Cellulosic Materials. *International Journal of Molecular Sciences* 15, 11922–11940. <https://doi.org/10.3390/ijms150711922>
- Isogai, A., Saito, T., Fukuzumi, H., 2011. TEMPO-oxidized cellulose nanofibers. *Nanoscale* 3, 71–85. <https://doi.org/10.1039/C0NR00583E>
- Ji, Q., Yu, X., Yagoub, A.E.-G.A., Chen, L., Zhou, C., 2021. Efficient cleavage of strong hydrogen bonds in sugarcane bagasse by ternary acidic deep eutectic solvent and

- ultrasonication to facile fabrication of cellulose nanofibers. *Cellulose* 28, 6159–6182. <https://doi.org/10.1007/s10570-021-03876-w>
- Jorfi, M., Foster, E.J., 2015. Recent advances in nanocellulose for biomedical applications. *Journal of Applied Polymer Science* 132. <https://doi.org/10.1002/app.41719>
- Kakuchi, R., Yamaguchi, M., Endo, T., Shibata, Y., Ninomiya, K., Ikai, T., Maeda, K., Takahashi, K., 2015. Efficient and rapid direct transesterification reactions of cellulose with isopropenyl acetate in ionic liquids. *RSC Advances* 5, 72071–72074. <https://doi.org/10.1039/C5RA14408F>
- Kalhor, P., Ghandi, K., 2019. Deep Eutectic Solvents for Pretreatment, Extraction, and Catalysis of Biomass and Food Waste. *Molecules* 24, 4012. <https://doi.org/10.3390/molecules24224012>
- Kang, T., 2007. Role of external fibrillation in pulp and paper properties. Helsinki University of Technology.
- Karimi, M., Hesarakhi, S., Alizadeh, M., Kazemzadeh, A., 2016. One-pot and sustainable synthesis of nanocrystalline hydroxyapatite powders using deep eutectic solvents. *Materials Letters* 175, 89–92. <https://doi.org/10.1016/j.matlet.2016.04.037>
- Karimi, Mehdi, Dadfarnia, S., Shabani, A.M.H., 2017. Application of Deep Eutectic Solvent Modified Cotton as a Sorbent for Online Solid-Phase Extraction and Determination of Trace Amounts of Copper and Nickel in Water and Biological Samples. *Biol Trace Elem Res* 176, 207–215. <https://doi.org/10.1007/s12011-016-0814-0>
- Karimi, Mohammad, Ramsheh, M.R., Ahmadi, S.M., Madani, M.R., Shamsi, M., Reshadi, R., Lotfi, F., 2017. Reline-assisted green and facile synthesis of fluorapatite nanoparticles. *Materials Science and Engineering: C* 77, 121–128. <https://doi.org/10.1016/j.msec.2017.03.217>
- Kaushik, A., Singh, M., 2011. Isolation and characterization of cellulose nanofibrils from wheat straw using steam explosion coupled with high shear homogenization. *Carbohydrate Research* 346, 76–85. <https://doi.org/10.1016/j.carres.2010.10.020>
- Kekäläinen, K., Liimatainen, H., Biale, F., Niinimäki, J., 2015. Nanofibrillation of TEMPO-oxidized bleached hardwood kraft cellulose at high solids content. *Holzforschung* 69, 1077–1088. <https://doi.org/10.1515/hf-2014-0269>

- Khadraoui, M., Khiari, R., Brosse, N., Bergaoui, L., Mauret, E., 2022. Combination of Steam Explosion and TEMPO-mediated Oxidation as Pretreatments to Produce Nanofibril of Cellulose from *Posidonia oceanica* Bleached Fibres. *BioResources* 17, 2933–2958.
- Khoshnevisan, K., Maleki, H., Samadian, H., Shahsavari, S., Sarrafzadeh, M.H., Larijani, B., Dorkoosh, F.A., Haghpanah, V., Khorramizadeh, M.R., 2018. Cellulose acetate electrospun nanofibers for drug delivery systems: Applications and recent advances. *Carbohydrate Polymers* 198, 131–141. <https://doi.org/10.1016/j.carbpol.2018.06.072>
- Klemm, D., Kramer, F., Moritz, S., Lindström, T., Ankerfors, M., Gray, D., Dorris, A., 2011. Nanocelluloses: A New Family of Nature-Based Materials. *Angewandte Chemie International Edition* 50, 5438–5466. <https://doi.org/10.1002/anie.201001273>
- Köhler, S., Liebert, T., Heinze, T., Vollmer, A., Mischnick, P., Möllmann, E., Becker, W., 2010. Interactions of ionic liquids with polysaccharides 9. Hydroxyalkylation of cellulose without additional inorganic bases. *Cellulose* 17, 437–448. <https://doi.org/10.1007/s10570-009-9379-9>
- Kovács, A., Neyts, E.C., Cornet, I., Wijnants, M., Billen, P., 2020. Modeling the Physicochemical Properties of Natural Deep Eutectic Solvents. *ChemSusChem* 13, 3789–3804. <https://doi.org/10.1002/cssc.202000286>
- Kudlak, B., Owczarek, K., Namieśnik, J., 2015. Selected issues related to the toxicity of ionic liquids and deep eutectic solvents—a review. *Environ Sci Pollut Res* 22, 11975–11992. <https://doi.org/10.1007/s11356-015-4794-y>
- Kulshrestha, U., Gupta, T., Kumawat, P., Jaiswal, H., Ghosh, S.B., Sharma, N.N., 2020. Cellulose nanofibre enabled natural rubber composites: Microstructure, curing behaviour and dynamic mechanical properties. *Polymer Testing* 90, 106676. <https://doi.org/10.1016/j.polymeresting.2020.106676>
- Kumar, A.K., Parikh, B.S., Pravakar, M., 2016. Natural deep eutectic solvent mediated pretreatment of rice straw: bioanalytical characterization of lignin extract and enzymatic hydrolysis of pretreated biomass residue. *Environ Sci Pollut Res* 23, 9265–9275. <https://doi.org/10.1007/s11356-015-4780-4>
- Kwon, G.-J., Bandi, R., Yang, B.-S., Park, C.-W., Han, S.-Y., Park, J.-S., Lee, E.-A., Kim, N.-H., Lee, S.-H., 2021. Choline chloride based deep eutectic solvents for the lignocellulose

- nanofibril production from Mongolian oak (*Quercus mongolica*). *Cellulose* 28, 9169–9185. <https://doi.org/10.1007/s10570-021-04102-3>
- Laitinen, O., Suopajarvi, T., Österberg, M., Liimatainen, H., 2017. Hydrophobic, Superabsorbing Aerogels from Choline Chloride-Based Deep Eutectic Solvent Pretreated and Silylated Cellulose Nanofibrils for Selective Oil Removal. *ACS Appl. Mater. Interfaces* 9, 25029–25037. <https://doi.org/10.1021/acsami.7b06304>
- Lavoine, N., Desloges, I., Dufresne, A., Bras, J., 2012. Microfibrillated cellulose – Its barrier properties and applications in cellulosic materials: A review. *Carbohydrate Polymers* 90, 735–764. <https://doi.org/10.1016/j.carbpol.2012.05.026>
- Lee, H., Abd Hamid, S.B., Zain, S., 2014. Conversion of Lignocellulosic Biomass to Nanocellulose: Structure and Chemical Process. *TheScientificWorldJournal* 2014, 631013. <https://doi.org/10.1155/2014/631013>
- Li, P., Sirviö, J.A., Asante, B., Liimatainen, H., 2018. Recyclable deep eutectic solvent for the production of cationic nanocelluloses. *Carbohydrate Polymers* 199, 219–227. <https://doi.org/10.1016/j.carbpol.2018.07.024>
- Li, P., Sirviö, J.A., Haapala, A., Liimatainen, H., 2017. Cellulose Nanofibrils from Nonderivatizing Urea-Based Deep Eutectic Solvent Pretreatments. *ACS Appl. Mater. Interfaces* 9, 2846–2855. <https://doi.org/10.1021/acsami.6b13625>
- Li, W., Xue, Y., He, M., Yan, J., Lucia, L.A., Chen, J., Yu, J., Yang, G., 2021. Facile Preparation and Characteristic Analysis of Sulfated Cellulose Nanofibril via the Pretreatment of Sulfamic Acid-Glycerol Based Deep Eutectic Solvents. *Nanomaterials* 11, 2778. <https://doi.org/10.3390/nano11112778>
- Li, Y., Wang, J., Liu, X., Zhang, S., 2018. Towards a molecular understanding of cellulose dissolution in ionic liquids: anion/cation effect, synergistic mechanism and physicochemical aspects. *Chemical Science* 9, 4027–4043. <https://doi.org/10.1039/C7SC05392D>
- Liao, H.-G., Jiang, Y.-X., Zhou, Z.-Y., Chen, S.-P., Sun, S.-G., 2008. Shape-Controlled Synthesis of Gold Nanoparticles in Deep Eutectic Solvents for Studies of Structure–Functionality Relationships in Electrocatalysis. *Angewandte Chemie International Edition* 47, 9100–9103. <https://doi.org/10.1002/anie.200803202>

- Liimatainen, H., Sirviö, J.A., Kekäläinen, K., Hormi, O., 2015. High-consistency milling of oxidized cellulose for preparing microfibrillated cellulose films. *Cellulose* 22, 3151–3160. <https://doi.org/10.1007/s10570-015-0700-5>
- Liimatainen, H., Suopajarvi, T., Sirviö, J., Hormi, O., Niinimäki, J., 2014. Fabrication of cationic cellulosic nanofibrils through aqueous quaternization pretreatment and their use in colloid aggregation. *Carbohydrate Polymers* 103, 187–192. <https://doi.org/10.1016/j.carbpol.2013.12.042>
- Lim, W.-L., Gunny, A.A.N., Kasim, F.H., AlNashef, I.M., Arbain, D., 2019. Alkaline deep eutectic solvent: a novel green solvent for lignocellulose pulping. *Cellulose* 26, 4085–4098. <https://doi.org/10.1007/s10570-019-02346-8>
- Ling, Z., Edwards, J.V., Guo, Z., Prevost, N.T., Nam, S., Wu, Q., French, A.D., Xu, F., 2019. Structural variations of cotton cellulose nanocrystals from deep eutectic solvent treatment: micro and nano scale. *Cellulose* 26, 861–876. <https://doi.org/10.1007/s10570-018-2092-9>
- Lionetto, F., Timo, A., Frigione, M., 2015. Curing kinetics of epoxy-deep eutectic solvent mixtures. *Thermochimica Acta* 612, 70–78. <https://doi.org/10.1016/j.tca.2015.05.004>
- Liu, C., Li, M.-C., Chen, W., Huang, R., Hong, S., Wu, Q., Mei, C., 2020. Production of lignin-containing cellulose nanofibers using deep eutectic solvents for UV-absorbing polymer reinforcement. *Carbohydrate Polymers* 246, 116548. <https://doi.org/10.1016/j.carbpol.2020.116548>
- Liu, G., Li, W., Chen, L., Zhang, X., Niu, D., Chen, Y., Yuan, S., Bei, Y., Zhu, Q., 2020. Molecular dynamics studies on the aggregating behaviors of cellulose molecules in NaOH/urea aqueous solution. *Colloids and Surfaces A: Physicochemical and Engineering Aspects* 594, 124663. <https://doi.org/10.1016/j.colsurfa.2020.124663>
- Liu, L., Wang, S.-M., Chen, W.-L., Lu, Y., Li, Y.-G., Wang, E.-B., 2012. A high nuclear lanthanide-containing polyoxometalate aggregate synthesized in choline chloride/urea eutectic mixture. *Inorganic Chemistry Communications* 23, 14–16. <https://doi.org/10.1016/j.inoche.2012.05.025>
- Liu, Q., Yuan, T., Fu, Q., Bai, Y., Peng, F., Yao, C., 2019. Choline chloride-lactic acid deep eutectic solvent for delignification and nanocellulose production of moso bamboo. *Cellulose* 26, 9447–9462. <https://doi.org/10.1007/s10570-019-02726-0>

- Liu, Y., Ahmed, S., Sameen, D.E., Wang, Y., Lu, R., Dai, J., Li, S., Qin, W., 2021. A review of cellulose and its derivatives in biopolymer-based for food packaging application. *Trends in Food Science & Technology* 112, 532–546. <https://doi.org/10.1016/j.tifs.2021.04.016>
- Liu, Y., Chen, W., Xia, Q., Guo, B., Wang, Q., Liu, S., Liu, Yixing, Li, J., Yu, H., 2017. Efficient Cleavage of Lignin–Carbohydrate Complexes and Ultrafast Extraction of Lignin Oligomers from Wood Biomass by Microwave-Assisted Treatment with Deep Eutectic Solvent. *ChemSusChem* 10, 1692–1700. <https://doi.org/10.1002/cssc.201601795>
- Liu, Zhang, Gou, Zhang, Wang, 2021. Esterification of cellulose using carboxylic acid-based deep eutectic solvents to produce high-yield cellulose nanofibers. *Carbohydrate Polymers* 251, 117018. <https://doi.org/10.1016/j.carbpol.2020.117018>
- Long, L., Tian, D., Hu, J., Wang, F., Saddler, J., 2017. A xylanase-aided enzymatic pretreatment facilitates cellulose nanofibrillation. *Bioresource Technology* 243, 898–904. <https://doi.org/10.1016/j.biortech.2017.07.037>
- López, F., Ariza, J., Pérez, I., Jiménez, L., 2000. Comparative study of paper sheets from olive tree wood pulp obtained by soda, sulphite or kraft pulping. *Bioresource Technology* 71, 83–86. [https://doi.org/10.1016/S0960-8524\(99\)00044-9](https://doi.org/10.1016/S0960-8524(99)00044-9)
- Ma, Y., Xia, Q., Liu, Yongzhuang, Chen, W., Liu, S., Wang, Q., Liu, Yixing, Li, J., Yu, H., 2019. Production of Nanocellulose Using Hydrated Deep Eutectic Solvent Combined with Ultrasonic Treatment. *ACS Omega* 4, 8539–8547. <https://doi.org/10.1021/acsomega.9b00519>
- Majová, V., Horanová, S., Škulcová, A., Šima, J., Jablonský, M., 2017. Deep Eutectic Solvent Delignification: Impact of Initial Lignin. *BioResources* 12, 7301–7310.
- Malaeke, H., Housaindokht, M.R., Monhemi, H., Izadyar, M., 2018. Deep eutectic solvent as an efficient molecular liquid for lignin solubilization and wood delignification. *Journal of Molecular Liquids* 263, 193–199. <https://doi.org/10.1016/j.molliq.2018.05.001>
- María, P.D. de, 2014. Recent trends in (ligno)cellulose dissolution using neoteric solvents: switchable, distillable and bio-based ionic liquids. *Journal of Chemical Technology & Biotechnology* 89, 11–18. <https://doi.org/10.1002/jctb.4201>
- Maugeri, Z., Domínguez de María, P., 2012. Novel choline-chloride-based deep-eutectic-solvents with renewable hydrogen bond donors: levulinic acid and sugar-based polyols. *RSC Adv.* 2, 421–425. <https://doi.org/10.1039/C1RA00630D>

- Mikkola, J.-P., Kirilin, A., Tuuf, J.-C., Pranovich, A., Holmbom, B., M. Kustov, L., Yu. Murzin, D., Salmi, T., 2007. Ultrasound enhancement of cellulose processing in ionic liquids: from dissolution towards functionalization. *Green Chemistry* 9, 1229–1237. <https://doi.org/10.1039/B708533H>
- Mjalli, F.S., Naser, J., Jibril, B., Alizadeh, V., Gano, Z., 2014. Tetrabutylammonium Chloride Based Ionic Liquid Analogues and Their Physical Properties. *J. Chem. Eng. Data* 59, 2242–2251. <https://doi.org/10.1021/je5002126>
- Mohammed, N., Grishkewich, N., Tam, K.C., 2018. Cellulose nanomaterials: promising sustainable nanomaterials for application in water/wastewater treatment processes. *Environ. Sci.: Nano* 5, 623–658. <https://doi.org/10.1039/C7EN01029J>
- Moon, R.J., Martini, A., Nairn, J., Simonsen, J., Youngblood, J., 2011. Cellulose nanomaterials review: structure, properties and nanocomposites. *Chem. Soc. Rev.* 40, 3941. <https://doi.org/10.1039/c0cs00108b>
- Moufawad, T., Gomes, M.C., Fourmentin, S., 2021. Solvants eutectiques profonds - Vers des procédés plus durables 27.
- Nader, S., Brosse, N., Daas, T., Mauret, E., 2022. Lignin containing micro and nano-fibrillated cellulose obtained by steam explosion: Comparative study between different processes. *Carbohydrate Polymers* 290, 119460. <https://doi.org/10.1016/j.carbpol.2022.119460>
- Nakagaito, A.N., Ikenaga, K., Takagi, H., 2015. Cellulose nanofiber extraction from grass by a modified kitchen blender. *Mod. Phys. Lett. B* 29, 1540039. <https://doi.org/10.1142/S0217984915400394>
- Nechyporchuk, O., Pignon, F., Belgacem, M.N., 2015. Morphological properties of nanofibrillated cellulose produced using wet grinding as an ultimate fibrillation process. *J Mater Sci* 50, 531–541. <https://doi.org/10.1007/s10853-014-8609-1>
- Nguyen, M.N., Kragl, U., Michalik, D., Ludwig, R., Hollmann, D., 2019. The Effect of Additives on the Viscosity and Dissolution of Cellulose in Tetrabutylphosphonium Hydroxide. *ChemSusChem* 12, 3458–3462. <https://doi.org/10.1002/cssc.201901316>
- Nie, S., Zhang, K., Lin, X., Zhang, C., Yan, D., Liang, H., Wang, S., 2018. Enzymatic pretreatment for the improvement of dispersion and film properties of cellulose nanofibrils. *Carbohydrate Polymers* 181, 1136–1142. <https://doi.org/10.1016/j.carbpol.2017.11.020>

- Nogi, M., Iwamoto, S., Nakagaito, A.N., Yano, H., 2009. Optically Transparent Nanofiber Paper. *Advanced Materials* 21, 1595–1598. <https://doi.org/10.1002/adma.200803174>
- Noguchi, Y., Homma, I., Matsubara, Y., 2017. Complete nanofibrillation of cellulose prepared by phosphorylation. *Cellulose* 24, 1295–1305. <https://doi.org/10.1007/s10570-017-1191-3>
- Nor, N.A.M., Mustapha, W.A.W., Hassan, O., 2015. Deep eutectic solvent (DES) as a pretreatment for oil palm empty fruit bunch (OPEFB) in production of sugar. *AIP Conference Proceedings* 1678, 050044. <https://doi.org/10.1063/1.4931323>
- Ogushi, Y., Sakai, S., Kawakami, K., 2007. Synthesis of enzymatically-gellable carboxymethylcellulose for biomedical applications. *Journal of Bioscience and Bioengineering* 104, 30–33. <https://doi.org/10.1263/jbb.104.30>
- Okita, Y., Saito, T., Isogai, A., 2010. Entire Surface Oxidation of Various Cellulose Microfibrils by TEMPO-Mediated Oxidation. *Biomacromolecules* 11, 1696–1700. <https://doi.org/10.1021/bm100214b>
- Olszewska, A., Eronen, P., Johansson, L.-S., Malho, J.-M., Ankerfors, M., Lindström, T., Ruokolainen, J., Laine, J., Österberg, M., 2011. The behaviour of cationic NanoFibrillar Cellulose in aqueous media. *Cellulose* 18, 1213–1226. <https://doi.org/10.1007/s10570-011-9577-0>
- Orts, W.J., Shey, J., Imam, S.H., Glenn, G.M., Guttman, M.E., Revol, J.-F., 2005. Application of Cellulose Microfibrils in Polymer Nanocomposites. *J Polym Environ* 13, 301–306. <https://doi.org/10.1007/s10924-005-5514-3>
- Pääkkö, M., Ankerfors, M., Kosonen, H., Nykänen, A., Ahola, S., Österberg, M., Ruokolainen, J., Laine, J., Larsson, P.T., Ikkala, O., Lindström, T., 2007. Enzymatic Hydrolysis Combined with Mechanical Shearing and High-Pressure Homogenization for Nanoscale Cellulose Fibrils and Strong Gels. *Biomacromolecules* 8, 1934–1941. <https://doi.org/10.1021/bm061215p>
- Parry, A., 2016. Nanocellulose and its Composites for Biomedical Applications. *Current medicinal chemistry* 23. <https://doi.org/10.2174/0929867323666161014124008>
- PAYEN, A., 1838. MÉMOIRE (MEMOIRE) SUR LA COMPOSITION DU TISSU PROPRE DES PLANTES ET DU LIGNEUX In *Comptes Rendus* vol. VII, 1838 pp. 1052-6. Academie des Sciences.

- Pei, A., Butchosa, N., Berglund, L.A., Zhou, Q., 2013. Surface quaternized cellulose nanofibrils with high water absorbency and adsorption capacity for anionic dyes. *Soft Matter* 9, 2047. <https://doi.org/10.1039/c2sm27344f>
- Perkins, S.L., Painter, P., Colina, C.M., 2014. Experimental and Computational Studies of Choline Chloride-Based Deep Eutectic Solvents. *J. Chem. Eng. Data* 59, 3652–3662. <https://doi.org/10.1021/je500520h>
- Phanthong, P., Karnjanakom, S., Reubroycharoen, P., Hao, X., Abudula, A., Guan, G., 2017. A facile one-step way for extraction of nanocellulose with high yield by ball milling with ionic liquid. *Cellulose* 24, 2083–2093. <https://doi.org/10.1007/s10570-017-1238-5>
- Pinkert, A., Marsh, K., Pang, S., Staiger, M., 2009. Ionic Liquids and Their Interaction with Cellulose. *Chemical reviews* 109, 6712–28. <https://doi.org/10.1021/cr9001947>
- Plotka-Wasyłka, J., de la Guardia, M., Andruch, V., Vilková, M., 2020. Deep eutectic solvents vs ionic liquids: Similarities and differences. *Microchemical Journal* 159, 105539. <https://doi.org/10.1016/j.microc.2020.105539>
- Procentese, A., Johnson, E., Orr, V., Campanile, A.G., Wood, J.A., Marzocchella, A., Rehmann, L., 2015. Deep eutectic solvent pretreatment and subsequent saccharification of corncob. *Bioresource Technology* 192, 31–36. <https://doi.org/10.1016/j.biortech.2015.05.053>
- Qi, H., Chang, C., Zhang, L., 2008. Effects of temperature and molecular weight on dissolution of cellulose in NaOH/urea aqueous solution. *Cellulose* 15, 779–787. <https://doi.org/10.1007/s10570-008-9230-8>
- Qi, H., Liebert, T., Meister, F., Heinze, T., 2009. Homogenous carboxymethylation of cellulose in the NaOH/urea aqueous solution. *Reactive and Functional Polymers* 69, 779–784. <https://doi.org/10.1016/j.reactfunctpolym.2009.06.007>
- Rahimi Kord Sofla, M., Batchelor, W., Kosinkova, J., Pepper, R., Brown, R., Rainey, T., 2019. Cellulose nanofibres from bagasse using a high speed blender and acetylation as a pretreatment. *Cellulose* 26, 4799–4814. <https://doi.org/10.1007/s10570-019-02441-w>
- Rahman, M.S., Hasan, M.S., Nitai, A.S., Nam, S., Karmakar, A.K., Ahsan, M.S., Shiddiky, M.J.A., Ahmed, M.B., 2021. Recent Developments of Carboxymethyl Cellulose. *Polymers* 13, 1345. <https://doi.org/10.3390/polym13081345>

- Rånby, B.G., 1951. Fibrous macromolecular systems. Cellulose and muscle. The colloidal properties of cellulose micelles. *Discuss. Faraday Soc.* 11, 158–164. <https://doi.org/10.1039/DF9511100158>
- Ren, F., Wang, J., Yu, J., Zhong, C., Xie, F., Wang, S., 2021. Dissolution of Cellulose in Ionic Liquid–DMSO Mixtures: Roles of DMSO/IL Ratio and the Cation Alkyl Chain Length. *ACS Omega* 6, 27225–27232. <https://doi.org/10.1021/acsomega.1c03954>
- Ren, H., Chen, C., Guo, S., Zhao, D., Wang, Q., 2016b. Synthesis of a Novel Allyl-Functionalized Deep Eutectic Solvent to Promote Dissolution of Cellulose. *BioResources* 11, 8457–8469.
- Ren, H., Chen, C., Wang, Q., Zhao, D., Guo, S., 2016a. The Properties of Choline Chloride-based Deep Eutectic Solvents and their Performance in the Dissolution of Cellulose. *BioResources* 11, 5435–5451.
- Rodríguez-Zúñiga, U.F., Cannella, D., Giordano, R. de C., Giordano, R. de L.C., Jørgensen, H., Felby, C., 2015. Lignocellulose pretreatment technologies affect the level of enzymatic cellulose oxidation by LPMO. *Green Chem.* 17, 2896–2903. <https://doi.org/10.1039/C4GC02179G>
- Rol, F., Banvillet, G., Meyer, V., Petit-Conil, M., Bras, J., 2018. Combination of twin-screw extruder and homogenizer to produce high-quality nanofibrillated cellulose with low energy consumption. *J Mater Sci* 53, 12604–12615. <https://doi.org/10.1007/s10853-018-2414-1>
- Rol, F., Belgacem, M.N., Gandini, A., Bras, J., 2019. Recent advances in surface-modified cellulose nanofibrils. *Progress in Polymer Science* 88, 241–264. <https://doi.org/10.1016/j.progpolymsci.2018.09.002>
- Rol, F., Karakashov, B., Nechyporchuk, O., Terrien, M., Meyer, V., Dufresne, A., Belgacem, M.N., Bras, J., 2017. Pilot-Scale Twin Screw Extrusion and Chemical Pretreatment as an Energy-Efficient Method for the Production of Nanofibrillated Cellulose at High Solid Content. *ACS Sustainable Chem. Eng.* 5, 6524–6531. <https://doi.org/10.1021/acssuschemeng.7b00630>
- Rol, F., Sillard, C., Bardet, M., Yarava, J.R., Emsley, L., Gablin, C., Léonard, D., Belgacem, N., Bras, J., 2020. Cellulose phosphorylation comparison and analysis of phosphate position on cellulose fibers. *Carbohydrate Polymers* 229, 115294. <https://doi.org/10.1016/j.carbpol.2019.115294>

- Ruesgas-Ramón, M., Figueroa-Espinoza, M.C., Durand, E., 2017. Application of Deep Eutectic Solvents (DES) for Phenolic Compounds Extraction: Overview, Challenges, and Opportunities. *J. Agric. Food Chem.* 65, 3591–3601. <https://doi.org/10.1021/acs.jafc.7b01054>
- Saini, S., Yücel Falco, Ç., Belgacem, M.N., Bras, J., 2016. Surface cationized cellulose nanofibrils for the production of contact active antimicrobial surfaces. *Carbohydrate Polymers* 135, 239–247. <https://doi.org/10.1016/j.carbpol.2015.09.002>
- Saito, T., Hirota, M., Tamura, N., Kimura, S., Fukuzumi, H., Heux, L., Isogai, A., 2009. Individualization of Nano-Sized Plant Cellulose Fibrils by Direct Surface Carboxylation Using TEMPO Catalyst under Neutral Conditions. *Biomacromolecules* 10, 1992–1996. <https://doi.org/10.1021/bm900414t>
- Saito, T., Isogai, A., 2004. TEMPO-Mediated Oxidation of Native Cellulose. The Effect of Oxidation Conditions on Chemical and Crystal Structures of the Water-Insoluble Fractions. *Biomacromolecules* 5, 1983–1989. <https://doi.org/10.1021/bm0497769>
- Saito, T., Isogai, A., 2006. Introduction of aldehyde groups on surfaces of native cellulose fibers by TEMPO-mediated oxidation. *Colloids and Surfaces A: Physicochemical and Engineering Aspects* 289, 219–225. <https://doi.org/10.1016/j.colsurfa.2006.04.038>
- Saito, T., Kimura, S., Nishiyama, Y., Isogai, A., 2007. Cellulose Nanofibers Prepared by TEMPO-Mediated Oxidation of Native Cellulose. *Biomacromolecules* 8, 2485–2491. <https://doi.org/10.1021/bm0703970>
- Salama, A., Hesemann, P., 2020. Recent Trends in Elaboration, Processing, and Derivatization of Cellulosic Materials Using Ionic Liquids. *ACS Sustainable Chem. Eng.* 8, 17893–17907. <https://doi.org/10.1021/acssuschemeng.0c06913>
- Santos, R.B., Capanema, E.A., Balakshin, M.Y., Chang, H.-M., Jameel, H., 2011. EFFECT OF HARDWOODS CHARACTERISTICS ON KRAFT PULPING PROCESS: EMPHASIS ON LIGNIN STRUCTURE. *BioResources* 6, 3623–3637.
- Sarko, A., Southwick, J., Hayashi, J., 1976. Packing Analysis of Carbohydrates and Polysaccharides. 7. Crystal Structure of Cellulose III and Its Relationship to Other Cellulose Polymorphs. *Macromolecules* 9, 857–863. <https://doi.org/10.1021/ma60053a028>
- Satlewal, A., Agrawal, R., Bhagia, S., Sangoro, J., Ragauskas, A.J., 2018. Natural deep eutectic solvents for lignocellulosic biomass pretreatment: Recent developments, challenges and novel

- opportunities. *Biotechnology Advances* 36, 2032–2050. <https://doi.org/10.1016/j.biotechadv.2018.08.009>
- Schaeffer, N., Conceição, J.H.F., Martins, M.A.R., Neves, M.C., Pérez-Sánchez, G., Gomes, J.R.B., Papaiconomou, N., Coutinho, J.A.P., 2020. Non-ionic hydrophobic eutectics – versatile solvents for tailored metal separation and valorisation. *Green Chem.* 22, 2810–2820. <https://doi.org/10.1039/D0GC00793E>
- Sehaqui, H., Liu, A., Zhou, Q., Berglund, L.A., 2010. Fast Preparation Procedure for Large, Flat Cellulose and Cellulose/Inorganic Nanopaper Structures. *Biomacromolecules* 11, 2195–2198. <https://doi.org/10.1021/bm100490s>
- Sehaqui, H., Zhou, Q., Berglund, L.A., 2011. High-porosity aerogels of high specific surface area prepared from nanofibrillated cellulose (NFC). *Composites Science and Technology* 71, 1593–1599. <https://doi.org/10.1016/j.compscitech.2011.07.003>
- Serpa Guerra, A.M., Gómez Hoyos, C., Velásquez-Cock, J.A., Vélez Penagos, L., Gañán Rojo, P., Vélez Acosta, L., Pereira, M.A., Zuluaga, R., 2020. Effect of ultra-fine friction grinding on the physical and chemical properties of curcuma (*Curcuma longa* L.) suspensions. *Journal of Food Science* 85, 132–142. <https://doi.org/10.1111/1750-3841.14973>
- Shahbaz, K., Mjalli, F.S., Hashim, M.A., AlNashef, I.M., 2012. Prediction of the surface tension of deep eutectic solvents. *Fluid Phase Equilibria* 319, 48–54. <https://doi.org/10.1016/j.fluid.2012.01.025>
- Sharma, G., Takahashi, K., Kuroda, K., 2021. Polar zwitterion/saccharide-based deep eutectic solvents for cellulose processing. *Carbohydrate Polymers* 267, 118171. <https://doi.org/10.1016/j.carbpol.2021.118171>
- Sharma, M., Mukesh, C., Mondal, D., Prasad, K., 2013. Dissolution of α -chitin in deep eutectic solvents. *RSC Advances* 3, 18149–18155. <https://doi.org/10.1039/C3RA43404D>
- Sharma, P.R., Joshi, R., Sharma, S.K., Hsiao, B.S., 2017. A Simple Approach to Prepare Carboxycellulose Nanofibers from Untreated Biomass. *Biomacromolecules* 18, 2333–2342. <https://doi.org/10.1021/acs.biomac.7b00544>
- Simeonov, S.P., Afonso, M.C.A., 2016. Basicity and stability of urea deep eutectic mixtures. *RSC Advances* 6, 5485–5490. <https://doi.org/10.1039/C5RA24558C>

- Siró, I., Plackett, D., 2010. Microfibrillated cellulose and new nanocomposite materials: a review. *Cellulose* 17, 459–494. <https://doi.org/10.1007/s10570-010-9405-y>
- Sirviö, J.A., 2018. Cationization of lignocellulosic fibers with betaine in deep eutectic solvent: Facile route to charge stabilized cellulose and wood nanofibers. *Carbohydrate Polymers* 198, 34–40. <https://doi.org/10.1016/j.carbpol.2018.06.051>
- Sirviö, J.A., Heiskanen, J.P., 2017. Synthesis of Alkaline-Soluble Cellulose Methyl Carbamate Using a Reactive Deep Eutectic Solvent. *ChemSusChem* 10, 455–460. <https://doi.org/10.1002/cssc.201601270>
- Sirviö, J.A., Heiskanen, J.P., 2020. Room-temperature dissolution and chemical modification of cellulose in aqueous tetraethylammonium hydroxide–carbamide solutions. *Cellulose* 27, 1933–1950. <https://doi.org/10.1007/s10570-019-02907-x>
- Sirviö, J.A., Hyypiö, K., Asaadi, S., Junka, K., Liimatainen, H., 2020. High-strength cellulose nanofibers produced via swelling pretreatment based on a choline chloride–imidazole deep eutectic solvent. *Green Chemistry* 22, 1763–1775. <https://doi.org/10.1039/C9GC04119B>
- Sirviö, J.A., Visanko, M., Liimatainen, H., 2015. Deep eutectic solvent system based on choline chloride-urea as a pre-treatment for nanofibrillation of wood cellulose. *Green Chemistry* 17, 3401–3406. <https://doi.org/10.1039/C5GC00398A>
- Sirviö, J.A., Visanko, M., Liimatainen, H., 2016. Acidic Deep Eutectic Solvents As Hydrolytic Media for Cellulose Nanocrystal Production. *Biomacromolecules* 17, 3025–3032. <https://doi.org/10.1021/acs.biomac.6b00910>
- Škulcová, A., Kamenská, L., Kalman, F., Ház, A., Jablonský, M., Čížová, K., Šurina, I., 2016. Deep Eutectic Solvents as Medium for Pretreatment of Biomass [WWW Document]. *Key Engineering Materials*. <https://doi.org/10.4028/www.scientific.net/KEM.688.17>
- Smith, E.L., Abbott, A.P., Ryder, K.S., 2014. Deep Eutectic Solvents (DESS) and Their Applications. *Chem. Rev.* 114, 11060–11082. <https://doi.org/10.1021/cr300162p>
- Soares, B., da Costa Lopes, A.M., Silvestre, A.J.D., Rodrigues Pinto, P.C., Freire, C.S.R., Coutinho, J.A.P., 2021. Wood delignification with aqueous solutions of deep eutectic solvents. *Industrial Crops and Products* 160, 113128. <https://doi.org/10.1016/j.indcrop.2020.113128>

- Song, Y., Sun, Y., Zhang, X., Zhou, J., Zhang, L., 2008. Homogeneous Quaternization of Cellulose in NaOH/Urea Aqueous Solutions as Gene Carriers. *Biomacromolecules* 9, 2259–2264. <https://doi.org/10.1021/bm800429a>
- Spence, K.L., Venditti, R.A., Rojas, O.J., Habibi, Y., Pawlak, J.J., 2011. A comparative study of energy consumption and physical properties of microfibrillated cellulose produced by different processing methods. *Cellulose* 18, 1097–1111. <https://doi.org/10.1007/s10570-011-9533-z>
- Spence, K.L., Venditti, R.A., Rojas, O.J., Habibi, Y., Pawlak, J.J., 2010. The effect of chemical composition on microfibrillar cellulose films from wood pulps: water interactions and physical properties for packaging applications. *Cellulose* 17, 835–848. <https://doi.org/10.1007/s10570-010-9424-8>
- Spiridon, I., Popa, V.I., 2008. Chapter 13 - Hemicelluloses: Major Sources, Properties and Applications, in: Belgacem, M.N., Gandini, A. (Eds.), *Monomers, Polymers and Composites from Renewable Resources*. Elsevier, Amsterdam, pp. 289–304. <https://doi.org/10.1016/B978-0-08-045316-3.00013-2>
- Suopajarvi, T., Ricci, P., Karvonen, V., Ottolina, G., Liimatainen, H., 2020. Acidic and alkaline deep eutectic solvents in delignification and nanofibrillation of corn stalk, wheat straw, and rapeseed stem residues. *Industrial Crops and Products* 145, 111956. <https://doi.org/10.1016/j.indcrop.2019.111956>
- Suopajarvi, T., Sirviö, J.A., Liimatainen, H., 2017. Nanofibrillation of deep eutectic solvent-treated paper and board cellulose pulps. *Carbohydrate Polymers* 169, 167–175. <https://doi.org/10.1016/j.carbpol.2017.04.009>
- Swatloski, R.P., Spear, S.K., Holbrey, J.D., Rogers, R.D., 2002. Dissolution of Cellose with Ionic Liquids. *J. Am. Chem. Soc.* 124, 4974–4975. <https://doi.org/10.1021/ja025790m>
- Swensson, B., Larsson, A., Hasani, M., 2020. Probing Interactions in Combined Hydroxide Base Solvents for Improving Dissolution of Cellulose. *Polymers* 12, 1310. <https://doi.org/10.3390/polym12061310>
- Taniguchi, T., Okamura, K., 1998. New films produced from microfibrillated natural fibres. *Polymer International* 47, 291–294. [https://doi.org/10.1002/\(SICI\)1097-0126\(199811\)47:3<291::AID-PI11>3.0.CO;2-1](https://doi.org/10.1002/(SICI)1097-0126(199811)47:3<291::AID-PI11>3.0.CO;2-1)

- Tanpichai, S., Witayakran, S., Boonmahitthisud, A., 2019. Study on structural and thermal properties of cellulose microfibrils isolated from pineapple leaves using steam explosion. *Journal of Environmental Chemical Engineering* 7, 102836. <https://doi.org/10.1016/j.jece.2018.102836>
- Tenhunen, T.-M., Lewandowska, A.E., Orelma, H., Johansson, L.-S., Virtanen, T., Harlin, A., Österberg, M., Eichhorn, S.J., Tammelin, T., 2018. Understanding the interactions of cellulose fibres and deep eutectic solvent of choline chloride and urea. *Cellulose* 25, 137–150. <https://doi.org/10.1007/s10570-017-1587-0>
- Tomé, L.I.N., Baião, V., da Silva, W., Brett, C.M.A., 2018. Deep eutectic solvents for the production and application of new materials. *Applied Materials Today* 10, 30–50. <https://doi.org/10.1016/j.apmt.2017.11.005>
- Turbak, A.F., Snyder, F.W., Sandberg, K.R., 1983. Microfibrillated cellulose, a new cellulose product: properties, uses, and commercial potential. *J. Appl. Polym. Sci.: Appl. Polym. Symp.;* (United States) 37.
- Uetani, K., Yano, H., 2011. Nanofibrillation of Wood Pulp Using a High-Speed Blender. *Biomacromolecules* 12, 348–353. <https://doi.org/10.1021/bm101103p>
- Van Nguyen, Q., Nomura, S., Hoshino, R., Ninomiya, K., Takada, K., Kakuchi, R., Takahashi, K., 2017. Recyclable and scalable organocatalytic transesterification of polysaccharides in a mixed solvent of 1-ethyl-3-methylimidazolium acetate and dimethyl sulfoxide. *Polym J* 49, 783–787. <https://doi.org/10.1038/pj.2017.49>
- Villares, A., Moreau, C., Bennati-Granier, C., Garajova, S., Foucat, L., Falourd, X., Saake, B., Berrin, J.-G., Cathala, B., 2017. Lytic polysaccharide monooxygenases disrupt the cellulose fibers structure. *Sci Rep* 7, 40262. <https://doi.org/10.1038/srep40262>
- Vuoti, S., Narasimha, K., Reinikainen, K., 2018. Green wastewater treatment flocculants and fixatives prepared from cellulose using high-consistency processing and deep eutectic solvents. *Journal of Water Process Engineering* 26, 83–91. <https://doi.org/10.1016/j.jwpe.2018.09.003>
- Wagle, D.V., Deakyne, C.A., Baker, G.A., 2016. Quantum Chemical Insight into the Interactions and Thermodynamics Present in Choline Chloride Based Deep Eutectic Solvents. *J. Phys. Chem. B* 120, 6739–6746. <https://doi.org/10.1021/acs.jpcc.6b04750>
- Walter, B., Gallatin, J.C., 1962. Enzymatic conversion of cellulosic fibers. US3041246A.

- Wang, H., Li, J., Zeng, X., Tang, X., Sun, Y., Lei, T., Lin, L., 2020. Extraction of cellulose nanocrystals using a recyclable deep eutectic solvent. *Cellulose* 27, 1301–1314. <https://doi.org/10.1007/s10570-019-02867-2>
- Wang, Q., Wei, W., Chang, F., Sun, J., Xie, S., Zhu, Q., 2016. Controlling the Size and Film Strength of Individualized Cellulose Nanofibrils Prepared by Combined Enzymatic Pretreatment and High Pressure Microfluidization. *BioResources* 11, 2536–2547.
- Wang, S., Cheng, Q., 2009. A novel process to isolate fibrils from cellulose fibers by high-intensity ultrasonication, Part 1: Process optimization. *Journal of Applied Polymer Science* 113, 1270–1275. <https://doi.org/10.1002/app.30072>
- Wang, X., Fang, G., Hu, C., Du, T., 2008. Application of ultrasonic waves in activation of microcrystalline cellulose. *Journal of Applied Polymer Science* 109, 2762–2767. <https://doi.org/10.1002/app.27975>
- Wang, Y., Wang, X., Xie, Y., Zhang, K., 2018. Functional nanomaterials through esterification of cellulose: a review of chemistry and application. *Cellulose* 25, 3703–3731. <https://doi.org/10.1007/s10570-018-1830-3>
- Wibowo, D., Lee, C.-K., 2010. Nonleaching antimicrobial cotton fibers for hyaluronic acid adsorption. *Biochemical Engineering Journal, Special Section: CHEMPOR2008 - Integration of Life Sciences and Engineering* 53, 44–51. <https://doi.org/10.1016/j.bej.2010.09.002>
- Wilkes S, J., 2002. A short history of ionic liquids—from molten salts to neoteric solvents. *Green Chemistry* 4, 73–80. <https://doi.org/10.1039/B110838G>
- Willberg-Keyriläinen, P., Hiltunen, J., Ropponen, J., 2018. Production of cellulose carbamate using urea-based deep eutectic solvents. *Cellulose* 25, 195–204. <https://doi.org/10.1007/s10570-017-1465-9>
- Willberg-Keyriläinen, P., Ropponen, J., 2019. Evaluation of esterification routes for long chain cellulose esters. *Heliyon* 5, e02898. <https://doi.org/10.1016/j.heliyon.2019.e02898>
- Wu, J., Zhang, J., Zhang, H., He, J., Ren, Q., Guo, M., 2004. Homogeneous Acetylation of Cellulose in a New Ionic Liquid. *Biomacromolecules* 5, 266–268. <https://doi.org/10.1021/bm034398d>

- Xia, Y., Yang, P., Sun, Y., Wu, Y., Mayers, B., Gates, B., Yin, Y., Kim, F., Yan, H., 2003. One-Dimensional Nanostructures: Synthesis, Characterization, and Applications. *Advanced Materials* 15, 353–389. <https://doi.org/10.1002/adma.200390087>
- Xu, G.-C., Ding, J.-C., Han, R.-Z., Dong, J.-J., Ni, Y., 2016. Enhancing cellulose accessibility of corn stover by deep eutectic solvent pretreatment for butanol fermentation. *Bioresource Technology* 203, 364–369. <https://doi.org/10.1016/j.biortech.2015.11.002>
- Xu, P., Zheng, G.-W., Zong, M.-H., Li, N., Lou, W.-Y., 2017. Recent progress on deep eutectic solvents in biocatalysis. *Bioresour. Bioprocess.* 4, 34. <https://doi.org/10.1186/s40643-017-0165-5>
- Yan, L., Tao, H., Bangal, P.R., 2009. Synthesis and Flocculation Behavior of Cationic Cellulose Prepared in a NaOH/Urea Aqueous Solution. *CLEAN – Soil, Air, Water* 37, 39–44. <https://doi.org/10.1002/clen.200800127>
- You, Y.H., Gu, C.D., Wang, X.L., Tu, J.P., 2012. Electrodeposition of Ni–Co alloys from a deep eutectic solvent. *Surface and Coatings Technology* 206, 3632–3638. <https://doi.org/10.1016/j.surfcoat.2012.03.001>
- Yu, W., Wang, C., Yi, Y., Wang, H., Yang, Y., Zeng, L., Tan, Z., 2021. Direct pretreatment of raw ramie fibers using an acidic deep eutectic solvent to produce cellulose nanofibrils in high purity. *Cellulose* 28, 175–188. <https://doi.org/10.1007/s10570-020-03538-3>
- Zahrina, I., Nasikin, M., Mulia, K., 2017. Evaluation of the interaction between molecules during betaine monohydrate-organic acid deep eutectic mixture formation. *Journal of Molecular Liquids* 225, 446–450. <https://doi.org/10.1016/j.molliq.2016.10.134>
- Zdanowicz, M., Wilpiszewska, K., Szychaj, T., 2018. Deep eutectic solvents for polysaccharides processing. A review. *Carbohydrate Polymers* 200, 361–380. <https://doi.org/10.1016/j.carbpol.2018.07.078>
- Zhang, C.-W., Xia, S.-Q., Ma, P.-S., 2016. Facile pretreatment of lignocellulosic biomass using deep eutectic solvents. *Bioresource Technology* 219, 1–5. <https://doi.org/10.1016/j.biortech.2016.07.026>
- Zhang, Jinming, Wu, J., Yu, J., Zhang, X., He, J., Zhang, Jun, 2017. Application of ionic liquids for dissolving cellulose and fabricating cellulose-based materials: state of the art and future trends. *Materials Chemistry Frontiers* 1, 1273–1290. <https://doi.org/10.1039/C6QM00348F>

- Zhang, L., Tsuzuki, T., Wang, X., 2015. Preparation of cellulose nanofiber from softwood pulp by ball milling. *Cellulose* 22, 1729–1741. <https://doi.org/10.1007/s10570-015-0582-6>
- Zhang, Q., Benoit, M., De Oliveira Vigier, K., Barrault, J., Jérôme, F., 2012a. Green and Inexpensive Choline-Derived Solvents for Cellulose Decrystallization. *Chemistry – A European Journal* 18, 1043–1046. <https://doi.org/10.1002/chem.201103271>
- Zhang, Q., Vigier, K.D.O., Royer, S., Jérôme, F., 2012b. Deep eutectic solvents: syntheses, properties and applications. *Chemical Society Reviews* 41, 7108–7146. <https://doi.org/10.1039/C2CS35178A>
- Zhao, M., Li, J., Mano, E., Song, Z., Tschäen, D.M., Grabowski, E.J.J., Reider, P.J., 1999. Oxidation of Primary Alcohols to Carboxylic Acids with Sodium Chlorite Catalyzed by TEMPO and Bleach. *J. Org. Chem.* 64, 2564–2566. <https://doi.org/10.1021/jo982143y>
- Zhao, Z., Chen, X., Ali, M.F., Abdeltawab, A.A., Yakout, S.M., Yu, G., 2018. Pretreatment of wheat straw using basic ethanolamine-based deep eutectic solvents for improving enzymatic hydrolysis. *Bioresource Technology* 263, 325–333. <https://doi.org/10.1016/j.biortech.2018.05.016>
- Zhekenov, T., Toksanbayev, N., Kazakbayeva, Z., Shah, D., Mjalli, F.S., 2017. Formation of type III Deep Eutectic Solvents and effect of water on their intermolecular interactions. *Fluid Phase Equilibria, 2016 Asian Thermophysical Properties Conference* 441, 43–48. <https://doi.org/10.1016/j.fluid.2017.01.022>
- Zhou, E., Liu, H., 2014. A Novel Deep Eutectic Solvents Synthesized by Solid Organic Compounds and Its Application on Dissolution for Cellulose. *Asian J. Chem.* 26, 3626–3630. <https://doi.org/10.14233/ajchem.2014.16995>
- Zhou, J., Qin, Y., Liu, S., Zhang, L., 2006. Homogenous Synthesis of Hydroxyethylcellulose in NaOH/Urea Aqueous Solution. *Macromolecular Bioscience* 6, 84–89. <https://doi.org/10.1002/mabi.200500148>
- Zhou, J., Zhang, L., Deng, Q., Wu, X., 2004. Synthesis and characterization of cellulose derivatives prepared in NaOH/urea aqueous solutions. *Journal of Polymer Science Part A: Polymer Chemistry* 42, 5911–5920. <https://doi.org/10.1002/pola.20431>

REFERENCES

- Zhou, S., Ingram, L.O., 2000. Synergistic Hydrolysis of Carboxymethyl Cellulose and Acid-Swollen Cellulose by Two Endoglucanases (CelZ and CelY) from *Erwinia chrysanthemi*. *J. Bacteriol.* 182, 5676–5682. <https://doi.org/10.1128/JB.182.20.5676-5682.2000>
- Zhu, S., Wu, Y., Chen, Q., Yu, Z., Wang, C., Jin, S., Ding, Y., Wu, G., 2006. Dissolution of cellulose with ionic liquids and its application: a mini-review. *Green Chemistry* 8, 325–327. <https://doi.org/10.1039/B601395C>

Chapter II. Study of DES pre-treatment effects on cellulose structure

Table of contents

Chapter II. Study of DES pre-treatment effects on cellulose structure.....	109
Introduction.....	115
II.1 Study of DES pre-treatment effects on cellulose fibres and paper properties.....	116
II.1.1 Introduction.....	117
II.1.2 Materials and Methods	120
II.1.2.1 Materials	120
II.1.2.2 DES pre-treatment.....	120
II.1.2.3 Enzymatic pre-treatment.....	121
II.1.2.4 Paper handsheet production	121
II.1.2.5 Spectroscopic analyses: ATR-FTIR and solid-state ¹³ C NMR	121
II.1.2.6 Chemical composition and degree of polymerisation	122
II.1.2.7 X-ray Diffraction XrD	123
II.1.2.8 Thermogravimetric analysis	123
II.1.2.9 Scanning electron microscopy (SEM).....	123
II.1.2.10 Morphological analysis of the fibres	124
II.1.2.11 Water retention value (WRV)	124
II.1.2.12 Mechanical properties of produced papers	124
II.1.3 Results and discussions	125
II.1.3.1 Effect of DES treatments on the chemical structure of the fibres.....	125
II.1.3.1.1 ATR-FTIR analysis.....	125
II.1.3.1.2 Solid-state ¹³ C NMR of DES/enzyme treated eucalyptus fibres.....	127
II.1.3.2 Chemical composition of DES-treated eucalyptus fibres.....	129
II.1.3.3 Degree of polymerisation	129

II.1.3.4 X-ray Diffraction and Crystallinity Index	131
II.1.3.5 Thermogravimetric analysis	134
II.1.3.6 Scanning Electron Microscopy (SEM).....	137
II.1.3.7 Morphological properties of fibres.....	138
II.1.3.8 Water Retention Value WRV of DES-treated fibres	139
II.1.3.9 Mechanical properties of produced papers from DES treated eucalyptus fibres	140
II.1.4 Conclusion	142
II.2 High-Performance Size Exclusion chromatography HPSEC to study DES effects on cellulose structure.....	145
II.2.1 Introduction.....	146
II.2.2 Materials and Methods	148
II.2.2.1 Materials	148
II.2.2.2 Fibre pre-treatment with DES.....	148
II.2.2.3 Fibre enzymatic pre-treatment	149
II.2.2.4 Cellulose carbanilation	149
II.2.2.5 HPSEC-multidetectors analysis	150
II.2.3 Results and discussion.....	150
II.2.3.1 SEC analysis of DES and/or enzyme-treated eucalyptus fibres	150
II.2.3.1.1 Molecular mass distribution (MMD)	150
II.2.3.1.2 Intrinsic viscosity, hydrodynamic radius and gyration radius.....	156
II.2.3.1.3 Comparison between the DP_v measured in cupriethylenediamine and DP averages measured by HPSEC	158
II.2.3.2 SEC analysis of DES and/or enzyme treated cotton fibres	160
II.2.3.2.1 Molecular mass distribution	160
II.2.3.2.2 Intrinsic viscosity, hydrodynamic radius and radius of gyration	163

II.2.3.2.3 Comparison between DP_v measured in cupriethylenediamine and DP averages measured by HPSEC	165
II.2.3.3 Comparison between eucalyptus and cotton fibres	165
II.2.4 Conclusion	166
Appendix II.2	168
References	169

Introduction

As described in the previous chapter, the use of Deep Eutectic Solvents as pre-treatment seems to be a promising way to reduce the toxicity and preserve the environment. However, there are many remaining challenges related to the effects of DES on cellulose and how their use facilitates the microfibrillation.

This chapter is divided into two main sections:

In the first section, the effects of DES on cellulose fibres and paper properties were studied. DES-treated fibres were characterised by various methods to study the structural, morphological, chemical, thermal and mechanical properties. DES-treated fibres were compared to those treated with enzymatic hydrolysis.

In the second section, the effects of these DES on cellulose structure at the molecular scale was investigated using high-performance size exclusion chromatography HPSEC. Cellulosic fibres pre-treated with DES were derivatised (tricarbanilated) and then analysed with HPSEC. Analysed fibres were compared to those treated with enzymatic pre-treatment.

II.1 Study of DES pre-treatment effects on cellulose fibres and paper properties

This section is adapted from Mnasri, A., Dhaouadi, H., Khiari, R., Halila, S., Mauret, E., 2022. Effects of Deep Eutectic Solvents on cellulosic fibres and paper properties: Green “chemical” refining. Carbohydrate Polymers 119606. <https://doi.org/10.1016/j.carbpol.2022.119606>.

Abstract

This work aims to study the effects of Deep Eutectic Solvents (DES) on cellulosic fibre structure. A focus was made on the induced fibrillation phenomena which could facilitate the further production of microfibrillated cellulose. Three DES of different pH (acid, neutral and alkaline), namely betaine hydrochloride-urea, choline chloride-urea and choline chloride-monoethanolamine, were tested. Eucalyptus and cotton pulps were used to investigate the effects of DES on both hemicelluloses and cellulose. Interestingly, cellulose was esterified during acidic DES treatment. Moreover, an internal and external fibrillation occurred with DES treatment without a great extent of modification in terms of chemical composition, crystallinity and degree of polymerisation. Compared to enzymatic hydrolysis (used as a conventional pre-treatment for cellulose microfibrillation), DES have significantly enhanced the mechanical properties of resulting papers. To conclude, DES treatment can be considered as a soft and green “chemical” refining that could be applied as a pre-treatment for cellulose microfibrillation.

Key words: Cellulose fibres, treatment, Deep Eutectic Solvents, fibrillation, chemical refining.

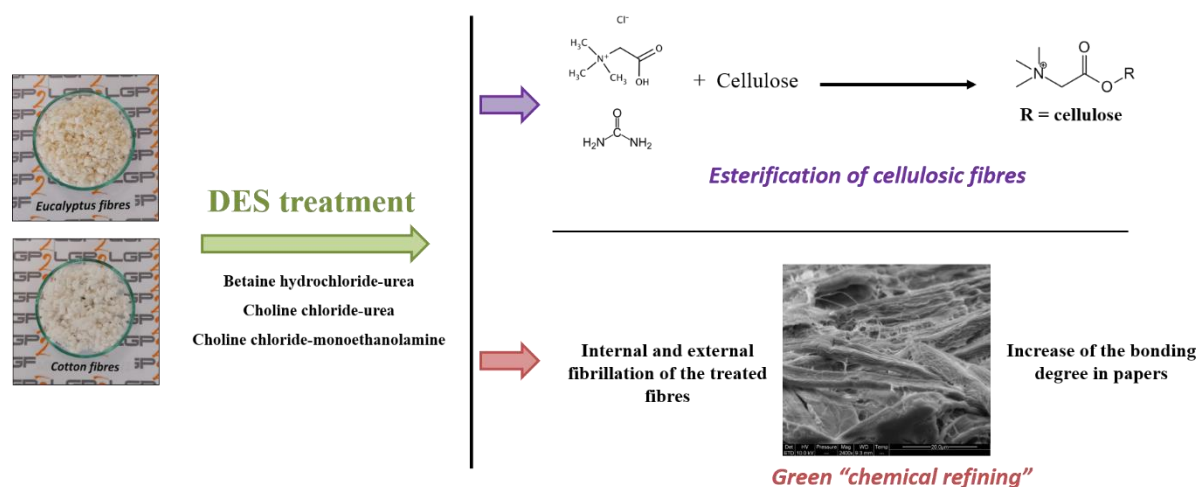


Figure II. 1. Graphical abstract of the section II.1

II.1.1 Introduction

Currently the development of “green” chemistry is one of the promising solutions to deal with environmental problems. This chemistry is particularly based on the use of non-toxic solvents and reagents. In this context, Deep Eutectic Solvents (DES) were proposed as an alternative to ionic liquids IL (Abbott et al., 2003). DES and IL share some similarities such as low volatility, high tunability and capacity of dissolving organic and inorganic compounds. However, they are distinguished in the method of their preparation and the starting reagents. DES exhibit more advantages than IL, including low or non-toxicity, easy preparation and the use of cheap and sustainable compounds. Moreover, the components of DES must not react with each other, while for IL their synthesis requires many steps using various reagents and organic volatile solvents (Płotka-Wasyłka et al., 2020).

DES could be described as a mixture of acids and Lewis or Bronsted bases. They can be also defined as the mixture of hydrogen bond donors (HBD) and hydrogen bond acceptors (HBA). Those made of quaternary ammonium and metal salts or hydrogen bond donor are the most studied systems. DES are classified into four groups (Smith et al., 2014): (I) combination of organic and metal salts; (II) mixture of organic salts and metal hydrates; (III) combination of organic salts and hydrogen bonding compounds and (IV) mixture of metal chlorides and hydrogen bond donor compounds. Many non-cationic DES have also been described in the literature. A fifth class (type V) was proposed (Abranches et al., 2019; Moufawad et al., 2021; Schaeffer et al., 2020), which is obtained from the mixture of non-ionic species.

Due to their interesting properties, DES are attracting more and more interest in the scientific community. They are used in several fields such as organic synthesis (Ruesgas-Ramón et al., 2017), polymer science (Tomé et al., 2018), electrochemical field (Fernandes et al., 2012; Hosu et al., 2017), and waste water treatment (AlOmar et al., 2016). Some DES are known to be treatment media for lignocellulosic biomass as described in many reviews (Selkälä et al., 2016; Zdanowicz et al., 2018).

When applied to lignocellulosic biomass, DES must have a selective solubilisation capacity which depends on both DES components and the nature of the biomass. As they do not solubilise cellulose, these DES make it possible to have a selective action.

CHAPTER II. STUDY OF DES PRE-TREATMENT EFFECTS ON CELLULOSE STRUCTURE

DES can also be used as pre-treatment media to enhance fibre fibrillation or microfibrillation, even though there are very few articles related to this subject compared to the selective extraction of biomass components. For instance, choline chloride-urea (CC-U) mixture was the first system used for treating cellulose fibres before microfibrillation (Sirviö et al., 2015). Another study showed that urea ammonium thiocyanate or guanidine hydrochloride-based DES can be used in wood pre-treatment to facilitate the microfibrillation (Li et al., 2017). These systems are able to swell the fibres and thus break the hydrogen bonds between the cellulose chains but without degrading the polysaccharide.

Furthermore, some studies reported the use of DES for microfibrillation with simultaneous modification. Cellulose cationization, for instance, can be carried out during DES treatment (Sirviö, 2018). Esterification reaction can also be performed in the presence of DES to produce esterified cellulose microfibrils (Liu et al., 2021).

For many years, one of the main topics of our group has been related to the reduction of the energy costs associated with cellulose microfibrillation (Banvillet et al., 2021; Khiari et al., 2019; Rol et al., 2020, 2017). For this purpose, various pre-treatments (biological or chemical) are used before the main mechanical treatment of microfibrillation (ultrafine grinding, homogenisation...) (Nechyporchuk et al., 2016; Rol et al., 2019). But conventional pre-treatments are expensive, such as enzymatic hydrolysis, or based on the use of toxic reagents like TEMPO-mediated oxidation. DES may represent an alternative solution to reduce the toxicity of chemical reagents and to protect the environment by the use of biodegradable components.

In addition, these solvents are sometimes nonreactive such as choline chloride-urea which can be an advantage especially for further modification (post-modification).

In the light of these promising results, this paper is part of the same strategy and aims at investigating the influence of three different DES systems (acidic, neutral and basic) on the chemical and physical properties, including internal and external fibrillation, of cellulose fibres from eucalyptus and cotton. The choice of these biomasses is based on their different composition. On one hand, eucalyptus fibres (kraft bleached pulp) were selected because they are widely used in papermaking and for producing microfibrillated cellulose. They are composed of cellulose and hemicelluloses which allows to see the effects of DES on both polysaccharides. On the other hand, cotton fibres were used as a model material because they

CHAPTER II. STUDY OF DES PRE-TREATMENT EFFECTS ON CELLULOSE STRUCTURE

contain only cellulose (almost 100%). The use of two different biomasses allows to give a better understanding of the involved phenomena.

In such a context, betaine hydrochloride-urea BHCl-U (acidic), choline chloride-urea CC-U (neutral) and choline chloride-monoethanolamine CC-M (basic) were chosen due to their non-toxicity and biodegradability. Moreover, they were selected to investigate the effects of the pH on cellulose fibres and because it was demonstrated that DES containing quaternary ammonium salts with chloride anion are efficient for the treatment of cellulose thanks to the interaction of chloride anion with cellulose (Chen et al., 2019).

To the best of our knowledge, BHCl-U and CC-M were never used as pre-treatment media for cellulose microfibrillation. Indeed, BHCl-U was studied to produce cellulose carbamate from hardwood dissolving pulp (Willberg-Keyriläinen et al., 2018), while CC-M was tested for wheat straw delignification (Zhao et al., 2018). CC-U was designated as a reference DES because it was already used in cellulose pre-treatment to produce microfibrillated cellulose, even if very few works are published on this subject. DES treated fibres were characterised according to the state-of-the-art techniques including infrared spectroscopy (ATR-FTIR), solid-state ^{13}C NMR, morphological analysis, water retention value (WRV), degree of polymerisation (DP), tensile tests of papers... So, the main purpose of this study was to evaluate the ability of these solvents, used as pre-treatment, to fibrillate the fibres and for the purpose of their microfibrillation without modifying in a great extent the cellulose structure.

It is interesting to note that there is no published paper focusing on the effects of DES of the fibre properties and those of the resulting papers. Understanding DES effects and how they act on cellulose fibres could improve this pre-treatment to then produce high quality MFC.

Enzymatic hydrolysis was also studied as a reference pre-treatment because it is the most frequently used for producing MFC without chemical modification. In the same way, the properties of enzymatically treated fibres, and papers produced from them, were investigated and the results were compared to those of DES treatment.

II.1.2 Materials and Methods

II.1.2.1 Materials

Dry sheets of bleached hardwood pulp (eucalyptus, Fibria T35) and cotton pulp (CELSUR, CS 21 DHS), referenced as EF and CF respectively, were used. These fibres were first disintegrated in water. The suspensions were then filtered, washed with ethanol and oven dried at 60 °C. Betaine hydrochloride ($C_5H_{12}ClNO_2$) was supplied from VWR (Milliporesigma), monoethanolamine (C_2H_7NO , >99%) from ROTH, choline chloride ($C_5H_{14}ClNO$, >98%) from Alfa Aesar. Urea ACS reagent (CH_4N_2O , 99.0-100.5%), bis(ethylenediamine)copper (II) hydroxide solution ($Cu(H_2NCH_2CH_2NH_2)_2(OH)_2$ 1.0 M in H_2O), sulfuric acid (H_2SO_4 , 72%), acetic acid (CH_3COOH), ethanol (CH_3OH , 96%) and sodium acetate ($C_2H_3NaO_2$) were obtained from Sigma Aldrich. Enzyme solution FiberCare (pH between 6 and 8) was purchased from Novozymes. Deionised water was used throughout the experiments.

II.1.2.2 DES pre-treatment

Acidic DES (BHCl-U) was obtained from the mixture of betaine hydrochloride and urea (1:4 molar ratio). The neutral DES (CC-U) was prepared by mixing choline chloride with urea (1:2 molar ratio) and the alkaline DES (CC-M) from choline chloride-monoethanolamine (1:6 molar ratio). DES mixtures were heated in an oil bath at 100 °C (for BHCl-U) or at 80 °C (for CC-M and CC-U) until a clear and transparent liquid is obtained.

The pH of each prepared DES was measured at 25 °C by mixing 2 mL of DES in 20 mL of deionised water using a pH meter (Toledo). The pH values of BHCl-U, CC-U and CC-M are 1.89, 7.13 and 11.96, respectively.

Cellulosic fibres (EF or CF) were mixed with prepared DES in a reactor vessel (Pressure reactor-600 mL) with a mass ratio of 2.5:100 (for CC-U and BHCl-U) and 5:100 for CC-M. The mass ratio was adjusted depending on the viscosity of the used DES. The suspension was left under mechanical stirring at 100 °C for 1 and/or 4 hours. After treatment, the suspension was filtered and washed first with hot and then cold water to remove the remaining DES. DES-treated fibres were finally stored at 4 °C until further use. The yield after DES pre-treatment was between 90-95%.

II.1.2.3 Enzymatic pre-treatment

The enzymatic hydrolysis using cellulase enzyme is designated as a reference pre-treatment. A 2 wt % fibre suspension was used. The enzymatic treatment was performed in 12 L reactor (Büchiglasuster), at a temperature of 50 °C and a pH adjusted at 5 using an acidic buffer solution (acetic acid and sodium acetate). Enzyme solution (FiberCare cellulase with an activity of 4948 ECU/g of solution) was added to the suspension with an enzyme's concentration of 300 ECU/g of cellulose. The reaction was left 2 h and then enzyme was deactivated by increasing the temperature to 80 °C for 10 min. The obtained suspension was then filtered through a nylon sieve (10 µm of mesh) and washed with hot water and cold water. The washed and filtered pulp was finally stored at 4 °C until further use. The yield after enzymatic hydrolysis was around 90%.

II.1.2.4 Paper handsheet production

Papers were prepared by filtration using a Rapid Köthen sheet former according to the ISO standard 5269-2:2004. Untreated, enzymatic treated, and DES-treated eucalyptus fibres (EF-CC-M) were used at a concentration of 2 g/L. One litre of the suspension was introduced into the bowl of the former. After dilution with 5 to 7 L of water, the suspension was filtered on a metallic sieve. The wet sheet is pressed and collected on blotting papers, protected between two sheets and dried under vacuum at 80 °C for 10 min. The weight of the sheets formed is generally around 60 g.m⁻².

Before any tests, the samples were placed in a conditioned atmosphere (T = 23 °C and relative humidity = 50%) for 48 h as recommended in ISO standard 187. For each pulp, 10 sheets were tested.

II.1.2.5 Spectroscopic analyses: ATR-FTIR and solid-state 13C NMR

Infrared spectroscopy analyses (ATR-FTIR) were done using a PerkinElmer spectrum 65. Spectra were collected with a single reflection horizontal ATR sampling accessory having a diamond ATR crystal. A small piece of sample (air dried fibres) was placed directly on the ATR crystal and pressed gradually using sample accessory until a sufficient signal intensity was obtained. The pressure was then fixed and the IR spectrum was measured at the absorbance mode (16 scans) with a resolution of 2 cm⁻¹ in the frequency from 600 to 4000 cm⁻¹.

CHAPTER II. STUDY OF DES PRE-TREATMENT EFFECTS ON CELLULOSE STRUCTURE

The NMR experiments were performed with a Bruker Avance III apparatus operating at 100.6 MHz and using a CP-MAS probe of 4 mm. All the spectra were recorded at 295 K using the combination of cross-polarisation, high-power proton decoupling and magic angle spinning (CP/MAS) methods. Glycine was used as a reference, with a carbonyl signal fixed at 176.03 ppm. The spinning speed was 12000 Hz with a contact time of 2000 μ s and repetition times of 2 s. The acquisition time was adjusted at 0.035 s and the sweep width at 29761.9 Hz.

Prior to performing NMR experiment, DES or enzyme treated eucalyptus fibres were air-dried and then grinded using a cryomill for 2 min. After grinding, sample was compacted in a 4 mm ZrO₂ rotors and then analysed. The analysis was done in the quantitative mode. The data were proceeded using TopSpin software and crystallinity index was measured by integration on C4. The degree of substitution (DS) of esterified cellulose is obtained by the integration of the new carbonyl group appeared with respect to the C1. The integration is done thanks to the TopSpin software.

The DS is calculated according as following:

$$DS = \frac{\text{Carbonyl group integral}}{\text{C1 integral}}$$

Betaine Hydrochloride, urea and the obtained DES (BHCl-U) were also analysed by liquid state NMR after dissolution in D₂O.

II.1.2.6 Chemical composition and degree of polymerisation

Chemical composition was analysed by ion chromatography (HPLC-dionex) according to the standard method (TAPPI T-249 cm-00). Fibres were first hydrolysed using sulfuric acid (72%) at 30 °C for 1 h. Then, an amount of water was added to the tube and heated at 120 °C for 1 h in autoclave. The mixture was then filtered and the filtrate was diluted and analysed by ion chromatography.

The DP was measured according to ISO 5351:2010 standard. Cellulose fibres were dissolved in a bis(ethylenediamine)copper(II) hydroxide solution. The intrinsic viscosity $[\eta]$ was measured at 25 °C with a capillary viscosimeter and the DP was deduced using the Mark–Houwink–Sakurada equation. Two measurements were made for each sample.

$$DP^{0.905} = 0.75 \times [\eta]$$

II.1.2.7 X-ray Diffraction XrD

X-ray Diffraction (XrD) was performed on paper samples deposited on a zero-background Si substrate. The measurements were carried out with a diffractometer X'Pert Pro MPD (PANalytical, Netherlands), equipped with a Bragg-Brentano geometry and a copper anode ($K\alpha$ $\lambda = 1.5419 \text{ \AA}$). The crystallinity index CrI (%) was calculated using Segal (1959) method:

$$CrI = \frac{I_{002} - I_{am}}{I_{002}} \times 100$$

where I_{002} represents the diffraction intensity of the main crystalline peak at $2\theta \approx 22.5^\circ$ and I_{am} is the intensity at $2\theta \approx 18.7^\circ$.

II.1.2.8 Thermogravimetric analysis

Thermogravimetric analyses (TGA) of cellulose fibres before and after DES or enzyme treatment were measured by a thermal analyser Mettler Toledo (TGA/DSC 3+) under air and/or nitrogen flow using a constant flow rate of 30 mL min^{-1} . Approximately 6 mg of paper were heated from 25 to $700 \text{ }^\circ\text{C}$, at a rate of $10 \text{ }^\circ\text{C.min}^{-1}$.

II.1.2.9 Scanning electron microscopy (SEM)

SEM is used to observe fibre surface aspect. This technique is based on the interaction between material and electrons. Dried fibre suspensions were coated with Au/Pd to make them conductive. Samples were analysed with SEM Quanta250 FEG using high voltage of 2.5 KV.

Cellulose fibres made of untreated, DES (after 4 h of treatment) and enzymatically treated pulps were analysed.

SEM images were also performed on the papers produced from untreated EF, EF-CC-M and EF-enzyme with SEM Quanta 200 (FEI, USA) in ETD mode, with a working distance of 10 mm and an acceleration voltage of 10.0 kV. Images were taken at an angle of 14° .

II.1.2.10 Morphological analysis of the fibres

Fibre morphology (arithmetic fibre length, fibre width, fine content...) was studied with a Morfi-Neo fibre analyser (Techpap, France). 40 mg (dry matter) of pulp were diluted in 1L of deionised water. Tests were performed during 5 min with a limit fibre/fine element fixed at 80 μm . For each sample, analysis was triplicated and the mean value of the measured parameters was calculated.

II.1.2.11 Water retention value (WRV)

The WRV is used to determine the amount of water retained in a fibre when it is subjected to a certain centrifugal force. Centrifugation is used to remove the capillary water retained between the fibres of a wet pulp pad. A handsheet (basis weight of 60 g/m^2) was made on an English former with a diameter of 159 mm and a water height of 350 mm above the mesh. Pads of 0.2 g were centrifuged at 3000 g for 15 minutes.

WRV was calculated according to the following equation:

$$WRV = \frac{m_{wet} - m_{dry}}{m_{dry}} \times 100$$

where m_{wet} is the weight of the sample after centrifugation and m_{dry} is the sample weight after oven drying at 105 $^{\circ}\text{C}$ for 24 h.

II.1.2.12 Mechanical properties of produced papers

Tensile tests were performed on the produced papers using an Instron 5965 machine (Instron, USA) according to ISO 1924-2 standard. Tests were done on samples with dimensions of 15×100 mm^2 and a tensile speed of 10 mm/min . The Young's modulus of each sample was calculated using the thickness values of the paper. For each handsheet, 2 measurements were done. The average of 20 measurements was calculated.

Tear resistance of papers was measured using a tear tester equipped with a 4000 mN pendulum (Noviprofibre, France) according to ISO 1974 standard. Tests were done on samples with dimensions of 50×65 mm^2 . 2 measurements were made for each handsheet. The average of 20 measurements was calculated.

CHAPTER II. STUDY OF DES PRE-TREATMENT EFFECTS ON CELLULOSE STRUCTURE

The internal bond strength or delamination resistance of papers was determined using an Internal pendulum Bond Tester IBT-IDM. This device leads to determine the adhesion of internal layers in paper using a Scott-Bond method according to ISO 16260 standard. The sample was placed between two double-layered adhesive substrates under a pressure of 100 psi for 30 s. The test sample was then subjected to a shear force by means of a pendulum. The internal bond strength is the energy required to delaminate the sample in the thickness. 10 measurements were done for each sample.

All the tests were carried out in conditioned atmosphere (Temperature = 23 °C and Relative humidity = 50%).

II.1.3 Results and discussions

II.1.3.1 Effect of DES treatments on the chemical structure of the fibres

II.1.3.1.1 ATR-FTIR analysis

Figure II. 2 presents the ATR-FTIR spectra of eucalyptus and cotton fibres before and after DES treatment (4 h). On the spectra, many of the observed peaks are typical of cellulose (Chung et al., 2004), such as a strong band around 3338 cm^{-1} corresponding to O-H stretching and a peak at 2892 cm^{-1} related to C-H stretching. The peak at 1640 cm^{-1} is related to absorbed water. However, a new peak at 1706 cm^{-1} was observed only with BHCl-U, for cotton and eucalyptus fibres, which is related to a carbonyl group (Figure II. 2a, red curve). The absence of this peak on the FT-IR spectrum of BHCl-U alone (see Figure II. 2c) leads to the conclusion that this group is covalently linked to the cellulose through either an ester (-O-C(O)-) or a carbamate (O-C(O)-NH-) function. Indeed, as already mentioned, BHCl-U system was reported to produce cellulose carbamate with a low degree of substitution by reacting with urea (Willberg-Keyriläinen et al., 2018). On the other side, ester bond could be envisioned by acid-catalysed esterification between alcohol of cellulose and carboxylic acid of BHCl. In order to determine the chemical nature of this carbonyl group, solid-state ^{13}C NMR have been performed.

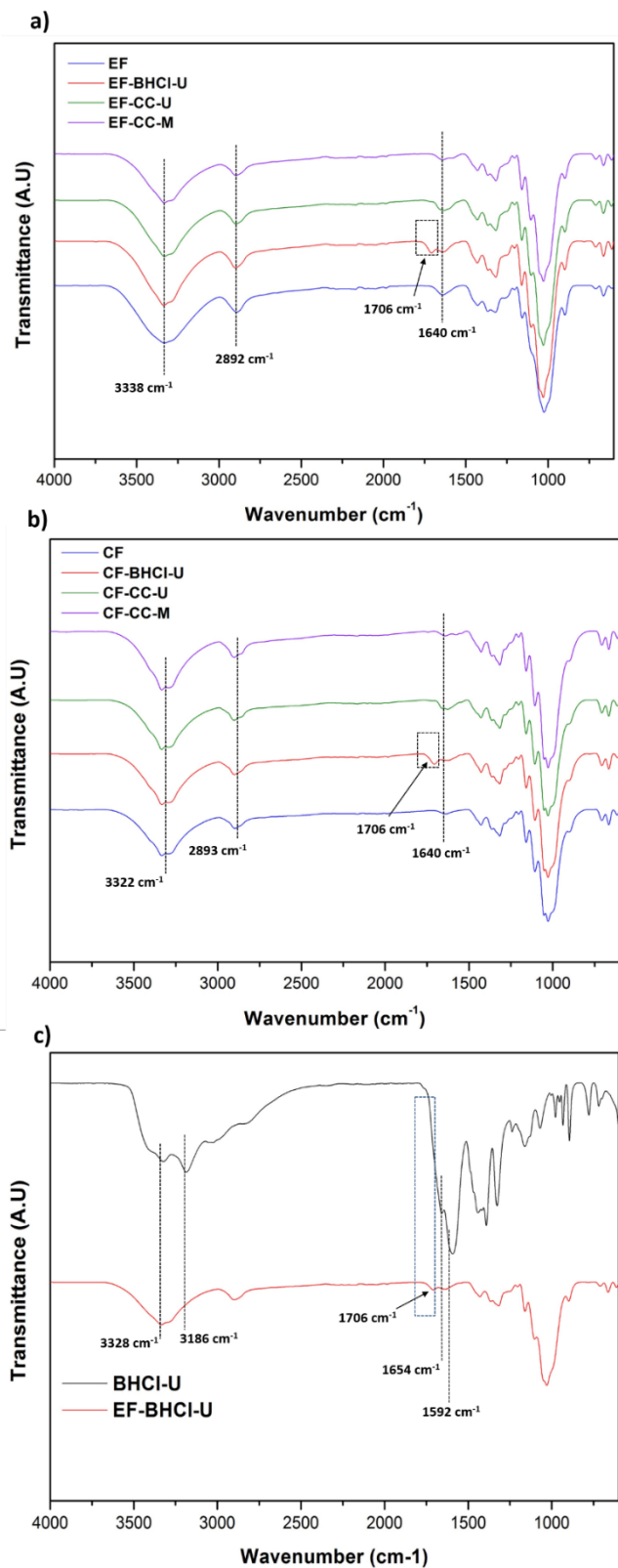


Figure II. 2. ATR-FTIR spectra of DES-treated eucalyptus(a), cotton fibres (b) and EF-BHCl-U compared to BHCl-U (c).

II.1.3.1.2 Solid-state ^{13}C NMR of DES/enzyme treated eucalyptus fibres

The NMR spectra of DES or enzyme treated eucalyptus fibres are presented in Figure II. 3a and compared to that of the cellulose fibres before any treatment. Here again, all the carbon peaks related to cellulose structure reported in the literature (Johan Foster et al., 2018; Kono et al., 2004) are observed. As expected, the chemical shifts are due to the contribution of C6 (62.8 ppm for amorphous cellulose, 65.3 for crystalline cellulose), C5 (72.8 ppm), C4 (82.9 ppm for amorphous cellulose and 89 ppm for crystalline cellulose), C3 (75.2 ppm), C2 (72.4 ppm) and C1 (104.9 ppm).

Additional peaks are observed with acidic and neutral DES-treatment. The spectrum of acidic DES-treated fibres presents two new small peaks. The first peak at 54.4 ppm is attributed to the methyl of quaternary ammonium ($-\text{N}(\text{CH}_3)_3^+$), while the second one at 158.7 ppm is related to a carbonyl group. This carbonyl group is different from that observed on the spectrum of the DES and its components (Figure II. 3b). This indicated that this is a new function group. The presence of the peaks related to the methyl of quaternary ammonium clearly evidenced that an esterification occurred between cellulose and BHCl with a relatively low degree of substitution (DS = 0.025).

At the opposite of the result present by Willberg-Keyriläinen et al. (2018) that reported only carbamation of cellulose with BHCl-U system, in our case we clearly demonstrated that an esterification occurred. The different reactivity of BHCl-U could be due to the experimental conditions since DES treatment was carried out during 1 or 4 h, while for Willberg-Keyriläinen et al. (2018) the reaction time was about 20 h. In conclusion, shorter duration of treatment seems to favour esterification. The proposed mechanism of the cellulose esterification is described in Figure II. 3c. Esterification mechanism can be occurred in three steps: (i) protonation of the carbonyl group of betaine hydrochloride; (ii) nucleophilic addition of the cellulose alcohol and (iii) deprotonation.

CHAPTER II. STUDY OF DES PRE-TREATMENT EFFECTS ON CELLULOSE STRUCTURE

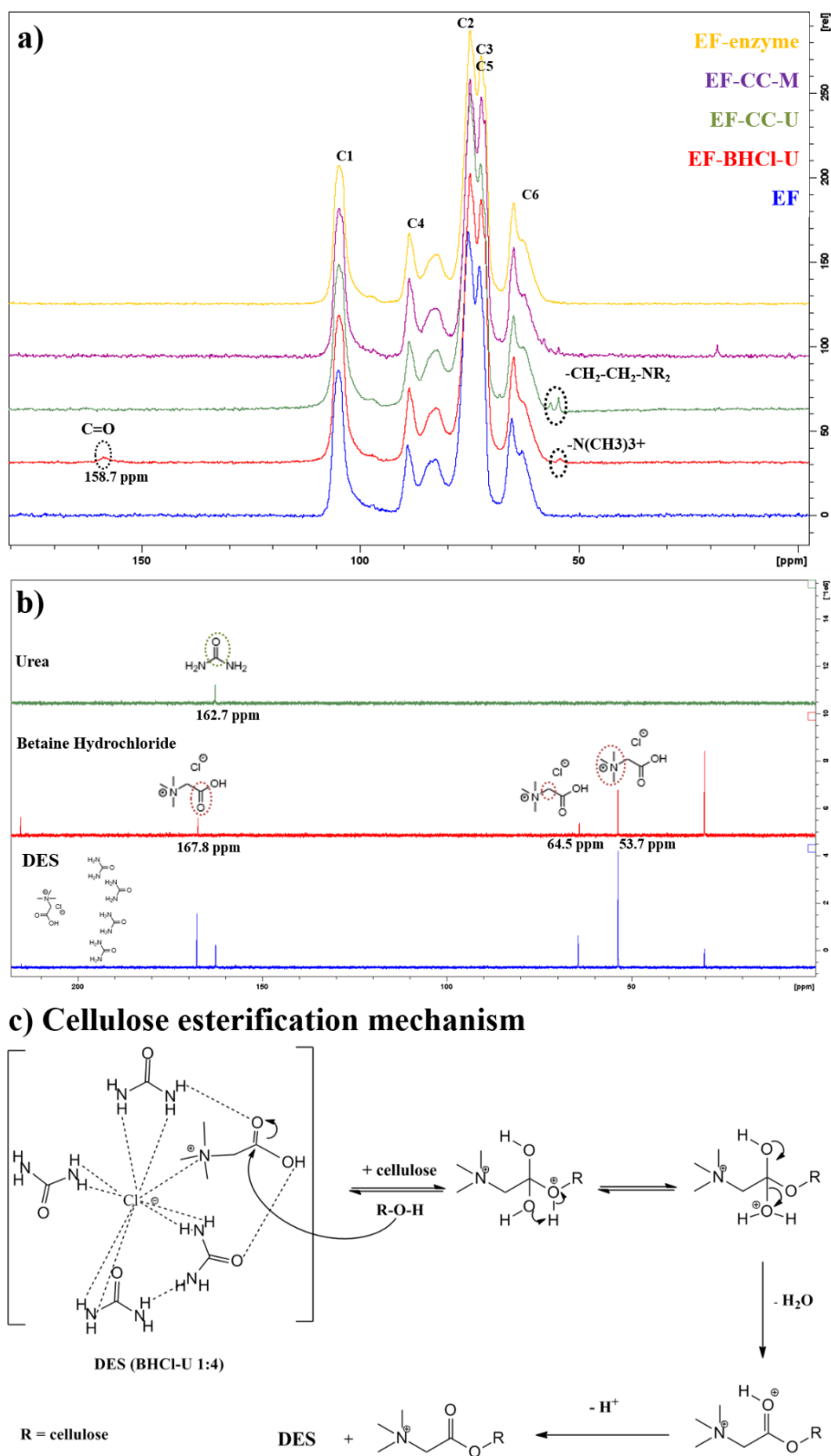


Figure II. 3. ¹³C NMR spectra of DES or enzymatic treated eucalyptus fibres (a), DES (BHCl-U) and its components (b) and the proposed mechanism of cellulose esterification (c).

It is interesting to note that there is only one article reported cellulose esterification using BHCl-based DES but in the presence of p-toluenesulfonyl (tosyl) chloride as catalyst (Sirviö, 2018). With neutral DES-treatment two small peaks also appeared around 54.7 and 56.4 ppm which can be assigned to the three methyl groups of the quaternary ammonium and the methylene group bounded to the alcohol of CC, respectively (Delso et al., 2019). However, we assumed that the peaks are rather CC contaminations, certainly by absorption, than an effective linkage onto cellulose because no reasonable coupling reaction could occur between cellulose and CC.

II.1.3.2 Chemical composition of DES-treated eucalyptus fibres

EF are mainly composed of cellulose, a polymer of β -(1,4)-linked glucose, and xylan, a polymer of β -(1,4)-linked xylose, which is the major component of hardwood hemicelluloses (Spiridon and Popa, 2008). Indeed, the carbohydrate composition of studied EF exclusively showed glucose and xylose, and no other sugar was detected (see Table II. 1). The chemical composition of DES-treated EF reveals that hemicellulose content decreases for both acidic and neutral DES, from 22 to 17 and 18%, respectively. However, alkaline CC-M system does not affect hemicellulose content. These results are in line with other studies showing that a selective dissolution or reactivity can be achieved, depending on the pH and components of DES (Mäki-Arvela et al., 2011; Suopajarvi et al., 2020). Generally speaking, the higher reactivity of hemicelluloses is due to their amorphous structure which facilitates their dissolution and their shorter chain lengths (Xiao et al., 2001).

II.1.3.3 Degree of polymerisation

The DP of DES or enzymatic-treated cellulose fibres was determined from intrinsic viscosity in cupri-ethylene-diamine. The evolution of the DP with the treatment time for both eucalyptus and cotton fibres is presented in Figure II. 4. For eucalyptus fibres, the DP decreased significantly with acidic DES from 848 to 692 and 657 after 1 and 4 h, respectively. This decrease is slightly less pronounced with alkaline DES treatment. However, DP is preserved after 1 and 4 h of CC-U treatment, with final values of 815 and 810 respectively.

DP of cotton fibres also decreased after DES treatment but not with the same trend. This behaviour is probably related to the weakness of this raw material, as illustrated by its very low initial DP, which may result from the preparation method of these fibres. Indeed,

CHAPTER II. STUDY OF DES PRE-TREATMENT EFFECTS ON CELLULOSE STRUCTURE

depolymerisation occurs in all cases, with similar DP values for acidic and neutral DES, effect being more marked in alkaline conditions.

Enzymatic hydrolysis leads to an expected decrease of the DP which is explained by enzyme's action (hydrolysis) on cellulose chains. Thus, DP decreases from 848 to 540 and from 572 to 446 for eucalyptus and cotton fibres respectively.

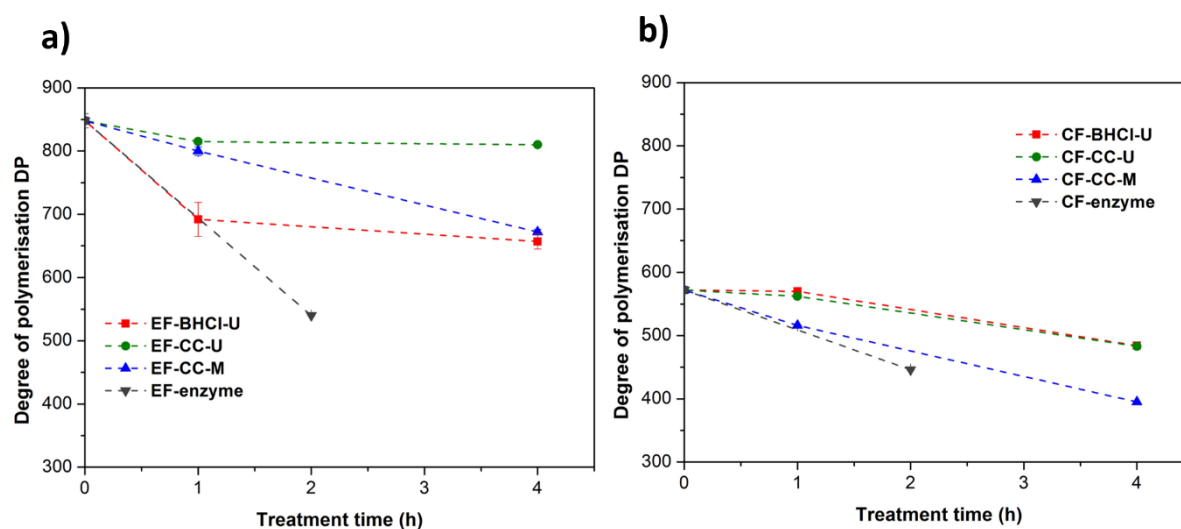


Figure II. 4. DP evolution of DES-treated eucalyptus (a) and cotton fibres (b).

The decrease of the DP in acidic DES is well discussed in the literature. In fact, this phenomenon results from glycosidic bond cleavage catalysed by acidic solvents and many acidic DES (formic acid, acetic acid, lactic acid-choline chloride) are known to lower the DP during delignification of lignocellulosic biomass (from 839 to 397, 367 and 323, respectively) (Tian et al., 2020). Thus, Sirviö and Heiskanen (2017) used acidic DES (dimethyl urea-ZnCl₂), as a reactive solvent, to produce cellulose methyl carbamate and observed a significant decrease of DP from 1820 to 686 after 1.5 h of treatment at 150 °C. For eucalyptus fibres, the fact that acidic and alkaline DES are able to reduce cellulose chain, while neutral CC-U system induces a small reduction of DP is in line with previous studies (Suopajarvi et al., 2017; Tenhunen et al., 2018).

II.1.3.4 X-ray Diffraction and Crystallinity Index

X-ray diffraction patterns (Figure II. 5) of cellulose fibres before and after DES or enzymatic treatment are typical of cellulose I β crystalline structure. The diffraction peaks at 2θ angles of 15.2, 16.5, 22.5 and 34.5° are related to the (11 $\bar{0}$), (110), (200) and (004) lattice planes respectively (French, 2014; Park et al., 2010). The diffractograms show that cellulose crystalline structure remained the same as the original fibres (cellulose I β) for both eucalyptus and cotton fibres due to the absence of other crystalline allomorphs of cellulose. From these results, it can be deduced that there was no regeneration even with alkaline DES. These results are in line with other studies in the literature (Hong et al., 2020; Suopajarvi et al., 2017). As expected, cotton fibres present a more crystalline structure than eucalyptus fibres: for the untreated fibres, CrI values i.e 87.0 and 80.2% were obtained from CF and EF respectively. In addition, the peaks at 15.2 and 16.5° of the diffractogram are more separated for cotton fibres which indicates that this structure is more crystalline. Indeed, the fact that this separation is not clearly observed with untreated eucalyptus fibres is due to the presence of more amorphous regions and also the presence of hemicelluloses.

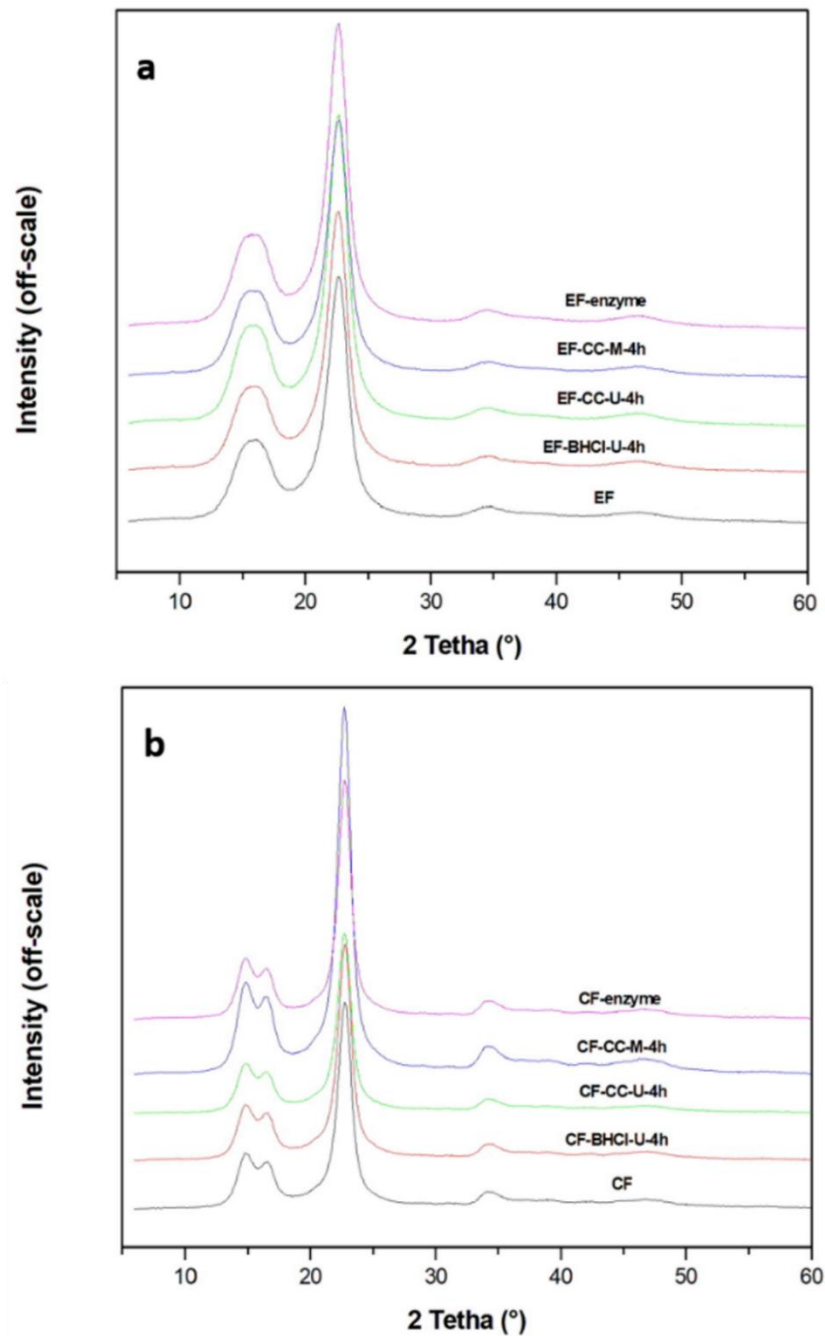


Figure II. 5. XrD diffractograms of treated-eucalyptus fibres (a) and cotton fibres (b)

It can be noticed that the cellulose crystallinity is almost unchanged with DES-treatment, while a slight increase with enzymatic hydrolysis was observed. In this case, the selective hydrolysis of amorphous regions may explain this behaviour.

CHAPTER II. STUDY OF DES PRE-TREATMENT EFFECTS ON CELLULOSE STRUCTURE

The crystallinity index of DES or enzymatic treated eucalyptus fibres was also analysed by ^{13}C NMR solid-state using the integration on C4. Table II. 1 gives the values obtained from XrD and ^{13}C NMR. CrI from ^{13}C NMR are lower than those obtained from XrD. This difference is explained by the better sensitivity of ^{13}C NMR and the fact that Segal method gives always higher values. Whereas CrI from XrD measurements are more or less constant, ^{13}C NMR allows observing a significant increase of CrI with alkaline DES, followed by acidic DES and enzymatic hydrolysis. Neutral DES only exhibits a slighter change. Consequently, amorphous parts are probably removed from cellulose fibres by alkaline DES. It is known that alkaline treatment allows increasing the crystallinity as observed with other treatments such as ammonia treatment at higher temperature (Mittal et al., 2011) or combination of NaOH (10 wt %) with enzymatic treatment (Banvillet et al., 2021). However, with these alkaline treatments, the initial allomorph of cellulose is changed which is not the case with DES-treatment. For BHCl-U, its effect on crystallinity is comparable to that of enzymatic hydrolysis which is probably due to the acidic pH of both treatments. For concluding, DES can be considered as mild treatment media for cellulose because it maintains the same cellulose allomorph during treatment.

CHAPTER II. STUDY OF DES PRE-TREATMENT EFFECTS ON CELLULOSE
STRUCTURE

Table II. 1. Chemical composition, Crystallinity Index CrI of DES and enzymatic treated eucalyptus fibres and cotton fibres.

		EF	BHCl-U	CC-U	CC-M	Enzyme
Eucalyptus fibres						
Chemical composition	Cellulose (%)	78	83	82	78	n.d
	Hemicelluloses (%)	22	17	18	22	n.d
CrI-XrD (%)		80.2	80.4	81.4	80.5	82.7
CrI-¹³C NMR (%)		38.2	41.0	37.8	45.4	41.6
Cotton fibres						
		CF	BHCl-U	CC-U	CC-M	Enzyme
CrI-XrD (%)		87.0	87.7	86.6	88.7	88.9

n.d: not determinate

II.1.3.5 Thermogravimetric analysis

The thermogravimetric analysis TGA/DTG of eucalyptus and cotton fibres (Figure II. 6) before and after treatment were analysed. All the curves showed the presence of two thermal degradation patterns translated into weight loss (%). The first stage (35-100 °C) is the water evaporation. Stage 2 is related to hemicelluloses in the case of EF (200-300 °C) and cellulose decomposition (270-400 °C).

Untreated EF were characterised by cellulose degradation onset temperature at 358 °C and 362 °C with air and nitrogen respectively. Cellulose decomposition onset temperature of treated EF was not modified in the significant way. For cotton fibres, cellulose decomposition onset temperature was 360 °C with both gases. Here again, thermal stability was maintained after the

CHAPTER II. STUDY OF DES PRE-TREATMENT EFFECTS ON CELLULOSE STRUCTURE

treatment, except for alkaline DES. In this case, decomposition onset temperature increased from 360 to 369 °C with both gases.

These results demonstrated that DES treatment did not negatively impact the thermal stability of cellulose.

CHAPTER II. STUDY OF DES PRE-TREATMENT EFFECTS ON CELLULOSE STRUCTURE

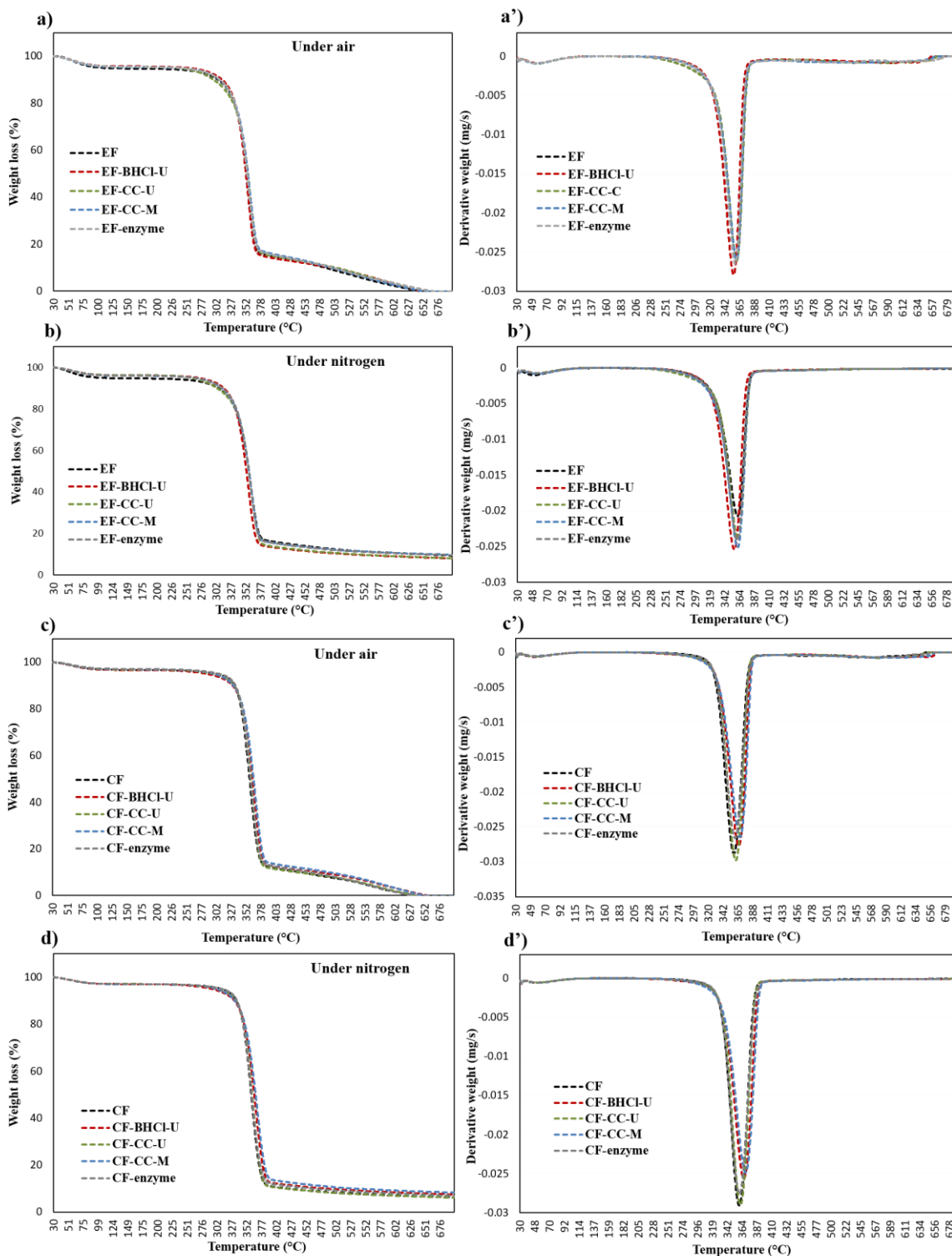


Figure II. 6. TGA and DTG curves of DES/enzyme treated eucalyptus (a, a' and b, b') and cotton fibres (c, c' and d, d') under air and nitrogen respectively.

II.1.3.6 Scanning Electron Microscopy (SEM)

SEM images of eucalyptus and cotton fibres before and after DES pre-treatment as well as enzymatic hydrolysis are illustrated in Figure II. 7. From these images, it clearly appears that the fibres have undergone changes during the treatment with neutral and alkaline DES. The most remarkable observation is the appearance of macrofibrils partially detached of the fibres which create a network between the fibres. The effect of the treatment seems to be the same for the two pulps, although it is more pronounced for cotton fibres. Compared to neutral and alkaline DES, acidic solvent has much less effect on the production of macrofibrils. Finally, no visible macrofibrils were detected after enzymatic treatment and the fibres seem to be less bound to each other. The observation of a network of macrofibrils after DES pre-treatment is similar to the refining effect as described in the literature (Banvillet et al., 2021).

SEM images of the produced papers from eucalyptus fibres, before and after alkaline DES pre-treatment or enzymatic hydrolysis, are also presented in Figure II. 7. These images confirm the presence of a network of macrofibrils created after DES pre-treatment indicating an external fibrillation of the fibres. This fibrillation is not observed with enzymatic hydrolysis. DES pre-treatment can thus be considered as a green and soft chemical refining of the cellulosic fibres.

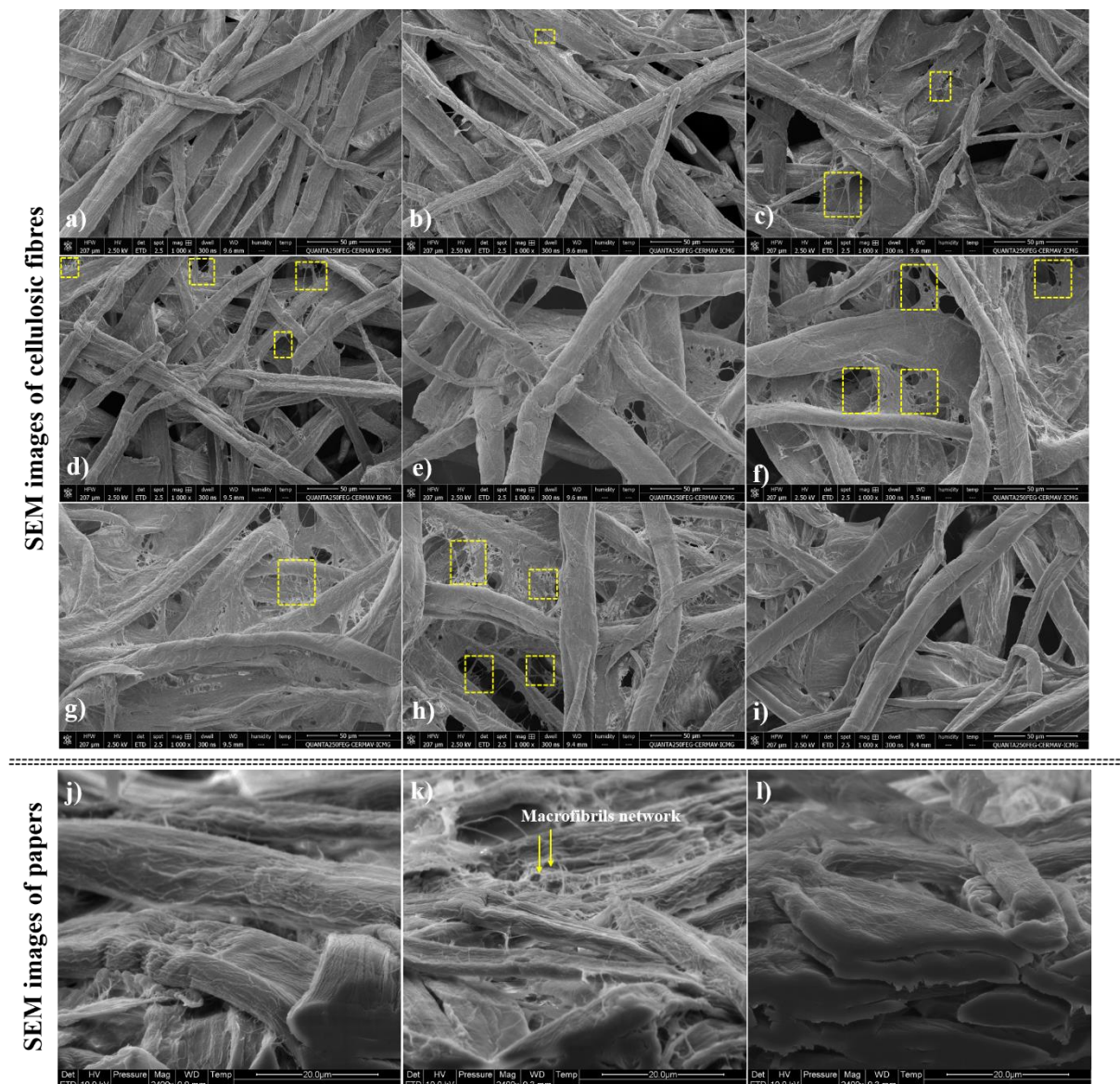


Figure II. 7. SEM images of eucalyptus fibres before and after acidic, neutral and alkaline DES treatment (a, b, c, d), cotton fibres before and after acidic DES, neutral, alkaline DES and enzymatic hydrolysis (e, f, g, h, i) respectively and images of papers produced from EF (j), alkaline DES (k) and enzymatic hydrolysis (l).

II.1.3.7 Morphological properties of fibres

Morphological properties were studied by analysing fibre length and width as well as fine content. According to the results reported in Table II. 2, there was no significant change in length and width of cellulose fibres (EF and CF), even after 4h of DES treatment. However, fine content slightly increased for eucalyptus fibres from 13.1 to 18.5, 16.4 and 15.3% after 4

CHAPTER II. STUDY OF DES PRE-TREATMENT EFFECTS ON CELLULOSE STRUCTURE

h of treatment in acidic, neutral and alkaline DES, respectively. For cotton fibres, it remained more or less constant whatever the treatment which can be attributable to the initial high content of fine elements in this pulp. Contrary to DES pre-treatment, enzymatic pre-treatment leads to a slight decrease in fibre length. In this case, the fine content increased much more significantly from 13.1 to 30.6% and from 35.8 to 56% for EF and CF, respectively. This increase was expected and it is related to the hydrolysis of cellulose chain by enzymes that leads to fine element liberation which is in accordance with literature (Banvillet et al., 2021).

Table II. 2. Morphological properties of DES/enzyme treated eucalyptus and cotton fibres

	EF	BHCl-U	CC-U	CC-M	Enzyme
Mean arithmetic length μm	523 \pm 4	511 \pm 1	508 \pm 1	512 \pm 3	446 \pm 3
Mean width μm	16.4 \pm 0.1	16.3 \pm 0	16.7 \pm 0.1	17.3 \pm 0.1	16.2 \pm 0.1
Fine content (% in length)	13.1 \pm 1.1	18.5 \pm 0.2	16.4 \pm 0.2	15.3 \pm 0.1	30.6 \pm 0.7
	CF	BHCl-U	CC-U	CC-M	Enzyme
Mean arithmetic length μm	453 \pm 3	480 \pm 4	434 \pm 3	481 \pm 3	415 \pm 1
Mean width μm	19.3 \pm 0.2	19.3 \pm 0.1	19.4 \pm 0.1	19.8 \pm 0.1	18 \pm 0
Fine content (% in length)	35.0 \pm 1.1	35.8 \pm 0.3	40.3 \pm 0.6	35.8 \pm 0.8	56 \pm 0.2

II.1.3.8 Water Retention Value WRV of DES-treated fibres

WRV of DES treated eucalyptus and cotton fibres are presented in Figure II. 8. These results show that WRV increased with DES treatment time. As expected, water swelling of eucalyptus fibres was more important than that of cotton fibres and the impact of DES treatment was also more pronounced. WRV increased after DES treatment from 100 to 110, 128 and 137% respectively with BHCl-U, CC-U and CC-M, for eucalyptus fibres, which corresponds to a maximum relative increase of 37%. In the case of cotton fibres, WRV varied from 66 to 81% with CC-M, the relative increase being of 23%. WRV, which is related to the swelling ability

of fibres, depends on the accessibility of the cell wall to water. This accessibility is promoted by internal fibrillation, which usually results from mechanical refining of the pulp suspension. DES treatment, and more precisely neutral and alkaline DES, seem to have the same effect than a mechanical treatment (refining): internal fibrillation occurs (revealed by WRV) as well as external fibrillation (revealed by the presence of macrofibrils) as observed by SEM. In contrast to what happens during a conventional refining process (Gharehkhani et al., 2015), the generation of fine elements is limited and the shortening of the fibres does not occur.

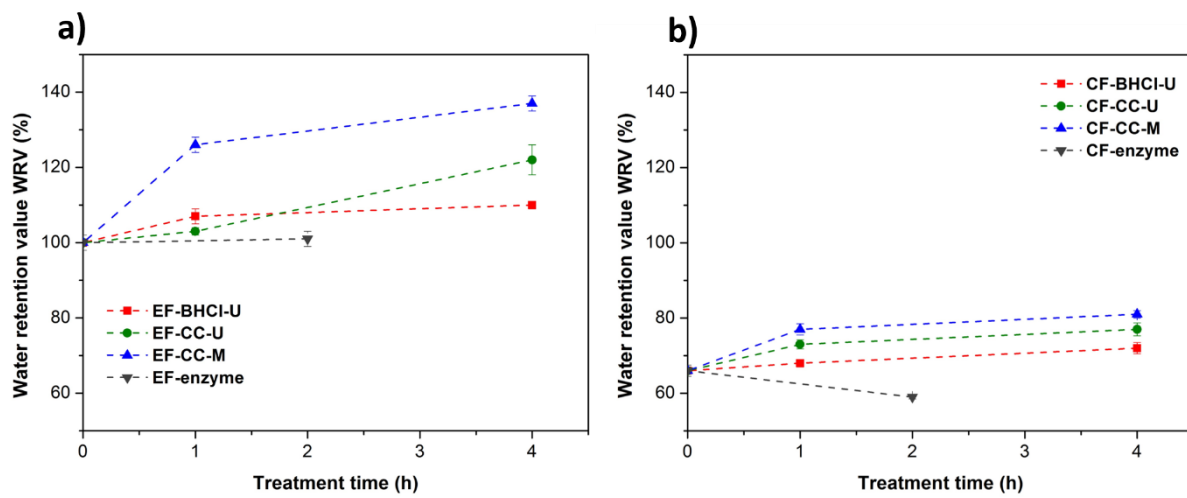


Figure II. 8. WRV evolution of cellulose fibres EF (image a) and CF (image b) according to DES/enzyme treatment time.

After enzymatic pre-treatment, WRV remains unchanged for eucalyptus fibres and decreases for cotton fibres. This decrease could be related to cellulose degradation by enzyme that attack amorphous regions of cellulose, that have the greatest affinity with water.

II.1.3.9 Mechanical properties of produced papers from DES treated eucalyptus fibres

The mechanical properties of papers produced from untreated eucalyptus fibres (EF), enzymatic treated fibres (EF-enzyme) and alkaline-DES treated fibres (EF-CC-M) were analysed. The evolution of the Young's modulus, density, internal bond strength, tensile strength index, tear resistance index and elongation at break is depicted in Figure II. 9.

A first observation is the significant increase of the density after DES treatment: it rises from 514 to 565 kg/m³. Oppositely, after enzymatic treatment, the change is neglectable. This

increase, for papers made of DES-treated fibres, reflects a densification of the fibrous network. This is in agreement with the results already discussed. The increase in internal fibrillation plays a role in the increase in fibre hydration, which leads to a better flexibility and conformability of the fibres. All these phenomena favour a larger contact surface area between the fibres in the fibre network: more hydrogen bonds are formed and a densification of the structure occurs after drying.

As expected, the previously discussed evolution of the microstructure of the paper leads to an improvement in its mechanical properties. For DES-treatment, the Young's modulus increases from 1.87 to 2.66 GPa. In the same way, tensile strength index and internal bond strength increased by 66% and 207%, respectively. Finally, it is worth noting that, as the length of the fibres is preserved, the tear strength was significantly improved after DES-treatment, varying from 2.9 to 4.3 mN.m²/g. Oppositely, the properties of the paper made from enzymatically treated fibres remain more or less constant.

To conclude, results show a very significant effect of DES on the properties of the papers produced. This effect is similar to a "chemical" refining of the fibre suspensions, but without the drawbacks of this mechanical process. DES are able to increase the bonding degree in papers in a great extent while preserving tear strength.

CHAPTER II. STUDY OF DES PRE-TREATMENT EFFECTS ON CELLULOSE STRUCTURE

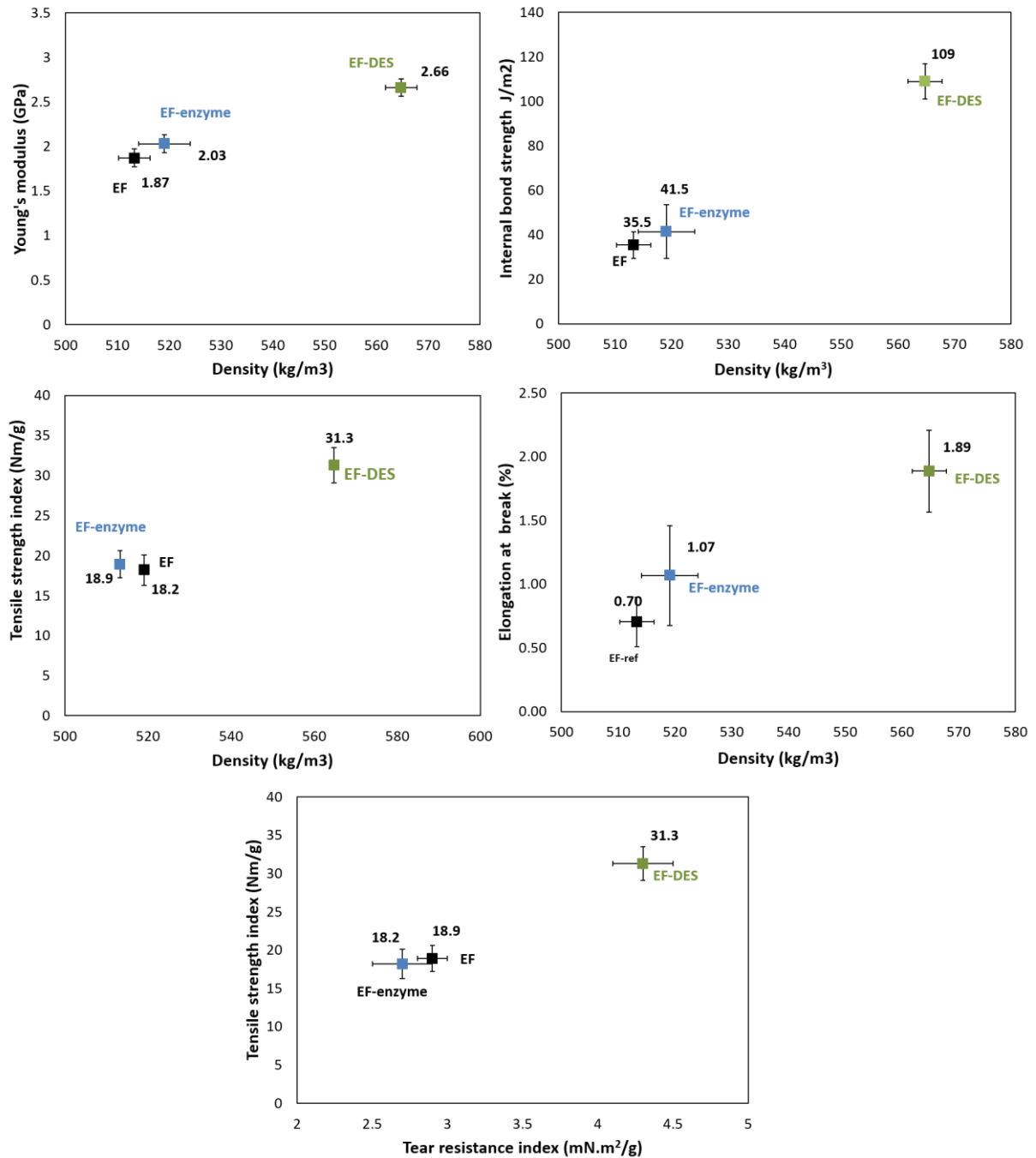


Figure II. 9. Evolution of the mechanical properties of produced papers from eucalyptus fibres before and after DES (CC-M) or enzymatic treatment.

II.1.4 Conclusion

In this study, three DES systems were used for the treatment of cellulose (eucalyptus and cotton) fibres. The structural characterisation of DES-treated cellulose using solid-state ¹³C NMR

CHAPTER II. STUDY OF DES PRE-TREATMENT EFFECTS ON CELLULOSE STRUCTURE

reveals cellulose esterification with BHCl using acidic DES, while no modification was observed with neutral or alkaline DES-treatment. The chemical composition of eucalyptus fibres was modified by DES treatment, but only with acidic and neutral DES. They promote the partial removal of xylan. Therefore, these findings highlight the reactive selectivity of these systems which depends on the DES components. DP and crystallinity index were impacted by the DES at different extents depending on the pH, whereas thermal properties were not modified.

In addition, it can be demonstrated that DES treatment causes both internal fibrillation (increase of the WRV) and external fibrillation (macrofibrils appearance). As a consequence, mechanical properties of the produced papers are enhanced in a very significant way by increasing the bonding degree and preserving fibre length. The obtained results are very interesting as the treatments proposed in this study may be similar to a chemical refining. The perspectives are to study the effect of these treatments for the production of microfibrillated cellulose and, more precisely, how they could facilitate the microfibrillation process. Moreover, the recycling of the DES must be also investigated to evaluate the stability and efficiency of the used DES and to assess their real impact on environment.

CRedit authorship contribution statement

A.M: Investigation, conceptualization, visualisation, writing - Original Draft. H.D: supervision. R.K: supervision. S.H: Supervision, conceptualization, validation, Writing-Reviewing and Editing, Funding acquisition. E.M: supervision, conceptualization, validation, Writing-Reviewing and Editing, Funding acquisition.

Acknowledgements

This work was financially supported by the “PHC Utique” program of the French Ministry of Foreign Affairs and Ministry of higher education, research and innovation and the Tunisian Ministry of higher education and scientific research in the CMCU project number TN 18G1132// FR 39316VF. LGP2 is part of the LabEx Tec 21 (Investissements d’Avenir - grant agreement n° ANR-11-LABX-0030) and of PolyNat Carnot Institute (Investissements d’Avenir - grant agreement n° ANR-16-CARN-0025-01). This research was made possible thanks to the

CHAPTER II. STUDY OF DES PRE-TREATMENT EFFECTS ON CELLULOSE STRUCTURE

facilities of the TekLiCell platform funded by the Région Rhône-Alpes (ERDF: European regional development fund).

The authors would like to thank Isabelle Jeacomine and Christine Lancelon-Pin from CERMAV Grenoble, France for solid-state ^{13}C NMR analysis and SEM observations respectively. We would like also to thank Thierry Encinas from CMTC – Grenoble, France for the XRD analysis.

II.2 High-Performance Size Exclusion chromatography HPSEC to study DES effects on cellulose structure

Abstract

High-Performance Size Exclusion Chromatography (HPSEC) has been widely investigated to analyse cellulose molecular mass distribution (MMD). In this paper, cellulose fibres (eucalyptus pulp and cotton linters pulp) treated by Deep Eutectic Solvents (DES) and enzymatic hydrolysis (used as a reference) were analysed by HPSEC. DES treatment was performed for 4 h at 100 °C using betaine hydrochloride-urea (BHCl-U), choline chloride-urea (CC-U) and choline chloride-monoethanolamine (CC-M). The obtained results showed that the polymer dispersity index (\mathcal{D}_M) has changed after fibre treatment; it is increased with CC-U and enzymatic hydrolysis, reduced with BHCl-U, and slightly changed with CC-M. It was suggested that enzymatic hydrolysis and CC-U act on cellulose fibres by cutting on their extremity (slight change in M_w and significant decrease of M_n), whereas, CC-M acts by cutting larger fragments (decrease of M_w only). Intrinsic viscosity (IV), hydrodynamic radius (R_h) and radius of gyration (R_g) are also modified after treatment. Radius evolution showed that, on the one hand, the polymer produced from CC-M is swollen, while that produced from BHCl-U is rigid and very elongated. On the other hand, spherical polymers were produced from eucalyptus and cotton fibres using enzymatic hydrolysis and CC-U treatment, respectively. This study highlights the potential of HPSEC to study cellulose changes after DES or enzymatic treatment, giving a better understanding of their effects.

Key words: High-performance size exclusion chromatography, molecular mass distribution, cellulose fibres, deep eutectic solvents, enzymatic hydrolysis.

II.2.1 Introduction

Size exclusion chromatography (SEC) is a separation technique that is widely used to characterise the molar mass distribution (MMD) of polymers (Brewer et al., 1968; Lauriol et al., 1987; Pawcenis et al., 2015). It has been widely applied on cellulose (Leskinen et al., 2015; Sjöholm and Wadsborn, 2022), in particular to observe the changes of cellulose MMD during chemical treatments (Wood et al., 1986). SEC was also used to study the degradation of papers (Dupont and Mortha, 2004; Łojewski et al., 2010).

Cellulose is the most abundant polymer on earth and it is described as a flat linear chain formed by the repetition of β -glucopyranose units. The polymer is characterised by an alternance of amorphous and ordered crystalline structures, due to the presence of many hydroxyl groups giving rise to a network of intra- and intermolecular hydrogen bonds. These linkages make the cellulose insoluble in common solvents, among which most classical solvents used for SEC (Wu, 2003). To resolve this, one possibility is cellulose derivatisation prior to dissolution in the chromatographic solvent (typically THF (tetrahydrofuran) or pyridine). Another possibility is direct dissolution in a particular suited solvent, DMAC-LiCl (8%). Prior to dissolution, an activation step is generally applied, to facilitate the disruption of the hydrogen bonds in the crystalline regions of the polymer and enhance swelling. This can be realised by solvent exchange (in water or amines) which facilitates direct dissolution or derivatisation (Ono and Isogai, 2021).

In our study, the cellulose derivatisation method using carbanilation was preferred to the direct dissolution method in DMAC-LiCl, since the former is generally more suitable for difficult-to-dissolve samples (Sjöholm et al., 1997). There are a variety of soluble cellulose derivatives which are suitable for SEC, such as cellulose acetate (Ghareeb et al., 2012), cellulose nitrate (Holt et al., 1978; Marx-Figini and Soubelet, 1984), carboxymethylcellulose, methylcellulose and trimethylcellulose (Wu, 2003). The conditions to fulfil are: derivatised cellulose should be fully soluble in the SEC solvent used as mobile phase; derivatisation and dissolution should not degrade cellulose; derivatives should be stable and suited to the stationary phase; the obtained solution should not be highly viscous. Among the different derivatives, cellulose tricarbanilation has been recognised as the best one for MMD analysis by SEC (Kleman-Leyer et al., 1996, 1994; Kleman-Leyer and Kirk, 1994; Srisodsuk et al., 1998). The derivatisation procedure has various advantages (Wood et al., 1986), cellulose is tri-substituted in a rather

CHAPTER II. STUDY OF DES PRE-TREATMENT EFFECTS ON CELLULOSE STRUCTURE

short time by the reagent, phenyl isocyanate, and no depolymerisation is generally observed, either in pyridine or in DMSO, if the limit of temperature is well respected: 65-70 °C in DMSO, 80 °C in pyridine (Henniges et al., 2007). Derivatised cellulose is recovered by precipitation and dissolved in THF, one of the best SEC solvents, and then analysed by SEC. A better alternative is the direct injection of the derivatisation reaction medium in the SEC column, after neutralizing the excess of phenyl isocyanate with methanol and dilution by THF.

Cellulose trinitrate, also easily dissolved in THF, is another possible derivative. Cellulose trinitrates have been much studied at the early time of using SEC for cellulose characterisation. They are rarely used today and only few studies on SEC of cellulose trinitrates have been reported during the past decade. This decrease of interest in using cellulose trinitrate for SEC characterisation is due to the uncertainty of the method, and to the possible cellulose depolymerisation by acid hydrolysis during derivatisation (Wu, 2003). Silylated cellulose has also been studied as a possible derivative for SEC analysis. It was investigated with various silylation agents and solvents such as chloromethylsilane, hexamethyldisilazane, and others. However, a main disadvantage is the need for strong purification after derivatisation, and there are a limited number of reports about SEC using silylated cellulose. Cellulose acetate, an important commercial derivative, also behaves very well in SEC analysis using THF, but the polymer is more or less depolymerised during the process of acetylation, and the possible presence of extra humps in the high molar mass region distort the MMD (Wu, 2003).

In the present study, HPSEC was used to study at the molecular scale the treatment of cellulose fibres using Deep Eutectic Solvents (DES). DES are a class of sustainable designer solvents that can be used as green solvents or reagents (Abbott et al., 2001). They have attracted considerable attention in the field of cellulose chemistry such as surface modification (Li et al., 2021; Liu et al., 2021; Sirviö, 2018; Sirviö et al., 2021, 2019), microfibrillation (Hong et al., 2020; Kwon et al., 2021; Sirviö et al., 2020, 2015; Suopajarvi et al., 2017; Yu et al., 2021) and nanocrystals production (Douard et al., 2021; Ling et al., 2019; Sirviö et al., 2016). In a previous study (Mnasri et al., 2022), cellulose fibres were treated with three DES systems namely betaine hydrochloride-urea (BHCl-U), choline chloride-urea (CC-U) and choline chloride-monoethanolamine (CC-M), used as acidic, neutral and alkaline systems, respectively. The morphological, structural and mechanical properties of DES-treated fibres were studied. It was established that with acidic DES treatment (BHCl-U), an esterification reaction occurs between

CHAPTER II. STUDY OF DES PRE-TREATMENT EFFECTS ON CELLULOSE STRUCTURE

BHCl and cellulose. Conversely, no chemical modification was observed with CC-U and CC-M. Moreover, it was shown that DES treatment (especially CC-M system) allows to increase the swelling capacity of the fibres and enhances the mechanical properties of produced paper handsheet. This treatment was compared to enzymatic hydrolysis used as a reference treatment. The comparison has shown that enzymatic hydrolysis has no effect on the swelling capacity of cellulose fibres and no enhancement of the mechanical properties was observed. The interesting results obtained with DES demonstrate their effectiveness and potential for use as pre-treatment to produce microfibrillated cellulose (MFC) with high quality.

Here, DES-treated fibres were characterised by HPSEC in order to understand DES effect at the molecular scale. This treatment is compared to enzymatic hydrolysis.

II.2.2 Materials and Methods

II.2.2.1 Materials

Dry sheets of bleached hardwood pulp (eucalyptus, Fibria T35, EF) and cotton linters pulp (CELSUR, CS 21 DHS, CF) were used as cellulose raw materials. These fibres were first disintegrated in water using a laboratory pulper (Lhomargy). Fibre suspensions were then filtered, washed with ethanol and oven dried at 60°C. Betaine hydrochloride ($C_5H_{12}ClNO_2$) and tetrahydrofuran THF (C_4H_8O) were supplied from VWR (Milliporesigma); monoethanolamine (C_2H_7NO , > 99%) and dimethylsulfoxide (C_2H_6OS) from ROTH; choline chloride ($C_5H_{14}ClNO$, > 98%) from Alfa Aeser; acetic acid (CH_3COOH), ethanol (CH_3OH , 96%), sodium acetate ($C_2H_3NaO_2$), urea ACS reagent (CH_4N_2O , 99.0-100.5%) and phenyl isocyanate (C_6H_5NCO , 98%) from Sigma Aldrich; Enzyme solution FiberCare (pH between 6 and 8) was purchased from Novozymes. Deionised water or Milli-Q water was used throughout the experiments.

II.2.2.2 Fibre pre-treatment with DES

DES pre-treatment was performed following the procedure explained in our previous study (Mnasri et al., 2022). The three DES were prepared (1) by mixing betaine hydrochloride with urea (1:4 molar ratio) at 100 °C, (2) choline chloride with urea (1:2 molar ratio), (3) choline chloride with monoethanolamine (1:6 molar ratio), at 80 °C, until transparent liquid is obtained.

CHAPTER II. STUDY OF DES PRE-TREATMENT EFFECTS ON CELLULOSE STRUCTURE

Cellulose fibres (EF or CF) were mixed with the prepared DES and the treatment was conducted for 4 h at 100 °C. After the treatment, the suspension was filtered and washed, first with hot water, and then, with cold water to remove all DES traces. DES-treated fibres were finally stored at 4 °C until further use.

II.2.2.3 Fibre enzymatic pre-treatment

Enzymatic pre-treatment is performed as described in our recently study (Mnasri et al., 2022). In brief, cellulose suspension (2%) was mixed with enzyme (FiberCare enzyme) at 50 °C for 2 h at pH 5. Enzyme was then deactivated by increasing the temperature to 80 °C for 10 min. The treated fibres were filtered and washed with hot and cold water to remove all chemical reagents.

II.2.2.4 Cellulose carbanilation

Cellulose tricarbanylation consists in the complete reaction (nucleophilic attack) of phenyl isocyanate, in excess in the medium, with the three hydroxyl groups attached to each anhydroglucose monomer unit of cellulose. The reaction is depicted on the scheme of Figure II. 10. The dried sample is first swelled in DMSO at 70°C in order to improve reagent accessibility in the cellulose interchain network.

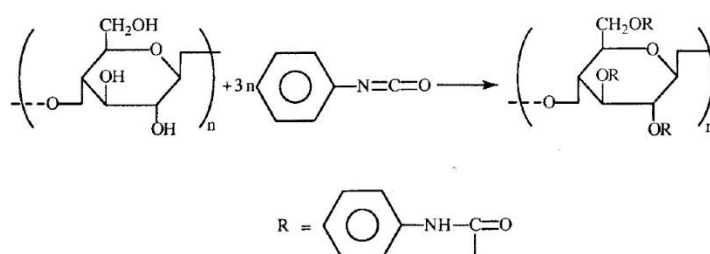


Figure II. 10. Cellulose tricarbanylation mechanism.

Reaction protocol: DES or enzymatic treated fibres were first ground using ball milling (cryomill) for 2 min to reduce their length (until some micrometres). The ground fibres were then oven-dried at 60 °C for 24 h. 125 mg of dried-ground fibres were mixed in glass bottle with 25 mL of DMSO. The mixture was slowly stirred with a magnet overnight at room temperature. After 18 h, the temperature was raised to 70 °C and 5 mL of phenyl isocyanate was slowly added to the mixture (drop by drop, under stirring), followed by the addition of 20 mL of DMSO. The carbanylation reaction was then left to proceed for 48 h at 70 °C. The reaction

CHAPTER II. STUDY OF DES PRE-TREATMENT EFFECTS ON CELLULOSE STRUCTURE

was finally stopped by adding 20 mL of acetone in order to neutralise the residual phenyl isocyanate. The final mixture containing the CTC polymer (cellulose tricarbanilate) was left to cool down under stirring.

II.2.2.5 HPSEC-multidetectors analysis

After cooling down, the reaction medium containing the CTC samples was diluted with THF and then injected in the HPSEC system for MMD analysis.

HPSEC system: Malvern-Viscotek GPC max-TDA 302 including the coupled detectors UV, DRI, LALS-RALS and viscometer. It is equipped with three (300×7.5mm) PLGEL mixed-B-LS columns and a (50 mm×7.5 mm) PLGEL-M-Guard pre-column. The injected volume was 100 μ l (loop injection) with a solvent (THF) flow rate of 1 mL.min⁻¹. The column and detectors temperature was set at 35 °C. The polymer concentration in the injected samples was close to 1 mg/mL. Molar mass calculation is based on the DRI-LALS coupling, with RALS and viscometer bringing some correction in the low mass region. A dn/dC value of 0.165 was taken for CTC dissolved in THF. Knowing the injected sample allows calculating the percentage of polymer recovery throughout the column. The DRI-viscometer coupling enables the calculation of the hydrodynamic radius by the Einstein formula. From the MMDs, weight-average (DP_w) and number-average (DP_n) degrees of polymerisation were calculated by dividing M_w and M_n , respectively, by 519 g/mol, which is the molar mass of the CTC monomer.

II.2.3 Results and discussion

II.2.3.1 SEC analysis of DES and/or enzyme-treated eucalyptus fibres

II.2.3.1.1 Molecular mass distribution (MMD)

In a monomodal polydispersed polymer, the weight average molar mass and DP (M_w , DP_w), number-average molar mass and DP (M_n , DP_n) and dispersity index (\mathcal{D}_M) are the conventional values to estimate the mean polymer chain length, and the width of the chain length distribution around mean values. They are calculated from molar mass distributions curves by the following formula:

$$M_w = \frac{\sum N_i M_i^2}{\sum N_i M_i} \quad M_n = \frac{\sum N_i M_i}{\sum N_i} \quad D_M = \frac{M_w}{M_n}$$

where N_i is the number of chains with molar mass M_i .

Table II. 3 illustrates the results for M_w , M_n , D_M , and the corresponding degree of polymerisation, obtained in the case of the DES-treated and enzyme-treated eucalyptus fibres samples. The recovery yield throughout the chromatographic columns is also reported.

It can be observed that M_w was decreased with both alkaline DES and enzymatic treatments, in a more pronounced way with the alkaline DES-treatment. All treatments, except the acidic DES, reduced M_n , and more significantly with the neutral DES and the enzymatic treatment.

However, both M_w and M_n increased with the acidic DES. The particular case of this sample can be explained by the chemical behaviour of cellulose, which was esterified during acidic DES pre-treatment. Indeed, it was shown by Mnasri et al. (2022) that cellulose pre-treatment using BHCl-U leads to an esterification reaction between cellulose and betaine hydrochloride. The presence of ester groups on cellulose fibres has probably influenced the derivatisation of this sample, for which a low recovery yield was observed during the chromatographic separation (61%).

(Notice. The polymer recovery yield is calculated on the basis of measuring the weight of recovered sample at column exit (by integration of the DRI signal, assuming a known dn/dc value (0.165), a complete derivatisation of the anhydroglucose units ($M = 519$ g/mol) and knowing the weight of the dry cellulosic sample used for derivatisation. Polymer losses may arise from incomplete derivatisation/solubilisation of the polymer, leading to particle or colloids retention at different locations: through the syringe filter used to purify the samples before the injection, through the LS detector filter, through the guard or SEC columns).

It is observed that the dispersity index D_M was changed after the DES and enzymatic treatments. It was decreased with BHCl-U and CC-M treatments, from 2.8 to 2.1 and 2.6, respectively. It was significantly increased with neutral DES and enzymatic treatments, from 2.8 to 3.5 and 3.4, respectively.

CHAPTER II. STUDY OF DES PRE-TREATMENT EFFECTS ON CELLULOSE STRUCTURE

The rise of \mathfrak{D}_M indicates that the polymer is more heterogenous, because of the formation of low molar mass fractions. However, the decrease of \mathfrak{D}_M especially in the case of acidic DES pre-treatment indicates that the polymer chain lengths becomes more uniform.

The average degree of polymerisation (DP_w and DP_n) also vary significantly. The CC-M treatment results in the lowest DP_w , while the enzymatic hydrolysis leads to a significant decrease of the DP_n .

Table II. 3. Molar mass distribution (MMD) and degree of polymerisation (DP) of DES-treated and/or enzymatic-treated eucalyptus fibres.

Sample	Recovery yield (%)	M_w (g/mol)	M_n (g/mol)	$\mathfrak{D}_M = \frac{M_w}{M_n}$	DP_w	DP_n
EF	91	349 000	125 000	2.80	673	240
EF-BHCl-U	61	437 000	201 000	2.18	843	387
EF-CC-U	100	354 000	102 000	3.47	682	197
EF-CC-M	100	294 000	111 000	2.65	566	213
EF-enzyme	100	332 000	97 000	3.41	639	187

The MMD curves before and after DES and enzyme treatments are presented in Figure II. 11.

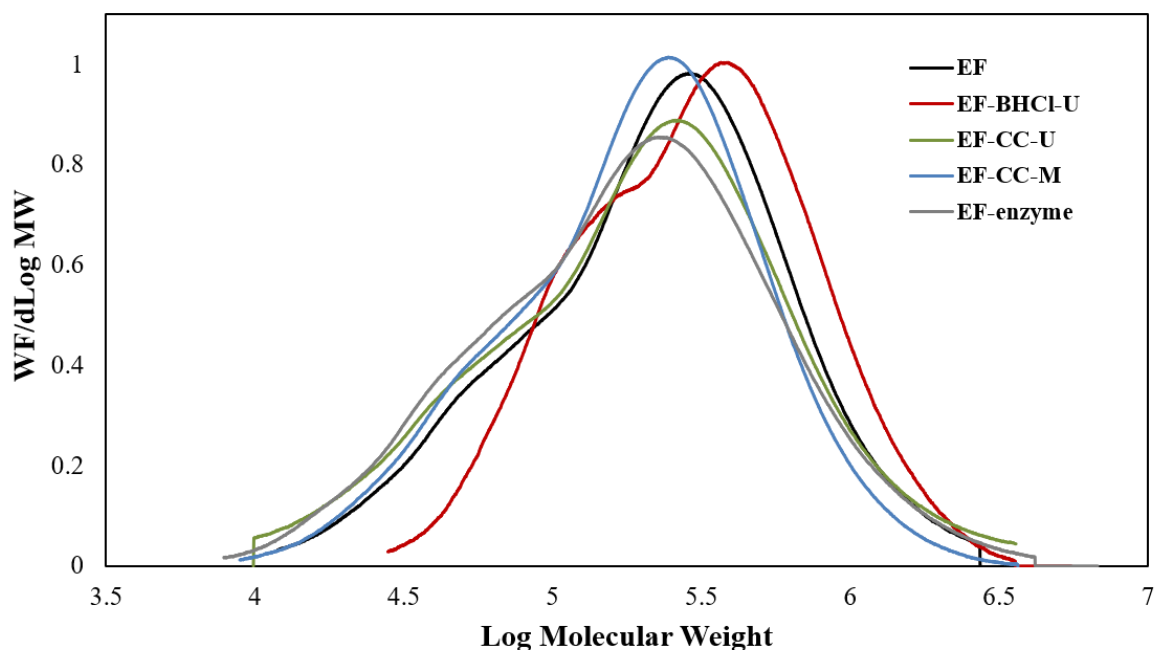


Figure II. 11. The molar weight distribution of DES and/or enzyme treated eucalyptus fibres.

On all curves, before and after treatment, two populations can be observed: a major population made of large molecules, centred at a peak around $\log M = 5.5$ (which corresponds to a DP of about $10^{5.5}/519 = 610$), and a minor population of small molecules, represented by the left shoulder on the curves at $\log M$ around 4.5 – 4.7 (corresponding to $DP = 75$). The first (major) population corresponds to main cellulose chains, whereas the second (minor) population corresponds to hemicelluloses chain (residual xylan).

Changes can be observed after all treatments. Alkaline and neutral DES samples, as well as enzymatic sample, exhibited curve shifts towards lower molar mass, while the acidic DES sample displayed a shift towards higher mass. Clearly, with neutral and alkaline DES, and with the enzymatic treatment, the frequency of the smaller molecule population increased (at $\log M$ around 4.5). Moreover, in the higher mass region ($\log M > 5.7$), the alkaline DES sample is the one that presented the most pronounced mass decrease, compared to the enzymatic and neutral DES samples.

From these observations, it can be suggested that the alkaline DES acts on cellulose by cutting some cellulose chains. Cutting the biggest chains leads to the highest decrease in M_w . Since \bar{D}_M remained rather constant, M_n was not very much decreased and thus, the smallest chains were probably extracted from the polymer matrix and dissolved in the DES solution.

CHAPTER II. STUDY OF DES PRE-TREATMENT EFFECTS ON CELLULOSE STRUCTURE

However, enzymatic hydrolysis and neutral DES treatment led to more significant decrease of M_n with quite moderate M_w reduction, thus increasing \mathcal{D}_M . This is probably due to very moderate attack at the chain centre, which would result into a significant decrease of M_w , like in the case of the alkaline DES. Thus, only the chain extremities are likely reacting, producing small chain fragments, poorly dissolved in the liquid medium (because of the lower alkalinity, compared to the alkaline DES case). The increased number of these small fragments in the polymer matrix led to the observed decrease of the M_n value.

The case of the acidic DES treatment appears different. After treatment, the population was shifted towards larger molar mass, the MMD curve is narrower than the others, and the population at $\log M$ around 4.5 had fully vanished. There is still a shoulder at $\log M$ around $\log M = 5.25$, but the peak of the big size, major population, had been shifted at $\log M$ around 5.7, instead of $\log M = 5.5$ before the treatment. It is noticeable that the recovery yield was weak. The loss of the population of small size might be related to column retention, due to the presence of the betaine group grafted on the cellulose fibres, which would impair the good dissolution of such derivatised molecules, thus enhancing their retention as partly dissolved colloids. The observed increase of the higher mass fraction, compared to the untreated fibres, probably results from some condensation reactions that might occur during the DES treatment, or from aggregation reactions between some polar chain fragments in the THF solvent (not a good solvent for polar molecules), and probably remain throughout the SEC columns.

The chromatographic elution curves for each sample (DRI signal versus retention volume) are shown in Figure II. 12.

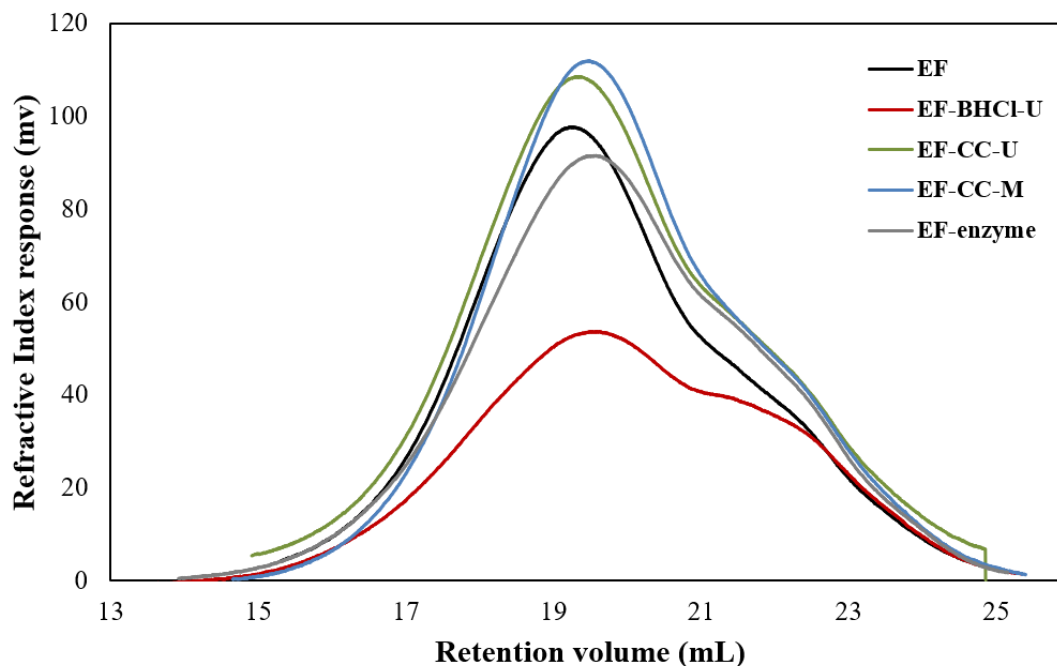


Figure II. 12. Refractive index response and retention volume of DES and/or enzyme treated eucalyptus fibres.

All treated samples except the acidic DES exhibited broader curves than the untreated sample. The total elution time was increased, because of the raise of the lower mass population.

Again, the case of the acidic DES sample is singular. Despite higher mass, this sample was eluted more slowly than the other samples. Moreover, the lower signal intensity illustrates the lower recovery yield throughout the SEC columns. Such an increased retention time in the columns is thus related to the higher polarity of polymer molecules, which causes poorer sample dissolution, likely to be due to imperfect derivatisation of the polymer.

The molar mass at the peak (M_p) and the corresponding DP_p values are displayed in Table II. 4.

CHAPTER II. STUDY OF DES PRE-TREATMENT EFFECTS ON CELLULOSE
STRUCTURE

Table II. 4. Peak molar mass (M_p) and DP_p of DES and/or enzyme treated eucalyptus fibres.

Sample	M _p (g/mol)	DP _p
EF	288 000	555
EF-BHCl-U	357 000	688
EF-CC-U	267 000	514
EF-CC-M	249 000	479
EF-enzyme	232 000	447

It is shown that the acidic DES presented the highest peak mass, whereas the other treated samples (alkaline and neutral DES, and enzymatic treatment) exhibited lower peak mass than the untreated sample. For the latter sample, the slight time shift of the peak position (slightly retarded) appears in agreement with the lower peak mass, compared to the untreated sample. The acidic DES was also slightly retarded, despite its higher mass, which again evidences some physiochemical interaction with the column.

II.2.3.1.2 Intrinsic viscosity, hydrodynamic radius and gyration radius

Table II. 5 presents the results for the intrinsic viscosity (IV), the hydrodynamic radius (R_h), and radius of gyration (R_g) of eucalyptus treated fibres.

The IV value for a polymer dissolved in a given solvent is representative of the swelled volume occupied by the dissolved polymer in this solvent. It depends mainly on the general shape, chain length, on polymer branching, and the solvent swelling effect. It can be also influenced by the presence of some aggregates which decrease the IV.

The reported IV values in Table II. 5 are weight-average values, derived from IV values measured in each solvent slice at column output by the viscosimetric detector. R_h is also a weight-average value, derived from the values in each solvent slice, and calculated by the Einstein formula:

$$R_h = \left(\frac{3 \cdot IV \cdot M}{10 \cdot \pi \cdot N_{av}} \right)^{1/3}$$

where N_{av} is the Avogadro number, IV is the intrinsic viscosity, and M is the molar mass.

CHAPTER II. STUDY OF DES PRE-TREATMENT EFFECTS ON CELLULOSE
STRUCTURE

Finally, the radius of gyration R_g (also a weight average value) is calculated from the slope of the well referred Zimm plot using the two angles of the light-scattering detector (low-angle at 7° , right-angle at 90°).

Table II. 5. Intrinsic viscosity IV , hydrodynamic radius R_h , and radius of gyration R_g of DES and/or enzymatic treated eucalyptus fibres

Sample	IV (mL/g)	R_h (nm)	R_g (nm)
EF	162	18.9	28.7
EF-BHCl-U	158	21.1	49.6
EF-CC-U	153	18.0	28.8
EF-CC-M	159	17.8	28.8
EF-enzyme	150	17.5	24.1

Again, it can be noticed in Table II. 5 that the acidic DES behaves differently than other samples. A trend for small decrease of IV and R_h was observed for the neutral and alkaline DES. Such a decrease is more pronounced for the enzymatic sample. R_g remained almost constant for the alkaline and neutral DES, but slightly decreased for the enzymatic sample.

Contrary to that, for the acidic DES sample, both R_h and R_g increased (more particularly R_g which almost doubles), while IV kept almost constant. The ratio of R_g/R_h increased quite much, compared to other samples. The moderate increase of R_h appears in correlation with the raise of molar mass, but the very important raise of R_g is typical of a change in the polymer structure. The polymer could be more elongated, while more rigid and partly cross-linked (looking at the decrease of IV).

For the other samples, the moderate decrease of all parameters in Table II. 5 are correlated with a similar decrease of molar mass and increase of elution time, compared to the untreated sample, as discussed in the previous paragraph.

Comparing neutral and alkaline DES, it seems that R_g and R_h are rather similar, while M_w is smaller for the alkaline DES. This could be typical of a more pronounced swelling effect of the alkaline DES, compared to the neutral DES and enzymatic hydrolysis. Compared to the latter, the R_g/R_h ratio is smaller, which could be typical of a more spherical shape.

Mark-Houwink-Sakurada (MHS) plots are represented in Figure II. 13.

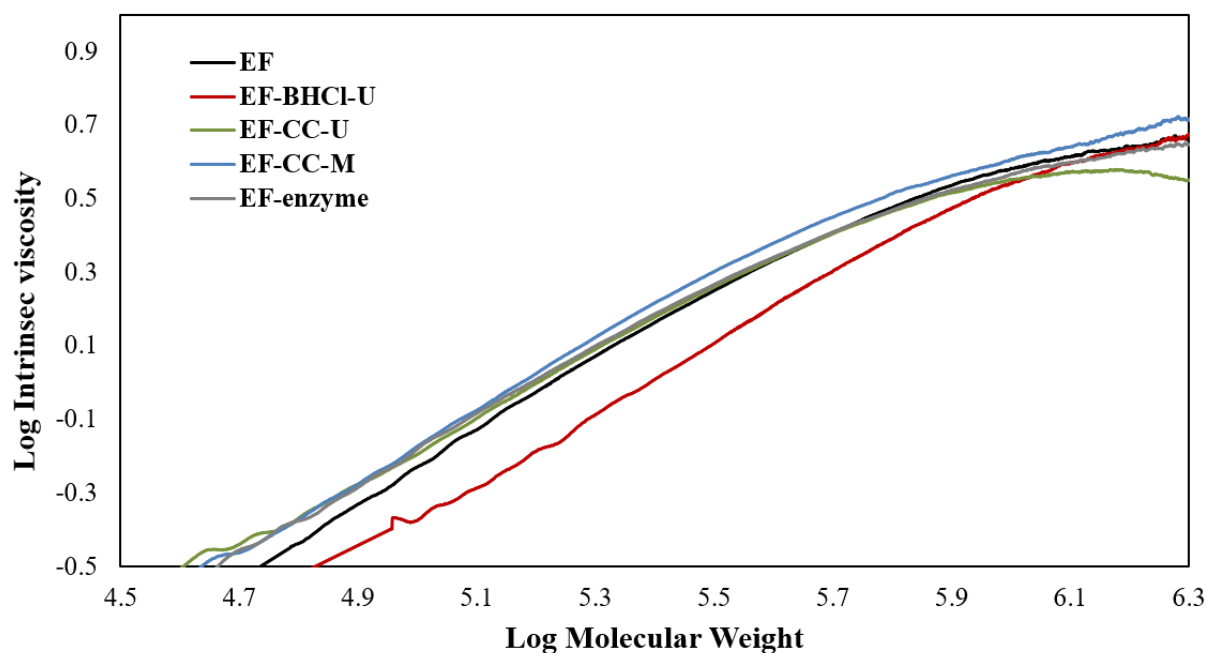


Figure II. 13. Intrinsic viscosity and molecular weight evolution of DES and/or enzyme treated eucalyptus fibres

The obtained curves are generally linear in a log M range of 4.7 – 5.9 (DP in a range of 100-1500). The acidic DES sample is clearly distinguished from other samples, with a lower intrinsic viscosity. As discussed before, the polymer has possibly a stick form, and it could also be influenced by the presence of aggregates that decrease the intrinsic viscosity.

II.2.3.1.3 Comparison between the DP_v measured in cupriethylenediamine and DP averages measured by HPSEC

The DP_v values from the HPSEC experiments were derived from the MHS equation:

$$DP_v = \frac{1}{519} \left(\frac{IV}{K} \right)^{1/a}$$

where K and a are the MHS-law parameters, identified for each sample analysis.

The DP_v and the DP_p measured by HPSEC can be compared to the DP_v measured by standard viscometry of cellulose in CuED (DP-CED), which is reported from our previous work (Mnasri et al., 2022). The evolution of these DP values is illustrated in Figure II. 14.

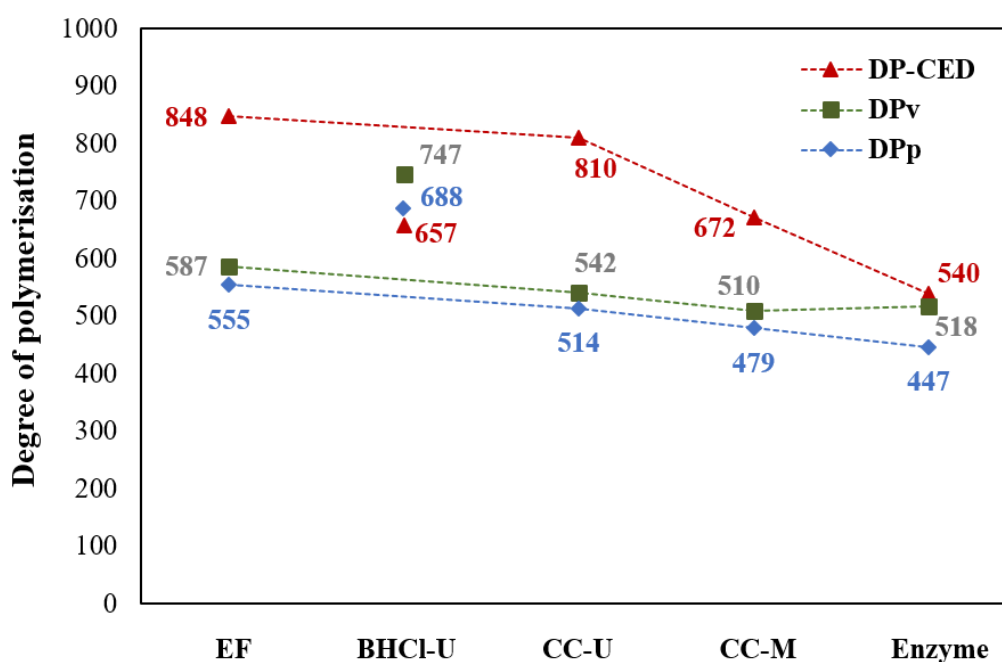


Figure II. 14. Correlation between the DP-CED, DP_v and DP_p of DES and/or enzyme treated eucalyptus fibres.

For all samples, except the acidic DES case, the general trend is a decrease of the DP's, the lowest value being obtained for the enzymatic sample. The slightly lower value of DP_p compared to DP_v-HPSEC appears logical. The difference with DP_v-CED is linked to the imprecision of the CED standard ISO method, related to the mathematical formula used to convert capillary viscosity measurement into DP_v.

In the case of the acidic DES, it is interesting to see that the DP_v-CED value is quite low. It is possibly related to molecule shape in CuED, as already discussed, or to some possible degradation of this cellulosic sample in this strongly alkaline solvent.

II.2.3.2 SEC analysis of DES and/or enzyme treated cotton fibres

II.2.3.2.1 Molecular mass distribution

Treated cotton fibres were also analysed and the results for dispersity index, molar mass and degree of polymerisation are summarized in the Table II. 6. The evolution of M_w followed the same trend as eucalyptus fibres treated with acidic and neutral DES. However, the decrease of the M_w is more noticeable with enzymatic treatment. M_n values also followed the same evolution as eucalyptus fibres. The decrease is more pronounced with neutral DES and enzymatic treatment. Dispersity values are generally smaller than for the eucalyptus treated fibres. Furthermore, the dispersity was not well affected by the acidic DES (slight decrease), while it slightly increased with the alkaline DES treatment (CC-M system). The highest dispersity value was obtained by the neutral DES treatment (CC-U system), and then, by enzymatic treatment. It is obvious that the different DES systems react in different ways on cellulose fibres.

Table II. 6. Molecular mass distribution and degree of polymerisation of DES and/or enzyme treated cotton fibres

Sample	Recovery yield (%)	M_w (g/mol)	M_n (g/mol)	M_w/M_n	DP_w	DP_n
CF	100	416 000	227 000	1.83	802	437
CF-BHCl-U	72	599 000	383 000	1.56	1154	739
CF-CC-U	100	432 000	175 000	2.47	832	337
CF-CC-M	97	386 000	195 000	1.98	744	376
CF-enzyme	100	376 000	177 000	2.13	725	340

MMD curves before and after DES and enzyme treatments are displayed in Figure II. 15. Contrary to eucalyptus fibres, the curves are monomodal in the case of cotton fibres, since the hemicelluloses population is absent. Except for the acidic DES case, rather slight changes in the cellulose population were generally produced by the different treatments. Curve width

slightly increased, with a small increase of smaller chains and small shift of peak maximum towards lower mass, more pronounced for the alkaline DES and enzymatic treatments. For the neutral DES changes were hardly observed. This generally followed the trend already observed with eucalyptus fibres.

Although changes were rather small with cotton fibres, it might be hypothesised the same conclusions as for eucalyptus fibres: neutral DES and enzymatic hydrolysis cut chains on their extremity, while alkaline DES cuts larger fragments, with deeper penetration in the interchain (decrease of Mw and slight reduction of Mn).

Acidic DES had a distinguished behaviour (narrow curve) and the population was shifted towards higher mass. As explained before, there is a loss of small molecules, possibly retained as colloids or aggregates in the column or on filters, as shown by the low recovery yield. This can be the result of incomplete derivatisation due to the presence of grafted ester group on cellulose as described previously (Mnasri et al., 2022).

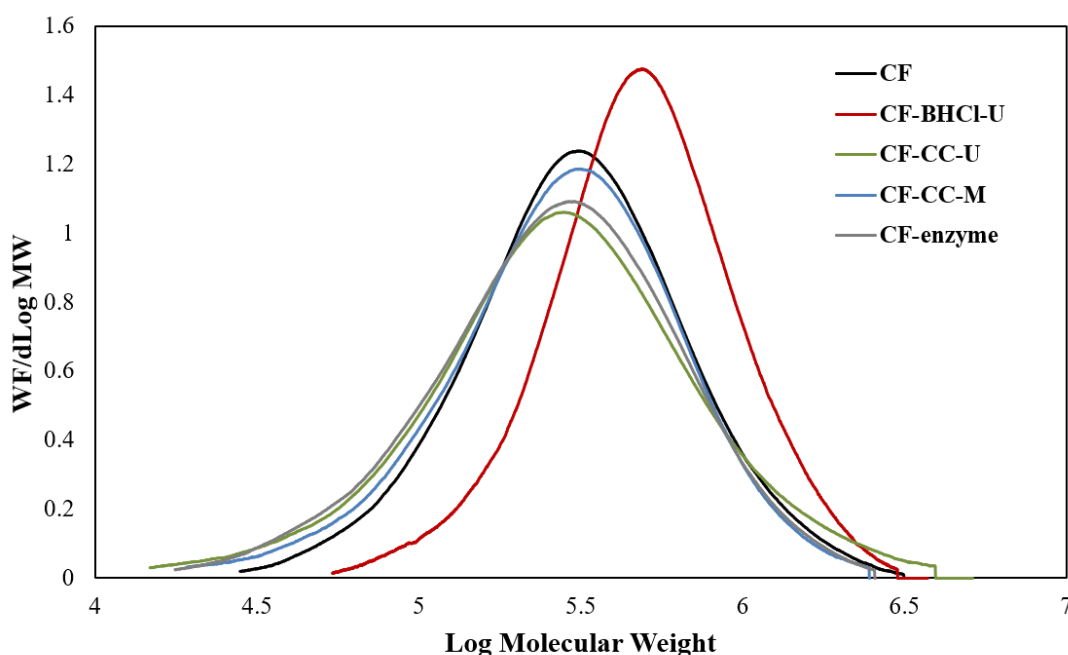


Figure II. 15. Molecular weight distribution of DES/enzyme treated cotton fibres

The evolution of the chromatographic elution curves (DRI signal versus retention volume) is displayed in Figure II. 16. Again, neutral and alkaline DES, as well as enzyme-treated samples behave similarly, while the acidic DES curve can be distinguished from the others by a singular

CHAPTER II. STUDY OF DES PRE-TREATMENT EFFECTS ON CELLULOSE STRUCTURE

behaviour. In the former case, only a small shift towards longer retention times, without significant peak broadening, can be observed, while in the latter case (acidic DES), peak shift is accompanied by an important broadening.

As a general trend, the column separation confirms the information obtained by the coupling of detectors: for all treatments except the acidic DES, slight cellulose degradation is noticeable (the most pronounced peak shift is the one observed with the enzymatic treatment) and in the case of the acidic DES treatment, slight cellulose degradation is accompanied by elution dispersion inside the column.

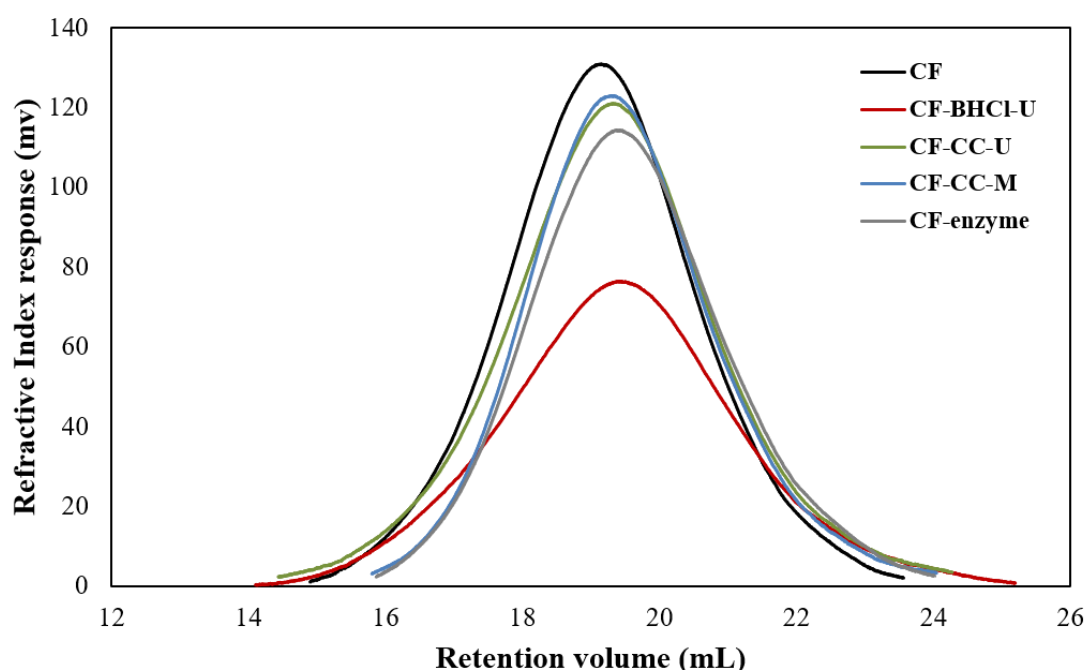


Figure II. 16. Refractive index response and retention volume of DES/enzyme treated cotton fibres

The molar mass at the peak (M_p) and the corresponding DP_p values, are presented in Table II. 7.

CHAPTER II. STUDY OF DES PRE-TREATMENT EFFECTS ON CELLULOSE
STRUCTURE

Table II. 7. Peak molar mass (M_p) and DP_p of DES and enzyme treated cotton fibres.

Sample	M_p (g/mol)	DP_p
CF	312 000	601
CF-BHCl-U	459 000	884
CF-CC-U	279 000	538
CF-CC-M	312 000	601
CF-enzyme	298 000	575

The same observations as eucalyptus fibres can be drawn with cotton fibres. The highest peak mass is given by the acidic DES, while the other treated sample (neutral DES, enzymatic treatment) exhibit lower peak mass than the untreated sample. However, in the case of alkaline DES, the highest peak mass remained the same as untreated fibres.

II.2.3.2.2 Intrinsic viscosity, hydrodynamic radius and radius of gyration

Table II. 8 illustrates the results of intrinsic viscosity (IV), hydrodynamic radius (R_h) and radius of gyration (R_g) of cotton treated fibres. The IV was decreased with all samples, the lowest value being obtained with CC-U (neutral DES). The hydrodynamic radius was significantly increased with acidic DES and slightly decreased with the other systems. As explained before, the IV is influenced by the general structure of the polymer, its chain length and branching. Except for the acidic DES case, the decrease of IV and R_h correlates with molar mass evolution, discussed in the previous paragraph. Both R_h , and even more, R_g , increase with the BHCl-U treatment (acidic DES), as already observed with eucalyptus fibres. In this case there is a deep modification in the polymer morphology, likely to be more elongated, rigid, and cross-links. For the other systems, the ratio of R_g/R_h tends to slightly increase after the treatments, showing that the structure of cellulose is slightly modified, the highest ratio being observed with the alkaline DES, which allows to get swollen polymer as observed with Eucalyptus fibres. However, neutral DES enables to produce more spherical structure which is not the case with eucalyptus fibres.

Table II. 8. Intrinsic viscosity, hydrodynamic radius, and radius of gyration of DES/enzyme treated cotton fibres

Sample	IV (dl/g)	R_h (nm)	R_g (nm)
CF	220	23.2	32.3
CF-BHCl-U	207	27.3	58.6
CF-CC-U	190	21.4	31.8
CF-CC-M	205	22.2	35.5
CF-enzyme	204	21.9	33.9

The MHS graph is displayed in Figure II. 17. As for eucalyptus fibres, the evolution is linear in a similar mass range, and the curves are superimposed except for the acidic DES case, with a much lower intrinsic viscosity at a given mass, which can be explained by the reasons discussed before (presence of aggregates, stick shape...).

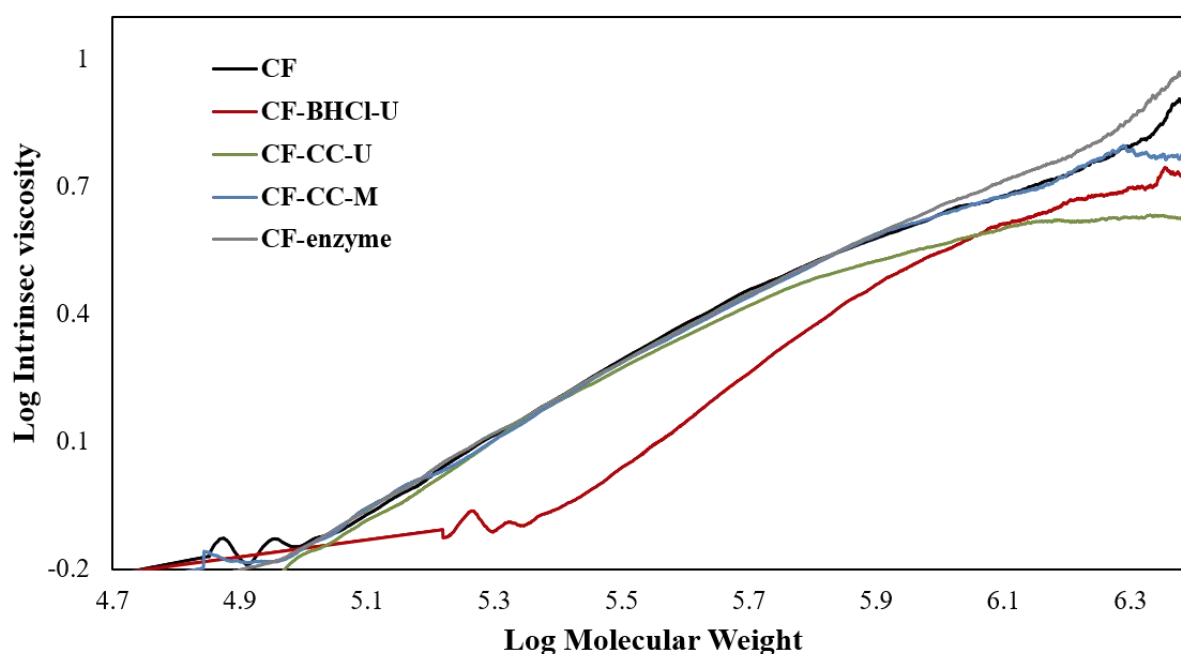


Figure II. 17. Graph for MHS law representation - $\log(IV)$ vs. $\log(M)$

II.2.3.2.3 Comparison between DP_v measured in cupriethylenediamine and DP averages measured by HPSEC

The comparison between the DP-CED and the DP obtained from the HPSEC measurements was not done for treated cotton fibres. This is due to DP values obtained with CED (Mnasri et al., 2022), which are lower than the others DP's values. It is suggested the DP-CED values are not representative for the cotton fibres, which could be due to the sensitive of this method. It can be supposed that CF were not completely dissolved in cupriethylene diamine due to their particular structure; the wall is thick and compact and the cellulose chains are in a less porous and more compact arrangement.

II.2.3.3 Comparison between eucalyptus and cotton fibres

The use of cellulosic fibres of different nature, cotton and hardwood pulp, aims to study the effect of the hemicelluloses. The main observed difference appears in the dispersity of the populations, the eucalyptus fibres having higher dispersity (2.8) than cotton fibres (1.8). This is obvious since hemicelluloses (mostly linear chains of xylan) are present at about 15-20% weight content in eucalyptus chemical pulps, fully delignified and bleached. Their average molar mass is about 5 to 10 times less than that of cellulose chains.

CF presented higher M_w than EF. This is generally the case, because the chemical cooking process to produce wood pulps takes place at much higher temperature (about 160 °C in the case of hardwoods) than the conditions applied for cooking cotton linters, typically around 110 to 140 °C. Therefore, the alkaline hydrolysis of cellulose, superimposed to peeling at temperatures above 130 °C, has lower importance in the CF pulp production.

In terms of molar mass distribution, it was observed for EF that enzymatic hydrolysis and neutral DES allowed to raise the dispersity by decreasing the M_n without affecting the M_w . For CF, the dispersity was also increased with the same systems. However, enzymatic hydrolysis affected greatly the M_w of CF, which was not the case for EF. This can be explained by the direct attack of the enzyme on the cellulose chains of CF, without any protection effect by hemicelluloses which are present in EF.

It is suggested that for both EF and CF, enzymatic hydrolysis as well as neutral DES-treatment act on cellulose chains by cutting on their extremity, since the decrease of M_w was

comparatively low compared to that of M_n . This may be explained by the fact that both media are non-swelling systems, and the reagents (enzyme and neutral DES) cannot diffuse deeply in the interchain network.

As a consequence of their chemical structure and cellulose accessibility, it is thus obvious that the DES systems exhibit a different reactivity on the cellulose fibres. For instance, alkaline DES (CC-M system) allowed to reduce the dispersity for EF, while it led to a slight increase with CF. This difference could be due to the presence of hemicelluloses and also to the low initial dispersity of untreated CF. Alkaline DES treatment enhanced the swelling of the polymer for both fibres. It was found a more spherical polymer from enzymatic treatment of EF, and from neutral DES treatment of CF.

II.2.4 Conclusion

In the present work, the analysis of the DES-treated substrates revealed some changes in the polymer structure. The neutral DES treatment and the enzymatic treatment increased the dispersity index (\mathcal{D}_M) by decreasing M_n , while the alkaline DES treatment slightly changed it by decreasing M_w . Studying the resulting MMD curves (molar mass distribution) showed that all treatments (except the acidic DES) shifted the population towards lower mass. However, studying the acidic DES showed that a large part of the small molecule population had vanished and, as a result, the population was shifted to higher mass. It was assumed that there is a condensation reaction occurs between polar fragments which allows obtaining higher DP values. It was also suggested that enzymatic hydrolysis and neutral DES act on cellulose fibres by cutting on their extremity (slight change of M_w and significant decrease of M_n). Contrary to that, the alkaline DES acts by cutting larger fragments (decrease of M_w with slight change of M_n). It was also shown that the polymer produced from an alkaline DES-treatment is swollen, while the one produced from an acidic DES is more dense, rigid and elongated (significant increase of R_h , R_g , and R_g/R_h). Moreover, enzymatic hydrolysis allowed to produce a polymer with a more spherical shape for eucalyptus fibres, while it is the neutral DES-treatment that ensured this effect with cotton fibres. Some other differences, like the position of the peak DP (DP_p), decreasing with the alkaline DES treatment on eucalyptus fibres, while unchanged for cotton fibres. This observation demonstrates the different behaviour of this DES in the presence or not of hemicelluloses which may act as a barrier.

CHAPTER II. STUDY OF DES PRE-TREATMENT EFFECTS ON CELLULOSE STRUCTURE

The acidic DES-treated sample showed a singular behaviour compared to the other DES-treated substrates. It is suggested that there is a loss of small molecules, aggregated as colloids, by retention inside the SEC columns or through the syringe or column filters. This could be caused by incomplete derivatisation of cellulosic chains bearing a carbonyl group brought by the acidic DES treatment. The low recovery yield during the chromatographic separation brings an evidence of such a loss of polymer, shifting the population towards higher mass, with a more dispersed elution through the columns.

Appendix II.2

The Mark-Houwink-Sakurada parameters of DES and/or enzyme treated eucalyptus and cotton fibres are presented in Table II. 9 and Table II. 10, respectively

Table II. 9. MHS parameters of DES and/or enzyme treated eucalyptus fibres

Sample	MHS parameters	
	a	logK
EF	0.859	-4.502
EF-BHCl-U	0.802	-4.284
EF-CC-U	0.786	-4.099
EF-CC-M	0.827	-4.282
EF-enzyme	0.806	-4.200

Table II. 10. MHS parameters of DES and/or enzyme treated cotton fibres

Sample	MHS parameters	
	a	logK
CF	0.772	-3.967
CF-BHCl-U	0.909	-4.921
CF-CC-U	0.727	-3.753
CF-CC-M	0.784	-4.04
CF-enzyme	0.803	-4.139

References

Abbott, A.P., Capper, G., Davies, D.L., Rasheed, R.K., Tambyrajah, V., 2003. Novel solvent properties of choline chloride/urea mixtures. *Chemical Communications* 0, 70–71. <https://doi.org/10.1039/B210714G>

Abbott, A.P., Capper, G., L. Davies, D., L. Munro, H., K. Rasheed, R., Tambyrajah, V., 2001. Preparation of novel, moisture-stable, Lewis-acidic ionic liquids containing quaternary ammonium salts with functional side chains. *Chemical Communications* 0, 2010–2011. <https://doi.org/10.1039/B106357J>

Abranches, D.O., Martins, M.A.R., Silva, L.P., Schaeffer, N., Pinho, S.P., Coutinho, J.A.P., 2019. Phenolic hydrogen bond donors in the formation of non-ionic deep eutectic solvents: the quest for type V DES. *Chem. Commun.* 55, 10253–10256. <https://doi.org/10.1039/C9CC04846D>

AlOmar, M.K., Alsaadi, M.A., Hayyan, M., Akib, S., Ibrahim, R.K., Hashim, M.A., 2016. Lead removal from water by choline chloride based deep eutectic solvents functionalized carbon nanotubes. *Journal of Molecular Liquids* 222, 883–894. <https://doi.org/10.1016/j.molliq.2016.07.074>

Banvillet, G., Depres, G., Belgacem, N., Bras, J., 2021. Alkaline treatment combined with enzymatic hydrolysis for efficient cellulose nanofibrils production. *Carbohydrate Polymers* 255, 117383. <https://doi.org/10.1016/j.carbpol.2020.117383>

Brewer, R.J., Tanghe, L.J., Bailey, S., Burr, J.T., 1968. Molecular weight distribution of cellulose esters by gel permeation chromatography and fractional precipitation. *Journal of Polymer Science Part A-1: Polymer Chemistry* 6, 1697–1704. <https://doi.org/10.1002/pol.1968.150060627>

Chen, Y.-L., Zhang, X., You, T.-T., Xu, F., 2019. Deep eutectic solvents (DESs) for cellulose dissolution: a mini-review. *Cellulose* 26, 205–213. <https://doi.org/10.1007/s10570-018-2130-7>

Chung, C., Lee, M., Choe, E.K., 2004. Characterization of cotton fabric scouring by FT-IR ATR spectroscopy. *Carbohydrate Polymers* 58, 417–420. <https://doi.org/10.1016/j.carbpol.2004.08.005>

- Delso, I., Lafuente, C., Muñoz-Embid, J., Artal, M., 2019. NMR study of choline chloride-based deep eutectic solvents. *Journal of Molecular Liquids* 290, 111236. <https://doi.org/10.1016/j.molliq.2019.111236>
- Douard, L., Bras, J., Encinas, T., Belgacem, M.N., 2021. Natural acidic deep eutectic solvent to obtain cellulose nanocrystals using the design of experience approach. *Carbohydrate Polymers* 252, 117136. <https://doi.org/10.1016/j.carbpol.2020.117136>
- Dupont, A.-L., Mortha, G., 2004. Comparative evaluation of size-exclusion chromatography and viscometry for the characterisation of cellulose. *Journal of Chromatography A* 1026, 129–141. <https://doi.org/10.1016/j.chroma.2003.11.002>
- Fernandes, P.M.V., Campiña, J.M., Pereira, N.M., Pereira, C.M., Silva, F., 2012. Biodegradable deep-eutectic mixtures as electrolytes for the electrochemical synthesis of conducting polymers. *J Appl Electrochem* 42, 997–1003. <https://doi.org/10.1007/s10800-012-0474-5>
- French, A.D., 2014. Idealized powder diffraction patterns for cellulose polymorphs. *Cellulose* 21, 885–896. <https://doi.org/10.1007/s10570-013-0030-4>
- Ghareeb, H.O., Malz, F., Kilz, P., Radke, W., 2012. Molar mass characterization of cellulose acetates over a wide range of high DS by size exclusion chromatography with multi-angle laser light scattering detection. *Carbohydrate Polymers* 88, 96–102. <https://doi.org/10.1016/j.carbpol.2011.11.071>
- Gharehkhani, S., Sadeghinezhad, E., Kazi, S.N., Yarmand, H., Badarudin, A., Safaei, M.R., Zubir, M.N.M., 2015. Basic effects of pulp refining on fiber properties—A review. *Carbohydrate Polymers* 115, 785–803. <https://doi.org/10.1016/j.carbpol.2014.08.047>
- Henniges, U., Kloser, E., Patel, A., Potthast, A., Kosma, P., Fischer, M., Fischer, K., Rosenau, T., 2007. Studies on DMSO-containing carbanilation mixtures: chemistry, oxidations and cellulose integrity. *Cellulose* 14, 497–511. <https://doi.org/10.1007/s10570-007-9130-3>
- Holt, C., Mackie, W., Sellen, D.B., 1978. Gel permeation chromatography of high molecular weight cellulose trinitrate. *Polymer* 19, 1421–1426. [https://doi.org/10.1016/0032-3861\(78\)90094-0](https://doi.org/10.1016/0032-3861(78)90094-0)

- Hong, S., Yuan, Y., Li, P., Zhang, K., Lian, H., Liimatainen, H., 2020. Enhancement of the nanofibrillation of birch cellulose pretreated with natural deep eutectic solvent. *Industrial Crops and Products* 154, 112677. <https://doi.org/10.1016/j.indcrop.2020.112677>
- Hosu, O., Bârsan, M.M., Cristea, C., Săndulescu, R., Brett, C.M.A., 2017. Nanostructured electropolymerized poly(methylene blue) films from deep eutectic solvents. Optimization and characterization. *Electrochimica Acta* 232, 285–295. <https://doi.org/10.1016/j.electacta.2017.02.142>
- Johan Foster, E., J. Moon, R., P. Agarwal, U., J. Bortner, M., Bras, J., Camarero-Espinosa, S., J. Chan, K., D. Clift, M.J., D. Cranston, E., J. Eichhorn, S., M. Fox, D., Y. Hamad, W., Heux, L., Jean, B., Korey, M., Nieh, W., J. Ong, K., S. Reid, M., Renneckar, S., Roberts, R., Anne Shatkin, J., Simonsen, J., Stinson-Bagby, K., Wanasekara, N., Youngblood, J., 2018. Current characterization methods for cellulose nanomaterials. *Chemical Society Reviews* 47, 2609–2679. <https://doi.org/10.1039/C6CS00895J>
- Kang, T., 2007. Role of external fibrillation in pulp and paper properties. Helsinki University of Technology.
- Khiari, R., Rol, F., Brochier Salon, M.-C., Bras, J., Belgacem, M.N., 2019. Efficiency of Cellulose Carbonates to Produce Cellulose Nanofibers. *ACS Sustainable Chem. Eng.* 7, 8155–8167. <https://doi.org/10.1021/acssuschemeng.8b06039>
- Kleman-Leyer, K.M., Gilkes, N.R., Miller, R.C., Kirk, T.K., 1994. Changes in the molecular-size distribution of insoluble celluloses by the action of recombinant *Cellulomonas fimi* cellulases. *Biochemical Journal* 302, 463–469. <https://doi.org/10.1042/bj3020463>
- Kleman-Leyer, K.M., Kirk, T.K., 1994. Three Native Cellulose-Depolymerizing Endoglucanases from Solid-Substrate Cultures of the Brown Rot Fungus *Meruliporia (Serpula) incrassata*. *Appl Environ Microbiol* 60, 2839–2845. <https://doi.org/10.1128/aem.60.8.2839-2845.1994>
- Kleman-Leyer, K.M., Siika-Aho, M., Teeri, T.T., Kirk, T.K., 1996. The Cellulases Endoglucanase I and Cellobiohydrolase II of *Trichoderma reesei* Act Synergistically To Solubilize Native Cotton Cellulose but Not To Decrease Its Molecular Size. *Appl Environ Microbiol* 62, 2883–2887. <https://doi.org/10.1128/aem.62.8.2883-2887.1996>

- Kono, H., Numata, Y., Erata, T., Takai, M., 2004. ¹³C and ¹H Resonance Assignment of Mercerized Cellulose II by Two-Dimensional MAS NMR Spectroscopies. *Macromolecules* 37, 5310–5316. <https://doi.org/10.1021/ma030465k>
- Kwon, G.-J., Bandi, R., Yang, B.-S., Park, C.-W., Han, S.-Y., Park, J.-S., Lee, E.-A., Kim, N.-H., Lee, S.-H., 2021. Choline chloride based deep eutectic solvents for the lignocellulose nanofibril production from Mongolian oak (*Quercus mongolica*). *Cellulose* 28, 9169–9185. <https://doi.org/10.1007/s10570-021-04102-3>
- Lauriol, J.-M., Froment, P., Pla, F., Robert, A., 1987. Molecular Weight Distribution of Cellulose by On-Line Size Exclusion Chromatography — Low Angle Laser Light Scattering Part I: Basic Experiments and Treatment of Data 41, 109–113. <https://doi.org/10.1515/hfsg.1987.41.2.109>
- Leskinen, T., Kelley, S.S., Argyropoulos, D.S., 2015. Determination of molecular weight distributions in native and pretreated wood. *Carbohydrate Polymers* 119, 44–52. <https://doi.org/10.1016/j.carbpol.2014.11.026>
- Li, P., Sirviö, J.A., Haapala, A., Liimatainen, H., 2017. Cellulose Nanofibrils from Nonderivatizing Urea-Based Deep Eutectic Solvent Pretreatments. *ACS Appl. Mater. Interfaces* 9, 2846–2855. <https://doi.org/10.1021/acsami.6b13625>
- Li, W., Xue, Y., He, M., Yan, J., Lucia, L.A., Chen, J., Yu, J., Yang, G., 2021. Facile Preparation and Characteristic Analysis of Sulfated Cellulose Nanofibril via the Pretreatment of Sulfamic Acid-Glycerol Based Deep Eutectic Solvents. *Nanomaterials* 11, 2778. <https://doi.org/10.3390/nano11112778>
- Ling, Z., Edwards, J.V., Guo, Z., Prevost, N.T., Nam, S., Wu, Q., French, A.D., Xu, F., 2019. Structural variations of cotton cellulose nanocrystals from deep eutectic solvent treatment: micro and nano scale. *Cellulose* 26, 861–876. <https://doi.org/10.1007/s10570-018-2092-9>
- Liu, S., Zhang, Q., Gou, S., Zhang, L., Wang, Z., 2021. Esterification of cellulose using carboxylic acid-based deep eutectic solvents to produce high-yield cellulose nanofibers. *Carbohydrate Polymers* 251, 117018. <https://doi.org/10.1016/j.carbpol.2020.117018>

- Łojewski, T., Zięba, K., Łojewska, J., 2010. Size exclusion chromatography and viscometry in paper degradation studies. New Mark-Houwink coefficients for cellulose in cupri-ethylenediamine. *Journal of Chromatography A* 1217, 6462–6468. <https://doi.org/10.1016/j.chroma.2010.07.071>
- Mäki-Arvela, P., Salmi, T., Holmbom, B., Willför, S., Murzin, D.Yu., 2011. Synthesis of Sugars by Hydrolysis of Hemicelluloses- A Review. *Chem. Rev.* 111, 5638–5666. <https://doi.org/10.1021/cr2000042>
- Marx-Figini, M., Soubelet, O., 1984. Size exclusion chromatography of cellulose nitrate. *Polymer Bulletin* 11, 281–286. <https://doi.org/10.1007/BF00255353>
- Mittal, A., Katahira, R., Himmel, M.E., Johnson, D.K., 2011. Effects of alkaline or liquid-ammonia treatment on crystalline cellulose: changes in crystalline structure and effects on enzymatic digestibility. *Biotechnology for Biofuels* 4, 41. <https://doi.org/10.1186/1754-6834-4-41>
- Mnasri, A., Dhaouadi, H., Khiari, R., Halila, S., Mauret, E., 2022. Effects of Deep Eutectic Solvents on cellulosic fibres and paper properties: Green “chemical” refining. *Carbohydrate Polymers* 119606. <https://doi.org/10.1016/j.carbpol.2022.119606>
- Moufawad, T., Gomes, M.C., Fourmentin, S., 2021. Solvants eutectiques profonds - Vers des procédés plus durables 27.
- Nechyporchuk, O., Belgacem, M.N., Bras, J., 2016. Production of cellulose nanofibrils: A review of recent advances. *Industrial Crops and Products* 93, 2–25. <https://doi.org/10.1016/j.indcrop.2016.02.016>
- Ono, Y., Isogai, A., 2021. Analysis of celluloses, plant holocelluloses, and wood pulps by size-exclusion chromatography/multi-angle laser-light scattering. *Carbohydrate Polymers* 251, 117045. <https://doi.org/10.1016/j.carbpol.2020.117045>
- Park, S., Baker, J.O., Himmel, M.E., Parilla, P.A., Johnson, D.K., 2010. Cellulose crystallinity index: measurement techniques and their impact on interpreting cellulase performance. *Biotechnol Biofuels* 3, 10. <https://doi.org/10.1186/1754-6834-3-10>

- Pawcenis, D., Thomas, J.L., Łojewski, T., Milczarek, J.M., Łojewska, J., 2015. Towards determination of absolute molar mass of cellulose polymer by size exclusion chromatography with multiple angle laser light scattering detection. *Journal of Chromatography A* 1409, 53–59. <https://doi.org/10.1016/j.chroma.2015.06.042>
- Plotka-Wasyłka, J., de la Guardia, M., Andruch, V., Vilková, M., 2020. Deep eutectic solvents vs ionic liquids: Similarities and differences. *Microchemical Journal* 159, 105539. <https://doi.org/10.1016/j.microc.2020.105539>
- Rol, F., Belgacem, M.N., Gandini, A., Bras, J., 2019. Recent advances in surface-modified cellulose nanofibrils. *Progress in Polymer Science* 88, 241–264. <https://doi.org/10.1016/j.progpolymsci.2018.09.002>
- Rol, F., Karakashov, B., Nechyporchuk, O., Terrien, M., Meyer, V., Dufresne, A., Belgacem, M.N., Bras, J., 2017. Pilot-Scale Twin Screw Extrusion and Chemical Pretreatment as an Energy-Efficient Method for the Production of Nanofibrillated Cellulose at High Solid Content. *ACS Sustainable Chem. Eng.* 5, 6524–6531. <https://doi.org/10.1021/acssuschemeng.7b00630>
- Rol, F., Sillard, C., Bardet, M., Yarava, J.R., Emsley, L., Gablin, C., Léonard, D., Belgacem, N., Bras, J., 2020. Cellulose phosphorylation comparison and analysis of phosphate position on cellulose fibers. *Carbohydrate Polymers* 229, 115294. <https://doi.org/10.1016/j.carbpol.2019.115294>
- Ruesgas-Ramón, M., Figueroa-Espinoza, M.C., Durand, E., 2017. Application of Deep Eutectic Solvents (DES) for Phenolic Compounds Extraction: Overview, Challenges, and Opportunities. *J. Agric. Food Chem.* 65, 3591–3601. <https://doi.org/10.1021/acs.jafc.7b01054>
- Schaeffer, N., Conceição, J.H.F., Martins, M.A.R., Neves, M.C., Pérez-Sánchez, G., Gomes, J.R.B., Papaiconomou, N., Coutinho, J.A.P., 2020. Non-ionic hydrophobic eutectics – versatile solvents for tailored metal separation and valorisation. *Green Chem.* 22, 2810–2820. <https://doi.org/10.1039/D0GC00793E>
- Selkälä, T., Sirviö, J.A., Lorite, G.S., Liimatainen, H., 2016. Anionically Stabilized Cellulose Nanofibrils through Succinylation Pretreatment in Urea–Lithium Chloride Deep Eutectic Solvent. *ChemSusChem* 9, 3074–3083. <https://doi.org/10.1002/cssc.201600903>

- Sirviö, J., Hyypiö, K., Asaadi, S., Junka, K., Liimatainen, H., 2020. High-strength cellulose nanofibers produced via swelling pretreatment based on a choline chloride–imidazole deep eutectic solvent. *Green Chemistry* 22, 1763–1775. <https://doi.org/10.1039/C9GC04119B>
- Sirviö, J.A., 2018. Cationization of lignocellulosic fibers with betaine in deep eutectic solvent: Facile route to charge stabilized cellulose and wood nanofibers. *Carbohydrate Polymers* 198, 34–40. <https://doi.org/10.1016/j.carbpol.2018.06.051>
- Sirviö, J.A., Heiskanen, J.P., 2017. Synthesis of Alkaline-Soluble Cellulose Methyl Carbamate Using a Reactive Deep Eutectic Solvent. *ChemSusChem* 10, 455–460. <https://doi.org/10.1002/cssc.201601270>
- Sirviö, J.A., Isokoski, E., Kantola, A.M., Komulainen, S., Ämmälä, A., 2021. Mechanochemical and thermal succinylation of softwood sawdust in presence of deep eutectic solvent to produce lignin-containing wood nanofibers. *Cellulose* 28, 6881–6898. <https://doi.org/10.1007/s10570-021-03973-w>
- Sirviö, J.A., Ukkola, J., Liimatainen, H., 2019. Direct sulfation of cellulose fibers using a reactive deep eutectic solvent to produce highly charged cellulose nanofibers. *Cellulose* 26, 2303–2316. <https://doi.org/10.1007/s10570-019-02257-8>
- Sirviö, J.A., Visanko, M., Liimatainen, H., 2015. Deep eutectic solvent system based on choline chloride-urea as a pre-treatment for nanofibrillation of wood cellulose. *Green Chemistry* 17, 3401–3406. <https://doi.org/10.1039/C5GC00398A>
- Sirviö, J.A., Visanko, M., Liimatainen, H., 2016. Acidic Deep Eutectic Solvents As Hydrolytic Media for Cellulose Nanocrystal Production. *Biomacromolecules* 17, 3025–3032. <https://doi.org/10.1021/acs.biomac.6b00910>
- Sjöholm, E., Gustafsson, K., Pettersson, B., Colmsjö, A., 1997. Characterization of the cellulosic residues from lithium chloride/N,N-dimethylacetamide dissolution of softwood kraft pulp. *Carbohydrate Polymers* 32, 57–63. [https://doi.org/10.1016/S0144-8617\(96\)00129-4](https://doi.org/10.1016/S0144-8617(96)00129-4)
- Sjöholm, E., Wadsborn, R., 2022. Minimizing interlaboratory deviations in the molecular mass determination of chemical pulps by lithium chloride/N,N-dimethylacetamide - size-exclusion chromatography.

- Smith, E.L., Abbott, A.P., Ryder, K.S., 2014. Deep Eutectic Solvents (DESs) and Their Applications. *Chem. Rev.* 114, 11060–11082. <https://doi.org/10.1021/cr300162p>
- Spiridon, I., Popa, V.I., 2008. Chapter 13 - Hemicelluloses: Major Sources, Properties and Applications, in: Belgacem, M.N., Gandini, A. (Eds.), *Monomers, Polymers and Composites from Renewable Resources*. Elsevier, Amsterdam, pp. 289–304. <https://doi.org/10.1016/B978-0-08-045316-3.00013-2>
- Srisodsuk, M., Kleman-Leyer, K., Keränen, S., Kirk, T.K., Teeri, T.T., 1998. Modes of action on cotton and bacterial cellulose of a homologous endoglucanase-exoglucanase pair from *Trichoderma reesei*. *European Journal of Biochemistry* 251, 885–892. <https://doi.org/10.1046/j.1432-1327.1998.2510885.x>
- Suopajarvi, T., Ricci, P., Karvonen, V., Ottolina, G., Liimatainen, H., 2020. Acidic and alkaline deep eutectic solvents in delignification and nanofibrillation of corn stalk, wheat straw, and rapeseed stem residues. *Industrial Crops and Products* 145, 111956. <https://doi.org/10.1016/j.indcrop.2019.111956>
- Suopajarvi, T., Sirviö, J.A., Liimatainen, H., 2017. Nanofibrillation of deep eutectic solvent-treated paper and board cellulose pulps. *Carbohydrate Polymers* 169, 167–175. <https://doi.org/10.1016/j.carbpol.2017.04.009>
- Tenhunen, T.-M., Lewandowska, A.E., Orelma, H., Johansson, L.-S., Virtanen, T., Harlin, A., Österberg, M., Eichhorn, S.J., Tammelin, T., 2018. Understanding the interactions of cellulose fibres and deep eutectic solvent of choline chloride and urea. *Cellulose* 25, 137–150. <https://doi.org/10.1007/s10570-017-1587-0>
- Tian, D., Guo, Y., Hu, J., Yang, G., Zhang, J., Luo, L., Xiao, Y., Deng, S., Deng, O., Zhou, W., Shen, F., 2020. Acidic deep eutectic solvents pretreatment for selective lignocellulosic biomass fractionation with enhanced cellulose reactivity. *International Journal of Biological Macromolecules* 142, 288–297. <https://doi.org/10.1016/j.ijbiomac.2019.09.100>
- Tomé, L.I.N., Baião, V., da Silva, W., Brett, C.M.A., 2018. Deep eutectic solvents for the production and application of new materials. *Applied Materials Today* 10, 30–50. <https://doi.org/10.1016/j.apmt.2017.11.005>

- Willberg-Keyriläinen, P., Hiltunen, J., Ropponen, J., 2018. Production of cellulose carbamate using urea-based deep eutectic solvents. *Cellulose* 25, 195–204. <https://doi.org/10.1007/s10570-017-1465-9>
- Wood, B.F., Conner, A.H., Hill Jr., C.G., 1986. The effect of precipitation on the molecular weight distribution of cellulose tricarbamate. *Journal of Applied Polymer Science* 32, 3703–3712. <https://doi.org/10.1002/app.1986.070320225>
- Wu, C.-S., 2003. *Handbook Of Size Exclusion Chromatography And Related Techniques: Revised And Expanded*. CRC Press.
- Xiao, B., Sun, X.F., Sun, R., 2001. Chemical, structural, and thermal characterizations of alkali-soluble lignins and hemicelluloses, and cellulose from maize stems, rye straw, and rice straw. *Polymer Degradation and Stability* 74, 307–319. [https://doi.org/10.1016/S0141-3910\(01\)00163-X](https://doi.org/10.1016/S0141-3910(01)00163-X)
- Yu, W., Wang, C., Yi, Y., Wang, H., Yang, Y., Zeng, L., Tan, Z., 2021. Direct pretreatment of raw ramie fibers using an acidic deep eutectic solvent to produce cellulose nanofibrils in high purity. *Cellulose* 28, 175–188. <https://doi.org/10.1007/s10570-020-03538-3>
- Zdanowicz, M., Wilpiszewska, K., Szychaj, T., 2018. Deep eutectic solvents for polysaccharides processing. A review. *Carbohydrate Polymers* 200, 361–380. <https://doi.org/10.1016/j.carbpol.2018.07.078>
- Zhao, Z., Chen, X., Ali, M.F., Abdeltawab, A.A., Yakout, S.M., Yu, G., 2018. Pretreatment of wheat straw using basic ethanolamine-based deep eutectic solvents for improving enzymatic hydrolysis. *Bioresource Technology* 263, 325–333. <https://doi.org/10.1016/j.biortech.2018.05>

Chapter III. Microfibrillated cellulose MFC production from DES pre-treatment

Table of contents

Chapter III. Microfibrillated cellulose MFC production from DES pre-treatment179

Introduction.....	185
III.1 MFC production from Deep Eutectic Solvents pre-treatment using ultra-fine friction grinder.....	186
III.1.1 Introduction	186
III.1.2 Materials and Methods.....	188
III.1.2.1 Materials	188
III.1.2.2 DES pre-treatment	189
III.1.2.3 Enzymatic pre-treatment	189
III.1.2.4 Cellulose microfibrillation	189
III.1.2.5 Nanopaper handsheet production.....	190
III.1.2.6 Microfibrillated cellulose MFC characterisation.....	190
III.1.2.6.1 Microscopic analyses: TEM, AFM and optical microscopy	190
III.1.2.6.2 Degree of Polymerisation	191
III.1.2.6.3 X-ray Diffraction.....	191
III.1.2.6.4 Morphological analysis of MFC suspension.....	191
III.1.2.6.5 Nanosized fraction and turbidity	191
III.1.2.6.6 Thermogravimetric analysis.....	192
III.1.2.6.7 Tensile tests.....	192
III.1.2.6.8 Oxygen permeability	192
III.1.2.6.9 Simplified Quality Index	193
III.1.3 Results and discussions.....	193
III.1.3.1 Morphological and structural properties of produced MFC.....	193
III.1.3.2 Thermogravimetric properties	198
Ahlem MNASRI – 2022	181

III.1.3.3 Mechanical properties and oxygen barrier properties	201
III.1.3.3.1 Mechanical properties of nanopapers	201
III.1.3.3.2 Oxygen permeability	204
III.1.3.3.3 Simplified quality index of produced MFC and energy consumption during ultra-fine grinding	205
III.1.4 Conclusion.....	208
III.2 High content MFC suspensions produced from DES-treated fibres using twin-screw extruder	210
III.2.1 Introduction	210
III.2.2 Materials and Methods.....	212
III.2.2.1 Materials	212
III.2.2.2 DES pretreatment.....	213
III.2.2.3 PFI-refining	213
III.2.2.4 Cellulose microfibrillation using twin-screw extruder TSE.....	213
III.2.2.5 Nanopaper handsheet production.....	214
III.2.2.6 Fibres/MFC characterisation	214
III.2.2.6.1 Optical microscopy.....	214
III.2.2.6.2 Scanning Electron Microscopy SEM	214
III.2.2.6.3 Morphological analysis.....	215
III.2.2.6.4 Degree of polymerisation (DP)	215
III.2.2.6.5 X-ray diffraction (XrD)	215
III.2.2.6.6 Macro size (μm^2).....	215
III.2.2.6.7 Nanosized fraction.....	216
III.2.2.6.8 Turbidity	216
III.2.2.6.9 Tensile tests.....	216
III.2.2.6.10 Simplified quality Index QI*	216

III.2.3 Results and discussions	217
III.2.3.1 Morphological properties of fibre/MFC suspensions	217
III.2.3.2 Crystallinity index CrI and Degree of polymerisation DP	221
III.2.3.3 Properties of papers and nanopapers.....	222
III.2.3.4 Simplified quality index QI*	224
III.2.4 Conclusion.....	225
References.....	227

Introduction

As discussed in chapter II, the effects of DES on cellulose fibres are mainly, the external and internal fibrillation of the fibres. This pre-treatment is regarded as a green and soft chemical refining. Therefore, the effectiveness of these DES to enhance the microfibrillation process was studied in this chapter.

The first section is dedicated to the production of cellulose microfibrils from DES-treated fibres using ultra-fine friction grinder. The produced MFC were characterised using different techniques and then compared to those produced from enzymatic hydrolysis.

The second section is devoted to produce high content MFC suspensions from DES-treated fibres using the twin-screw extruder. The properties of the extruded-MFC were studied and compared the ground-MFC.

III.1 MFC production from Deep Eutectic Solvents pre-treatment using ultra-fine friction grinder

This section is inspired from Mnasri, A., Khiari, R., Dhaouadi, H., Halila, S., & Mauret, E. Acidic and alkaline Deep Eutectic Solvents pre-treatment to produce high aspect ratio microfibrillated cellulose. Under revision in Bioresource & Technology.

Abstract

This study aims to investigate the microfibrillation potential of three Deep Eutectic Solvents (DES) namely betaine hydrochloride-urea, choline chloride-urea and choline chloride-monoethanolamine. Cellulose fibres (eucalyptus EF and cotton CF) were first treated in DES at 100 °C for 4 h and then ground with ultra-fine friction grinder to produce microfibrillated cellulose MFC. DES pre-treatment has significantly improved the microfibrillation process with an energy consumption during grinding comparable to that of enzymatic hydrolysis (used as a reference pre-treatment). Long and thin microfibril bundles with widths around 50 nm and individualised microfibrils having widths between 5 and 10 nm were obtained. MFC gels and nanopapers were then characterised using several techniques. It is worth noting that nanopapers produced from DES treated MFC showed good mechanical properties with Young's modulus higher than 10 GPa. In addition, they exhibited higher quality index (between 73 and 76) than those produced from enzymatic hydrolysis (quality index around 68). Indeed, DES pre-treatment appears to be a promising way to enhance the microfibrillation and produce MFC with high aspect ratio.

Key words: Cellulose fibres, pre-treatment, Deep Eutectic Solvents, microfibrillation, microfibrillated cellulose, ultra-fine friction grinder.

III.1.1 Introduction

Nanocellulose has gained great attention from the scientific community due to its fascinating properties. Two kinds of nanocellulose can be extracted depending on the isolation process: microfibrillated cellulose MFC or cellulose microfibrils CMF and cellulose nanocrystals CNC.

Microfibrillated cellulose has been extensively studied (Abdul Khalil et al., 2014; Nechyporchuk et al., 2016) because of their interesting properties; biodegradability, biocompatibility (Fukuzumi et al., 2009; Nogi et al., 2009) high aspect ratio and specific surface

CHAPTER III. Microfibrillated cellulose MFC PRODUCTION FROM DES PRE-TREATMENT

area (Moon et al., 2011). MFC were first studied in 1983 by Turbak et al. (1983). They are produced by subjecting cellulose suspension to high shear mechanical treatments such as high-pressure homogeniser, microfluidiser, ultrafine friction grinder, extruder, ball milling... (Khiari, 2017; Nechyporchuk et al., 2016; Rol et al., 2017). These processes are energy consuming because of the high shear forces required to release cellulose microfibrils from cellulosic fibres. To reduce this energy, pre-treatments are applied before the mechanical step. Enzymatic and chemical pre-treatments are the most commonly used to facilitate microfibrillation process. Enzymatic treatment is based on cellulose hydrolysis using enzyme and the resulting MFC are not functionalised (Banvillet et al., 2021a; Henriksson et al., 2007; Pääkkö et al., 2007). Chemical pre-treatments are based on cellulose modification such as TEMPO oxidation (Habibi et al., 2006; Isogai et al., 2011; Saito et al., 2007, 2006; Saito and Isogai, 2006, 2004), quaternisation (Ho et al., 2011; Liimatainen et al., 2014; Pei et al., 2013; Song et al., 2008) and phosphorylation (Ghanadpour et al., 2015; Luneva and Ezovitova, 2014; Noguchi et al., 2017; Rol et al., 2020). Among these chemical pre-treatments, TEMPO oxidation is the most effective one and leads to obtain MFC with high quality. However, this pre-treatment has some limits such as the toxicity of the used reagents.

Deep Eutectic Solvents (DES) were first discovered in 2001 by Abbott et al. (2001). They are obtained by the combination of two components (two solids or solid and liquid) and sometimes were formed by more than two components. They are characterised by their biodegradability, eco-friendly character, low or non-toxicity, thermal stability, easy use, recyclability... Due to their interesting properties, they are studied in many fields such as electrochemistry, polymer science and polysaccharides treatment (Smith et al., 2014; Zdanowicz et al., 2018). Many works are dedicated to the treatment of cellulose fibres by DES and more precisely to the selective extraction of lignin (Francisco et al., 2012; Majová et al., 2017) or hemicelluloses (Hou et al., 2018; Tenhunen et al., 2018). Indeed, DES are considered as a mild pre-treatment medium because many systems preserve the degree of polymerisation and also the crystallinity index of cellulose (Hong et al., 2020; Suopajarvi et al., 2017; Tenhunen et al., 2016). DES were first studied in 2015 as a pre-treatment medium for producing MFC (Sirviö et al., 2015). The authors used a mixture of choline chloride-urea to pretreat cellulose fibres in order to facilitate their subsequent microfibrillation during microfluidisation. They showed that this system allows obtaining a mixture of microfibril bundles with widths of 15-200 nm and individualised

microfibrils (widths between 2 and 5 nm). For the same purpose, other systems have been recently investigated (Li et al., 2021; Ma et al., 2019; Yu et al., 2021). Nevertheless, apart from these studies, DES potential for microfibrillation process and MFC production remains under-explored until now. Very recently, Mnasri et al. (2022) studied the effects of three eutectic systems on cellulosic fibres and paper properties. These systems are mixture of betaine hydrochloride-urea (BHCl-U, acidic), choline chloride-urea (CC-U, neutral) and choline chloride-monoethanolamine (CC-M, alkaline). It was shown that an esterification reaction of cellulose occurs with acidic DES, while no modification was observed with neutral and alkaline DES. The crystallinity index of the treated fibres was not impacted by DES treatment. Moreover, an internal and external fibrillation of the fibres was identified after DES pre-treatment, which led to a significant improvement of mechanical properties of the produced papers (Young's modulus, internal bond strength...). It was concluded that DES pre-treatment can be considered as a relevant green and soft treatment which is similar to a chemical refining. This paper is a continuation of this previous work. It aims at investigating the production of cellulose microfibrils from DES-treated cellulosic fibres. DES systems (acidic and alkaline), that were never used for this purpose, have been studied to pre-treat cellulosic fibres and promote internal and external fibrillation. Then, the DES-treated fibres were ground by an ultra-fine grinder and characterised using several methods, including transmission electron microscopy, X-ray diffraction, tensile tests of nanopapers, etc. Finally, the MFC obtained after DES treatment were compared to those obtained from enzymatic hydrolysis (used as a reference pre-treatment).

III.1.2 Materials and Methods

III.1.2.1 Materials

Dry sheets of bleached hardwood pulp (eucalyptus, Fibria T35) and cotton pulp (Celsur) were chosen as cellulose materials and referenced as EF and CF, respectively. These fibres were first disintegrated in water, filtered and washed with ethanol and then oven dried at 60 °C. Betaine hydrochloride ($C_5H_{12}ClNO_2$) was supplied from VWR (Milliporesigma), monoethanolamine (C_2H_7NO , >99%) from ROTH, choline chloride ($C_5H_{14}ClNO$, >98%) from Alfa Aesar. Urea ACS reagent (CH_4N_2O , 99.0-100.5%), bis(ethylenediamine)copper (II) hydroxide solution ($Cu(H_2NCH_2CH_2NH_2)_2(OH)_2$ 1.0 M in H_2O), sulfuric acid (H_2SO_4 , 72%), acetic acid

CHAPTER III. Microfibrillated cellulose MFC PRODUCTION FROM DES PRE-TREATMENT

(CH₃COOH), ethanol (CH₃OH, 96%) and sodium acetate (C₂H₃NaO₂) were obtained from Sigma Aldrich. Enzyme solution FiberCare (pH between 6 and 8) was purchased from Novozymes. Deionised water was used throughout the experiments.

III.1.2.2 DES pre-treatment

Cellulose fibres (EF and CF) were treated in three eutectic mixtures; (i) betaine hydrochloride-urea BHCl-U (1:4) (ii) choline chloride-urea CC-U (1:2) and (iii) choline chloride-monoethanolamine CC-M (1:6) as described in our previous study (Mnasri et al., 2022). Cellulose fibres were mixed with DES in a reactor vessel (Pressure reactor-600 mL) with a mass ratio of 2.5:100 (for BHCl-U and CC-U) and 5:100 for CC-M. These ratios were selected based on the viscosity of the obtained DES. The mixture of cellulose and DES was left under mechanical stirring at 100 °C for 4 hours. After treatment, the suspension was filtered and washed with hot and cold water to remove the remaining DES.

III.1.2.3 Enzymatic pre-treatment

An enzymatic hydrolysis using cellulase was used as a reference pre-treatment. The treatment of the fibre suspension (2 wt %) was performed in a 12 L reactor (Büchiglasuster, Germany) at 50 °C in acidic conditions (pH = 5), using an acidic buffer solution (acetic acid and sodium acetate). Enzyme solution (FiberCare cellulase with an activity of 4948 ECU/g of solution) was added to the suspension with an enzyme's concentration of 300 ECU/g of cellulose. The fibres were left 2h under stirring and then enzyme was deactivated by raising the temperature to 80 °C for 10 min. The suspension was then filtered through a nylon sieve (10 µm of mesh) and washed by hot and cold water.

III.1.2.4 Cellulose microfibrillation

Cellulose microfibrillation was performed with supermasscolloider ultra-fine friction grinder (model MKZA6-2, disk model MKG-C 80, Masuko Sangyo Co., Ltd., Japan). DES and/or enzymatic treated fibres were suspended in water (2 wt %) and ground at 1500 rpm. The suspension was passed through the disks by adjusting the gap (distance) between them: 5 passes at a gap (0), 10 passes with a gap (-5) and 20 passes with a gap (-10).

III.1.2.5 Nanopaper handsheet production

Nanopapers were prepared by filtration using a Rapid Köthen sheet former according to ISO standard 5269-2:2004. MFC suspension (0.5 wt %) was filtered through the sheet former equipped with a nylon sieve (mesh size of 1 μm). After filtering, the obtained shandheets were dried under vacuum at 85 °C for 20 min. 3 nanopapers were made for each kind of MFC. Before any tests, dried nanopapers were stored in a conditioned room (23 °C and 50% RH) for 48 h as recommended in ISO 187 standard.

III.1.2.6 Microfibrillated cellulose MFC characterisation

III.1.2.6.1 Microscopic analyses: TEM, AFM and optical microscopy

Transmission Electron Microscopy (TEM) was performed with a JEOL JEM-2100-Plus microscope operating at 200 kV equipped with a Gatan Rio 16 digital camera. Diluted MFC suspensions were deposited onto glow-discharged carbon-coated TEM grids. During sample preparation, a negative dye composed of uranyl acetate was added. After drying, the sample was placed inside the microscope and images were recorded.

Atomic Force Microscopy (AFM) was done in tapping mode using a dimension Icon atomic force microscope (DI, Veeco, Instrumentation Group). MFC suspensions at a concentration of 10^{-3} wt % were prepared and sonicated for 3 min. One drop of the sonicated suspension was deposited on a mica plate, dried overnight at room temperature and then analysed.

Optical microscopy images were made with an Axio Imager M1 microscope (Carl Zeiss, Germany) equipped with an AxioCam MRc 5 digital camera. MFC suspensions diluted at 0.1 wt % and mixed with an Ultra-TurraxT-25 disperser (5 min at 5000 rpm) was used. Magnifications of 50 and 100 were used and 5 images were taken for each magnification.

The *macro size* (μm^2) was determined from optical microscopy images using Fuji software. Images were transformed to 8-byte format and thresholded. Then, the average size of the particles was calculated. The macro-size, which represents the average surface of the visible particles, is obtained by dividing the total surface by the number of particles. Six images per sample were analysed.

III.1.2.6.2 Degree of Polymerisation

The degree of polymerisation DP was determined according to ISO 5351:2010 standard. Microfibrillated cellulose were dissolved in a bis(ethylenediamine)copper(II) hydroxide solution. The intrinsic viscosity $[\eta]$ was measured at 25°C with a capillary viscosimeter and the DP was deduced using the Mark–Houwink–Sakurada equation. Three measurements were made for each sample.

$$DP^{0.905} = 0.75 \times [\eta]$$

III.1.2.6.3 X-ray Diffraction

X-ray diffraction (XrD) was performed on nanopaper samples deposited on a zero-background Si substrate. The measurements were carried out with a diffractometer X'Pert Pro MPD (PANalytical, Netherlands), equipped with a Bragg-Brentano geometry and a copper anode ($K\alpha$ $\lambda = 1.5419 \text{ \AA}$). The crystallinity index CrI (%) was calculated by the Segal method (Segal et al., 1959):

$$CrI = \frac{I_{002} - I_{am}}{I_{002}} \times 100$$

where I_{002} represents the diffraction intensity of the main crystalline peak at $2\theta \approx 22.5^\circ$ and I_{am} is the intensity at $2\theta \approx 18.7^\circ$.

III.1.2.6.4 Morphological analysis of MFC suspension

MFC suspensions were analysed with a Morfi-Neo fibre analyser (techpap, France) to determine the main morphological properties of the remaining visible elements (arithmetic fibre length, fibre width, fine content). 40 mg of the materials (dry matter) were diluted in 1 L of deionised water. Analyses were performed during 5 min with limit fibre/fine elements fixed at 80 μ m. For each sample, a triplicate analysis was done and the mean value s was determined. Morphological properties were compared to those of the original cellulosic fibres (EF and CF).

III.1.2.6.5 Nanosized fraction and turbidity

The nanosized fraction was measured by a gravimetric method, adapted from Naderi et al. (2015). This method allows determining the quantity of nanoscale particles contained in the

MFC suspension. For this purpose, MFC suspensions were first diluted to 0.02 wt % and then centrifuged at 1000 g for 15 min in order to remove the largest fragments. Concentrations of the suspension before and after centrifugation (in the supernatant) were measured after 24 h of drying at 105 °C. The nanosized fraction was calculated as following:

$$\text{Nanosized fraction (w/w\%)} = \frac{C_{ac}}{C_{bc}} \times 100$$

where C_{ac} and C_{bc} correspond to the mass concentration after and before centrifugation, respectively. NF (%) corresponds not only to MFC and microfibril aggregates, but also to larger particles.

Turbidity of the MFC suspensions was measured using a portable turbidimeter AL-250 (Aqualitic, Germany) with a range between 0.01 and 1100 NTU. The diluted MFC suspensions (0.1 wt %) were homogenized for 2 min with an Ultra Turrax T-25 disperser at 8000 rpm and then 10 measurements were done. The turbidity value is mainly influenced by the size of the suspended elements, their shape and concentration.

III.1.2.6.6 Thermogravimetric analysis

Thermogravimetric analyses (TGA) of microfibrillated cellulose were done with a thermal analyser Mettler Toledo (TGA/DSC 3⁺) under nitrogen or air flow (dynamic air) using a constant flow rate of 30 mL min⁻¹. Approximately 6 mg of the sample (nanopaper) were heated from 25 to 700 °C, at a rate of 10 °C min⁻¹.

III.1.2.6.7 Tensile tests

Tensile tests were performed on the produced nanopapers using an Instron 5965 machine (Instron, USA), according to ISO 1924-2 standard and in conditioned atmosphere (23 °C and 50% RH). Tests were done on samples with dimensions of 15 × 100 mm² and a tensile speed of 10 mm/min. The Young's modulus and tensile strength of each sample were determined. The average of 6 measurements was calculated.

III.1.2.6.8 Oxygen permeability

The oxygen transmission rate (OTR) was analysed with an oxygen permeation analyser (model 8001 systech Illinois Inc., USA) at 2 bar partial oxygen pressure. The nanopaper was exposed

to 100% oxygen on one side and to oxygen-free nitrogen on the other side. The oxygen permeability (OP) was calculated by multiplying the obtained OTR by the thickness of the nanopaper and dividing it by the difference in the partial oxygen pressure. The measurements were made at 23 °C, under normal atmospheric pressure, and at 0, 50 and 80% RH.

III.1.2.6.9 Simplified Quality Index

The quality of produced MFC has been evaluated by using the simplified Quality Index QI^* (Desmaisons et al. (2017)). QI^* combines four simple tests which are nanosized fraction (%), turbidity (NTU), Young's modulus (GPa) and macro size (μm^2) and it is calculated as following:

$$QI^* = 0.3 x_1 + (-0.03 x_2) - 0.071 x_3^2 + 2.54 x_3 - 5.35 \ln(x_4) + 59.9$$

where x_1 corresponds to the nanosized fraction value, x_2 represents the turbidity value, x_3 is the value of the Young's modulus and x_4 corresponds to the macro size value.

III.1.3 Results and discussions

III.1.3.1 Morphological and structural properties of produced MFC

DES-treated fibres (EF and CF) were passed through the ultrafine grinder without any clogging. The obtained aqueous microfibril suspensions were viscous and gel-like materials. AFM, TEM images of MFC from EF and CF and the resulting nanopapers are presented in Figure III. 1. These images confirm the effectiveness of this pre-treatment to produce a mixture of microfibril bundles having widths around 50 nm and individualised microfibrils with widths between 5 and 10 nm.

CHAPTER III. Microfibrillated cellulose MFC PRODUCTION FROM DES
PRE-TREATMENT

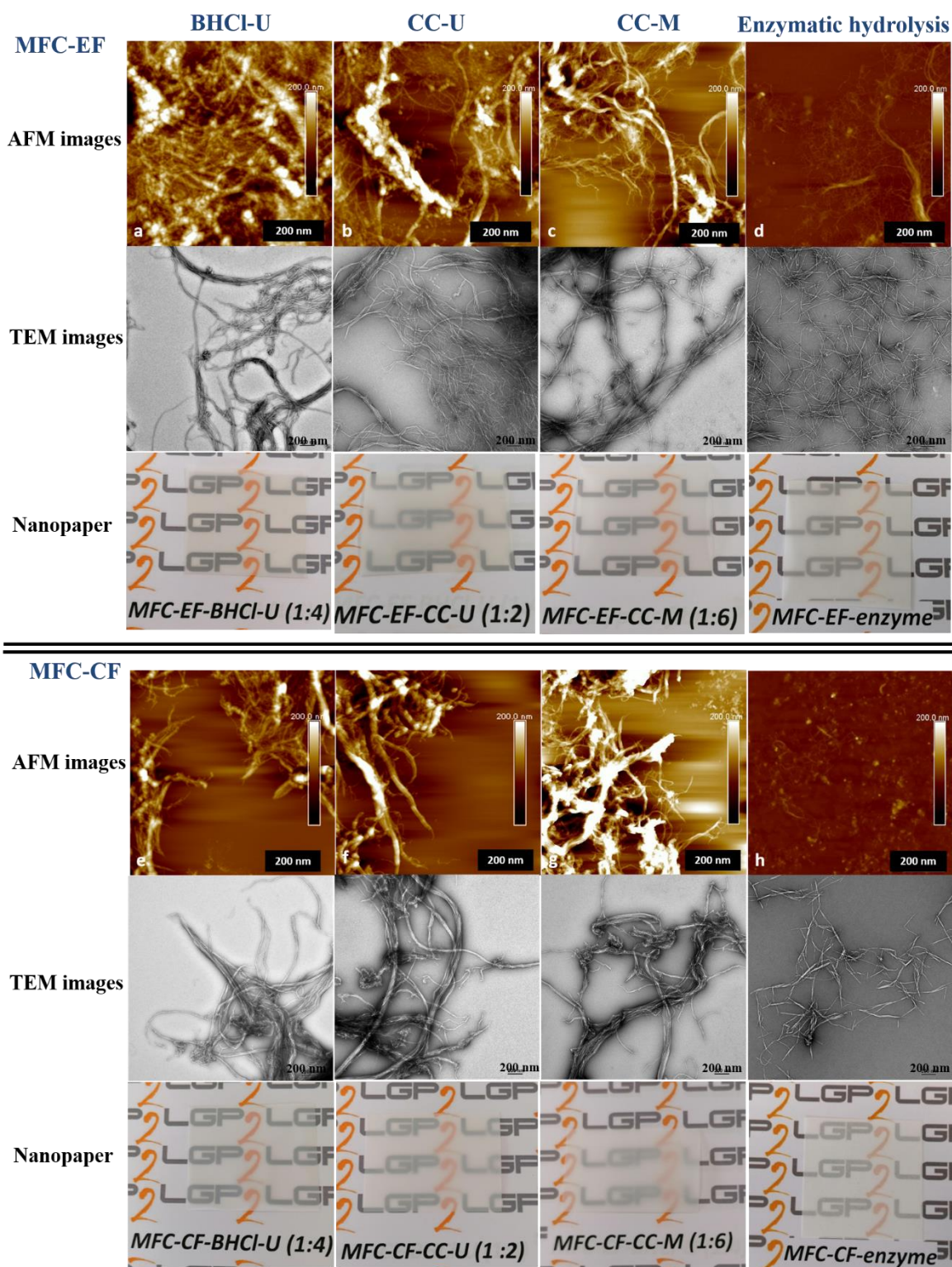


Figure III. 1. AFM, TEM and nanopapers images of produced MFC-EF and MFC-CF treated with BHCl-U (a, e), CC-U (b, f), CC-M (c, g) and enzymatic hydrolysis (d, h) respectively.

CHAPTER III. Microfibrillated cellulose MFC PRODUCTION FROM DES PRE-TREATMENT

It is worth noting that the length of the obtained MFC after DES-treatment (Figure III. 1a, b, c and e, f, g) is very different from that obtained when an enzymatic treatment is used (Figure III. 1d, h) and this difference is visible on both AFM and TEM images. It can be explained by the way how DES and enzyme react on cellulose. As reported by Mnasri et al. (2022), DES has a specific action on the fibre cell wall: it enhances internal and external fibrillation especially in the case of alkaline and neutral DES-treatment. In addition, acidic-DES treated fibres undergo chemical modification and cellulose is esterified. Thus, the grafted betaine, which bears a cationic charge (quaternary ammonium), induces repulsion between the microfibrils. This phenomenon facilitates both fibrillation (internal and external) and microfibrillation. This is in line with another study on cellulose quaternisation using betaine hydrochloride and glycerol, as reported by Hong et al. (2020). It can be concluded that DES allows the production of MFC with very high aspect ratio compared to enzymatic hydrolysis. Indeed, this later reduces the cellulose chain length which leads to short and kinked MFC. Oppositely, the width of the enzymatic MFC is not very different from that of the individualised DES-treated MFC, especially for eucalyptus MFC. The presence of bundles and aggregates of MFC after DES treatment is probably related to their very high aspect ratio.

As expected, the degree of polymerisation (see Figure III. 2) of MFC-EF and MFC-CF decreased after mechanical treatment which results from the high shear forces applied during grinding (Sirviö et al., 2015). Moreover, this decrease is more pronounced for enzymatic MFC and this is the result of the enzymatic hydrolysis itself, DP of fibres being already significantly lowered before the grinding (Mnasri et al., 2022). The relative decrease of the DP is, in all cases, lower for cotton MFC which may be due to their very low initial DP.

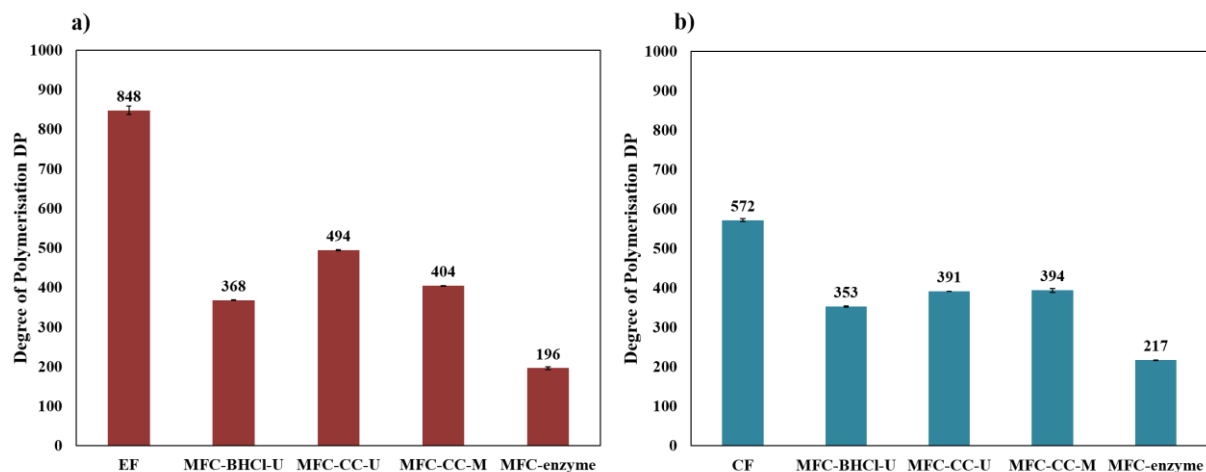


Figure III. 2. Degree of Polymerisation DP of MFC produced from Eucalyptus (a) and Cotton fibres (b).

The XrD diffractograms of the MFC are reported in Figure III. 3. They show the presence of only the allomorph cellulose I_{β} for all MFC. It is important to note that the DES treatment does not impact the crystallinity of the fibres as shown by Mnasri et al. (2022). Consequently, the observed decrease of the crystallinity index (CrI) of the DES-treated MFC (EF and CF) is only attributable to grinding. It results from the weakening of interfibrillar hydrogen bonds and disruption of crystalline parts due to the high shear forces as reported in many studies (Hong et al., 2020; Suopajarvi et al., 2017). From our results, it appears that the relative decrease of CrI induced by grinding is of 26 and 27% after acidic DES, 32 and 37% after neutral DES, 42 and 44% after alkaline DES and 38 and 34% with enzymatic hydrolysis for MFC produced from EF and CF, respectively. Thus, the grinding of fibres pre-treated by acidic DES led to the lowest decrease of the CrI for both MFC. This result may be due to the electrical charges of the fibres and their positive impact on microfibrillation which is facilitated.

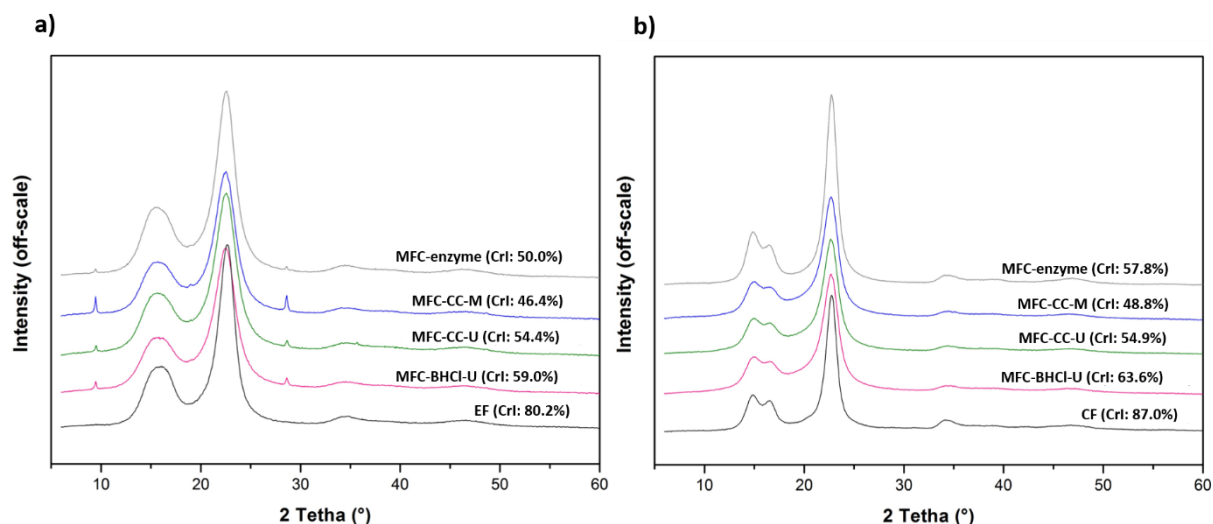


Figure III. 3. XrD diffractograms of MFC produced from Eucalyptus (a) and Cotton fibres (b).

The morphological properties (Morfi analyses) of MFC suspensions and their turbidity values are presented in Figure III. 4. The visible elements present in the MFC suspensions are cellulosic fines (more than 85% and 90 % for eucalyptus and cotton MFC suspensions, respectively) which is in line with the turbidity of the different suspensions.

In fact, after DES treatment, the eucalyptus MFC suspensions are characterised by smaller turbidity values (between 388 and 424 NTU) compared to those obtained from cotton MFC suspensions (between 745 and 774 NTU).

Regarding the enzymatic treatment, the MFC suspensions present lower turbidity (228 and 558 NTU for MFC-EF and MFC-CF, respectively) than those obtained from DES-treatment. This is related to the hydrolysis effect of enzyme which reduced the length of MFC and their aspect ratio, thus limiting entanglement between MFC and the presence of bundles that could impact the turbidity values.

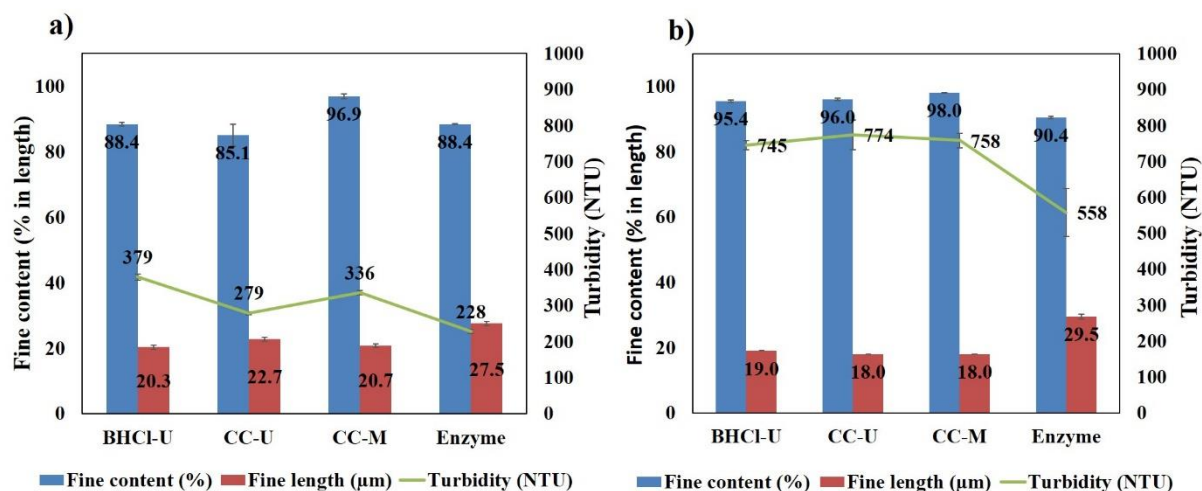


Figure III. 4. Morphological properties of remained elements in MFC-EF (a) and MFC-CF suspensions (b).

III.1.3.2 Thermogravimetric properties

The thermal behaviour (TGA/DTG) of MFC produced from DES or enzymatic pre-treatment were analysed and compared to untreated fibres. The curves of TGA/DTG of the different samples are reported in Figure III. 5. The thermal degradation of cellulose has been widely studied (Banyasz et al., 2001; Zhu et al., 2012) and the most accepted mechanism is based on three coupled reactions. The first reaction is an activation or induction step resulting in “active cellulose”. The nature of this active cellulose is not well understood. However, it was postulated based on the necessity to have an initial step involving no weight loss. This is followed by a pair of competing reactions, that lead to weight loss. The first is supposed to occur via depolymerisation of cellulose which results in the production of levoglucosan and its degradation products. These are identified as 'volatiles'. The other reaction is intended to produce char and gases such as CO₂ and water (Banyasz et al., 2001; Zhu et al., 2012).

CHAPTER III. Microfibrillated cellulose MFC PRODUCTION FROM DES
PRE-TREATMENT

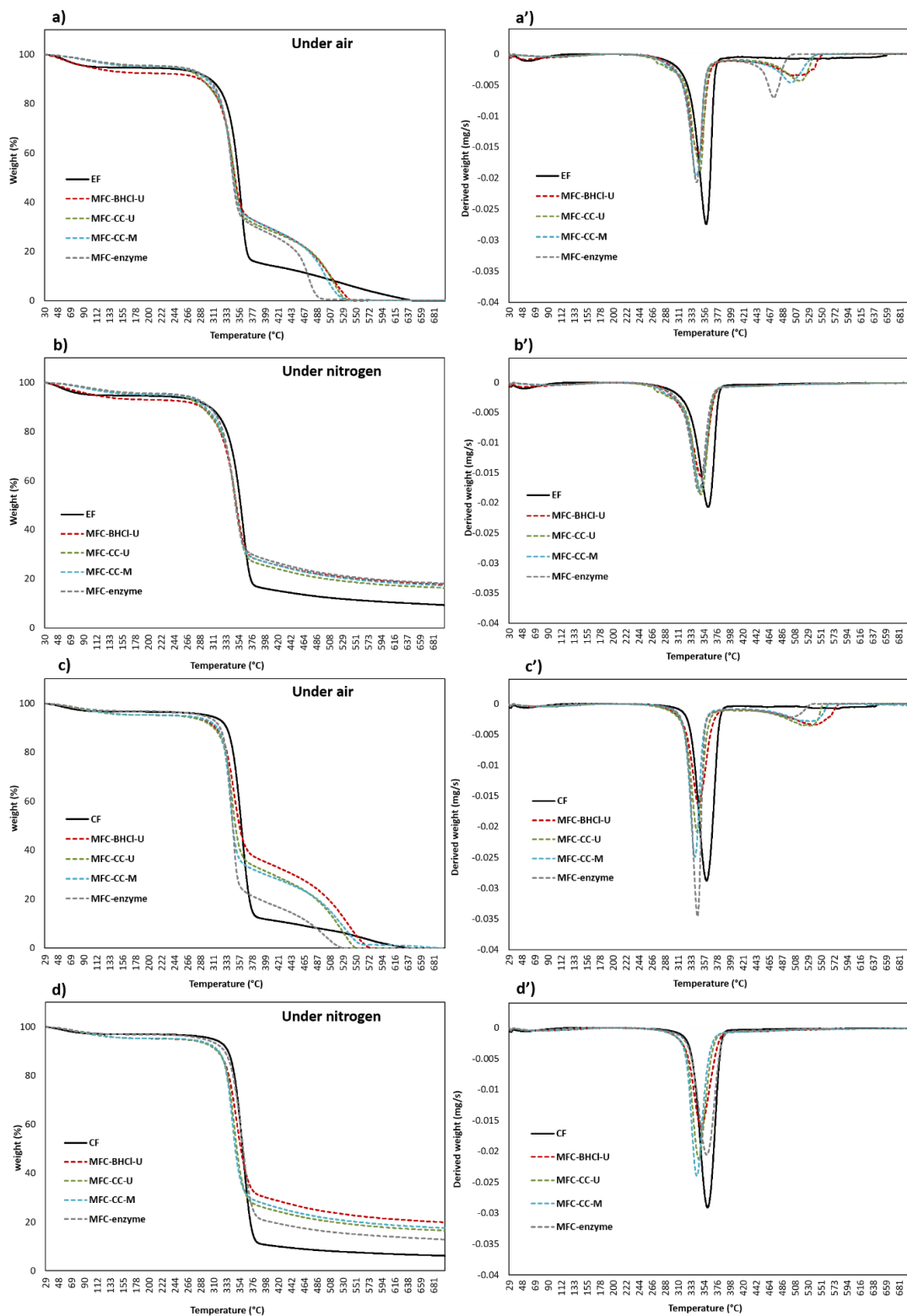


Figure III. 5. TGA and DTG curves of MFC produced from EF (a, a', b and b') and CF (c, c', d and d') under and nitrogen flow respectively.

CHAPTER III. Microfibrillated cellulose MFC PRODUCTION FROM DES PRE-TREATMENT

Table III. 1 summarizes the starting decomposition temperature (T_{start}), onset decomposition temperature (T_{onset}), maximum weight-loss rate temperature (T_{max}) and residual weight of the MFC samples and untreated eucalyptus and cotton fibres. In the initial stage, where the temperature was below T_{start} , the weight loss was due to the evaporation of the moisture. The main cellulose degradation, between approximately 200 °C and 400 °C, was caused by depolymerisation, dehydration of the cellulose or decomposition of the glycosyl units. The T_{start} of untreated cellulose was around 277 and 287 °C under air and nitrogen flow respectively. For MFC samples, T_{start} decreased and its value was between 257-266 °C and 261-276 °C under air and nitrogen respectively. The onset temperature of decomposition as well as T_{max} were lower for MFC. It indicates the decrease of cellulose thermal stability which may be affected by the decrease of its crystallinity after grinding.

The residual weight after cellulose pyrolysis was 9% for eucalyptus fibres while it was between 16 and 18% for MFC samples. This higher residual weight reveals the presence, in small quantity, of relatively stable zones which lower the degradation rate.

As expected, under nitrogen flow, it is clearly observed that all the temperatures of cellulose decomposition were higher than those obtained under air. This observation indicates more thermal stability of all samples in nitrogen which is in accordance with other studies (Hafid et al., 2021; Li et al., 2017).

For cotton, the tendency and the results are similar. However, the starting temperature of decomposition of untreated fibres was higher than that of eucalyptus due to the absence of hemicelluloses in cotton fibres.

Table III. 1. Temperatures of cellulose degradation process of produced MFC.

Sample	Under air			Under nitrogen			Residual weight (%)
	T _{start} (°C)	T _{onset} (°C)	T _{max} (°C)	T _{start} (°C)	T _{onset} (°C)	T _{max} (°C)	
Eucalyptus fibres							
EF	277	358	380	287	361	389	9
MFC-BHCl-U	262	349	374	268	351	384	18
MFC-CC-U	257	349	373	261	349	381	16
MFC-CC-M	261	342	371	268	348	380	17
MFC-enzyme	266	344	370	276	347	377	18
Cotton fibres							
CF	295	360	388	306	360	394	6
MFC-BHCl-U	279	346	384	289	349	387	20
MFC-CC-U	280	344	378	287	346	381	17
MFC-CC-M	296	341	375	289	342	381	18
MFC-enzyme	296	345	373	305	360	390	13

III.1.3.3 Mechanical properties and oxygen barrier properties

III.1.3.3.1 Mechanical properties of nanopapers

Density, Young's modulus and tensile strength index were determined as depicted in Figure III. 6.

It clearly appears that nanopapers produced from DES-treated MFC exhibit higher density than those obtained from enzymatic MFC, for both EF and CF. The highest densities for MFC-EF and MFC-CF were obtained with alkaline DES (1255 and 1254 kg/m³ respectively), followed

by acidic system (1228 and 1210 kg/m³ respectively) and neutral DES (1162 and 1087 kg/m³ respectively). After enzymatic treatment, the density of nanopapers made of eucalyptus and cotton fibres is lower with values of 1064 and 844.5 kg/m³, respectively. The significant densification of the nanopapers after DES treatment reveals their specific effect. In fact, obtaining such a densification with elements having very high aspect ratio is quite unexpected. It may be attributable to a different microfibrillation, leading to MFC more flexible and very conformable, with high specific surface area that are linked together via strong hydrogen bonding.

It is worth noting that Young's modulus and tensile strength index tend to increase with nanopaper density (see Figure III. 6) but at a minor extent. In the same way, Young modulus of eucalyptus nanopapers is not greatly impacted by the different treatments (values are all comprised between 10 and 11 GPa) whereas DES treatment improves the elastic modulus of cotton nanopapers compared to enzymatic treatment (Young's modulus rises from 6.0 to 8.4 GPa). The most important effect is observed for the tensile strength index at break: DES treatment, and especially acidic and neutral DES, allows increasing the tensile strength of EF and CF nanopapers by 25 and 33 %, respectively when compared to enzymatic treatment. Finally, the vegetal fibre source plays a major role: strength of nanopapers from eucalyptus fibres is significantly higher. This difference may be due to the presence of hemicellulose in eucalyptus fibres which enhances the mechanical properties of nanopapers. The hemicelluloses are strongly bound onto the MFC surface in the form of "shell" coating, and act as a binder which favours stress-transfer among microfibrils (Galland et al., 2015; Meng and Wang, 2019).

Mechanical properties of nanopapers are related to many parameters (MFC width, length, orientation, flexibility, etc.) as reviewed by Meng and Wang (2019). Fukuzumi et al. (2013) demonstrated that, for a given MFC diameter, longer MFC lead to higher fracture toughness of the nanopapers. As a result, the elastic modulus, toughness and tensile strength increase simultaneously while increasing MFC length. In our work, we have shown that DES-treated MFC clearly have high aspect ratio compared to enzymatic MFC which promotes the entanglement of the MFC. The combination of this property with high density of nanopapers probably enhances strength as well as load transfer in the network which allows obtaining higher elastic modulus and tensile strength, as already discussed in the literature (Henriksson et al., 2008; Sehaqui et al., 2014).

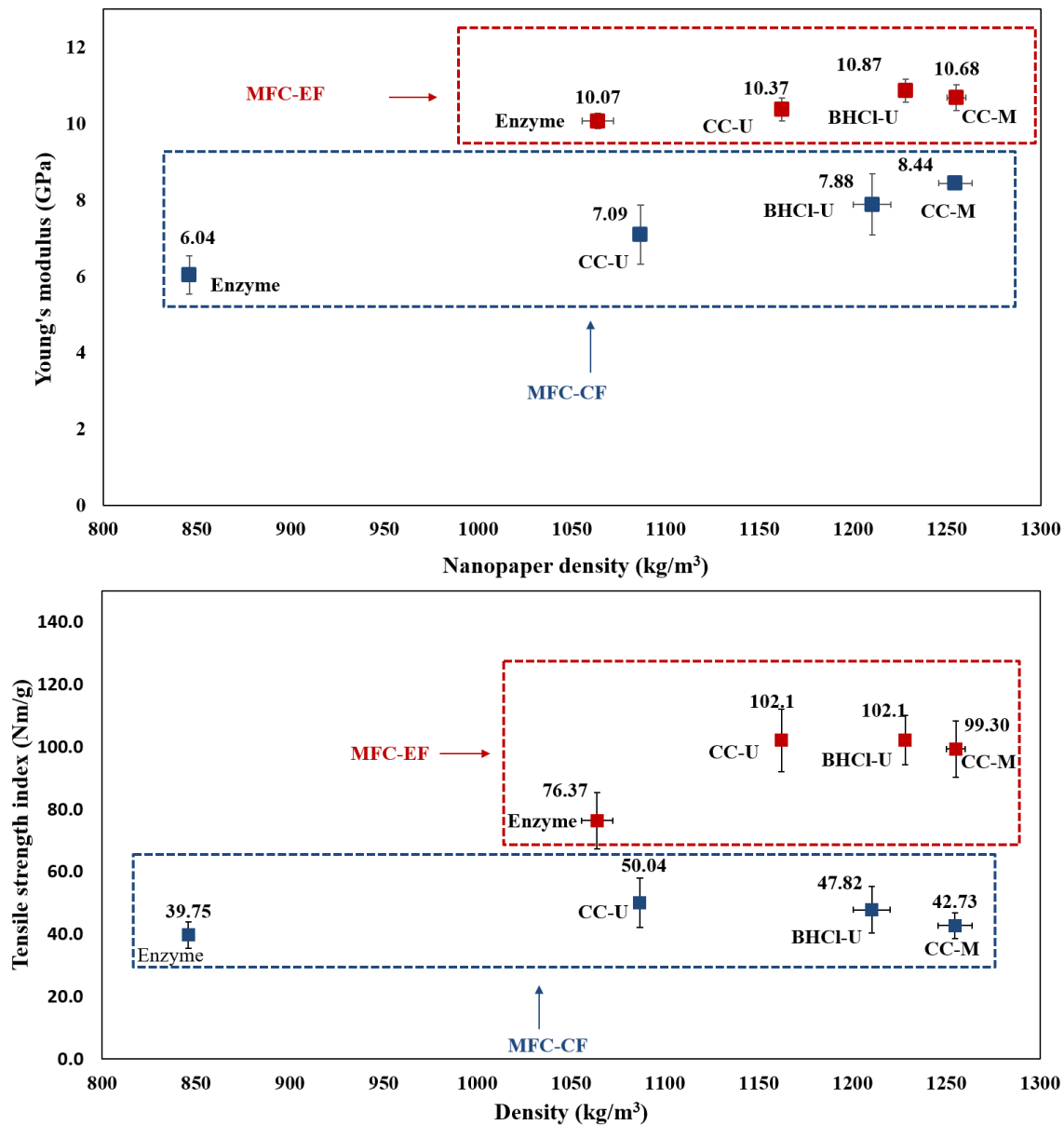


Figure III. 6. Evolution of the Young's modulus and tensile strength index with nanopaper density.

III.1.3.3.2 Oxygen permeability

Oxygen permeability of nanopapers is presented in Table III. 2. The OP values are higher than 400 ($\text{cm}^3 \cdot \mu\text{m} / \text{m}^2 \cdot \text{d} \cdot \text{atm}$), indicating a medium permeability of the nanopapers (Wang et al., 2018), even if they present high density (greater than 1000 kg/m^3).

For eucalyptus, the OP of nanopapers made from DES-terated MFC is smaller compared to those obtained from enzymatic MFC, the values even being not measurable in the case of enzyme-CF-MFC. These results demonstrate the potential of DES pre-treatment to control the OP of the nanopapers. Regarding the different tested DES, there is no visible tendency and the differences between the different treatments remains low. As expected, OP rises with relative humidity whatever the samples, which is related to the presence of water that breaks the hydrogen bonds holding the MFC together. Thus, at high humidity, nanopapers swell, allowing oxygen permeability to increase. It can be also noted that OP of eucalyptus is also lower than that of cotton nanopapers.

Table III. 2. Oxygen permeability of produced MFC

Sample	0 % RH		50% RH		80% RH	
	OTR (cm^3 ($\text{m}^2 \cdot \text{d}$) ⁻¹)	OP ($\text{cm}^3 \cdot \mu\text{m}$ ($\text{m}^2 \cdot \text{d} \cdot \text{atm}$) ⁻¹)	OTR (cm^3 ($\text{m}^2 \cdot \text{d}$) ⁻¹)	OP ($\text{cm}^3 \cdot \mu\text{m}$ ($\text{m}^2 \cdot \text{d} \cdot \text{atm}$) ⁻¹)	OTR (cm^3 ($\text{m}^2 \cdot \text{d}$) ⁻¹)	OP ($\text{cm}^3 \cdot \mu\text{m}$ ($\text{m}^2 \cdot \text{d} \cdot \text{atm}$) ⁻¹)
MFC-EF-BHCl-U	20.9	499	40.1	956	116	2744
MFC-EF-CC-U	19.2	487	42.0	1066	96.8	2457
MFC-EF-CC-M	20.6	523	49.9	1088	108	2754
MFC-EF-enzyme	22.8	671	42.9	1365	108	5167
MFC-CF-BHCl-U	20.1	500	47.4	1179	149	3719
MFC-CF-CC-U	36.7	893	48.6	1184	153	3728
MFC-CF-CC-M	17.9	450	36.0	905	176	4410
MFC-CF-enzyme	>1000	>10000	>1000	>100000	>1000	>100000

d: day

It was reported that the barrier properties of non-modified MFC nanopapers were less than those of modified MFC through carboxymethylation (Aulin et al., 2012, 2010) or TEMPO-oxidation (Kumar et al., 2014) which is in line with our results. Nevertheless, Sirviö et al. (2020) showed that DES allows obtaining high barrier properties (OP < 40) using CC-U and CC-imidazole

system. This is not in accordance with the present study and one of the possible reasons, and may be the main one, is the method used for sample preparation. Thus, Sirviö et al. (2020) prepared microfibrillated cellulose films by a casting method, while, in our case, the nanopapers were prepared by filtration.

III.1.3.3.3 Simplified quality index of produced MFC and energy consumption during ultra-fine grinding

The quality index allows evaluating the produced MFC. It was developed to characterise MFC and gives an idea of the homogeneity and the level of microfibrillation. Quality index value allows to classify the different MFC (Desmaisons et al., 2017). The obtained data are listed in Table III. 3 and show that MFC produced from eucalyptus fibres exhibit higher quality index (between 74 to 76) than those produced from cotton fibres (between 43 and 52). This is consistent with the results presented in the previous sections. Moreover, the obtained values are comparable to those of the literature. For instance, commercial grades of enzymatic MFC produced from eucalyptus fibres by ultrafine grinding has QI^* between 60 and 75 and those produced from cotton fibres are around 46 (Desmaisons et al., 2017).

Eucalyptus MFC prepared from DES pre-treatment exhibited higher QI^* (between 72 and 76) than those produced from enzymatic hydrolysis (69). This result confirmed the effectiveness of DES to produce MFC with high quality that is comparable to marketed MFC.

Table III. 3. Simplified quality index of produced MFC

Sample	Macro size (μm^2)	Nanosized fraction (%)	Turbidity (NTU)	Young's modulus (GPa)	Simplified QI*
Eucalyptus fibres					
MFC-EF-BHCl-U	12.22 \pm 1.31	61.67 \pm 8.94	379 \pm 8	10.9 \pm 0.3	72.86 \pm 2.70
MFC-EF-CC-U	13.85 \pm 6.73	67.26 \pm 0.51	279 \pm 4	10.4 \pm 0.3	76.43 \pm 1.35
MFC-EF-CC-M	16.08 \pm 1.33	65.96 \pm 6.86	336 \pm 6	10.7 \pm 0.3	73.77 \pm 1.77
MFC-EF-enzyme	69.21 \pm 3.40	65.87 \pm 4.04	228 \pm 6	10.07 \pm 0.2	68.52 \pm 0.61
Cotton fibres					
MFC-CF-BHCl-U	97.05 \pm 52.4	63.61 \pm 5.35	745 \pm 13	7.88 \pm 0.4	47.77 \pm 3.68
MFC-CF-CC-U	70.57 \pm 25.5	75.12 \pm 12.44	774 \pm 41	7.09 \pm 0.5	50.88 \pm 6.09
MFC-CF-CC-M	64.34 \pm 0.10	56.49 \pm 1.36	758 \pm 20	8.44 \pm 0.1	48.22 \pm 0.01
MFC-CF-enzyme	138.4 \pm 49.3	43.95 \pm 7.83	558 \pm 67	6.04 \pm 0.5	42.73 \pm 6.08

The energy consumption (KWh/t) during MFC grinding was calculated as following:

$$E = \frac{P_{net} \times t}{m_{dry}}$$

P_{net} correspond to the net power (KW), t is the fibrillation time (h) and m_{dry} is the fibres/MFC dry mass (t).

The net power was measured for each pass through the ultrafine grinder and then summed to get the energy consumption during grinding.

The evolution of the simplified quality index QI* and the energy consumption is presented in Figure III. 7. The obtained values of energy consumption are comparable to those find in the literature (Banvillet et al., 2021; Desmaisons et al., 2017).

CHAPTER III. Microfibrillated cellulose MFC PRODUCTION FROM DES PRE-TREATMENT

Despite, the low-quality index of MFC produced from cotton, their grinding consumed more energy (except for that produced from enzymatic hydrolysis) than those obtained from eucalyptus. This difference is due to the presence of hemicelluloses in eucalyptus fibres which facilitated MFC liberation and then reduced the energy consumption.

The energy consumed during grinding could be related to the nanopaper density (Figure III. 7). Thus, MFC (EF and CF) obtained from alkaline DES required more energy than the others because the resulting nanopapers have the highest density. The enzymatic treatment did not consume a lot of energy especially for CF. However, in the case of EF-MFC, the values of energy consumption for acidic DES and enzymatic treatments were the same. The low energy consumption for acidic DES resulted from the presence of cationic charges which enhances the repulsion between microfibrils and thus facilitates their liberation during grinding.

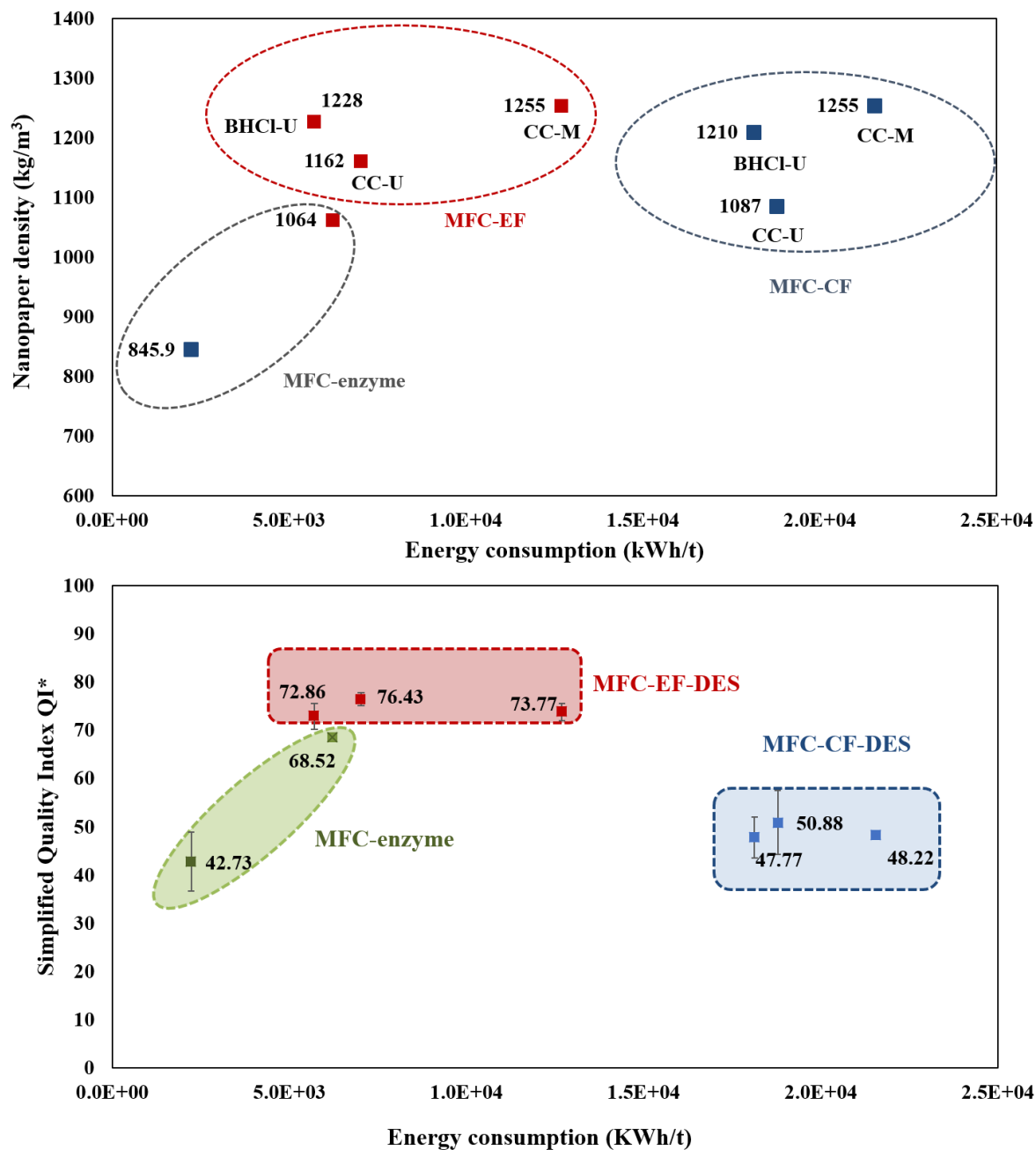


Figure III. 7. Nanopaper density and simplified quality index QI* evolution with grinding energy.

III.1.4 Conclusion

New DES systems were tested as green pre-treatment media for cellulose (eucalyptus and cotton fibres) microfibrillation. The obtained results are very promising and confirmed the effectiveness of DES as pre-treatment media. As shown in a previous study (Mnasri et al.,

2022), DES treatment of fibres promotes their internal and external microfibrillation. In this work, we have demonstrated that this effect observed for the fibres helps facilitating the ensuing microfibrillation process. The characterisations revealed that the quality of MFC obtained from DES was significantly different from those obtained from enzymatic treatment. DES-treated MFC have, in particular, very high aspect ratio. Nanopapers produced from DES-treated MFC (EF and CF) exhibited high density and Young's modulus and very high tensile strength. These properties result from network made of long, conformable and entangled MFC in which load transfer is efficient.

Moreover, DES-treated MFC from eucalyptus fibres show good quality index (between 73 and 76). It is worth noting that presence of ester function with quaternary ammonium grafted on cellulose in the case of acidic DES treatment enhanced the mechanical microfibrillation with a reduced energy consumption. This phenomenon results from to charge repulsion between microfibrils which decreases energy consumption during grinding compared to unmodified MFC.

Finally, the results confirm the importance of hemicelluloses in the microfibrillation process and their positive effects on the mechanical properties of nanopapers.

III.2 High content MFC suspensions produced from DES-treated fibres using twin-screw extruder

Abstract

In this study, cellulosic fibres (bleached kraft pulp of Eucalyptus), pre-treated with Deep Eutectic Solvents (DES), have been microfibrillated using a twin-screw extruder (TSE). DES pre-treatment was performed for 4 h at 100 °C with three eutectic systems: betaine hydrochloride-urea, choline chloride-urea and choline chloride-monoethanolamine. DES-treated fibres were first refined (PFI-mill) and then passed four times through the TSE whose advantage is to obtain MFC at high solid content (20%). Several characterisations were carried out before and after TSE to evaluate the effects of these treatments on both the fibres and MFC. The Young's modulus of the obtained nanopapers was, for instance, around 6 GPa. Extruded-MFC were compared to those produced by ultrafine grinding. The comparison showed that the ultrafine grinding allows obtaining MFC of better quality. This result can be attributed to the slipping phenomenon occurred during extrusion.

Key words: Cellulose, microfibrillated cellulose, pre-treatment, Deep Eutectic Solvents, twin-screw extruder.

III.2.1 Introduction

Cellulose, defined as the most abundant polymer on earth, is characterised by fascinating properties, including biodegradability, sustainability and renewability (Siró and Plackett, 2010). In the cell wall, cellulose is present in the form of macrofibrils, that are themselves composed of microfibrils resulting from the association of elementary fibrils (Cousins and Brown, 1995). Cellulose microfibrils (CMF), called also microfibrillated cellulose (MFC), cellulose nanofibrils (CNF) and nanofibrillated cellulose (NFC), can be extracted from cellulose fibres by subjecting the fibrous suspension to a high shear mechanical treatment such as ultrafine grinding (Spence et al., 2011), homogenisation and microfluidisation (Abdul Khalil et al., 2014; Boufi and Gandini, 2015). However, these treatments are energy consuming that is why there is a need to pre-treat the cellulose fibres (Nechyporchuk et al., 2016). Various pre-treatments exist in the literature such as TEMPO-oxidation (Besbes et al., 2011; Isogai et al., 2011; Saito et al., 2007, 2006), quaternisation (Chaker and Boufi, 2015; Liimatainen et al., 2014),

CHAPTER III. Microfibrillated cellulose MFC PRODUCTION FROM DES PRE-TREATMENT

enzymatic hydrolysis (Henriksson et al., 2007; Pääkkö et al., 2007) and Deep Eutectic Solvents (DES) even if, for these emerging solvents, there are very few publications (Hong et al., 2020; Liu et al., 2020; Ma et al., 2019).

Even with the use of pre-treatments, the energy consumption remains high (Rol et al., 2019a) and the obtained MFC suspensions are generally at low solid contents (< 5%) which causes transport and storage problems with limitations when used in some applications. Research is thus focusing on the production of MFC at higher solid contents with lower energy consumption. For this purpose, some researchers have obtained promising results by studying twin-screw extrusion (TSE) for MFC production (Hietala et al., 2014; Ho et al., 2015; Suzuki et al., 2013). TSE is widely used, mainly for packaging applications (Navarchian et al., 2015), pharmaceutical industries (Dhaval et al., 2020) and for vegetable oil extraction (Uitterhaegen and Evon, 2017).

The use of extrusion in cellulose microfibrillation was patented by Heisknen et al. (2014). An extruder can be composed of a single screw, twin screw or conical extruder. This latter was shown as the most efficient process, due to the high shear forces, and it allows producing MFC with less energy cost (Heisknen et al., 2014). In addition, TSE was shown to be an effective process of microfibrillation. For instance, the properties of extruded cellulosic pulp in terms of degree of microfibrillation and degradation were studied during the extrusion process (Ho et al., 2015). It was demonstrated that the fibrillation degree was improved by increasing the number of passes. However, cellulose degradation occurred during extrusion. Rol et al. (2017) have also used TSE to produce MFC at high solid content (20-25 wt %). This process allowed reducing energy consumption by 60% compared to conventional processes. MFC having widths of 20 - 30 nm and nanopapers with high mechanical properties (Young's modulus higher than 15 GPa) were obtained. The combination of TSE with homogenisation was proposed as a route to produce high quality MFC from enzymatically pre-treated cellulosic fibres (Rol et al., 2018). The pre-treated fibres were passed once through the TSE followed by four passes through the homogeniser. This combination resulted in MFC with high properties (higher transparency and Young's modulus of nanopapers, higher quality index of MFC). Energy consumption was decreased and it was possible to increase without any problem the concentration in the homogeniser (from 2 to 4 wt %). However, the depolymerisation of cellulosic fibres is still observed. TSE was also tested with cationised cellulose fibres, after reaction with epoxypropyl

trimethyl ammonium chloride (Rol et al., 2019b). The cationisation improves the microfibrillation process and the quality of produced MFC. One important drawback of TSE is the slipping effect that may occur in the TSE resulting in high size distribution of elements in the MFC suspension which affects the quality of the produced MFC.

TSE profile requires optimisations that depends on the targeted effects and can be performed using a simulation software. An optimised profile was thus proposed by Rol et al. (2020). It was composed of six zones of kneading disks with left-handed offset. This profile allows applying high shear forces and deformation. After one pass, the authors demonstrated that the produced MFC had comparable to those obtained after four passes in the classical profile.

Deep Eutectic Solvents (DES) can be described as the mixture of hydrogen bond donors (HBD) and hydrogen bond acceptors (HBA) (Abbott et al., 2003). DES pre-treatment is considered as an emerging pre-treatment that can be used to facilitate microfibrillation for the production of MFC (Liu et al., 2021; Sirviö et al., 2020; Suopajarvi et al., 2017). In a previous study (Mnasri et al., submitted 2022), these pre-treatments were found to be efficient to produce MFC with high quality using ultrafine grinding.

In the present work, cellulose fibres (bleached kraft Eucalyptus fibres) pre-treated with DES were tested to produce MFC suspensions at high solid content, using extrusion with the optimised profile proposed by Rol et al. (2020). Three DES systems have been investigated: betaine hydrochloride-urea, choline chloride-urea and choline chloride-monoethanolamine. DES-treated fibres were then refined using a PFI-mill to reduce fibre length and to avoid clogging during extrusion. The obtained fibres, MFC and papers/nanopapers were characterised at each step to study the effects on the different treatments on their properties. Finally, extruded-MFC were compared to ground-MFC to evaluate the effectiveness of TSE in producing MFC.

III.2.2 Materials and Methods

III.2.2.1 Materials

Dry sheets of bleached kraft hardwood pulp (Eucalyptus, Fibria T35) were used in this study. Cellulosic fibres were first disintegrated in water, filtered and washed with ethanol and then oven dried at 60 °C. Betaine hydrochloride ($C_5H_{12}ClNO_2$) was supplied from VWR

CHAPTER III. Microfibrillated cellulose MFC PRODUCTION FROM DES PRE-TREATMENT

(Milliporesigma), monoethanolamine (C_2H_7NO , >99%) from ROTH, choline chloride ($C_5H_{14}ClNO$, >98%) from Alfa Aesar, bis(ethylenediamine)copper (II) hydroxide solution ($Cu(H_2NCH_2CH_2NH_2)_2(OH)_2$ 1.0 M in H_2O) and urea ACS reagent (CH_4N_2O , 99.0-100.5%) were obtained from Sigma Aldrich. Deionised water was used throughout the experiments.

III.2.2.2 DES pretreatment

The cellulose fibres (EF) were pre-treated in three eutectic mixtures: (i) betaine hydrochloride-urea BHCl-U (1:4) (ii) choline chloride-urea CC-U (1:2) and (iii) choline chloride-monoethanolamine CC-M (1:6) as described in a previous study (Mnasri et al., 2022). Cellulose fibres were mixed with DES in a Parr reactor vessel (pressure reactor-600mL) with a mass ratio of 2.5:100 (for BHCl-U and CC-U) and 5:100 for CC-M. The mixture of cellulose and DES was left under mechanical stirring at 100 °C for 4 hours. Then, the suspension was filtered and washed with hot and cold water to remove all DES traces.

III.2.2.3 PFI-refining

Untreated and DES-treated fibres were refined using a PFI mill (ISO 5264-2 standard). 30 g of dry pulp (10% w/w) were introduced into the refiner bowl and distributed uniformly along its vertical wall. Pulps were refined until reaching 80°SR (Schopper Riegler degree).

III.2.2.4 Cellulose microfibrillation using twin-screw extruder TSE

The microfibrillation was performed using a twin-screw extruder TSE (Model Thermoscientific HAAKE Rheomex OS PTW 16+ HAAKE PolyLab OS RheoDrive 7) with a ratio (L/D) of 45. Refined pulps were pressed until a solid content of 20 wt % and then entered into the TSE. The TSE is mainly composed of mixing disks and fully open-ended conveying screws as described in Figure III. 8. The screw profile was optimised and tested by Rol et al. (2020). This profile has 6 shear zones with reverse elements that allow to increase the residence time of the pulp in these zones. The shearing zones are constituted of kneading disks with different degree of orientation. These disks are able to apply high shear forces to the pulp and, thus, to facilitate their microfibrillation.

CHAPTER III. Microfibrillated cellulose MFC PRODUCTION FROM DES PRE-TREATMENT

The speed was adjusted at 400 rpm and the temperature at 10 °C, through cold water circulation. The pulps were passed 4 times through the TSE and, after each pass, pulp was sampled before characterisation.

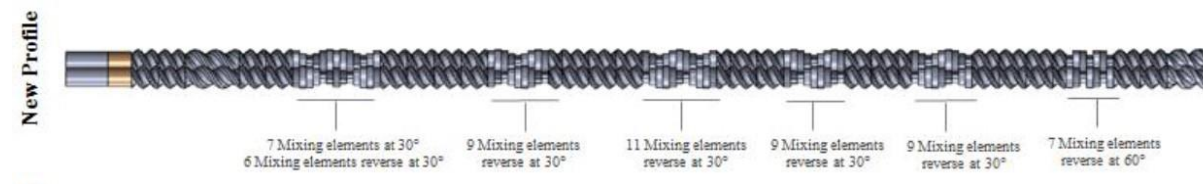


Figure III. 8. Optimised screw profile (Rol et al., 2020).

III.2.2.5 Nanopaper handsheet production

Papers/nanopapers were produced by filtration using a Rapid Köthen sheet former (ISO standard 5269-2:2004). Fibre (0.2 wt %) or MFC (0.5 wt %) suspensions were filtered through the sheet former equipped with a nylon sieve (mesh size of 1 µm). Sheets were dried under vacuum at 85 °C for 20 min, then stored in conditioned room (23 °C and 50% RH) for 48 h before any tests, as recommended by ISO 187.

III.2.2.6 Fibres/MFC characterisation

III.2.2.6.1 Optical microscopy

Fibre or MFC suspensions (0.1 wt %) were mixed with an Ultra-TurraxT-25-disperser for 5 min at 5000 rpm. Optical images were collected with an Axio Imager M1 microscope (Carl Zeiss, Germany) equipped with an AxioCam MRc 5 digital camera. For each sample, at least 5 images were taken.

III.2.2.6.2 Scanning Electron Microscopy SEM

The surface aspect of fibre and MFC was studied by SEM. Diluted fibre or MFC suspensions were dried under vacuum on a carbon adhesive and coated with Au/Pd layer. Samples were analysed with a Quanta 200 (FEI, USA) in ETD mode, with a working distance of 10 mm and an acceleration voltage of 10.0 kV. For each sample, at least 10 images were taken with magnifications between x 150 and x 8000.

III.2.2.6.3 Morphological analysis

The morphology of the fibres or, after microfibrillation, that of the remaining coarse elements (arithmetic fibre length, fibre width, fine content...) was studied using a Morfi-Neo fibre analyser (techpap, France). Analyses were made during 5 min with a limit fibre/fine elements fixed at 80 µm. Suspensions were prepared by suspending 40 mg (dried matter) of fibre or MFC in 1L of deionised water. Analysis were done twice and the mean value of the measured parameters was determined.

III.2.2.6.4 Degree of polymerisation (DP)

DP were determined according to ISO 5351:2010 standard. Cellulose fibre or MFC were dissolved in bis(ethylenediamine)copper(II) hydroxide solution. The intrinsic viscosity $[\eta]$ was measured at 25 °C with a capillary viscosimeter and the DP was deduced from the Mark–Houwink–Sakurada equation. Two measurements were made for each sample.

$$DP^{0.905} = 0.75 \times [\eta]$$

III.2.2.6.5 X-ray diffraction (XrD)

X-ray Diffraction (XrD) was carried out on paper or nanopaper samples deposited on a zero-background Si substrate. The measurements were done with a diffractometer X'Pert Pro MPD (PANalytical, Netherlands), equipped with a Bragg-Brentano geometry and a copper anode ($K\alpha$ $\lambda = 1.5419 \text{ \AA}$). The crystallinity index CrI (%) was calculated using Segal method:

$$CrI = \frac{I_{002} - I_{am}}{I_{002}} \times 100$$

where I_{002} represents the diffraction intensity of the main crystalline peak at $2\theta \approx 22.5^\circ$ and I_{am} is the intensity at $2\theta \approx 18.7^\circ$.

III.2.2.6.6 Macro size (μm^2)

The macro size was determined from optical microscopy images using Fuji software. Images were transformed to 8-byte format and thresholded. Then, the average size of the visible particles was calculated. The macro-size which presents the average surface of the visible

particles was obtained by dividing the total surface by the number of particles. Six images per sample were considered.

III.2.2.6.7 Nanosized fraction

The nanosized fraction NF was measured by a gravimetric method, adapted from Naderi et al. (2015). MFC suspensions at 0.02 wt % were centrifuged at 1000 g (2484 rpm) for 15 min. The concentrations of the suspension before and after centrifugation (in the supernatant part) were measured after 24 h of drying at 105 °C. The nanosized fraction was calculated as following:

$$\text{Nanosized fraction (w/w\%)} = \frac{C_{ac}}{C_{bc}} \times 100$$

where C_{ac} and C_{bc} correspond to the mass concentration after and before centrifugation, respectively. NF (%) corresponds not only to MFC and microfibril aggregates, but also to larger particles.

III.2.2.6.8 Turbidity

Turbidity of the MFC suspensions was measured using a portable turbidimeter AL-250 (Aqualitic, Germany) with a range between 0.01 and 1100 NTU. MFC suspensions (0.1 wt %) were mixed for 2 min with an Ultra Turrax T-25 disperser at 8000 rpm and then 10 measurements were taken.

III.2.2.6.9 Tensile tests

Tensile tests were done using an Instron 5965 machine (Instron, USA), according to ISO 1924-2 standard. Measurements were performed on nanopaper samples with dimensions of 15 x 100 mm² and a tensile speed of 10 mm/min. The Young's modulus of each sample was determined. The average of 6 measurements was calculated.

III.2.2.6.10 Simplified quality Index QI*

The quality index is used to evaluate the produced MFC and allows a comparison between different grades. The simplified Quality Index QI* was developed by Desmaisons et al. (2017).

This QI^* includes four simple tests which are nanosized fraction (%), turbidity (NTU), Young's modulus (GPa) and macro size (μm^2) used in the equation as x_1 , x_2 , x_3 and x_4 respectively.

$$QI^* = 0.3 x_1 + (-0.03 x_2) - 0.071 x_3^2 + 2.54 x_3 - 5.35 \ln(x_4) + 59.9$$

III.2.3 Results and discussions

III.2.3.1 Morphological properties of fibre/MFC suspensions

The refining of the EF fibres in a PFI-mill allowed reaching a Schopper Riegler degree of 80°SR after 9000, 10000 and 11000 revolutions for EF treated pulps with CC-U, BHCl-U and CC-M, respectively. After refining, the fibre structure was studied by SEM as depicted in Figure III. 9. As expected, refining causes an external fibrillation that is clearly observed on the images. This fibrillation seems to be more pronounced for fibres treated with neutral and alkaline DES: the corresponding images show the presence of a network of macrofibrils between the fibres. As demonstrated in a previous study (Mnasri et al., 2022), neutral and alkaline DES are able to promote an internal and external fibrillation of the treated fibres, similar to the effects of a conventional refining, but without cutting the fibres and with a reduced generation of fine elements. In this previously published study, DES treatments were thus assimilated to a soft “chemical refining”. In the present work, it appears that the effects of the neutral and alkaline DES treatments on the fibre structure are still observable even after high levels of refining in a PFI-mill.

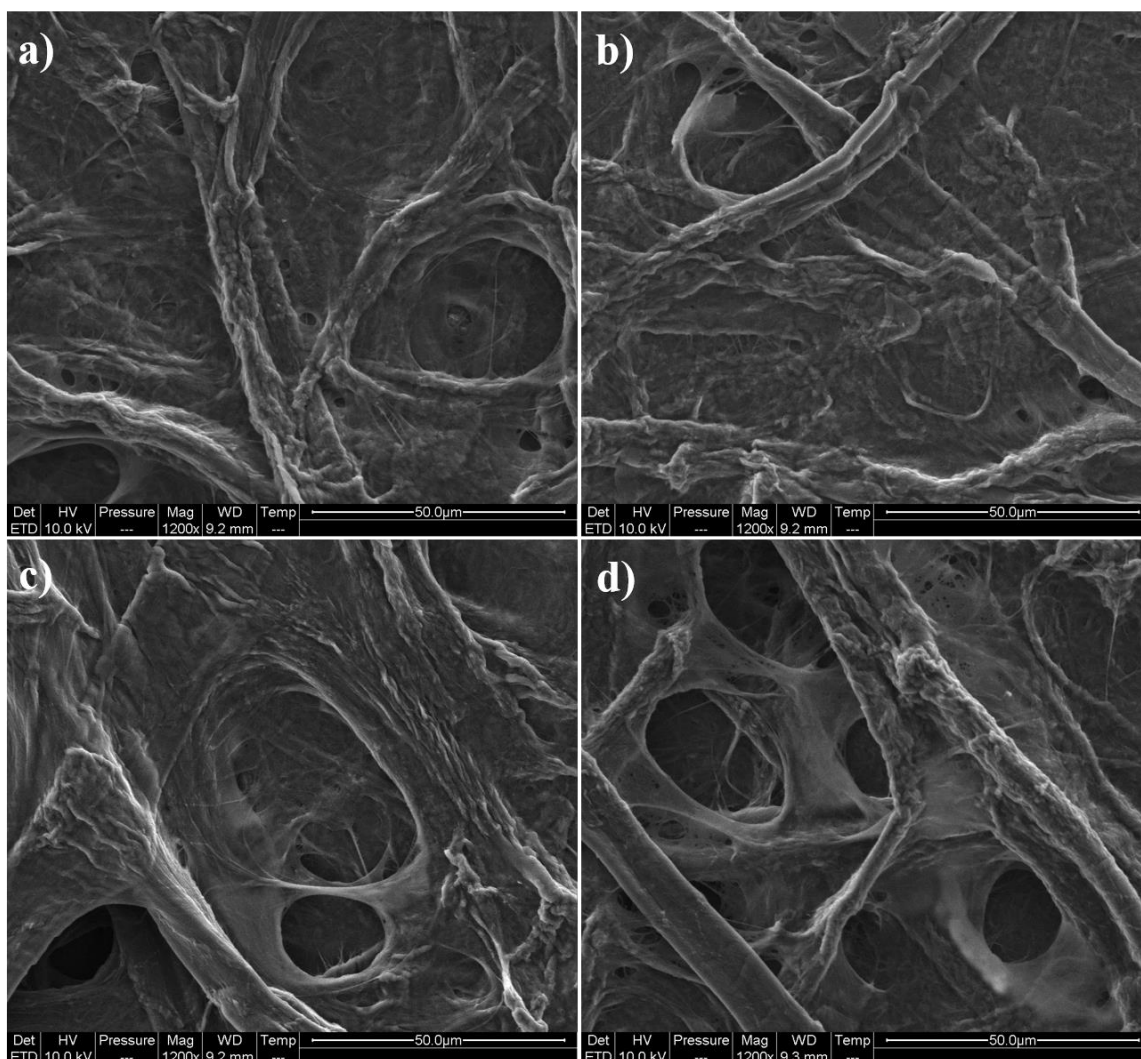


Figure III. 9. SEM images of refined EF (a), refined EF-BHCl-U (b), refined EF-CC-U (c) and refined EF-CC-M (d).

The characterisation of the produced MFC was done at the end of each pass. The MFC structure was observed by microscopy (optical and SEM images - see Figure III. 10). Optical images show the presence of residual coarse elements even after 4 passes in TSE. SEM images allow observing these elements, whose length is between 10 and 100 μm, as well as their structure which shows the presence of macro- and microfibrils, partially individualised.

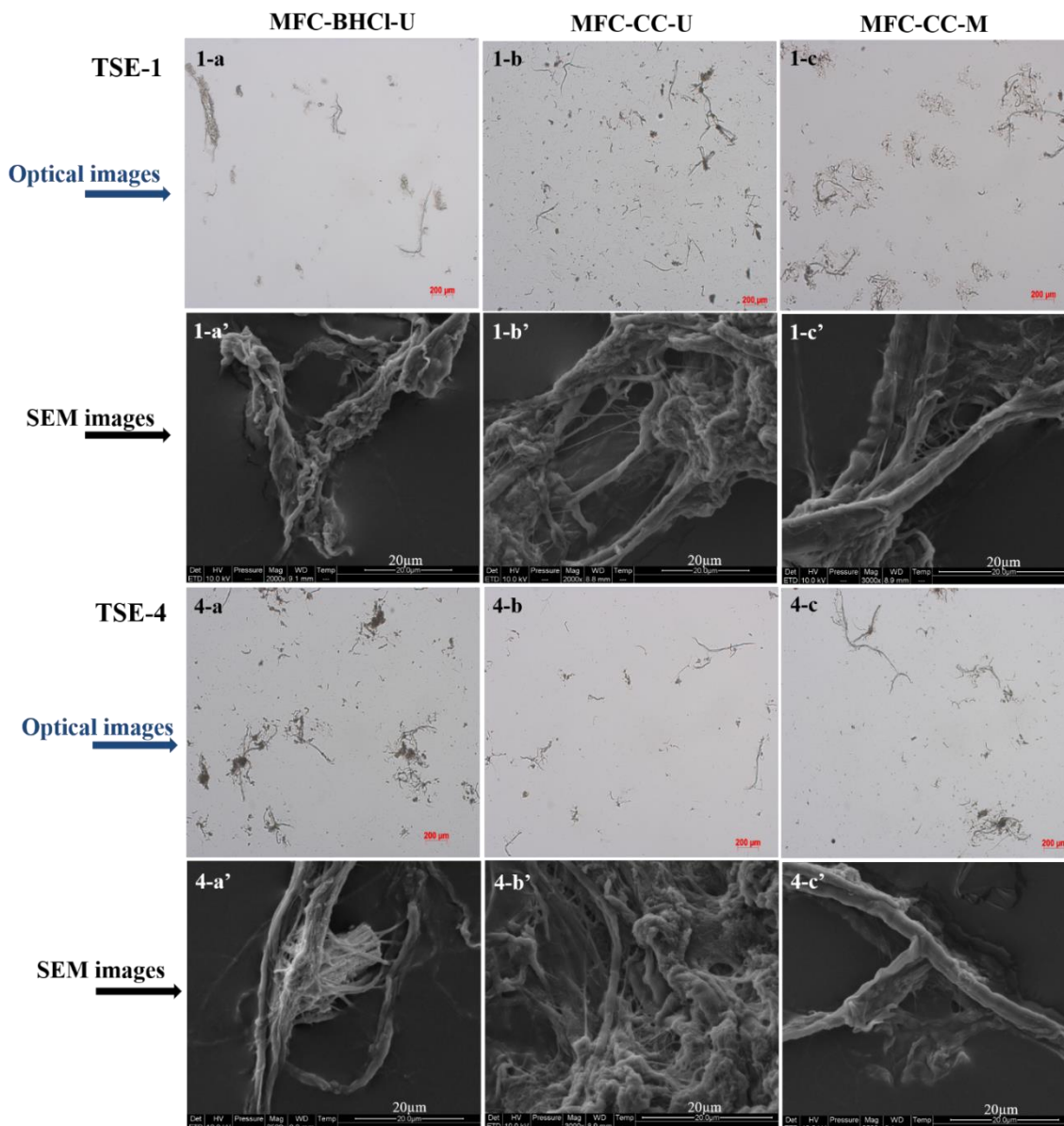


Figure III. 10. Optical and SEM images of MFC produced from BHCl-U (a, a'), CC-U (b, b') and CC-M (c, c') after one and four passes of TSE, respectively.

The morphological properties of the refined DES-treated fibres were analysed and the results are given in Table III. 4. After refining, the mean arithmetic fibre length was reduced, while an increase in fine content was observed for all the samples. This increase is related to the effect of refining. There are two kind of fines, primary fines that are present in the fibres before refining and secondary fines which are generated during the refining process. The fibre width was slightly increased which reflects a swelling of the fibre.

Table III. 4. Morphological properties of PFI-EF and PFI-DES-EF.

Sample	EF	EF-PFI	BHCl-U-PFI	CC-U-PFI	CC-M-PFI
Mean arithmetic length (μm)	523 ± 4	397 ± 2	360 ± 2	418 ± 3	401 ± 4
Mean fibre width (μm)	16.4 ± 0.1	18.5 ± 0.4	18.0 ± 0.1	18.4 ± 0.1	18.4 ± 0.3
Fine element (% in length)	13.1 ± 1.1	41.7 ± 0.6	45.6 ± 0.5	35.9 ± 0.2	41.9 ± 0.6

The morphological properties of the MFC suspensions were also analysed. Figure III. 11 illustrates the evolution of fine content and turbidity with TSE passes. The fine content was between 77 and 80% and was not influenced by the number of passes during extrusion. On the other hand, turbidity was reduced after 4 passes from 722, 715 and 742 to 645, 696 and 690 NTU for acidic, neutral and alkaline DES-treated fibres.

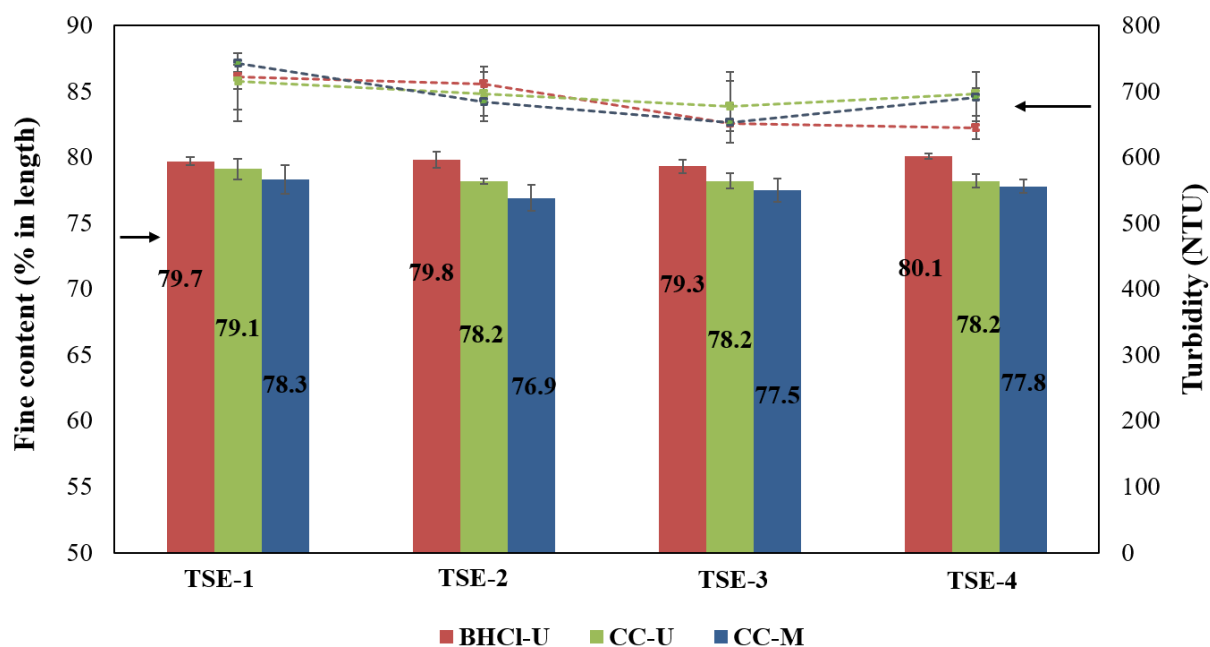


Figure III. 11. Evolution of the morphological properties of MFC suspensions with TSE passes.

III.2.3.2 Crystallinity index CrI and Degree of polymerisation DP

The evolution of DP and CrI of the fibres before and after refining are depicted in Figure III. 12. The DP was slightly reduced when compared to the unrefined pulp which results from the intense action of the PFI-mill. It is worth noting that the DP of acidic, neutral and alkaline DES-treated fibres, before refining, were 657, 810 and 672, respectively (Mnasri et al., 2022): the tendency is thus the same after refining. As expected, CrI is almost not impacted.

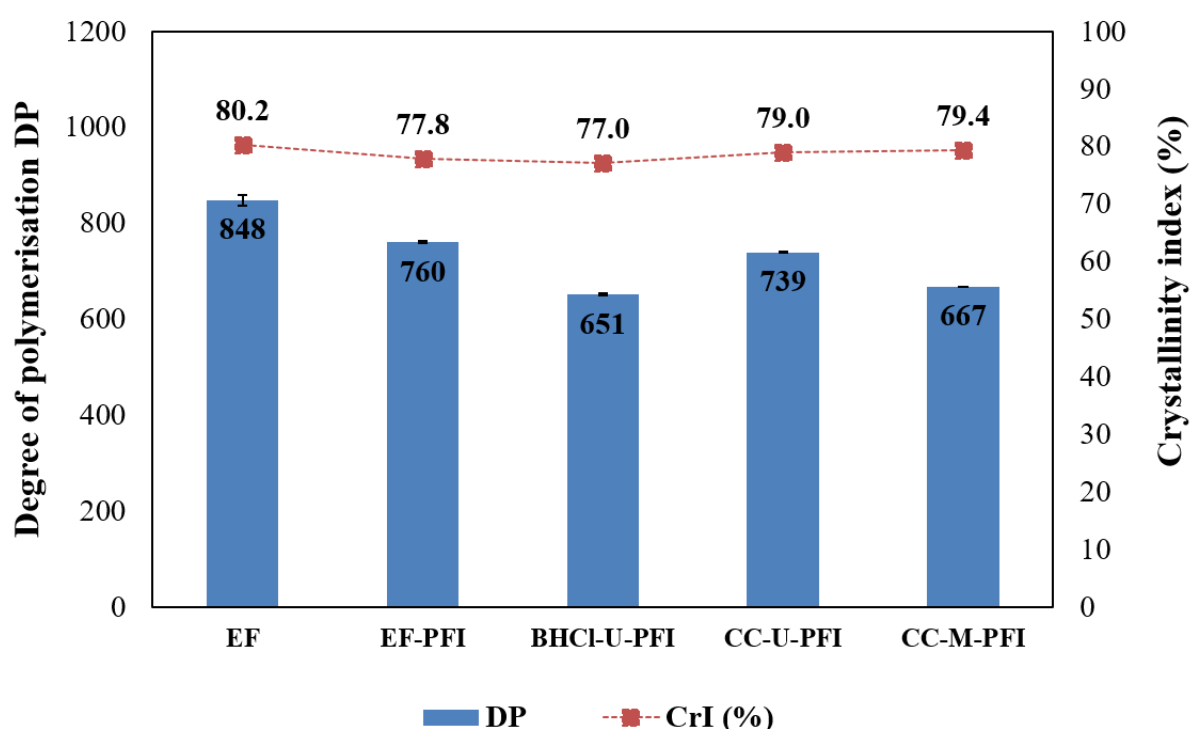


Figure III. 12. Evolution of the degree of polymerisation and crystallinity index after refining.

During extrusion, the DP and CrI were followed after each pass and the results are depicted in Figure III. 13. The CrI was negatively impacted by the number of passes. This decrease is related to the destruction of cellulose crystalline regions caused by the high shear rates applied on the fibres. The values of the CrI are similar to those obtained with ultra-fine friction grinder as reported in our previous work (Mnasri et al., 2022b).

The DP follows a similar trend: it was reduced by 6.6 and 14% for BHCl-U treated fibres, 13.3 and 13.4% for CC-U treated fibres and by 3.6 and 7.5% for CC-M treated fibres after 1 and 4 passes through the TSE, respectively. The lowest value of the DP is always given by the acidic

DES as expected because this system allows to reduce significantly the DP during DES-treatment as shown before in our previous work (Mnasri et al., 2022). The reduce of the DP was not pronounced with alkaline DES.

The final DP values of extruded-MFC obtained with BHCl-U, CC-U and CC-M are 560, 640 and 617, respectively, while for ground-MFC, the values are 368, 494 and 404, respectively (Mnasri et al., 2022b). From these results, it can be mentioned that the DP was impacted in a significant way during grinding. However, the extrusion did not significantly affect the DP.

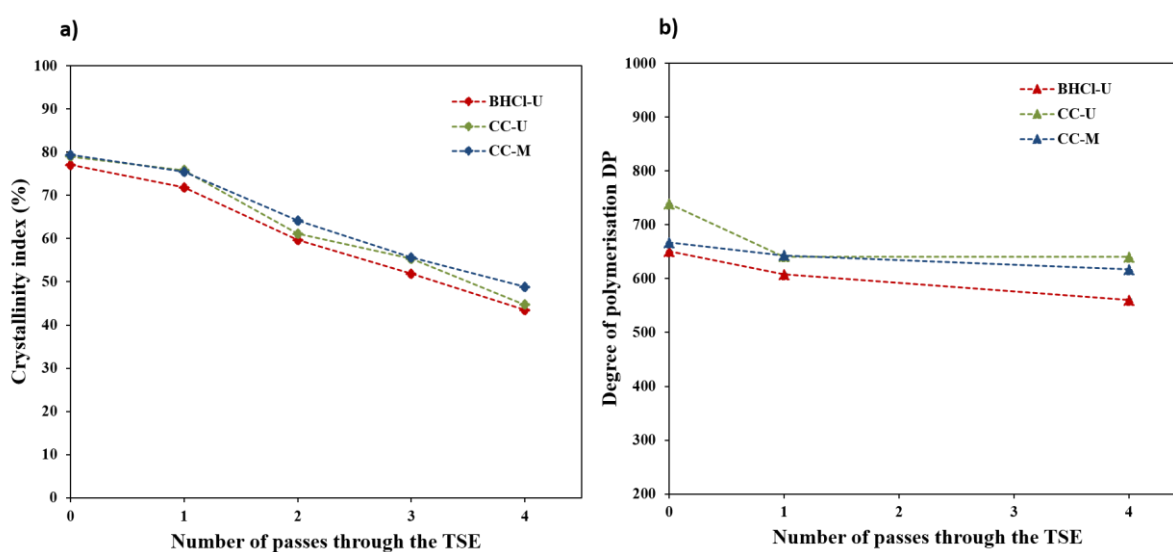


Figure III. 13. Evolution of the crystallinity index (a) and degree of polymerisation (b) during extrusion.

III.2.3.3 Properties of papers and nanopapers

The sheet densities and mechanical properties (Young's modulus, tensile strength index and elongation at break) of papers/nanopapers are depicted in Figure III. 14. The sheet density was slightly increased after the extrusion. This increase indicates a densification of the microfibrils network.

The Young's modulus, tensile strength index and elongation at break were also changed during extrusion. The Young's modulus values of are between 5.17 - 6.42, 5.84 - 6.95 and 6.06 – 6.88 GPa for BHCl-U, CC-U and CC-M treated MFC, respectively. The greatest values of the Young's modulus were reached after the fourth pass for acidic DES, the second pass for neutral

one, and after one pass for alkaline DES. The highest values of the tensile strength are given after the same passes where the greatest Young's modulus values are obtained.

The different evolution may be explained by the high dispersity of MFC suspension after each pass through the extruder.

Regarding the elongation at break, the maximum values are 1.99, 4.09 and 3.14% for acidic DES (fourth pass), neutral DES (fourth pass) and alkaline DES (one pass), respectively.

From these results, it can be mentioned that the neutral DES led to obtaining the better mechanical properties, followed by alkaline and acidic DES. The average quality of obtained MFC can be due to the presence of coarse elements in the MFC suspension and also the high heterogeneity.

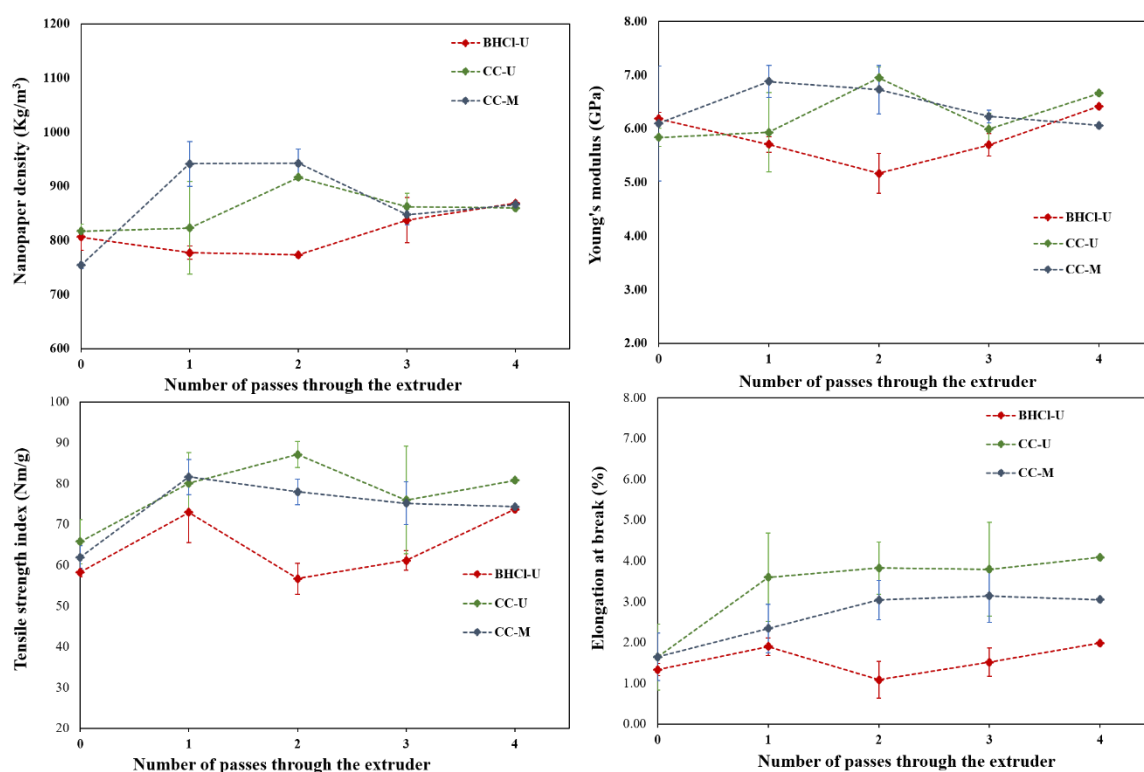


Figure III. 14. Young's modulus and nanopaper density evolution during extrusion

III.2.3.4 Simplified quality index QI^*

Table III. 5 recapitulates the QI^* of MFC produced from TSE (after four passes) compared to those obtained by ultrafine grinding extracted from previous work. The QI^* values were 43.25, 45.99 and 45.77 for MFC produced from acidic, neutral and alkaline DES, respectively. These results indicate that the quality of the MFC obtained after TSE is poor. On the other hand, MFC produced from ultrafine grinding have good qualities which are comparable to commercialized MFC (Mnasri et al., 2022b). The lower qualities of MFC-TSE are due to the high macro sized fraction turbidity of the suspensions and low Young's modulus of the resulting nanopapers.

The extrusion and grinding processes are different which lead to obtain different products. In the case of ultrafine grinding, the fibre suspension is passed through the two disks. Forces are applied on the fibres including compression, shearing and rolling friction forces which enhances the microfibrillation (Serpa Guerra et al., 2020). Their relatively narrow size distribution, high specific surface area as well as their flexibility, conformability and ability to entangle directly impact the microstructure of the resulting nanopapers.

Consequently, such MFC allows creating numerous bonds between the microfibrils and entanglement which densifies the network, as illustrated by the values of density which are greater than 1000 kg/m^3 . The shear rate applied during grinding was evaluated and values between 5.10^6 s^{-1} and 3.108 s^{-1} were reported (Baati et al, 2017; Rol, 2019). It depends on the gap between the disks (it increases when the disks are very close).

However, during extrusion the shear rate applied on cellulose fibres are generated by the kneading zones which are different from those occurring during grinding. The shear rate reported for the TSE is lower than that of ultrafine grinding and was estimated to be around $300\text{-}3000 \text{ s}^{-1}$ (Baati et al., 2017; Mohamed et al., 1990; Suparno et al., 2011). This shear rate is significantly impacted by the kneading disks, the shearing increases in these parts.

Moreover, in the TSE, there is a slipping phenomenon that could occur during extrusion. The fibres behaviour in the TSE is not the same, fibres are not sheared in the kneading zones. This led to the generation of coarse elements which causes high heterogeneity of the suspension. The slipping of the fibres, the slight reduces of the DP during the extrusion affect thus the microfibrillation efficiency and the quality of produced MFC.

CHAPTER III. Microfibrillated cellulose MFC PRODUCTION FROM DES
PRE-TREATMENT

In the case of ultrafine grinding, the fibres behaviour is quite similar, which led obtaining more homogenous MFC suspensions. The DP decreases in a significant way during grinding which enhances the microfibrillation and results in high quality MFC.

Table III. 5. Quality index of produced MFC by TSE (after four passes) compared to ground MFC.

Sample	Macro size (μm^2)	Nanosized fraction (%)	Turbidity (NTU)	Young's modulus (GPa)	Simplified QI*
MFC-BHCl-U-TSE-P4	254.3 \pm 21	63.16 \pm 13	645 \pm 18	6.42 \pm 0.2	43.25 \pm 4.14
MFC-CC-U-TSE-P4	145.3 \pm 25	66.14 \pm 4.2	696 \pm 8	6.66 \pm 0.3	45.99 \pm 1.56
MFC-CC-M-TSE-P4	160.5 \pm 7.9	69.85 \pm 2.2	690 \pm 32	6.06 \pm 0.1	45.77 \pm 0.69
MFC-BHCl-U	12.22 \pm 1.3	61.67 \pm 8.9	379 \pm 8	10.9 \pm 0.3	72.86 \pm 2.70
MFC-CC-U	13.85 \pm 6.7	67.26 \pm 0.5	279 \pm 4	10.4 \pm 0.3	76.43 \pm 1.35
MFC-CC-M	16.08 \pm 1.3	65.96 \pm 6.9	336 \pm 6	10.7 \pm 0.3	73.77 \pm 1.77

III.2.4 Conclusion

In this work, the microfibrillation of DES-treated fibres using TSE was investigated. This process allows producing MFC with the presence of coarse elements and even residual fibres. The properties of extruded MFC were studied and compared to those obtained from ultrafine grinding. The degree of polymerisation was reduced after extrusion. The crystallinity index was significantly decreased by increasing the number of passes through the TSE, which indicates the degradation of cellulose. The mechanical properties of extruded MFC were close (between 6.06 and 6.30 GPa). These values are lower than those obtained from ultrafine grinding which could be due to the different process of microfibrillation.

Despite the very interesting results obtained with the combination of DES pre-treatment and ultrafine grinding, the TSE was thus not suitable for the production of MFC from DES-treated fibres with high quality. This can be due to the used profile which is may be not adequate for

DES-treated fibres. The perspectives of this work will be the use of another profile (classic one) with adjustable conditions (solid content, speed...). or the possibility to combine DES pre-treatment with enzymatic hydrolysis (in order to reduce the DP) and eliminate the refining step to enhance the microfibrillation using the TSE.

References

- Abbott, A.P., Capper, G., Davies, D.L., Rasheed, R.K., Tambyrajah, V., 2003. Novel solvent properties of choline chloride/urea mixtures. *Chemical Communications* 0, 70–71. <https://doi.org/10.1039/B210714G>
- Abbott, A.P., Capper, G., L. Davies, D., L. Munro, H., K. Rasheed, R., Tambyrajah, V., 2001. Preparation of novel, moisture-stable, Lewis-acidic ionic liquids containing quaternary ammonium salts with functional side chains. *Chemical Communications* 0, 2010–2011. <https://doi.org/10.1039/B106357J>
- Abdul Khalil, H.P.S., Davoudpour, Y., Islam, Md.N., Mustapha, A., Sudesh, K., Dungani, R., Jawaid, M., 2014. Production and modification of nanofibrillated cellulose using various mechanical processes: A review. *Carbohydrate Polymers* 99, 649–665. <https://doi.org/10.1016/j.carbpol.2013.08.069>
- Aulin, C., Gällstedt, M., Lindström, T., 2010. Oxygen and oil barrier properties of microfibrillated cellulose films and coatings. *Cellulose* 17, 559–574. <https://doi.org/10.1007/s10570-009-9393-y>
- Aulin, C., Salazar-Alvarez, G., Lindström, T., 2012. High strength, flexible and transparent nanofibrillated cellulose–nanoclay biohybrid films with tunable oxygen and water vapor permeability. *Nanoscale* 4, 6622. <https://doi.org/10.1039/c2nr31726e>
- Baati, R., Magnin, A., Boufi, S., 2017. High Solid Content Production of Nanofibrillar Cellulose via Continuous Extrusion. *ACS Sustainable Chem. Eng.* 5, 2350–2359. <https://doi.org/10.1021/acssuschemeng.6b02673>
- Banvillet, G., Depres, G., Belgacem, N., Bras, J., 2021a. Alkaline treatment combined with enzymatic hydrolysis for efficient cellulose nanofibrils production. *Carbohydrate Polymers* 255, 117383. <https://doi.org/10.1016/j.carbpol.2020.117383>
- Banvillet, G., Gatt, E., Belgacem, N., Bras, J., 2021b. Cellulose fibers deconstruction by twin-screw extrusion with in situ enzymatic hydrolysis via bioextrusion. *Bioresource Technology* 327, 124819. <https://doi.org/10.1016/j.biortech.2021.124819>
- Banyasz, J.L., Li, S., Lyons-Hart, J.L., Shafer, K.H., 2001. Cellulose pyrolysis: the kinetics of hydroxyacetaldehyde evolution. *Journal of Analytical and Applied Pyrolysis* 57, 223–248. [https://doi.org/10.1016/S0165-2370\(00\)00135-2](https://doi.org/10.1016/S0165-2370(00)00135-2)

- Besbes, I., Alila, S., Boufi, S., 2011. Nanofibrillated cellulose from TEMPO-oxidized eucalyptus fibres: Effect of the carboxyl content. *Carbohydrate Polymers* 84, 975–983. <https://doi.org/10.1016/j.carbpol.2010.12.052>
- Boufi, S., Gandini, A., 2015. Triticale crop residue: a cheap material for high performance nanofibrillated cellulose. *RSC Adv.* 5, 3141–3151. <https://doi.org/10.1039/C4RA12918K>
- Chaker, A., Alila, S., Mutjé, P., Vilar, M.R., Boufi, S., 2013. Key role of the hemicellulose content and the cell morphology on the nanofibrillation effectiveness of cellulose pulps. *Cellulose* 20, 2863–2875. <https://doi.org/10.1007/s10570-013-0036-y>
- Chaker, A., Boufi, S., 2015. Cationic nanofibrillar cellulose with high antibacterial properties. *Carbohydrate Polymers* 131, 224–232. <https://doi.org/10.1016/j.carbpol.2015.06.003>
- Cousins, S.K., Brown, R.M., 1995. Cellulose I microfibril assembly: computational molecular mechanics energy analysis favours bonding by van der Waals forces as the initial step in crystallization. *Polymer* 36, 3885–3888. [https://doi.org/10.1016/0032-3861\(95\)99782-P](https://doi.org/10.1016/0032-3861(95)99782-P)
- Desmaisons, J., Boutonnet, E., Rueff, M., Dufresne, A., Bras, J., 2017. A new quality index for benchmarking of different cellulose nanofibrils. *Carbohydrate Polymers* 174, 318–329. <https://doi.org/10.1016/j.carbpol.2017.06.032>
- Dhaval, M., Sharma, S., Dudhat, K., Chavda, J., 2020. Twin-Screw Extruder in Pharmaceutical Industry: History, Working Principle, Applications, and Marketed Products: an In-depth Review. *J Pharm Innov.* <https://doi.org/10.1007/s12247-020-09520-7>
- Francisco, M., Bruinhorst, A. van den, Kroon, M., 2012. New natural and renewable low transition temperature mixtures (LTTMs): screening as solvents for lignocellulosic biomass processing. *Green Chemistry* 14, 2153–2157. <https://doi.org/10.1039/C2GC35660K>
- Fukuzumi, H., Saito, T., Isogai, A., 2013. Influence of TEMPO-oxidized cellulose nanofibril length on film properties. *Carbohydrate Polymers* 93, 172–177. <https://doi.org/10.1016/j.carbpol.2012.04.069>
- Fukuzumi, H., Saito, T., Iwata, T., Kumamoto, Y., Isogai, A., 2009. Transparent and High Gas Barrier Films of Cellulose Nanofibers Prepared by TEMPO-Mediated Oxidation. *Biomacromolecules* 10, 162–165. <https://doi.org/10.1021/bm801065u>

- Galland, S., Berthold, F., Prakobna, K., Berglund, L.A., 2015. Holocellulose Nanofibers of High Molar Mass and Small Diameter for High-Strength Nanopaper. *Biomacromolecules* 16, 2427–2435. <https://doi.org/10.1021/acs.biomac.5b00678>
- Ghanadpour, M., Carosio, F., Larsson, P.T., Wågberg, L., 2015. Phosphorylated Cellulose Nanofibrils: A Renewable Nanomaterial for the Preparation of Intrinsically Flame-Retardant Materials. *Biomacromolecules* 16, 3399–3410. <https://doi.org/10.1021/acs.biomac.5b01117>
- Habibi, Y., Chanzy, H., Vignon, M.R., 2006. TEMPO-mediated surface oxidation of cellulose whiskers. *Cellulose* 13, 679–687. <https://doi.org/10.1007/s10570-006-9075-y>
- Hafid, H.S., Omar, F.N., Zhu, J., Wakisaka, M., 2021. Enhanced crystallinity and thermal properties of cellulose from rice husk using acid hydrolysis treatment. *Carbohydrate Polymers* 260, 117789. <https://doi.org/10.1016/j.carbpol.2021.117789>
- Heiskanen, I., Harlin, A., Backfolk, K., Laitinen, R., 2014. Process for the production of microfibrillated cellulose in an extruder and microfibrillated cellulose produced according to the process. US8747612B2.
- Henriksson, M., Berglund, L.A., Isaksson, P., Lindström, T., Nishino, T., 2008. Cellulose Nanopaper Structures of High Toughness. *Biomacromolecules* 9, 1579–1585. <https://doi.org/10.1021/bm800038n>
- Henriksson, M., Henriksson, G., Berglund, L.A., Lindström, T., 2007. An environmentally friendly method for enzyme-assisted preparation of microfibrillated cellulose (MFC) nanofibers. *European Polymer Journal* 43, 3434–3441. <https://doi.org/10.1016/j.eurpolymj.2007.05.038>
- Hietala, M., Rollo, P., Kekäläinen, K., Oksman, K., 2014. Extrusion processing of green biocomposites: Compounding, fibrillation efficiency, and fiber dispersion. *Journal of Applied Polymer Science* 131. <https://doi.org/10.1002/app.39981>
- Ho, T.T.T., Abe, K., Zimmermann, T., Yano, H., 2015. Nanofibrillation of pulp fibers by twin-screw extrusion. *Cellulose* 22, 421–433. <https://doi.org/10.1007/s10570-014-0518-6>
- Ho, T.T.T., Zimmermann, T., Hauert, R., Caseri, W., 2011. Preparation and characterization of cationic nanofibrillated cellulose from etherification and high-shear disintegration processes. *Cellulose* 18, 1391–1406. <https://doi.org/10.1007/s10570-011-9591-2>

- Hong, S., Yuan, Y., Li, P., Zhang, K., Lian, H., Liimatainen, H., 2020. Enhancement of the nanofibrillation of birch cellulose pretreated with natural deep eutectic solvent. *Industrial Crops and Products* 154, 112677. <https://doi.org/10.1016/j.indcrop.2020.112677>
- Hou, X.-D., Li, A.-L., Lin, K.-P., Wang, Y.-Y., Kuang, Z.-Y., Cao, S.-L., 2018. Insight into the structure-function relationships of deep eutectic solvents during rice straw pretreatment. *Bioresource Technology* 249, 261–267. <https://doi.org/10.1016/j.biortech.2017.10.019>
- Isogai, A., Saito, T., Fukuzumi, H., 2011. TEMPO-oxidized cellulose nanofibers. *Nanoscale* 3, 71–85. <https://doi.org/10.1039/C0NR00583E>
- Jonoobi, M., Mathew, A.P., Oksman, K., 2012. Producing low-cost cellulose nanofiber from sludge as new source of raw materials. *Industrial Crops and Products* 40, 232–238. <https://doi.org/10.1016/j.indcrop.2012.03.018>
- Khiari, R., 2017. Valorization of Agricultural Residues for Cellulose Nanofibrils Production and Their Use in Nanocomposite Manufacturing. *International Journal of Polymer Science* 2017, e6361245. <https://doi.org/10.1155/2017/6361245>
- Kumar, V., Bollström, R., Yang, A., Chen, Q., Chen, G., Salminen, P., Bousfield, D., Toivakka, M., 2014. Comparison of nano- and microfibrillated cellulose films. *Cellulose* 21, 3443–3456. <https://doi.org/10.1007/s10570-014-0357-5>
- Li, P., Sirviö, J.A., Haapala, A., Liimatainen, H., 2017. Cellulose Nanofibrils from Nonderivatizing Urea-Based Deep Eutectic Solvent Pretreatments. *ACS Appl. Mater. Interfaces* 9, 2846–2855. <https://doi.org/10.1021/acsami.6b13625>
- Li, W., Xue, Y., He, M., Yan, J., Lucia, L.A., Chen, J., Yu, J., Yang, G., 2021. Facile Preparation and Characteristic Analysis of Sulfated Cellulose Nanofibril via the Pretreatment of Sulfamic Acid-Glycerol Based Deep Eutectic Solvents. *Nanomaterials* 11, 2778. <https://doi.org/10.3390/nano11112778>
- Liimatainen, H., Suopajarvi, T., Sirviö, J.A, Hormi, O., Niinimäki, J., 2014. Fabrication of cationic cellulosic nanofibrils through aqueous quaternization pretreatment and their use in colloid aggregation. *Carbohydrate Polymers* 103, 187–192. <https://doi.org/10.1016/j.carbpol.2013.12.042>
- Liu, C., Li, M.-C., Chen, W., Huang, R., Hong, S., Wu, Q., Mei, C., 2020. Production of lignin-containing cellulose nanofibers using deep eutectic solvents for UV-absorbing polymer

- reinforcement. Carbohydrate Polymers 246, 116548. <https://doi.org/10.1016/j.carbpol.2020.116548>
- Liu, S., Zhang, Q., Gou, S., Zhang, L., Wang, Z., 2021. Esterification of cellulose using carboxylic acid-based deep eutectic solvents to produce high-yield cellulose nanofibers. Carbohydrate Polymers 251, 117018. <https://doi.org/10.1016/j.carbpol.2020.117018>
- Luneva, N.K., Ezovitova, T.I., 2014. Cellulose phosphorylation with a mixture of orthophosphoric acid and ammonium polyphosphate in urea medium. Russ J Appl Chem 87, 1558–1565. <https://doi.org/10.1134/S1070427214100243>
- Ma, Y., Xia, Q., Liu, Yongzhuang, Chen, W., Liu, S., Wang, Q., Liu, Yixing, Li, J., Yu, H., 2019. Production of Nanocellulose Using Hydrated Deep Eutectic Solvent Combined with Ultrasonic Treatment. ACS Omega 4, 8539–8547. <https://doi.org/10.1021/acsomega.9b00519>
- Majová, V., Horanová, S., Škulcová, A., Šima, J., Jablonský, M., 2017. Deep Eutectic Solvent Delignification: Impact of Initial Lignin. BioResources 12, 7301–7310.
- Meng, Q., Wang, T.J., 2019. Mechanics of Strong and Tough Cellulose Nanopaper. Applied Mechanics Reviews 71, 040801. <https://doi.org/10.1115/1.4044018>
- Mnasri, A., Dhaouadi, H., Khiari, R., Halila, S., Mauret, E., 2022. Effects of Deep Eutectic Solvents on cellulosic fibres and paper properties: Green “chemical” refining. Carbohydrate Polymers 119606. <https://doi.org/10.1016/j.carbpol.2022.119606>
- Mohamed, I.O., Ofoli, R.Y., Morgan, R.G., 1990. MODELING the AVERAGE SHEAR RATE IN A CO-ROTATING TWIN SCREW EXTRUDER. Journal of Food Process Engineering 12, 227–246. <https://doi.org/10.1111/j.1745-4530.1990.tb00052.x>
- Moon, R.J., Martini, A., Nairn, J., Simonsen, J., Youngblood, J., 2011. Cellulose nanomaterials review: structure, properties and nanocomposites. Chem. Soc. Rev. 40, 3941. <https://doi.org/10.1039/c0cs00108b>
- Naderi, A., Lindström, T., Sundström, J., 2015. Repeated homogenization, a route for decreasing the energy consumption in the manufacturing process of carboxymethylated nanofibrillated cellulose? Cellulose 22, 1147–1157. <https://doi.org/10.1007/s10570-015-0576-4>

- Navarchian, A.H., Jalalian, M., Pirooz, M., 2015. Characterization of starch/poly(vinyl alcohol)/clay nanocomposite films prepared in twin-screw extruder for food packaging application. *Journal of Plastic Film & Sheeting* 31, 309–336. <https://doi.org/10.1177/8756087914568904>
- Nechyporchuk, O., Belgacem, M.N., Bras, J., 2016. Production of cellulose nanofibrils: A review of recent advances. *Industrial Crops and Products* 93, 2–25. <https://doi.org/10.1016/j.indcrop.2016.02.016>
- Nogi, M., Iwamoto, S., Nakagaito, A.N., Yano, H., 2009. Optically Transparent Nanofiber Paper. *Advanced Materials* 21, 1595–1598. <https://doi.org/10.1002/adma.200803174>
- Noguchi, Y., Homma, I., Matsubara, Y., 2017. Complete nanofibrillation of cellulose prepared by phosphorylation. *Cellulose* 24, 1295–1305. <https://doi.org/10.1007/s10570-017-1191-3>
- Pääkkö, M., Ankerfors, M., Kosonen, H., Nykänen, A., Ahola, S., Österberg, M., Ruokolainen, J., Laine, J., Larsson, P.T., Ikkala, O., Lindström, T., 2007. Enzymatic Hydrolysis Combined with Mechanical Shearing and High-Pressure Homogenization for Nanoscale Cellulose Fibrils and Strong Gels. *Biomacromolecules* 8, 1934–1941. <https://doi.org/10.1021/bm061215p>
- Pei, A., Butchosa, N., Berglund, L.A., Zhou, Q., 2013. Surface quaternized cellulose nanofibrils with high water absorbency and adsorption capacity for anionic dyes. *Soft Matter* 9, 2047. <https://doi.org/10.1039/c2sm27344f>
- Rol, F., 2019. Prétraitements de la cellulose pour une nanofibrillation par extrusion (thesis). <http://www.theses.fr>. Université Grenoble Alpes (ComUE).
- Rol, F., Banvillet, G., Meyer, V., Petit-Conil, M., Bras, J., 2018. Combination of twin-screw extruder and homogenizer to produce high-quality nanofibrillated cellulose with low energy consumption. *J Mater Sci* 53, 12604–12615. <https://doi.org/10.1007/s10853-018-2414-1>
- Rol, F., Belgacem, M.N., Gandini, A., Bras, J., 2019a. Recent advances in surface-modified cellulose nanofibrils. *Progress in Polymer Science* 88, 241–264. <https://doi.org/10.1016/j.progpolymsci.2018.09.002>
- Rol, F., Karakashov, B., Nechyporchuk, O., Terrien, M., Meyer, V., Dufresne, A., Belgacem, M.N., Bras, J., 2017. Pilot-Scale Twin Screw Extrusion and Chemical Pretreatment as an Energy-Efficient Method for the Production of Nanofibrillated Cellulose at High Solid Content. *ACS Sustainable Chem. Eng.* 5, 6524–6531. <https://doi.org/10.1021/acssuschemeng.7b00630>

- Rol, F., Saini, S., Meyer, V., Petit-Conil, M., Bras, J., 2019b. Production of cationic nanofibrils of cellulose by twin-screw extrusion. *Industrial Crops and Products* 137, 81–88. <https://doi.org/10.1016/j.indcrop.2019.04.031>
- Rol, F., Sillard, C., Bardet, M., Yarava, J.R., Emsley, L., Gablin, C., Léonard, D., Belgacem, N., Bras, J., 2020. Cellulose phosphorylation comparison and analysis of phosphate position on cellulose fibers. *Carbohydrate Polymers* 229, 115294. <https://doi.org/10.1016/j.carbpol.2019.115294>
- Rol, F., Vergnes, B., El Kissi, N., Bras, J., 2020. Nanocellulose Production by Twin-Screw Extrusion: Simulation of the Screw Profile To Increase the Productivity. *ACS Sustainable Chem. Eng.* 8, 50–59. <https://doi.org/10.1021/acssuschemeng.9b01913>
- Saito, T., Isogai, A., 2004. TEMPO-Mediated Oxidation of Native Cellulose. The Effect of Oxidation Conditions on Chemical and Crystal Structures of the Water-Insoluble Fractions. *Biomacromolecules* 5, 1983–1989. <https://doi.org/10.1021/bm0497769>
- Saito, T., Isogai, A., 2006. Introduction of aldehyde groups on surfaces of native cellulose fibers by TEMPO-mediated oxidation. *Colloids and Surfaces A: Physicochemical and Engineering Aspects* 289, 219–225. <https://doi.org/10.1016/j.colsurfa.2006.04.038>
- Saito, T., Kimura, S., Nishiyama, Y., Isogai, A., 2007. Cellulose Nanofibers Prepared by TEMPO-Mediated Oxidation of Native Cellulose. *Biomacromolecules* 8, 2485–2491. <https://doi.org/10.1021/bm0703970>
- Saito, T., Nishiyama, Y., Putaux, J.-L., Vignon, M., Isogai, A., 2006. Homogeneous Suspensions of Individualized Microfibrils from TEMPO-Catalyzed Oxidation of Native Cellulose. *Biomacromolecules* 7, 1687–1691. <https://doi.org/10.1021/bm060154s>
- Segal, L., Creely, J.J., Martin, A.E., Conrad, C.M., 1959. An Empirical Method for Estimating the Degree of Crystallinity of Native Cellulose Using the X-Ray Diffractometer. *Textile Research Journal* 29, 786–794. <https://doi.org/10.1177/004051755902901003>
- Sehaqui, H., Zimmermann, T., Tingaut, P., 2014. Hydrophobic cellulose nanopaper through a mild esterification procedure. *Cellulose* 21, 367–382. <https://doi.org/10.1007/s10570-013-0110-5>
- Serpa Guerra, A.M., Gómez Hoyos, C., Velásquez-Cock, J.A., Vélez Penagos, L., Gañán Rojo, P., Vélez Acosta, L., Pereira, M.A., Zuluaga, R., 2020. Effect of ultra-fine friction grinding on

the physical and chemical properties of curcuma (*Curcuma longa* L.) suspensions. *Journal of Food Science* 85, 132–142. <https://doi.org/10.1111/1750-3841.14973>

Siró, I., Plackett, D., 2010. Microfibrillated cellulose and new nanocomposite materials: a review. *Cellulose* 17, 459–494. <https://doi.org/10.1007/s10570-010-9405-y>

Sirviö, J.A., Hyypiö, K., Asaadi, S., Junka, K., Liimatainen, H., 2020. High-strength cellulose nanofibers produced via swelling pretreatment based on a choline chloride–imidazole deep eutectic solvent. *Green Chem.* 22, 1763–1775. <https://doi.org/10.1039/C9GC04119B>

Sirviö, J.A., Visanko, M., Liimatainen, H., 2015. Deep eutectic solvent system based on choline chloride-urea as a pre-treatment for nanofibrillation of wood cellulose. *Green Chemistry* 17, 3401–3406. <https://doi.org/10.1039/C5GC00398A>

Smith, E.L., Abbott, A.P., Ryder, K.S., 2014. Deep Eutectic Solvents (DESs) and Their Applications. *Chem. Rev.* 114, 11060–11082. <https://doi.org/10.1021/cr300162p>

Song, Y., Sun, Y., Zhang, X., Zhou, J., Zhang, L., 2008. Homogeneous Quaternization of Cellulose in NaOH/Urea Aqueous Solutions as Gene Carriers. *Biomacromolecules* 9, 2259–2264. <https://doi.org/10.1021/bm800429a>

Spence, K.L., Venditti, R.A., Rojas, O.J., Habibi, Y., Pawlak, J.J., 2011. A comparative study of energy consumption and physical properties of microfibrillated cellulose produced by different processing methods. *Cellulose* 18, 1097–1111. <https://doi.org/10.1007/s10570-011-9533-z>

Suopajarvi, T., Sirviö, J.A., Liimatainen, H., 2017. Nanofibrillation of deep eutectic solvent-treated paper and board cellulose pulps. *Carbohydrate Polymers* 169, 167–175. <https://doi.org/10.1016/j.carbpol.2017.04.009>

Suparno, M., Dolan, K.D., Ng, P.K.W., Steffe, J.F., 2011. AVERAGE SHEAR RATE IN A TWIN-SCREW EXTRUDER AS A FUNCTION OF DEGREE OF FILL, FLOW BEHAVIOR INDEX, SCREW SPEED AND SCREW CONFIGURATION: AVERAGE SHEAR RATE IN EXTRUDER. *Journal of Food Process Engineering* 34, 961–982. <https://doi.org/10.1111/j.1745-4530.2009.00381.x>

Suzuki, K., Okumura, H., Kitagawa, K., Sato, S., Nakagaito, A.N., Yano, H., 2013. Development of continuous process enabling nanofibrillation of pulp and melt compounding. *Cellulose* 20, 201–210. <https://doi.org/10.1007/s10570-012-9843-9>

- Tenhunen, T.-M., Kouko, J., Salminen, A., Härkäsalmi, T., Pere, J., Harlin, A., Hänninen, T., 2016. Method for Forming Pulp Fibre Yarns Developed by a Design-driven Process. *BioResources* 11, 2492–2503.
- Tenhunen, T.-M., Lewandowska, A.E., Orelma, H., Johansson, L.-S., Virtanen, T., Harlin, A., Österberg, M., Eichhorn, S.J., Tammelin, T., 2018. Understanding the interactions of cellulose fibres and deep eutectic solvent of choline chloride and urea. *Cellulose* 25, 137–150. <https://doi.org/10.1007/s10570-017-1587-0>
- Turbak, A.F., Snyder, F.W., Sandberg, K.R., 1983. Microfibrillated cellulose, a new cellulose product: properties, uses, and commercial potential. *J. Appl. Polym. Sci.: Appl. Polym. Symp.;* (United States) 37.
- Uitterhaegen, E., Evon, P., 2017. Twin-screw extrusion technology for vegetable oil extraction: A review. *Journal of Food Engineering* 212, 190–200. <https://doi.org/10.1016/j.jfoodeng.2017.06.006>
- Wang, J., Gardner, D.J., Stark, N.M., Bousfield, D.W., Tajvidi, M., Cai, Z., 2018. Moisture and Oxygen Barrier Properties of Cellulose Nanomaterial-Based Films. *ACS Sustainable Chem. Eng.* 6, 49–70. <https://doi.org/10.1021/acssuschemeng.7b03523>
- Yu, W., Wang, C., Yi, Y., Wang, H., Yang, Y., Zeng, L., Tan, Z., 2021. Direct pretreatment of raw ramie fibers using an acidic deep eutectic solvent to produce cellulose nanofibrils in high purity. *Cellulose* 28, 175–188. <https://doi.org/10.1007/s10570-020-03538-3>
- Zdanowicz, M., Wilpiszewska, K., Szychaj, T., 2018. Deep eutectic solvents for polysaccharides processing. A review. *Carbohydrate Polymers* 200, 361–380. <https://doi.org/10.1016/j.carbpol.2018.07.078>
- Zhu, G., Zhu, X., Xiao, Z., Yi, F., 2012. Study of cellulose pyrolysis using an in situ visualization technique and thermogravimetric analyzer. *Journal of Analytical and Applied Pyrolysis* 94, 126–130. <https://doi.org/10.1016/j.jaap.2011.11.016>

General conclusions and perspectives

Conclusions

This PhD project aimed at studying some pre-treatments in order to facilitate the production of microfibrillated cellulose MFC. The selected pre-treatment was based on the use of Deep Eutectic Solvents (DES) and was compared to the well-known enzymatic hydrolysis. Three DES of different pH (acidic, neutral and alkaline) were proposed, consisting in the mixture of betaine hydrochloride-urea (BHCl-U), choline chloride-urea (CC-U) and choline chloride-monoethanolamine (CC-M), respectively.

In **chapter II**, the effects of DES pre-treatment on cellulose fibres (eucalyptus and cotton) and papers properties were studied. The chemical structure of DES-treated fibres was highlighted that no relevant modifications were observed except for the acidic DES treatment where cellulose esterification was clearly evidenced. The crystallinity index and degree of polymerisation were changed after DES pre-treatment. The swelling capacity of DES-treated fibres was enhanced with the appearance of some macrofibrils at their surface indicating that DES pre-treatment led mainly to an internal and external fibrillation. Moreover, the mechanical properties of resulting produced papers were significantly improved after DES pre-treatment (increase of the Young's modulus, tensile strength, internal bond strength...) which is considered as an interesting result. Owing to the given results, the effects of DES pre-treatment is similar to that of a chemical refining. Therefore, DES pre-treatment can be considered as a relevant green and soft chemical refining.

In the second section of this chapter, High-Performance Size Exclusion Chromatography HPSEC was used to study the molecular mass distribution of cellulose fibres after DES pre-treatment or enzymatic hydrolysis. DES-treated fibres were successfully tricarbanilated and analysed by HPSEC. All samples presented high recovery yield between 90 and 100% except for acidic DES-treated fibres (lower recovery yield) which is certainly due to their chemical modification (esterification). SEC analysis showed that the polydispersity was increased by CC-U and enzymatic hydrolysis, slightly changed with CC-M and decreased with BHCl-U pre-treatment. It was suggested that CC-U and enzymatic hydrolysis acted on cellulose fibres by cutting on their extremity, while CC-M acted by cutting larger fragments (decrease of Mw) with a compensation detected by the increase of Mn. It was also deduced that CC-M led to swollen polymer, while CC-U and enzymatic hydrolysis led to spherical polymers or glucans for cotton and eucalyptus fibres, respectively.

The perspectives of this chapter could be the optimisation of the esterification reaction in order to increase the degree of substitution. This could improve the microfibrillation by the presence of high cationic charge. The resulted cationic MFC could be used in various applications such as a stabiliser in oil-water emulsions, in the absorption of anionic dyes or in antibacterial applications.

It could be also interesting to investigate some applications related to papers produced from DES pre-treatment (reinforcement of polylactic acid, for instance), since it significantly improves their mechanical properties. The recycling of the used DES is an important parameter and the effectiveness and the stability of these systems must be evaluated.

Chapter III was dedicated to the effectiveness of DES pre-treatment to facilitate the microfibrillation process. In the first section, the ultra-fine friction grinder was used to produce MFC from DES-treated fibres (4 h at 100 °C). DES pre-treatment allowed to produce a mixture of microfibril bundles (widths around 50 nm) and individualised microfibrils (widths between 5 and 10 nm). The produced MFC from DES are very long with high aspect ratio, while those obtained from enzymatic hydrolysis, are shorter with more kinks. It appears that the internal and external fibrillation of the fibres during DES pre-treatment improved the microfibrillation process, which is also enhanced by the esterification of cellulose during acidic DES pre-treatment. This improvement is explained by the presence of charged group (quaternary ammonium), that between themselves make a repulsion which facilitates the microfibrils release. The morphological, structural and mechanical properties of produced MFC were explored. The results showed that MFC-DES obtained from eucalyptus exhibited higher densities and higher quality index QI^* (between 72 and 76). However, those obtained from cotton fibres were with modest qualities. This difference was explained by the presence of hemicellulose (xylan) in eucalyptus fibres which has a positive impact on the quality of produced MFC. The energy consumption was calculated during grinding and its value was close to enzymatic hydrolysis. The presence of cationic charge group on acidic DES-treated fibres required less energy demand. The effectiveness of DES pre-treatment was thus highlighted and DES could be considered as a valuable green and soft pre-treatment alternative allowing the production of MFC with high quality.

In the second part of this chapter, the possibility of the scaling-up of DES pre-treatment was studied using a twin-screw extruder TSE. DES-treated fibres were refined and then passed

through the TSE for 4 times. TSE allowed to produce MFC at high solid content (20%) with the presence of residual fibres. The evolution of the morphological, structural and mechanical properties was done after each pass through the TSE. The DP of and crystallinity index were impacted by the TSE. It was shown that the increase of the number of passes through the TSE causes fibre degradation. Moreover, the mechanical properties were slightly improved after the first or the second pass and then reduced. TSE facilitates the microfibrillation process, but the qualities of produced MFC are modest and significantly lower than those obtained from ultrafine grinding.

One of the main conclusions of this chapter is that the use of DES-treated fibres (4 h at 100 °C) followed with an ultrafine grinding enables an energy-efficient production of MFC with high-quality. The applications of produced MFC using ultra-fine friction grinder could be extended. For instance, MFC produced from DES-treated eucalyptus fibres could be used in bio-composite reinforcement due to their high mechanical properties. Other applications could be envisaged such as the antibacterial properties of cationic MFC produced from BHCl-U pre-treatment.

For the second section, the perspectives are the use of another TSE profile with adjustable conditions (solid content, speed...). The possibility of combining DES pre-treatment with enzymatic hydrolysis could be also envisaged.

Extended French abstract – Résumé étendu en français

Résumé étendu en français

Aujourd'hui, il existe un réel besoin de remplacer les polymères synthétiques produits à partir du pétrole par des polymères biodégradables et biosourcés. Ce besoin résulte de l'utilisation intensive de ces polymères qui conduit à de nombreux problèmes, notamment l'épuisement des ressources pétrolières, la pollution...

Dans ce contexte, la cellulose présente de nombreux atouts pour remplacer les polymères synthétiques. La cellulose est en effet le polymère le plus abondant sur terre avec une production d'environ 300 Gt par an (Delmer and Amor, 1995). Ce polymère biosourcé est caractérisé par sa biodégradabilité, sa durabilité et son caractère renouvelable. Il peut être extrait de différentes biomasses lignocellulosiques, notamment le bois (résineux et feuillus), le coton, le lin... Malgré ses propriétés intéressantes, la cellulose, en tant que matière première, présente certaines limites en raison de son affinité avec l'eau (matériau hygroscopique). Aujourd'hui, de nombreux travaux de recherche s'intéressent à la nanocellulose qui est extraite des fibres de cellulose. La nanocellulose présente des propriétés chimiques et physiques très intéressantes, notamment du fait de sa grande surface spécifique et des facteurs de forme qu'elle possède. Deux types de nanocellulose peuvent être identifiés à savoir : les microfibrilles de cellulose (MFC) et les nanocristaux de cellulose (NCC). Les MFC sont produites principalement par désintégration des fibres végétales par un traitement mécanique (Turbak et al., 1983), tandis que les NCC sont obtenus par hydrolyse en milieu acide (Habibi et al., 2010).

La production de MFC est très coûteuse, en raison de la consommation énergétique des procédés mécaniques utilisés comme le broyage, l'homogénéisation... (Abdul Khalil et al., 2014). La nécessité de réduire cette consommation d'énergie a conduit les chercheurs à proposer des nouvelles voies des prétraitements chimiques ou biologiques. De nombreux prétraitements sont bien décrits dans la littérature comme l'oxydation TEMPO (Isogai et al., 2011; Nooy et al., 1994; Saito et al., 2009) et l'hydrolyse enzymatique (Henriksson et al., 2007; Hu et al., 2011; Nie et al., 2018; Pääkkö et al., 2007) pour ne citer que les plus fréquemment mis en oeuvre. L'oxydation avec le radical TEMPO est en effet le prétraitement le plus répandu qui permet de produire des MFC de haute qualité avec un faible coût énergétique. Malgré son efficacité, il présente certaines limites comme sa toxicité et l'utilisation d'un catalyseur (généralement à base d'ion bromure), qui n'est pas toujours approprié en fonction des applications envisagées.

Récemment, un nouveau prétraitement basé sur l'utilisation de solvants eutectiques profonds (DES) a été proposé. Les DES sont définis comme des mélanges de donneurs et d'accepteurs de liaisons hydrogène qui, ensemble, présentent un point de fusion inférieur à leur température de fusion individuelle (Abbott et al., 2003). Les DES sont considérés comme des solvants et réactifs verts avec des propriétés intéressantes, notamment leur biodégradabilité, leur faible toxicité, leur recyclabilité et leur sélectivité. Les systèmes les plus étudiés sont ceux composés d'ammonium quaternaire et de sels métalliques ou de donneurs de liaison hydrogène. Selon Smith et al. (2014), les DES sont classés en quatre groupes :

- (I) Combinaison de sels organiques et métalliques
- (II) Mélange de sels organiques et d'hydrates métalliques
- (III) Combinaison de sels organiques et de composés à liaison hydrogène
- (IV) Mélange de chlorures métalliques et de composés donneurs de liaison hydrogène.

De nombreux DES non cationiques ont également été bien décrits dans la littérature. Une cinquième classe (type V) a été proposée (Abranches et al., 2019 ; Moufawad et al., 2021 ; Schaeffer et al., 2020). Cette dernière est obtenue à partir du mélange d'espèces non ioniques.

En raison de leurs propriétés intéressantes, les DES suscitent de plus en plus d'intérêt dans la communauté scientifique. Ils sont utilisés dans plusieurs domaines tels que la synthèse organique (Ruesgas-Ramón et al., 2017), la science des polymères (Tomé et al., 2018), le domaine électrochimique (Fernandes et al., 2012 ; Hosu et al., 2017) et le traitement des eaux usées (AlOmar et al., 2016). Certains DES sont également connus pour être des supports de traitement de la biomasse lignocellulosique, comme décrit dans de nombreuses revues (Selkälä et al., 2016 ; Zdanowicz et al., 2018).

Lorsqu'ils sont appliqués à la biomasse lignocellulosique, ils doivent avoir une capacité de solubilisation sélective qui dépend à la fois de leurs composants et de la nature de la biomasse. Comme ils ne solubilisent pas ou peu la cellulose, ils permettent d'avoir une action sélective.

Les DES peuvent ainsi être potentiellement utilisés comme milieu de prétraitement pour améliorer la fibrillation ou la microfibrillation des fibres, même s'il existe très peu d'articles sur ce sujet par rapport à l'extraction sélective des composants de la biomasse. Par exemple, le mélange chlorure de choline-urée (CC-U) a été le premier système utilisé pour traiter les fibres de cellulose avant une étape de microfibrillation mécanique (Sirviö et al., 2015). Une autre étude a montré que le mélange de thiocyanate d'urée avec l'ammonium ou le chlorhydrate de

guanidine peut être utilisé dans le prétraitement du bois pour faciliter ultérieurement la microfibrillation (Li et al., 2017). Ces systèmes sont capables de gonfler les fibres et donc de rompre les liaisons hydrogène (inter et intra) entre les chaînes de cellulose sans dégrader le polysaccharide.

Par ailleurs, certaines études ont rapporté l'utilisation de DES pour la microfibrillation avec une modification chimique simultanée. La cationisation de la cellulose, par exemple, peut être effectuée pendant le traitement par DES (Sirviö, 2018). Une réaction d'estérification peut également être réalisée en présence de DES pour produire des CNF estérifiés (Liu et al., 2021).

Depuis de nombreuses années, l'un des principaux sujets de notre groupe de recherche est lié à la réduction des coûts énergétiques associés à la microfibrillation mécanique de la cellulose (Banvillet et al., 2021 ; Khiari et al., 2019 ; Rol et al., 2020, 2017). Pour cela, différents prétraitements (biologiques ou chimiques) sont utilisés avant le traitement mécanique principal de microfibrillation (broyage ultrafin, homogénéisation...) (Nechyporchuk et al., 2016 ; Rol et al., 2019). En revanche, les prétraitements conventionnels sont généralement coûteux, comme l'hydrolyse enzymatique, ou basés sur l'utilisation de réactifs toxiques, comme l'oxydation par le réactif TEMPO. Les DES peuvent être considérés comme une bonne alternative pour réduire la toxicité des réactifs chimiques et protéger l'environnement par l'utilisation de composants biodégradables. Enfin, ces solvants sont parfois non réactifs, comme le chlorure de choline-urée, ce qui peut être un avantage, surtout pour une modification ultérieure (post-modification).

En raison des résultats prometteurs obtenus avec le prétraitement DES, ce travail s'inscrit dans la même stratégie et vise à étudier l'influence de prétraitements DES sur les fibres de cellulose et leur efficacité à faciliter le processus de microfibrillation.

Cette thèse a été réalisée dans le cadre d'une cotutelle entre le Laboratoire de Génie des Procédés Papetiers LGP2 (Université de Grenoble Alpes, France) et le Laboratoire d'Environnement Chimique et de Procédés Propres LCE2P- LR21ES04 (Faculté des Sciences de Monastir-université de Monastir, Tunisie), en collaboration avec le CERMAV (CNRS, France). Ce travail a été soutenu financièrement par le programme « PHC Utique » du ministère français des affaires étrangères, du ministère de l'enseignement supérieur, de la recherche et de l'innovation et du ministère tunisien de l'enseignement supérieur et de la recherche scientifique dans le cadre du projet CMCU ayant le numéro TN 18G1132// FR 39316VF.

Le manuscrit est divisé en trois chapitres principaux comme décrit dans la Figure 1.

Le **chapitre I** est un état de l'art : la première partie porte sur la cellulose, sa structure, ses propriétés, sa dissolution et sa modification. La deuxième partie est consacrée aux propriétés de la nanocellulose (nanofibrilles de cellulose et nanocristaux de cellulose) et à leur extraction. Ensuite, les propriétés des nanofibrilles de cellulose, leur production et les prétraitements utilisés sont discutés. La dernière partie est consacrée aux propriétés des solvants eutectiques profonds DES, leurs applications et, plus spécifiquement, leur utilisation pour le traitement de la biomasse cellulosique.

Le **chapitre II** rassemble les résultats expérimentaux relatifs à l'étude des effets des DES sur les fibres de cellulose et les propriétés des papiers. Dans cette partie, les propriétés morphologiques, chimiques, structurelles et mécaniques des fibres de cellulose sont étudiées. Un deuxième volet est consacré à l'étude des effets des DES sur les fibres de cellulose en utilisant la chromatographie d'exclusion stérique à haute performance (HPSEC) pour comprendre les phénomènes se produisant à l'échelle moléculaire.

Le **chapitre III** s'intéresse à l'efficacité des prétraitements DES pour la production de MFC. La première partie étudie la microfibrillation des fibres traitées par les DES à l'aide d'un broyage ultrafin. Dans un deuxième temps, une extrudeuse bi-vis TSE est utilisée pour produire des suspensions concentrées de MFC en vue de faciliter leur industrialisation.

Le manuscrit par une conclusion et la proposition de perspectives pour des travaux ultérieurs.

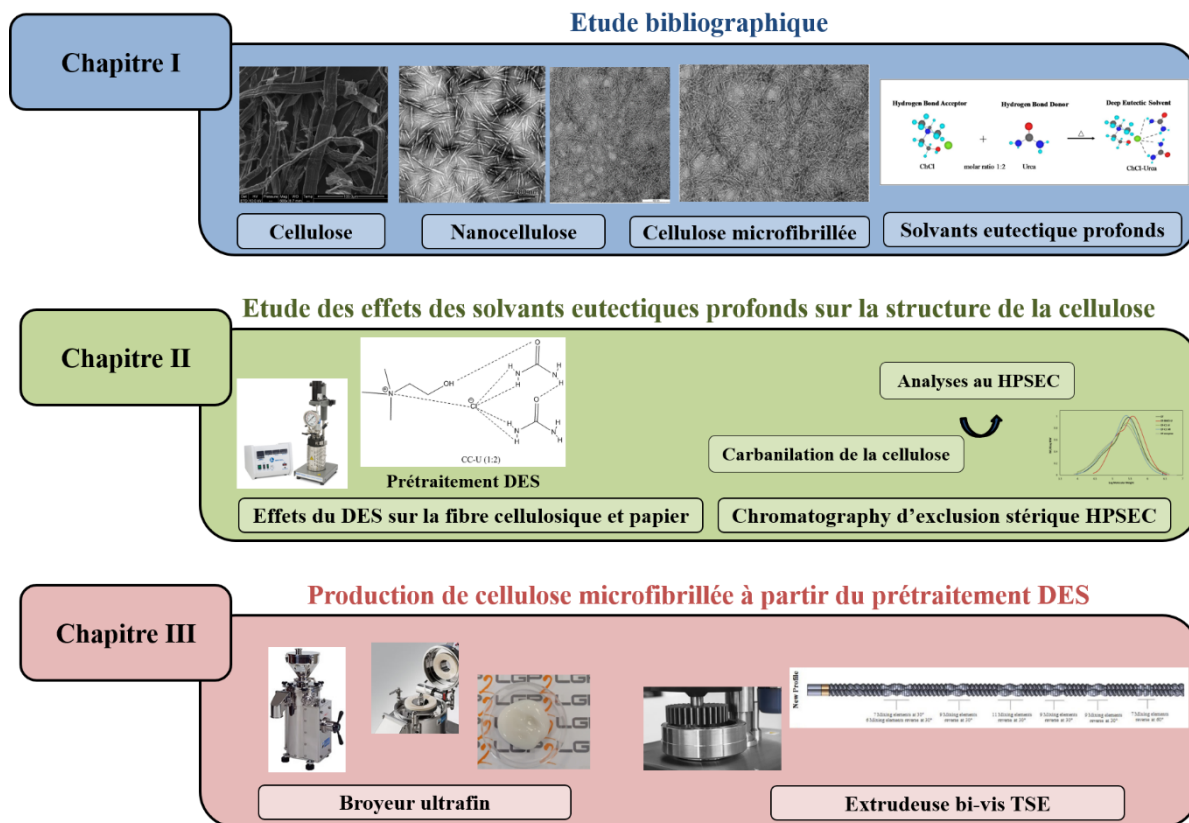


Figure 1 : Schéma général de l'organisation du manuscrit.

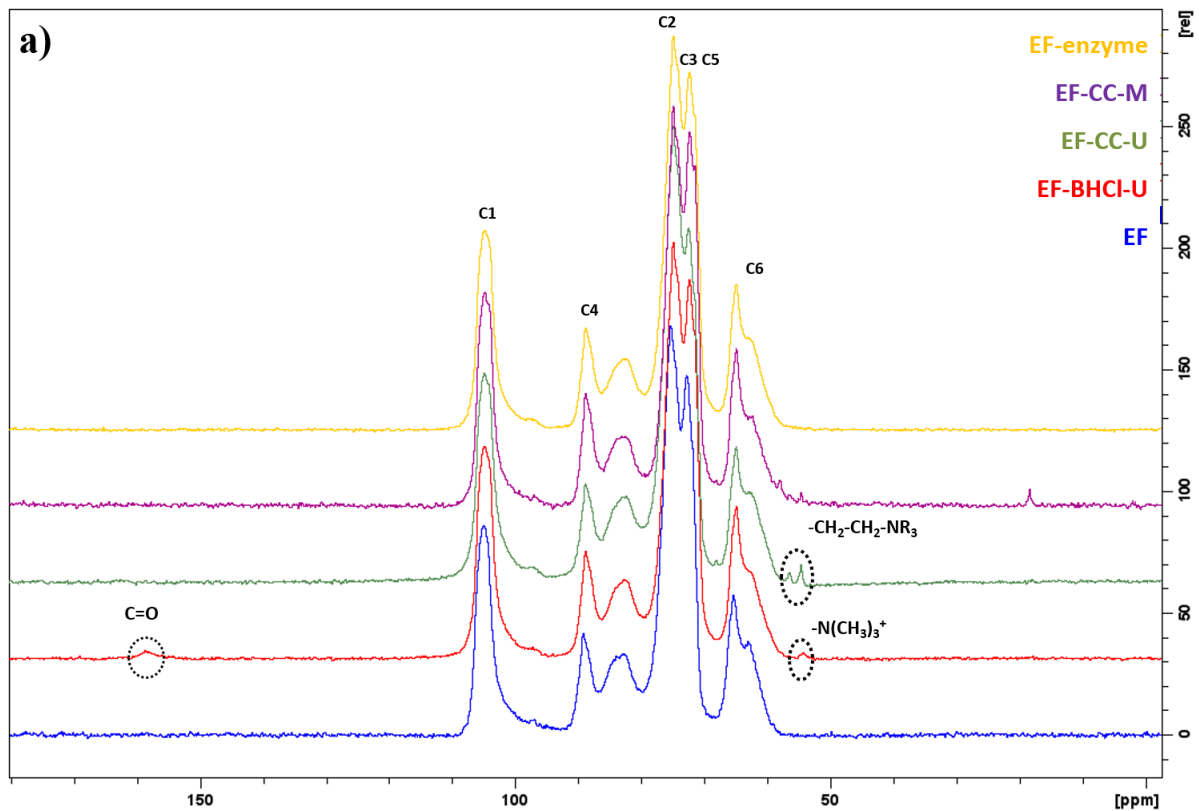
Principaux résultats

Dans ce travail de recherche, trois différents systèmes eutectiques sont choisis en fonction de leur pH et leur efficacité pour le traitement de la cellulose. Ces solvants sont : (i) un mélange chlorhydrate de bétaïne-urée BHCl-U (système acide), (ii) un mélange chlorure de choline-urée CC-U (système neutre), et (iii) un mélange chlorure de choline/mono-éthanolamine CC-M (système alcalin). Il est important de signaler que le système acide est utilisé pour la première fois comme un prétraitement pour la microfibrillation de la cellulose. Le système alcalin a quant à lui été utilisé comme un prétraitement de la biomasse lignocellulosique pour extraire la lignine (Zhao et al., 2018). Enfin, le DES neutre est choisi comme un système de référence puisqu'il est le plus connu pour le traitement de la biomasse cellulosique (Sirviö et al., 2015). En plus du traitement des fibres dans les DES, nous avons effectué un traitement enzymatique classique (traitement de référence) pour faire la comparaison entre les MFC produites. Le traitement enzymatique se base sur l'hydrolyse des chaînes de cellulose grâce à des enzymes (cellulase

FiberCare avec une activité de 4948 ECU/g de solution). La réaction s'effectue à 50°C et dans un pH égal à 5 durant 2h.

Deux types de fibres cellulosiques ont été utilisés à savoir : des fibres d'eucalyptus (pâte kraft blanchie, FE) et des fibres de coton (FC). Ce choix se base sur le fait que les fibres d'eucalyptus sont largement utilisées dans le domaine papetier, en particulier pour la production de MFC et qu'elles contiennent un pourcentage d'hémicelluloses non négligeable. Les fibres de coton sont à l'opposé essentiellement constituées de cellulose. Cette approche permet de comprendre à la fois les effets des DES sur la cellulose seule (coton) et sur les hémicelluloses (fibres blanchies d'eucalyptus).

Dans le **chapitre II**, les effets du prétraitement DES sur les fibres de cellulose (FE et FC) et les propriétés des papiers ont été étudiés. La structure chimique des fibres traitées au DES a été étudiée par diverses techniques (RMN ^{13}C solide et FT-IR-ATR). Les résultats ont montré qu'une estérification s'est produite pendant le traitement au DES acide comme illustré dans la Figure 2. La cellulose a réagi avec le chlorure de bétaïne pour former un ester de cellulose. Aucune modification n'a été détectée avec les autres systèmes.



b) Cellulose esterification mechanism

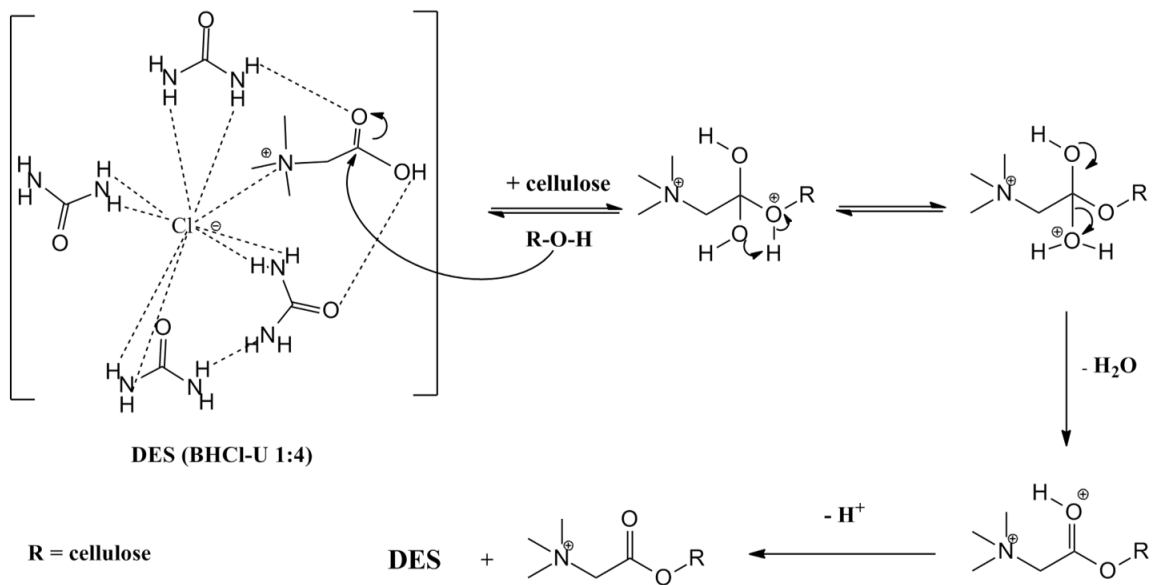


Figure 2 : Spectres RMN solide ^{13}C des fibres d'eucalyptus traitées par les DES ou par hydrolyse enzymatique (a) et mécanisme réactionnel proposé pour l'estérification de la cellulose (b).

La composition chimique des fibres d'eucalyptus (à partir du dosage des sucres) a été modifiée uniquement au cours du traitement par les DES acide et neutre comme le montre le Tableau 1. Ces deux systèmes favorisent l'élimination partielle du xylane. Ces résultats révèlent donc la sélectivité de ces systèmes qui dépend de leur composition.

Tableau 1 : Composition chimique des fibres cellulosiques traitées par les solvants eutectiques.

	Cellulose (%)	Hemicelluloses (%)
EF	78	22
EF-BHCl-U	83	17
EF-CC-U	82	18
EF-CC-M	78	22
CF	100	n.d
CF-BHCl-U	100	n.d
CF-CC-U	100	n.d
CF-CC-M	100	n.d

n.d : non déterminé

Le DP et l'indice de cristallinité ont été influencés par le DES alors que les propriétés thermiques n'ont pas été modifiées.

La valeur de rétention d'eau des fibres traitées a augmenté surtout avec le système alcalin comme le montre la Figure 3. Ceci reflète une action spécifique du DES sur la structure de la paroi des fibres : les DES étudiés semblent favoriser une fibrillation interne.

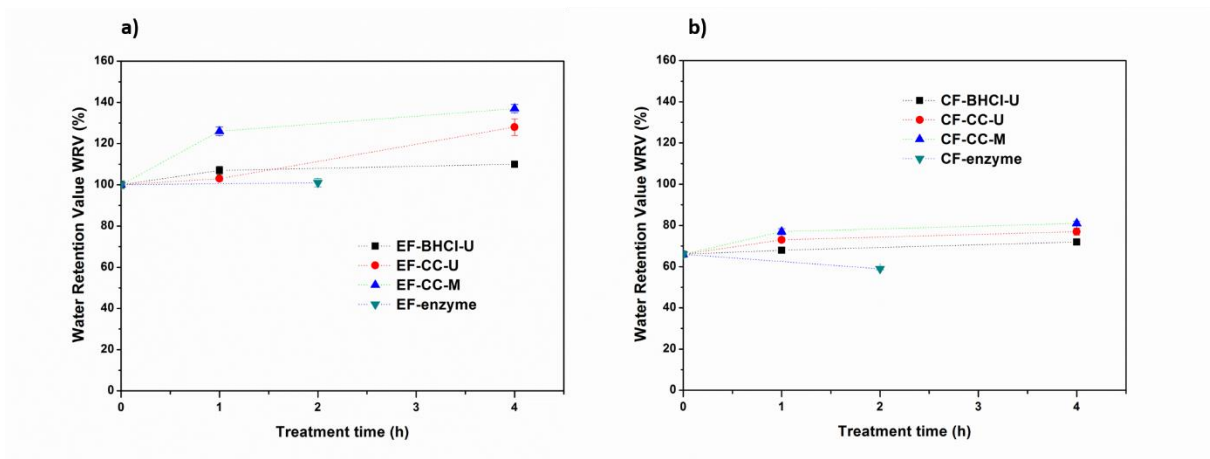


Figure 3: Evolution de la valeur de rétention d'eau des fibres d'eucalyptus (a) et de coton (b) traitées par les DES ou par voie enzymatique.

Une fibrillation externe a également été identifiée par microscopie électronique à balayage MEB comme le montre la Figure 4. L'observation la plus remarquable est l'apparition de macrofibrilles partiellement détachées des fibres qui créent un réseau entre les fibres après séchage. A l'inverse, aucune macrofibrille visible n'a été détectée après un traitement enzymatique et les fibres semblent moins liées les unes aux autres. L'observation d'un réseau de macrofibrilles après le traitement DES est similaire à l'effet de raffinage de la suspension fibreuse (Banvillet et al., 2021; Kang, 2007).

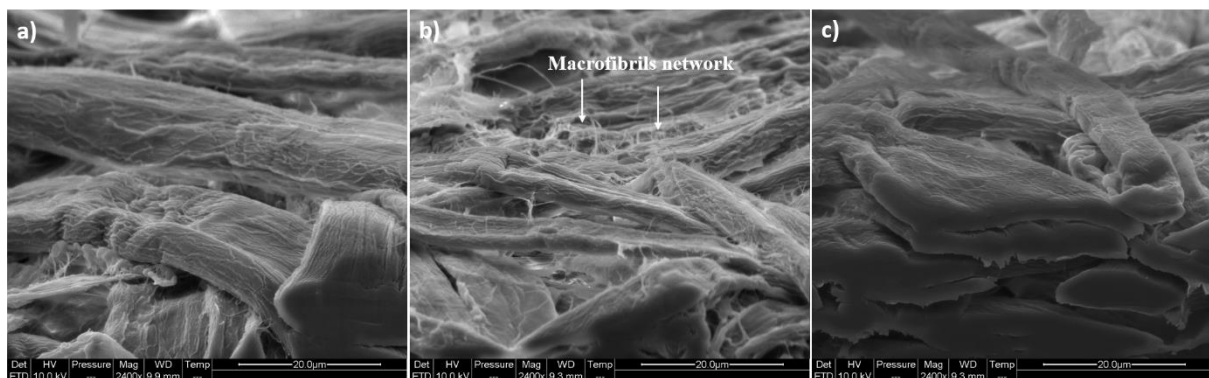


Figure 4 : Images MEB des papiers produits à partir de fibres d'eucalyptus non traitées (a), traitées par le DES alcalin (b) et par voie enzymatique (c).

En conséquence, les propriétés mécaniques des papiers produits sont améliorées de manière très significative (augmentation du module d'Young, de la résistance à la traction, de la cohésion

interne...), en augmentant le degré de liaison et en préservant la longueur des fibres (Figure 5). Les résultats obtenus sont très intéressants : le traitement DES peut ainsi être considéré comme un raffinage "chimique" vert et doux des fibres de cellulose.

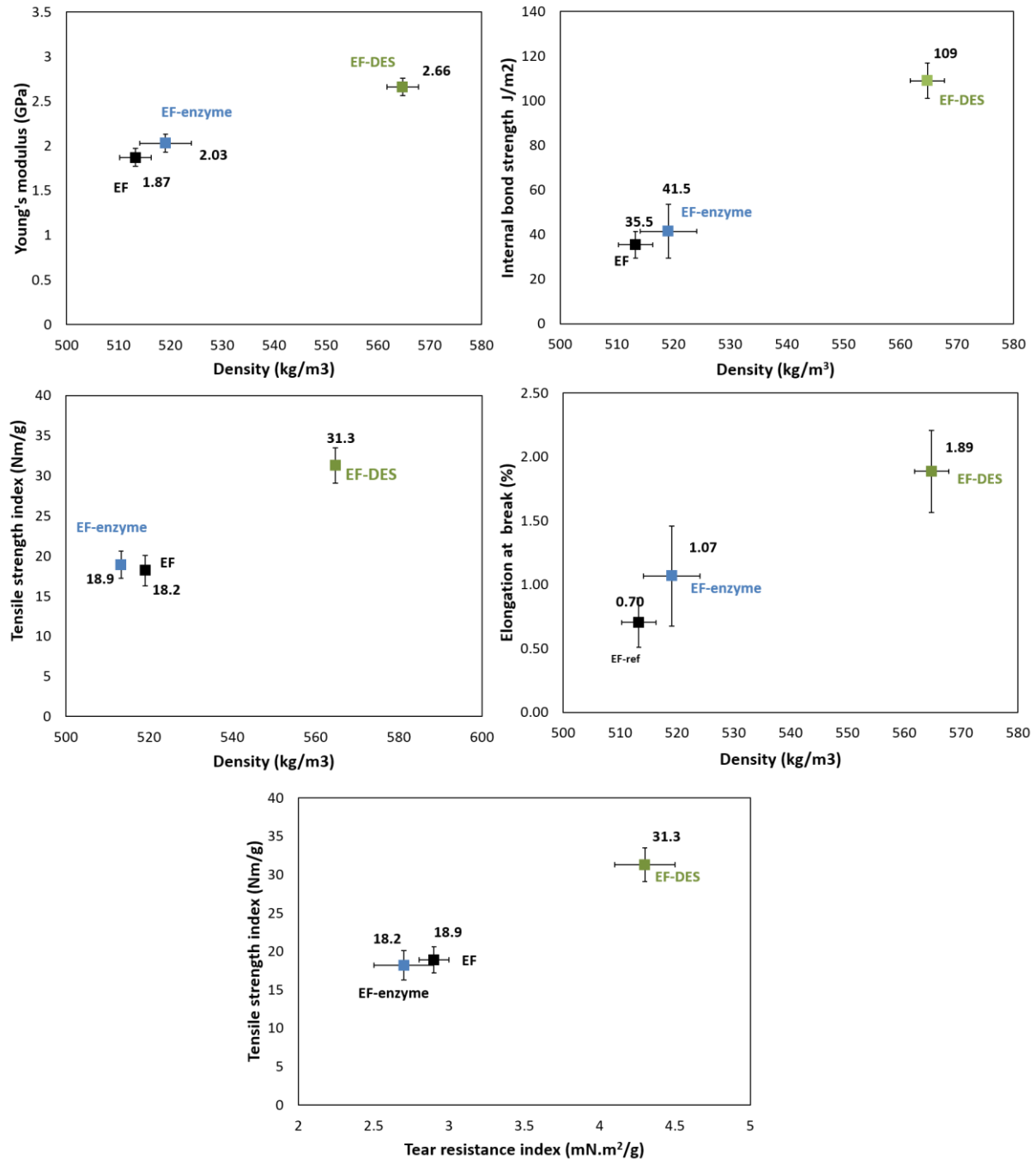


Figure 5 : Evolution des propriétés mécaniques des papiers produits après traitement avec le DES alcalin ou le traitement enzymatique.

Dans la deuxième partie de ce chapitre, la chromatographie d'exclusion stérique à haute performance HPSEC a été utilisée pour étudier la distribution de la masse moléculaire de la cellulose après prétraitement DES ou après hydrolyse enzymatique. Les fibres traitées au DES ont été tricarbanilées avec l'isocyanate de phényle en présence de diméthyle sulfoxyde DMSO. Cette modification a pour but de fonctionnaliser la cellulose pour la solubiliser dans le tétrahydrofurane THF, qui est le solvant utilisé pour la technique SEC. Les fibres tricarbanilées ont été dissoutes dans le THF, puis injectées dans la colonne du HPSEC.

Les résultats ont montré que tous les échantillons présentent un taux de rendement élevé (celui de la colonne) compris entre 90 et 100%, à l'exception des fibres traitées par le DES acide (rendement plus faible), ce qui peut résulter de leur modification chimique (estérification). L'analyse HPSEC a montré que la dispersité a augmenté après un traitement par le système neutre et après l'hydrolyse enzymatique. Elle a été légèrement modifiée par le DES alcalin et diminuée par le DES acide.

On peut penser que le système CC-U et l'hydrolyse enzymatique permettent d'augmenter la dispersité en coupant les extrémités des chaînes de cellulose (légère diminution de la masse moléculaire en poids M_w et forte réduction de la masse moléculaire en nombre M_n). En revanche, le DES alcalin semble avoir une action différente : il permettrait de diminuer la dispersité en coupant de gros fragments de la chaîne cellulosique (diminution significative du M_w) avec une augmentation du M_n .

Par ailleurs, le système CC-M favorise la production de polymères gonflés. Le système CC-U et l'hydrolyse enzymatique favorisent l'obtention des polymères sphériques respectivement pour les fibres de coton et d'eucalyptus.

Les perspectives de cette étude pourraient être l'optimisation de la réaction d'estérification afin d'augmenter le degré de substitution de la cellulose. Il serait également possible d'étudier certaines applications liées aux papiers produits à partir d'un prétraitement au DES, puisque celui-ci améliore significativement leurs propriétés mécaniques. Le recyclage des DES utilisé doit enfin être étudié pour évaluer l'efficacité et la stabilité de ces systèmes.

Le **chapitre III** est consacré à l'étude de l'efficacité des prétraitements DES pour faciliter l'étape ultérieure de microfibrillation des fibres cellulosiques. Dans un premier temps, nous avons produit des MFC par broyage (broyeur ultrafin Masuko) à partir de fibres cellulosiques (eucalyptus et coton) traitées dans les DES pendant 4h à 100°C. Une suspension aqueuse de

fibres cellulosiques à 2% (fraction massique) est traitée mécaniquement dans un broyeur (Masuko) à 1500 tours/minute selon le protocole suivant : 10 passages entre les disques avec un écart de -5 et 20 passages avec un écart de -10. Les MFC obtenues ont été caractérisés par plusieurs techniques (AFM, TEM, Morfi, essai de traction...).

Les images d'AFM, TEM des MFC obtenues à partir des fibres d'eucalyptus et de coton ainsi que celles des nanopapiers produits à partir des suspensions de MFC sont regroupées dans la Figure 6. Ces images montrent la présence de faisceaux de microfibrilles (diamètre d'environ 50 nm) et des microfibrilles individualisées (diamètre compris entre 5 et 10 nm). Elles prouvent la production de MFC présentant des longueurs bien supérieures à celles obtenues après un traitement enzymatique.

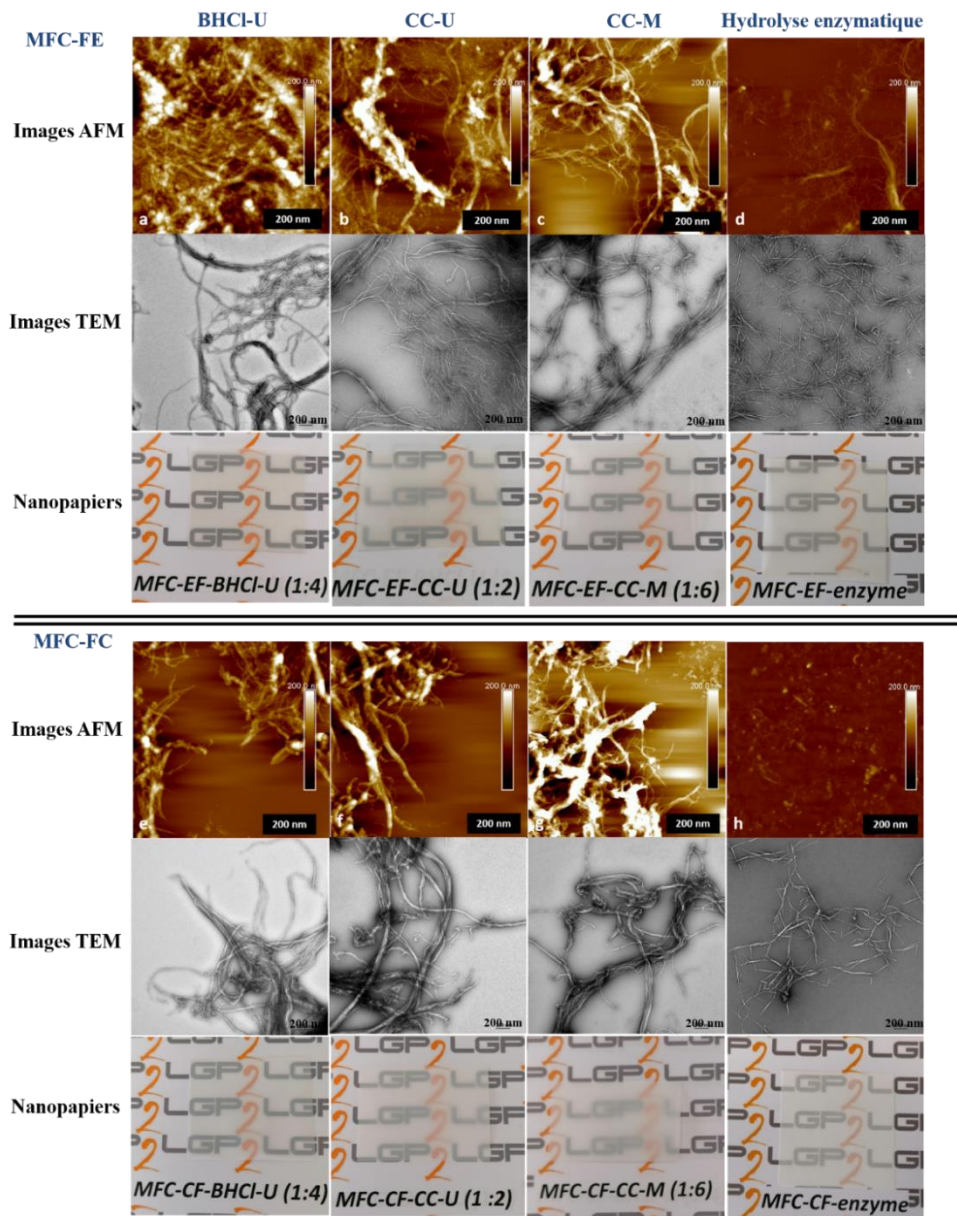


Figure 6 : Images de MFC obtenues à partir des fibres celluloses (eucalyptus et coton) traitées aux DES ou par l'hydrolyse enzymatique.

La fibrillation interne et externe qui s'est produite pendant le prétraitement par les DES améliore le processus de microfibrillation. En outre, l'estérification de la cellulose au cours du prétraitement DES acide semble avoir contribué à améliorer la microfibrillation. Les propriétés morphologiques, structurales et mécaniques des MFC produites ont été étudiées en utilisant différentes techniques de caractérisation. Les résultats regroupés dans le Tableau 2 montrent que les MFC-DES obtenues à partir de fibres d'eucalyptus présentent un bon indice de qualité QI^* (entre 72 et 76). Le module de Young des nanopapiers est élevé. En revanche, les MFC

obtenues à partir des fibres de coton présentent de moins bonnes caractéristiques. Cette différence peut s'expliquer par la présence d'hémicelluloses dans les fibres d'eucalyptus qui améliore la qualité des MFC produites.

Tableau 2 : Indice de qualité simplifié de MFC produites par broyage ultrafin.

Echantillon	Taille macro (μm^2)	Fraction nanométrique (%)	Turbidité (NTU)	Module de Young (GPa)	Indice de qualité QI*
MFC-EF-BHCl-U	12.22 \pm 1.31	61.67 \pm 8.94	379 \pm 8	10.9 \pm 0.3	72.86 \pm 2.70
MFC-EF-CC-U	13.85 \pm 6.73	67.26 \pm 0.51	279 \pm 4	10.4 \pm 0.3	76.43 \pm 1.35
MFC-EF-CC-M	16.08 \pm 1.33	65.96 \pm 6.86	336 \pm 6	10.7 \pm 0.3	73.77 \pm 1.77
MFC-EF-enzyme	69.21 \pm 3.40	65.87 \pm 4.04	228 \pm 6	10.1 \pm 0.2	68.52 \pm 0.61
MFC-CF-BHCl-U	97.05 \pm 52.4	63.61 \pm 5.35	745 \pm 13	7.88 \pm 0.4	47.77 \pm 3.68
MFC-CF-CC-U	70.57 \pm 25.5	75.12 \pm 12.44	774 \pm 41	7.06 \pm 0.5	50.88 \pm 6.09
MFC-CF-CC-M	64.34 \pm 0.10	56.49 \pm 1.36	758 \pm 20	8.44 \pm 0.1	48.22 \pm 0.01
MFC-CF-enzyme	138.4 \pm 49.3	43.95 \pm 7.83	558 \pm 67	6.04 \pm 0.5	42.73 \pm 6.08

La consommation d'énergie a été calculée (Figure 7) pendant le broyage pour les fibres traitées par les DES et sa valeur est proche de celle obtenue pour des fibres traitées par voie enzymatique. La présence de groupements cationiques pour les fibres traitées par le DES acide semble faciliter la microfibrillation en limitant la consommation d'énergie. L'efficacité d'un prétraitement des fibres cellulosiques par des DES a ainsi été démontrée et les résultats sont très intéressants : les DES permettent de réaliser un prétraitement vert et doux qui conduit à l'obtention de MFC de bonne qualité. D'autre part, les MFC produites à partir d'un broyage ultrafin présentent de bonnes qualités comparables aux MFC commercialisées (Mnasri et al., 2022b).

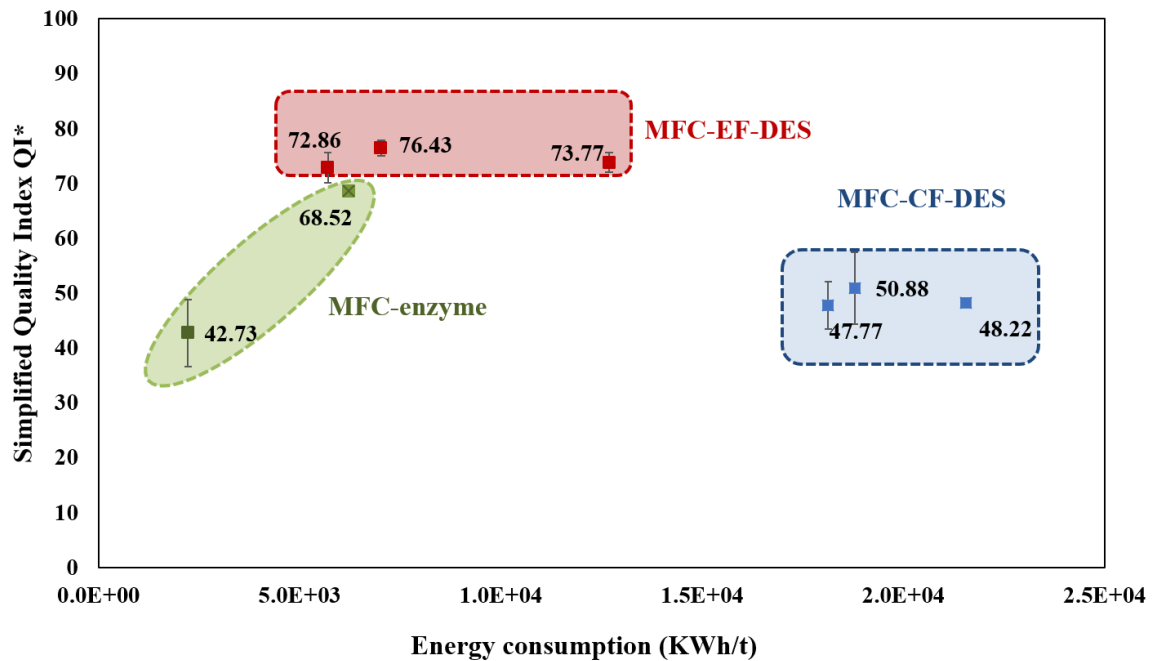


Figure 7 : Evolution de l'indice de qualité en fonction de l'énergie consommée au cours du broyage ultrafin.

Dans la deuxième partie de ce chapitre, la possibilité de produire de la cellulose microfibrillée à haute concentration après un prétraitement par les DES a été étudiée en utilisant une extrudeuse bi-vis (TSE). Des fibres traitées par les DES pendant 4h à 100°C ont été raffinées et passées 4 fois dans l'extrudeuse. Les résultats obtenus montrent que la TSE permet certes de produire des MFC à haute teneur en solides (20%) mais la présence d'éléments cellulosiques grossiers constitue une limitation. L'évolution des propriétés morphologiques des suspensions a été suivie après chaque passage dans le TSE comme le montre la Figure 8. Les images MEB indiquent la présence d'éléments présentant une longueur comprise entre 20 et 100 μm avec quelques microfibrilles attachées aux fibres.

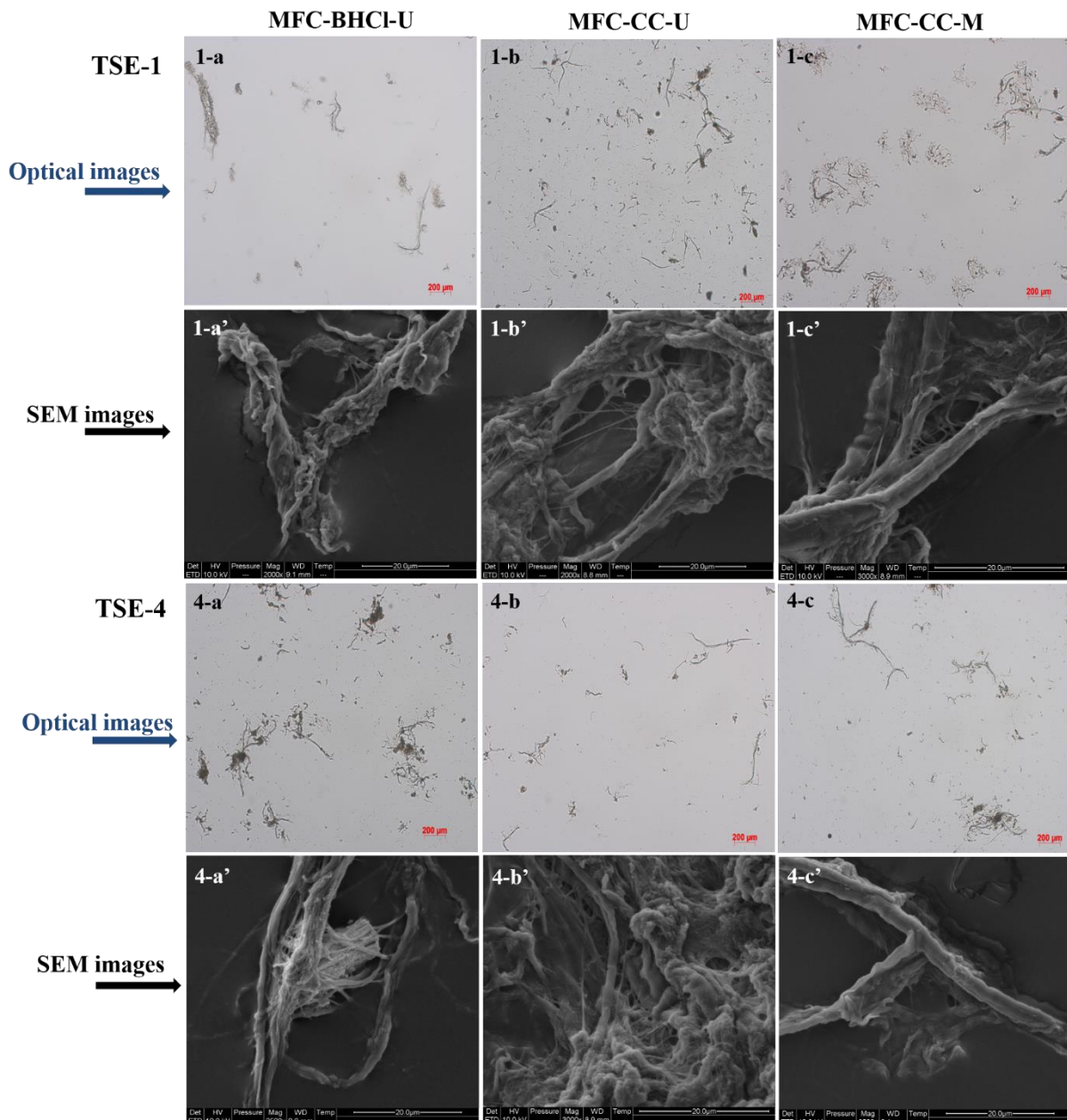


Figure 8 : Images MEB et de microscopie optique de MFC produites par extrusion après la première et quatrième passe au TSE.

Le DP de et l'indice de cristallinité ont été influencés par la TSE comme illustré dans la Figure 9. L'augmentation du nombre de passages à travers la TSE provoque une diminution de ces valeurs.

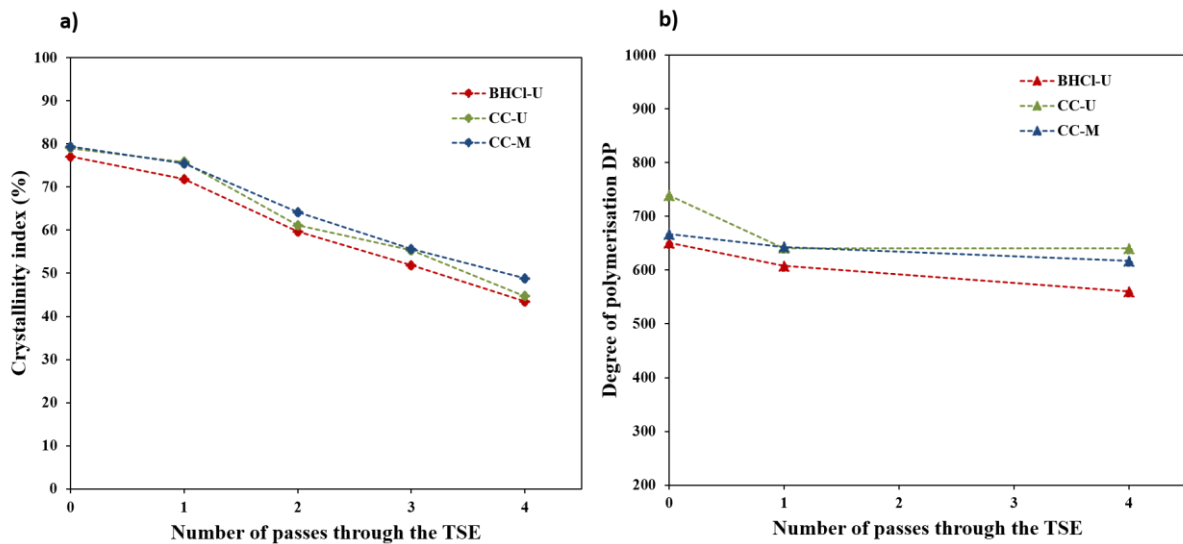


Figure 9 : Evolution de la cristallinité (a) et le degré de polymérisation (b) en fonction du nombre de passe dans l'extrudeuse.

Les masses volumiques des papiers/nanopapiers obtenus à partir des suspensions de MFC et leurs propriétés mécaniques (module de Young, indice de résistance à la traction et allongement à la rupture) sont illustrées dans la Figure 10.

La masse volumique du papier a été légèrement influencée par l'extrusion. Le module d'Young, l'indice de résistance à la traction et l'allongement à la rupture ont également été modifiés pendant l'extrusion. Les valeurs du module de Young des papiers/nanopapiers se situent entre 5,17 et 6,95 GPa. Les plus grandes valeurs du module ont été atteintes après le quatrième passage pour le DES acide, le deuxième passage pour le DES neutre et après un passage pour le DES alcalin. Les valeurs les plus élevées de la résistance à la traction sont obtenues pour les mêmes conditions de traitement.

L'évolution différente peut être expliquée par la forte hétérogénéité de la suspension après chaque passage dans l'extrudeuse.

En ce qui concerne les déformations à la rupture, les valeurs maximales sont de 1.99, 4.09 et 3.14% respectivement pour le DES acide (quatrième passage), le DES neutre (quatrième passage) et le DES alcalin (un passage).

A partir de ces résultats, on peut mentionner qu'un traitement par le DES neutre permet d'obtenir les meilleures valeurs des propriétés mécaniques des papiers/nanopapiers, suivi par le DES alcalin et le DES acide.

La qualité moyenne des MFC obtenues par extrusion, bien inférieure à celle des MFC obtenues par broyage ultrafin (Tableau 3), est liée à la présence d'éléments grossiers dans la suspension de MFC mais également à l'hétérogénéité des MFC produites.

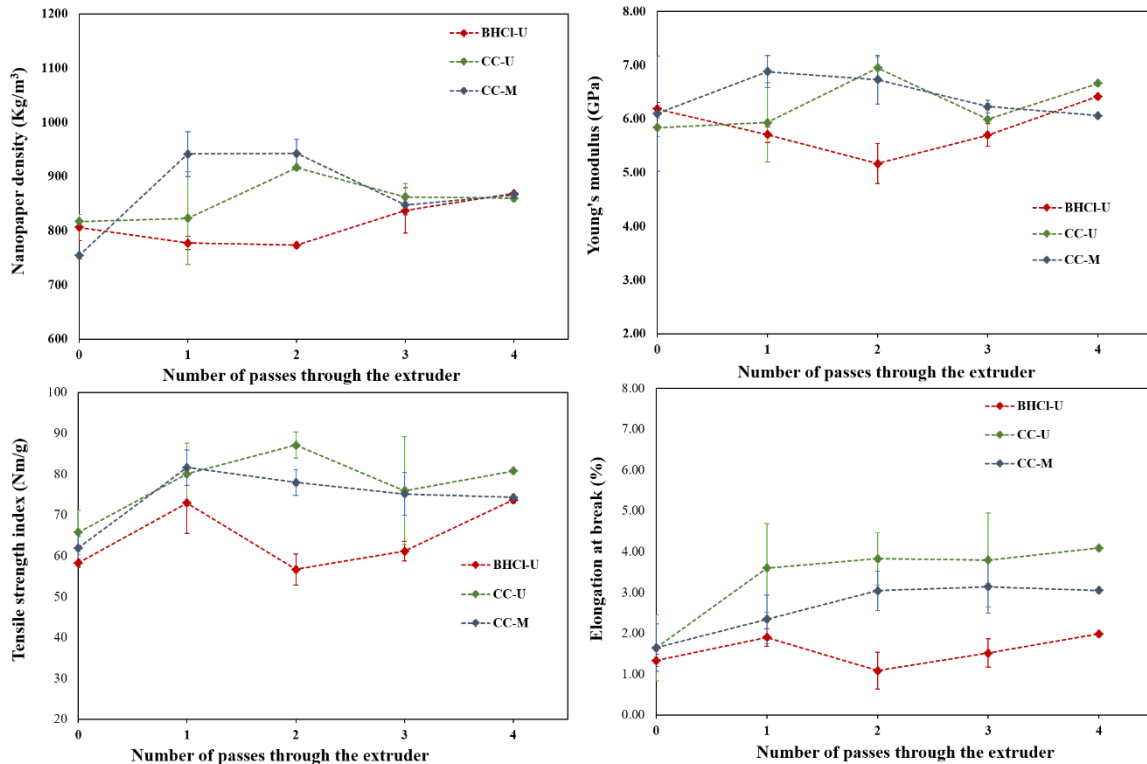


Figure 10 : Evolution des propriétés mécaniques de papiers/nanopapiers en fonction du nombre de passes dans l'extrudeuse.

Les valeurs de QI^* , voisines de 45 pour les trois DES, démontrent que la qualité des MFC obtenues après TSE est effectivement médiocre. Elles sont dues à la turbidité élevée des suspensions, résultant elle-même d'une fraction macroscopique plus grande, et au faible module de Young des nanopapiers obtenus.

Les procédés d'extrusion et de broyage sont différents, ce qui conduit à des produits différents. Dans le cas du broyage ultrafin, la suspension de fibres passe à travers deux disques. Des forces sont appliquées sur les fibres, notamment des forces de compression, de cisaillement et de friction, ce qui favorise la microfibrillation (Serpa Guerra et al., 2020). Quand les conditions sont bien choisies, la distribution de taille des MFC est relativement étroite, leur surface spécifique élevée. Leur flexibilité, leur conformabilité et leur capacité à s'enchevêtrer ont un impact direct sur la microstructure des nanopapiers obtenus.

Par conséquent, les propriétés des MFC obtenues permettent de former des réseaux enchevêtrés, capables de créer de nombreuses liaisons entre les microfibrilles. Les nanopapiers présentent alors une masse volumique importante (valeurs supérieures à 1000 kg/m^3). Le taux de cisaillement appliqué lors du broyage a été évalué et des valeurs comprises entre 5.10^6 s^{-1} et 3.10^8 s^{-1} ont été rapportées (Baati et al, 2017 ; Rol, 2019). Ces valeurs dépendent de l'écart entre les disques et de la vitesse de rotation des disques.

Lors de l'extrusion, le cisaillement appliqué sur les fibres de cellulose est généré par les disques malaxeurs. Le taux de cisaillement rapporté pour la TSE reste généralement bien inférieur à celui du broyage ultrafin et il a été estimé à environ $300\text{-}3000 \text{ s}^{-1}$ (Baati et al., 2017 ; Mohamed et al., 1990 ; Suparno et al., 2011). Ce taux de cisaillement est significativement impacté par les disques malaxeurs, le cisaillement augmente dans ces parties.

De plus, il existe au cours de l'extrusion un phénomène potentiel de glissement. Dans ce cas, le comportement des fibres dans le TSE n'est pas le même et les fibres ne sont pas cisillées. Ceci peut conduire à la présence d'éléments grossiers résiduels qui provoquent une forte hétérogénéité de la suspension. Le glissement des fibres et la faible diminution du DP pendant l'extrusion affectent donc l'efficacité de la microfibrillation et la qualité des MFC produites.

Le broyage ultrafin qui assure un traitement plus homogène des fibres, permet d'obtenir des suspensions de MFC de meilleure qualité. Le DP diminue de manière significative pendant le broyage, ce qui améliore la microfibrillation.

Tableau 3 : Indice de qualité simplifié de MFC produites par extrusion

Echantillon	Macro size (μm^2)	Fraction nanométrique (%)	Turbidité (NTU)	Module de Young (GPa)	Indice de qualité simplifié QI*
MFC-BHCl-U-TSE-P4	254.3 \pm 21	63.16 \pm 13	645 \pm 18	6.42 \pm 0.2	43.25 \pm 4.14
MFC-CC-U-TSE-P4	145.3 \pm 25	66.14 \pm 4.2	696 \pm 8	6.66 \pm 0.3	45.99 \pm 1.56
MFC-CC-M-TSE-P4	160.5 \pm 7.9	69.85 \pm 2.2	690 \pm 32	6.06 \pm 0.1	45.77 \pm 0.69
MFC-BHCl-U	12.22 \pm 1.3	61.67 \pm 8.9	379 \pm 8	10.9 \pm 0.3	72.86 \pm 2.70
MFC-CC-U	13.85 \pm 6.7	67.26 \pm 0.5	279 \pm 4	10.4 \pm 0.3	76.43 \pm 1.35
MFC-CC-M	16.08 \pm 1.3	65.96 \pm 6.9	336 \pm 6	10.7 \pm 0.3	73.77 \pm 1.77

Ce travail a permis de démontrer l'intérêt des DES utilisés en prétraitement des fibres cellulosiques pour la production de MFC. Les perspectives à cette thèse sont très nombreuses et des travaux ultérieurs pourraient ainsi s'intéresser à l'étude d'autres DES, à l'optimisation poussée des conditions du prétraitement, à la modification chimique in-situ de la cellulose, mais également au comportement au recyclage des DES les plus appropriés. Un deuxième volet de perspectives est lié aux domaines d'application des MFC obtenues qui présentent des caractéristiques spécifiques et en particulier un fort facteur de forme (application dans le domaine des bio-composites, modification des propriétés rhéologiques de suspension, etc.) Dans le cas où une modification de la cellulose intervient, et plus précisément une cationisation (prétraitement BHCl-U), les propriétés antibactériennes des MFC cationiques peuvent être testées.

Ces travaux ont également montré que la TSE n'était pas adaptée à la production de MFC de bonne qualité à partir de fibres prétraitées par les DES. Ceci peut être bien sûr dû au profil utilisé qui n'est peut-être pas adapté aux fibres traitées par les DES. Les perspectives de ce travail seraient donc l'utilisation d'un autre profil (classique) couplée à l'étude des conditions opératoires (teneur en solides, vitesse, débit...). Une autre voie consisterait à étudier la possibilité de combiner le prétraitement DES avec une hydrolyse enzymatique afin de réduire le DP et en éliminant l'étape de raffinage. Cependant, il apparaît que l'utilisation de fibres

traitées par les DES sélectionnés dans cette étude, qui préservent relativement bien l'intégrité de la cellulose, risque de ne pas être vraiment adaptée au traitement TSE. Une dernière voie pourrait être l'étude de DES ayant un effet plus marqué sur la cellulose et son DP.

Références

- Abbott, A.P., Capper, G., Davies, D.L., Rasheed, R.K., Tambyrajah, V., 2003. Novel solvent properties of choline chloride/urea mixtures. *Chemical Communications* 0, 70–71. <https://doi.org/10.1039/B210714G>
- Abbott, A.P., Capper, G., L. Davies, D., L. Munro, H., K. Rasheed, R., Tambyrajah, V., 2001. Preparation of novel, moisture-stable, Lewis-acidic ionic liquids containing quaternary ammonium salts with functional side chains. *Chemical Communications* 0, 2010–2011. <https://doi.org/10.1039/B106357J>
- Abdul Khalil, H.P.S., Davoudpour, Y., Islam, Md.N., Mustapha, A., Sudesh, K., Dungani, R., Jawaid, M., 2014. Production and modification of nanofibrillated cellulose using various mechanical processes: A review. *Carbohydrate Polymers* 99, 649–665. <https://doi.org/10.1016/j.carbpol.2013.08.069>
- Aulin, C., Gällstedt, M., Lindström, T., 2010. Oxygen and oil barrier properties of microfibrillated cellulose films and coatings. *Cellulose* 17, 559–574. <https://doi.org/10.1007/s10570-009-9393-y>
- Aulin, C., Salazar-Alvarez, G., Lindström, T., 2012. High strength, flexible and transparent nanofibrillated cellulose–nanoclay biohybrid films with tunable oxygen and water vapor permeability. *Nanoscale* 4, 6622. <https://doi.org/10.1039/c2nr31726e>
- Banvillet, G., Depres, G., Belgacem, N., Bras, J., 2021a. Alkaline treatment combined with enzymatic hydrolysis for efficient cellulose nanofibrils production. *Carbohydrate Polymers* 255, 117383. <https://doi.org/10.1016/j.carbpol.2020.117383>
- Banvillet, G., Gatt, E., Belgacem, N., Bras, J., 2021b. Cellulose fibers deconstruction by twin-screw extrusion with in situ enzymatic hydrolysis via bioextrusion. *Bioresource Technology* 327, 124819. <https://doi.org/10.1016/j.biortech.2021.124819>
- Banyasz, J.L., Li, S., Lyons-Hart, J.L., Shafer, K.H., 2001. Cellulose pyrolysis: the kinetics of hydroxyacetaldehyde evolution. *Journal of Analytical and Applied Pyrolysis* 57, 223–248. [https://doi.org/10.1016/S0165-2370\(00\)00135-2](https://doi.org/10.1016/S0165-2370(00)00135-2)
- Chaker, A., Alila, S., Mutjé, P., Vilar, M.R., Boufi, S., 2013. Key role of the hemicellulose content and the cell morphology on the nanofibrillation effectiveness of cellulose pulps. *Cellulose* 20, 2863–2875. <https://doi.org/10.1007/s10570-013-0036-y>

- Delmer, D.P., Amor, Y., 1995. Cellulose biosynthesis. *Plant Cell* 7, 987–1000.
- Desmaisons, J., Boutonnet, E., Rueff, M., Dufresne, A., Bras, J., 2017. A new quality index for benchmarking of different cellulose nanofibrils. *Carbohydrate Polymers* 174, 318–329. <https://doi.org/10.1016/j.carbpol.2017.06.032>
- Fukuzumi, H., Saito, T., Isogai, A., 2013. Influence of TEMPO-oxidized cellulose nanofibril length on film properties. *Carbohydrate Polymers* 93, 172–177. <https://doi.org/10.1016/j.carbpol.2012.04.069>
- Fukuzumi, H., Saito, T., Iwata, T., Kumamoto, Y., Isogai, A., 2009. Transparent and High Gas Barrier Films of Cellulose Nanofibers Prepared by TEMPO-Mediated Oxidation. *Biomacromolecules* 10, 162–165. <https://doi.org/10.1021/bm801065u>
- Galland, S., Berthold, F., Prakobna, K., Berglund, L.A., 2015. Holocellulose Nanofibers of High Molar Mass and Small Diameter for High-Strength Nanopaper. *Biomacromolecules* 16, 2427–2435. <https://doi.org/10.1021/acs.biomac.5b00678>
- Ghanadpour, M., Carosio, F., Larsson, P.T., Wågberg, L., 2015. Phosphorylated Cellulose Nanofibrils: A Renewable Nanomaterial for the Preparation of Intrinsically Flame-Retardant Materials. *Biomacromolecules* 16, 3399–3410. <https://doi.org/10.1021/acs.biomac.5b01117>
- Habibi, Y., Chanzy, H., Vignon, M.R., 2006. TEMPO-mediated surface oxidation of cellulose whiskers. *Cellulose* 13, 679–687. <https://doi.org/10.1007/s10570-006-9075-y>
- Habibi, Y., Lucia, L.A., Rojas, O.J., 2010. Cellulose Nanocrystals: Chemistry, Self-Assembly, and Applications. *Chem. Rev.* 110, 3479–3500. <https://doi.org/10.1021/cr900339w>
- Hafid, H.S., Omar, F.N., Zhu, J., Wakisaka, M., 2021. Enhanced crystallinity and thermal properties of cellulose from rice husk using acid hydrolysis treatment. *Carbohydrate Polymers* 260, 117789. <https://doi.org/10.1016/j.carbpol.2021.117789>
- Henriksson, M., Berglund, L.A., Isaksson, P., Lindström, T., Nishino, T., 2008. Cellulose Nanopaper Structures of High Toughness. *Biomacromolecules* 9, 1579–1585. <https://doi.org/10.1021/bm800038n>
- Henriksson, M., Henriksson, G., Berglund, L.A., Lindström, T., 2007. An environmentally friendly method for enzyme-assisted preparation of microfibrillated cellulose (MFC)

- nanofibers. *European Polymer Journal* 43, 3434–3441. <https://doi.org/10.1016/j.eurpolymj.2007.05.038>
- Ho, T.T.T., Zimmermann, T., Hauert, R., Caseri, W., 2011. Preparation and characterization of cationic nanofibrillated cellulose from etherification and high-shear disintegration processes. *Cellulose* 18, 1391–1406. <https://doi.org/10.1007/s10570-011-9591-2>
- Hong, S., Yuan, Y., Li, P., Zhang, K., Lian, H., Liimatainen, H., 2020. Enhancement of the nanofibrillation of birch cellulose pretreated with natural deep eutectic solvent. *Industrial Crops and Products* 154, 112677. <https://doi.org/10.1016/j.indcrop.2020.112677>
- Hu, J., Arantes, V., Saddler, J.N., 2011. The enhancement of enzymatic hydrolysis of lignocellulosic substrates by the addition of accessory enzymes such as xylanase: is it an additive or synergistic effect? *Biotechnol Biofuels* 4, 36. <https://doi.org/10.1186/1754-6834-4-36>
- Isogai, A., Saito, T., Fukuzumi, H., 2011. TEMPO-oxidized cellulose nanofibers. *Nanoscale* 3, 71–85. <https://doi.org/10.1039/C0NR00583E>
- Jonoobi, M., Mathew, A.P., Oksman, K., 2012. Producing low-cost cellulose nanofiber from sludge as new source of raw materials. *Industrial Crops and Products* 40, 232–238. <https://doi.org/10.1016/j.indcrop.2012.03.018>
- Khiari, R., 2017. Valorization of Agricultural Residues for Cellulose Nanofibrils Production and Their Use in Nanocomposite Manufacturing. *International Journal of Polymer Science* 2017, e6361245. <https://doi.org/10.1155/2017/6361245>
- Khiari, R., Rol, F., Brochier Salon, M.-C., Bras, J., Belgacem, M.N., 2019. Efficiency of Cellulose Carbonates to Produce Cellulose Nanofibers. *ACS Sustainable Chem. Eng.* 7, 8155–8167. <https://doi.org/10.1021/acssuschemeng.8b06039>
- Kumar, V., Bollström, R., Yang, A., Chen, Q., Chen, G., Salminen, P., Bousfield, D., Toivakka, M., 2014. Comparison of nano- and microfibrillated cellulose films. *Cellulose* 21, 3443–3456. <https://doi.org/10.1007/s10570-014-0357-5>
- Laitinen, O., Suopajarvi, T., Österberg, M., Liimatainen, H., 2017. Hydrophobic, Superabsorbing Aerogels from Choline Chloride-Based Deep Eutectic Solvent Pretreated and Silylated Cellulose Nanofibrils for Selective Oil Removal. *ACS Appl. Mater. Interfaces* 9, 25029–25037. <https://doi.org/10.1021/acsmi.7b06304>

- Li, P., Sirviö, J.A., Haapala, A., Liimatainen, H., 2017. Cellulose Nanofibrils from Nonderivatizing Urea-Based Deep Eutectic Solvent Pretreatments. *ACS Appl. Mater. Interfaces* 9, 2846–2855. <https://doi.org/10.1021/acsami.6b13625>
- Li, W., Xue, Y., He, M., Yan, J., Lucia, L.A., Chen, J., Yu, J., Yang, G., 2021. Facile Preparation and Characteristic Analysis of Sulfated Cellulose Nanofibril via the Pretreatment of Sulfamic Acid-Glycerol Based Deep Eutectic Solvents. *Nanomaterials* 11, 2778. <https://doi.org/10.3390/nano11112778>
- Liimatainen, H., Suopajarvi, T., Sirviö, J., Hormi, O., Niinimäki, J., 2014. Fabrication of cationic cellulosic nanofibrils through aqueous quaternization pretreatment and their use in colloid aggregation. *Carbohydrate Polymers* 103, 187–192. <https://doi.org/10.1016/j.carbpol.2013.12.042>
- Luneva, N.K., Ezovitova, T.I., 2014. Cellulose phosphorylation with a mixture of orthophosphoric acid and ammonium polyphosphate in urea medium. *Russ J Appl Chem* 87, 1558–1565. <https://doi.org/10.1134/S1070427214100243>
- Ma, Y., Xia, Q., Liu, Yongzhuang, Chen, W., Liu, S., Wang, Q., Liu, Yixing, Li, J., Yu, H., 2019. Production of Nanocellulose Using Hydrated Deep Eutectic Solvent Combined with Ultrasonic Treatment. *ACS Omega* 4, 8539–8547. <https://doi.org/10.1021/acsomega.9b00519>
- Meng, Q., Wang, T.J., 2019. Mechanics of Strong and Tough Cellulose Nanopaper. *Applied Mechanics Reviews* 71, 040801. <https://doi.org/10.1115/1.4044018>
- Mnasri, A., Dhaouadi, H., Khiari, R., Halila, S., Mauret, E., 2022. Effects of Deep Eutectic Solvents on cellulosic fibres and paper properties: green "chemical" refining. Submitted to be published in *Carbohydrate Polymers*.
- Moon, R.J., Martini, A., Nairn, J., Simonsen, J., Youngblood, J., 2011. Cellulose nanomaterials review: structure, properties and nanocomposites. *Chem. Soc. Rev.* 40, 3941. <https://doi.org/10.1039/c0cs00108b>
- Naderi, A., Lindström, T., Sundström, J., 2015. Repeated homogenization, a route for decreasing the energy consumption in the manufacturing process of carboxymethylated nanofibrillated cellulose? *Cellulose* 22, 1147–1157. <https://doi.org/10.1007/s10570-015-0576-4>

- Nechyporchuk, O., Belgacem, M.N., Bras, J., 2016. Production of cellulose nanofibrils: A review of recent advances. *Industrial Crops and Products* 93, 2–25. <https://doi.org/10.1016/j.indcrop.2016.02.016>
- Nie, S., Zhang, K., Lin, X., Zhang, C., Yan, D., Liang, H., Wang, S., 2018. Enzymatic pretreatment for the improvement of dispersion and film properties of cellulose nanofibrils. *Carbohydrate Polymers* 181, 1136–1142. <https://doi.org/10.1016/j.carbpol.2017.11.020>
- Nogi, M., Iwamoto, S., Nakagaito, A.N., Yano, H., 2009. Optically Transparent Nanofiber Paper. *Advanced Materials* 21, 1595–1598. <https://doi.org/10.1002/adma.200803174>
- Noguchi, Y., Homma, I., Matsubara, Y., 2017. Complete nanofibrillation of cellulose prepared by phosphorylation. *Cellulose* 24, 1295–1305. <https://doi.org/10.1007/s10570-017-1191-3>
- Nooy, A.E.J. de, Besemer, A.C., Bekkum, H. van, 1994. Highly selective tempo mediated oxidation of primary alcohol groups in polysaccharides. *Recueil des Travaux Chimiques des Pays-Bas* 113, 165–166. <https://doi.org/10.1002/recl.19941130307>
- Pääkkö, M., Ankerfors, M., Kosonen, H., Nykänen, A., Ahola, S., Österberg, M., Ruokolainen, J., Laine, J., Larsson, P.T., Ikkala, O., Lindström, T., 2007. Enzymatic Hydrolysis Combined with Mechanical Shearing and High-Pressure Homogenization for Nanoscale Cellulose Fibrils and Strong Gels. *Biomacromolecules* 8, 1934–1941. <https://doi.org/10.1021/bm061215p>
- Pei, A., Butchosa, N., Berglund, L.A., Zhou, Q., 2013. Surface quaternized cellulose nanofibrils with high water absorbency and adsorption capacity for anionic dyes. *Soft Matter* 9, 2047. <https://doi.org/10.1039/c2sm27344f>
- Rol, F., Belgacem, M.N., Gandini, A., Bras, J., 2019. Recent advances in surface-modified cellulose nanofibrils. *Progress in Polymer Science* 88, 241–264. <https://doi.org/10.1016/j.progpolymsci.2018.09.002>
- Rol, F., Karakashov, B., Nechyporchuk, O., Terrien, M., Meyer, V., Dufresne, A., Belgacem, M.N., Bras, J., 2017. Pilot-Scale Twin Screw Extrusion and Chemical Pretreatment as an Energy-Efficient Method for the Production of Nanofibrillated Cellulose at High Solid Content. *ACS Sustainable Chem. Eng.* 5, 6524–6531. <https://doi.org/10.1021/acssuschemeng.7b00630>
- Rol, F., Sillard, C., Bardet, M., Yarava, J.R., Emsley, L., Gablin, C., Léonard, D., Belgacem, N., Bras, J., 2020. Cellulose phosphorylation comparison and analysis of phosphate position

on cellulose fibers. *Carbohydrate Polymers* 229, 115294. <https://doi.org/10.1016/j.carbpol.2019.115294>

Saito, T., Hirota, M., Tamura, N., Kimura, S., Fukuzumi, H., Heux, L., Isogai, A., 2009. Individualization of Nano-Sized Plant Cellulose Fibrils by Direct Surface Carboxylation Using TEMPO Catalyst under Neutral Conditions. *Biomacromolecules* 10, 1992–1996. <https://doi.org/10.1021/bm900414t>

Saito, T., Isogai, A., 2004. TEMPO-Mediated Oxidation of Native Cellulose. The Effect of Oxidation Conditions on Chemical and Crystal Structures of the Water-Insoluble Fractions. *Biomacromolecules* 5, 1983–1989. <https://doi.org/10.1021/bm0497769>

Saito, T., Isogai, A., 2006. Introduction of aldehyde groups on surfaces of native cellulose fibers by TEMPO-mediated oxidation. *Colloids and Surfaces A: Physicochemical and Engineering Aspects* 289, 219–225. <https://doi.org/10.1016/j.colsurfa.2006.04.038>

Saito, T., Kimura, S., Nishiyama, Y., Isogai, A., 2007. Cellulose Nanofibers Prepared by TEMPO-Mediated Oxidation of Native Cellulose. *Biomacromolecules* 8, 2485–2491. <https://doi.org/10.1021/bm0703970>

Saito, T., Nishiyama, Y., Putaux, J.-L., Vignon, M., Isogai, A., 2006. Homogeneous Suspensions of Individualized Microfibrils from TEMPO-Catalyzed Oxidation of Native Cellulose. *Biomacromolecules* 7, 1687–1691. <https://doi.org/10.1021/bm060154s>

Segal, L., Creely, J.J., Martin, A.E., Conrad, C.M., 1959. An Empirical Method for Estimating the Degree of Crystallinity of Native Cellulose Using the X-Ray Diffractometer. *Textile Research Journal* 29, 786–794. <https://doi.org/10.1177/004051755902901003>

Sehaqui, H., Zimmermann, T., Tingaut, P., 2014. Hydrophobic cellulose nanopaper through a mild esterification procedure. *Cellulose* 21, 367–382. <https://doi.org/10.1007/s10570-013-0110-5>

Serpa Guerra, A.M., Gómez Hoyos, C., Velásquez-Cock, J.A., Vélez Penagos, L., Gañán Rojo, P., Vélez Acosta, L., Pereira, M.A., Zuluaga, R., 2020. Effect of ultra-fine friction grinding on the physical and chemical properties of curcuma (*Curcuma longa* L.) suspensions. *Journal of Food Science* 85, 132–142. <https://doi.org/10.1111/1750-3841.14973>

- Sirviö, J.A., Hyypiö, K., Asaadi, S., Junka, K., Liimatainen, H., 2020. High-strength cellulose nanofibers produced via swelling pretreatment based on a choline chloride–imidazole deep eutectic solvent. *Green Chem.* 22, 1763–1775. <https://doi.org/10.1039/C9GC04119B>
- Sirviö, J.A., Visanko, M., Liimatainen, H., 2015. Deep eutectic solvent system based on choline chloride-urea as a pre-treatment for nanofibrillation of wood cellulose. *Green Chemistry* 17, 3401–3406. <https://doi.org/10.1039/C5GC00398A>
- Sirviö, J.A., Visanko, M., Liimatainen, H., 2015. Deep eutectic solvent system based on choline chloride-urea as a pre-treatment for nanofibrillation of wood cellulose. *Green Chemistry* 17, 3401–3406. <https://doi.org/10.1039/C5GC00398A>
- Smith, E.L., Abbott, A.P., Ryder, K.S., 2014. Deep Eutectic Solvents (DESs) and Their Applications. *Chem. Rev.* 114, 11060–11082. <https://doi.org/10.1021/cr300162p>
- Song, Y., Sun, Y., Zhang, X., Zhou, J., Zhang, L., 2008. Homogeneous Quaternization of Cellulose in NaOH/Urea Aqueous Solutions as Gene Carriers. *Biomacromolecules* 9, 2259–2264. <https://doi.org/10.1021/bm800429a>
- Suopajarvi, T., Sirviö, J.A., Liimatainen, H., 2017. Nanofibrillation of deep eutectic solvent-treated paper and board cellulose pulps. *Carbohydrate Polymers* 169, 167–175. <https://doi.org/10.1016/j.carbpol.2017.04.009>
- Tenhunen, T.-M., Kouko, J., Salminen, A., Härkäsalmi, T., Pere, J., Harlin, A., Hänninen, T., 2016. Method for Forming Pulp Fibre Yarns Developed by a Design-driven Process. *BioResources* 11, 2492–2503.
- Turbak, A.F., Snyder, F.W., Sandberg, K.R., 1983. Microfibrillated cellulose, a new cellulose product: properties, uses, and commercial potential. *J. Appl. Polym. Sci.: Appl. Polym. Symp.;* (United States) 37.
- Wang, J., Gardner, D.J., Stark, N.M., Bousfield, D.W., Tajvidi, M., Cai, Z., 2018. Moisture and Oxygen Barrier Properties of Cellulose Nanomaterial-Based Films. *ACS Sustainable Chem. Eng.* 6, 49–70. <https://doi.org/10.1021/acssuschemeng.7b03523>
- Yu, W., Wang, C., Yi, Y., Wang, H., Yang, Y., Zeng, L., Tan, Z., 2021. Direct pretreatment of raw ramie fibers using an acidic deep eutectic solvent to produce cellulose nanofibrils in high purity. *Cellulose* 28, 175–188. <https://doi.org/10.1007/s10570-020-03538-3>

- Zdanowicz, M., Wilpiszewska, K., Szychaj, T., 2018. Deep eutectic solvents for polysaccharides processing. A review. *Carbohydrate Polymers* 200, 361–380. <https://doi.org/10.1016/j.carbpol.2018.07.078>
- Zhao, Z., Chen, X., Ali, M.F., Abdeltawab, A.A., Yakout, S.M., Yu, G., 2018. Pretreatment of wheat straw using basic ethanolamine-based deep eutectic solvents for improving enzymatic hydrolysis. *Bioresource Technology* 263, 325–333. <https://doi.org/10.1016/j.biortech.2018.05.016>
- Zhu, G., Zhu, X., Xiao, Z., Yi, F., 2012. Study of cellulose pyrolysis using an in situ visualization technique and thermogravimetric analyzer. *Journal of Analytical and Applied Pyrolysis* 94, 126–130. <https://doi.org/10.1016/j.jaap.2011.11.016>

Appendix

Table of contents

Appendix.....	275
1) Modification of MG using DMC in the presence of BHCl-U	279
2) MCC modification with DMC in the presence of BHCl-U	280
3) Treatment of eucalyptus fibres.....	283
References.....	289

The modification of the hydroxyl functions of cellulose by grafting coupled with the use of green and inexpensive reagents thus makes it possible to facilitate the release of MFC on the one hand and to obtain high quality MFC on the other hand. This part is devoted to cellulose modification with dimethyl carbonate (DMC).

A study in our team conducted by Khiari et al. (2016, 2017, 2019) showed that the reaction of DMC with cellulose or cellobiose lead to a carbonation reaction instead of methoxycarbonylation or methylation. This study consists of reacting a quantity of cellobiose/cellulose with a 15% (w/v) potassium ethanoic hydroxide (KOH/ethanol) solution for 2h at room temperature. Then DMC was added with ethanol and the mixture left to stir for a few hours at a fixed temperature. For cellobiose, the highest degree of substitution (DS = 2.45) is obtained at 70°C for 6h. Microcrystalline cellulose has a maximum DS of 0.28 which is obtained when the reaction was carried out at 90°C for 24h. Finally, the DS of eucalyptus fibres (bleached kraft pulp) reaches a value of 0.29 obtained for the following conditions: reaction conducted at 20°C for 24 hours. In this part, we chose to test reactions on methyl- α -glucopyranoside MG as monomer, microcrystalline cellulose (MCC) as model (containing only cellulose) and on eucalyptus fibres as cellulosic biomass. These reactions correspond to chemical modifications (methylation or methoxycarbonylation) using DMC in the presence of eutectic solvent (betaine hydrochloride-urea BHCl-U or choline chloride-urea CC-U). These reactions were carried out in the synthesis microwave for the monomer and MCC and in the pressure reactor for eucalyptus fibres.

The eutectic system, BHCl-U is chosen because it allows to dissolve MCC (2.5%) as reported in the literature (Sharma et al., 2013). Moreover, the modification of cellulose with DMC necessitates the use of reagent that do not react with DMC such as acidic group.

The experimental conditions were inspired from the study of Labafzadeh et al. (2015).

1) Modification of MG using DMC in the presence of BHCl-U

The reaction is performed in four steps:

- (i) DES preparation (BHCl-U (1:4)): 0.045 moles (7 g) of betaine hydrochloride were mixed with 0.182 moles of urea (10.94 g) at 100°C until a colourless liquid was obtained.

- (ii) Dissolution of MG in DES: 0.018 moles (3.52 g) of MG are dissolved in 17.94 g of DES for 15min at 100°C
- (iii) Reaction with DMC: 4 eq/M-G (0.072 moles) of DMC are added to the tube containing the mixture. The reaction is carried out at 60°C for 15min.
- (iv) Purification: precipitation in ethyl acetate and water then extraction with ethyl acetate 3 times.

The purification is so difficult to carry out because of the hard separation between the sugar and the DES. This problem is linked to the close solubilities of DES and sugar in water and in several other organic solvents (methanol, ethyl acetate, ethanol).

2) MCC modification with DMC in the presence of BHCl-U

The procedure is done according to the following steps:

- (i) Preparation of DES (BHCl-U (1:4)): as described before.
- (ii) Solvation of MCC in DES: 0.0027 moles (0.45 g) of microcrystalline cellulose (Avicel pH-101) were dissolved in DES for 10 hours at 100°C. The mixture is then transferred directly into the microwave reactor tube.
- (iii) Reaction with DMC: 1.36ml (6 eq/AGU) of DMC was added to the tube containing the MCC+DES mixture. Two temperatures were tested (60 and 100°C) and the reaction time was set at 15min.
- (iv) Product purification: The mixture obtained after reaction was filtered, washed with ethanol and then with distilled water.

The FT-IR-ATR spectra of obtained products are illustrated in Figure A. 1.

On these spectra, it can be observed the appearance of a new peak at around 1700 cm^{-1} for the reaction at 60°C and at around 1709 cm^{-1} for that at 100°C. This peak corresponds to the carbonyl function.

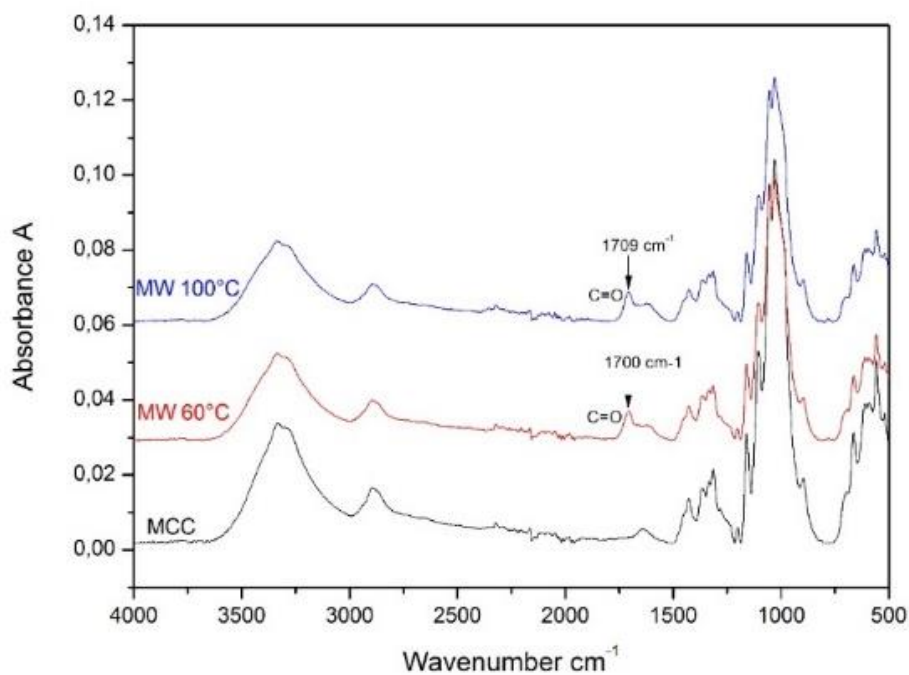


Figure A. 1. FT-IR ATR spectra of MCC treated with DMC in the presence of BHCl-U at 60 and 100°C.

To confirm the modification, the products were characterised by solid state NMR spectroscopy. Figure A. 2 shows the three NMR spectra of the original MCC, modified MCC at 60°C and modified MCC at 100°C.

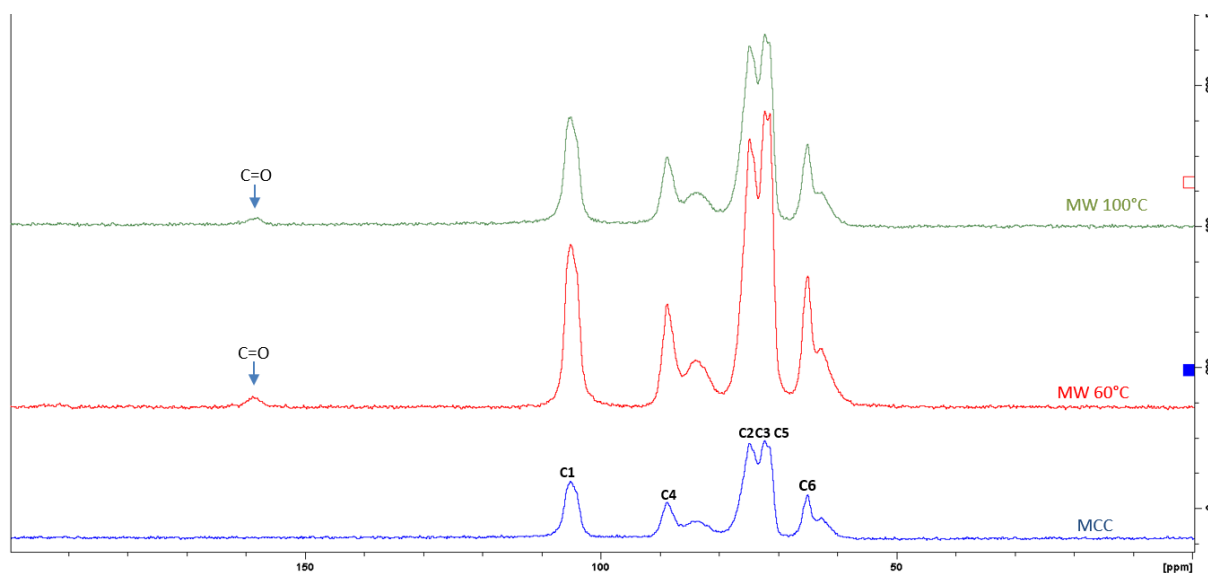


Figure A. 2. ^{13}C solid-state NMR spectra of MCC treated with DMC in BHCl-U at 60 and 100°C.

On the NMR spectrum of the MCC, it can be noticed that all the peaks related to the cellulose structure. The first peak corresponds to the C6 carbon and appears at around 65ppm. Then the peaks relating to carbons C5, C3 and C2 appear at 71, 73 and 74 ppm, respectively. The peak appearing at around 88ppm corresponds to the C4 carbon and finally the last peak which appears at around 104ppm corresponds to the C1 carbon.

On the two spectra of the modified MCC at 60°C and 100°C, the same peaks with the appearance of a new small peak at around 159 ppm were observed. It corresponds to the carbonyl group but we did not observe the methyl peak which normally emerges around 54ppm. This peak does not correspond to impurities, given the purification protocol adopted, DES being soluble in water. Nor a trace of DMC (no methyl peak).

Afterwards, if this peak corresponds to the carbonyl group and reflects the presence of carbonate functions linked to the cellulose, we could expect a shift in the peaks of the modified cellulose compared to the unmodified one, which is not the case. However, due to the crystal structure of MCC, the amount of grafted carbonate functions remains low (DS = 0.06 and 0.05 for 60 and 100°C, respectively) and the resulting shift may not be detectable. In conclusion, it can be assumed that the peak at 159 ppm corresponds to the carbonate group.

The crystallinity of the cellulose is studied by XrD. From the obtained spectra (Figure A. 3), it is noticed that the starting structure of the cellulose (I_{α}) has not changed after the modification. The appearance of a peak around 28° is observed which corresponds to the triurea.

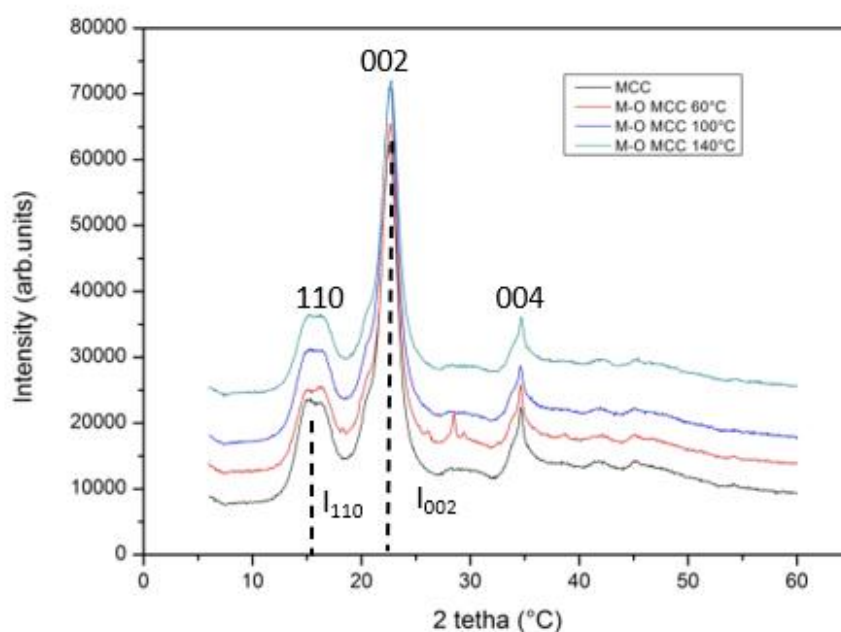


Figure A. 3. X-rD diffractograms of MCC treated with DMC in BHCl-U at 60, 100 and 140°C.

3) Treatment of eucalyptus fibres

The treatment of eucalyptus fibres was carried out in a pressure reactor (Parr reactor) following the same steps as those already applied to microcrystalline cellulose (preparation of DES, solvation, reaction with DMC and then purification).

- (i) Preparation of DES (BHCl-U (1 :4)): 0.65 moles (100 g) of BHCl were mixed with 2.60 moles of urea (156.40g) at 100°C until a colourless liquid is obtained.
- (ii) Solvation of cellulose fibres in DES: 0.022 moles (3.57 g) of fibres are dissolved in DES for 1h at 100°C in the reactor.
- (iii) Reaction with DMC: 22.43 ml (12 eq/AGU) of DMC was added to the cellulose + DES mixture. Three temperatures were tested (120, 140 and 180°C) and the reaction time was set at 4h.
- (iv) Product purification: the mixture obtained after reaction is filtered, and washed with distilled water to neutral pH.

Then the fibres were characterised by ATR-IR (Figure A. 4) and solid NMR (Figure A. 5) in order to identify the modification.

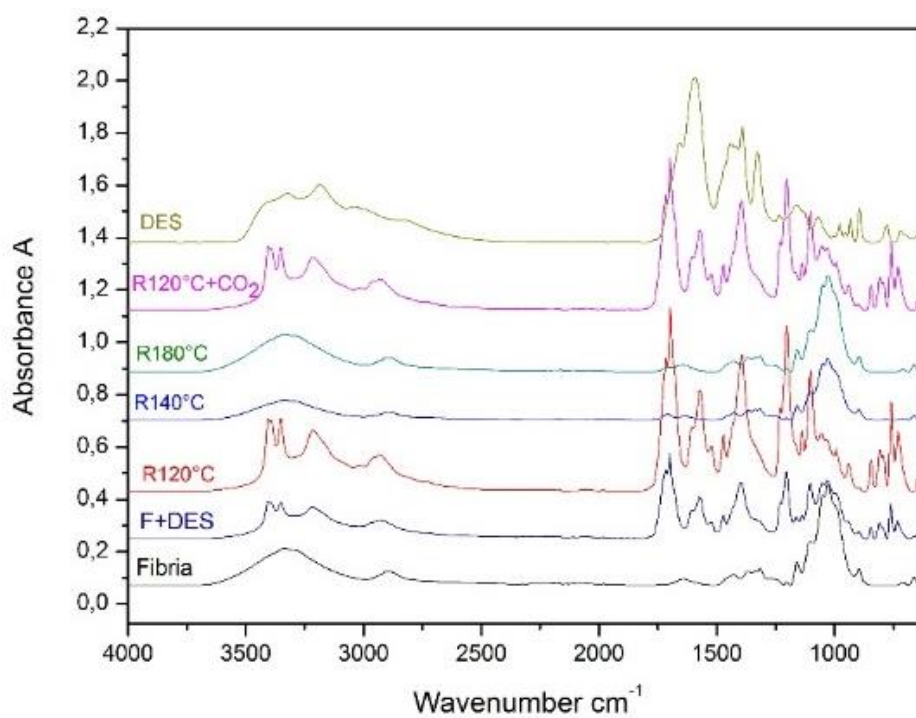


Figure A. 4. FT-IR ATR spectra of eucalyptus fibres treated with DES in the presence or not of carbon dioxide.

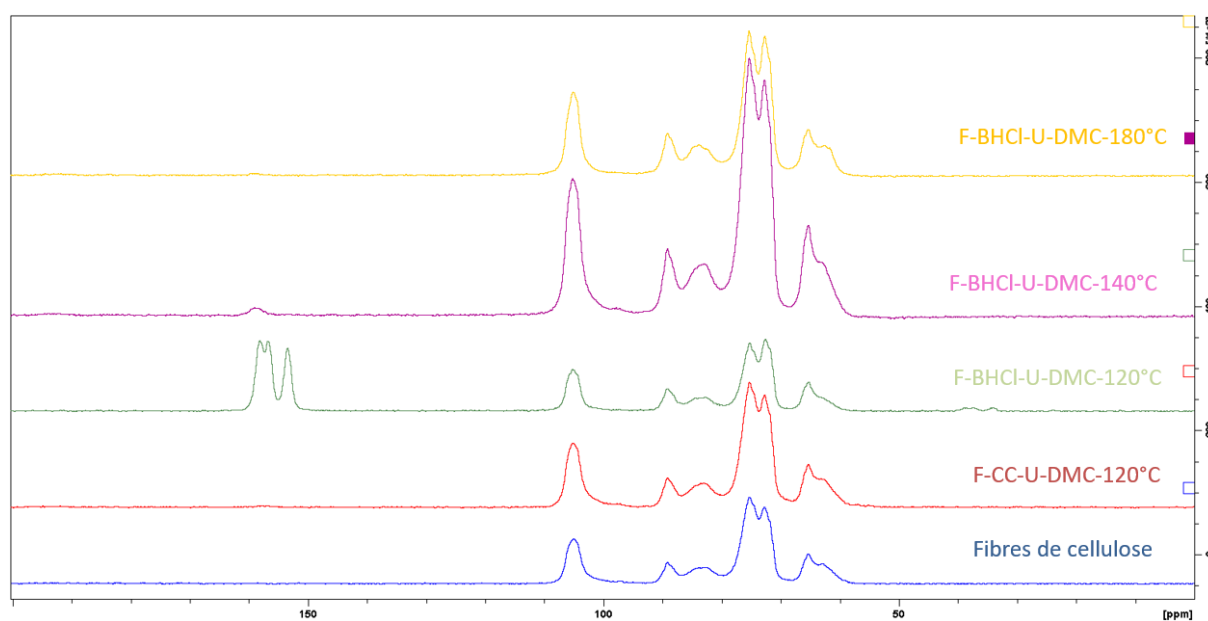


Figure A. 5. ^{13}C solid-state NMR of eucalyptus fibres treated with DMC in the presence of BHCl-U at 120, 140 and 180°C and CC-U at 120°C

The ^{13}C solid-state NMR results showed the appearance of new peaks between 153 and 159 ppm. These peaks are observed only on the spectrum of the reaction carried out at 120°C in BHCl-U. These three peaks correspond to three carbonyl functions (two symmetrical carbonyls). The analysis of these peaks showed that this is the structure of the triurea which is also confirmed by X-ray Diffraction (XrD) (Figure A. 6).

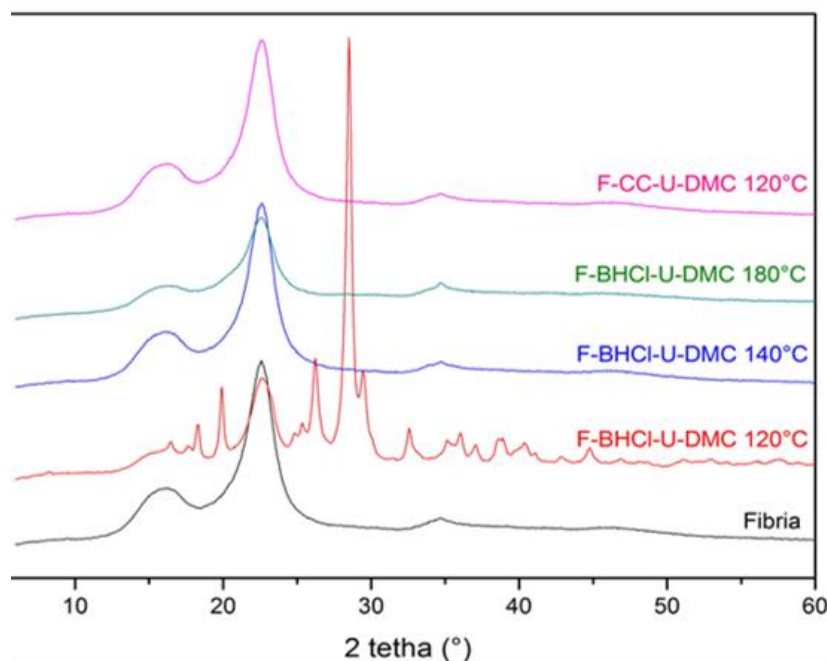


Figure A. 6. XrD diffractograms of DES treated eucalyptus fibres

These results can be explained by the existence of a competition between two reactions involving the urea molecules forming the DES, this phenomenon occurring at a certain temperature (between 100 and 120°C). At this temperature, it is possible that the hydrogen bonds between the urea molecules (4 moles) and the betaine hydrochloride (1 mol) are weakened in the presence of cellulose. The weakening of this bond would result in the formation of new hydrogen bonds between the betaine hydrochloride and the cellulose. Consequently, three urea molecules react together rapidly to form triurea (between 100 and 120°C).

To confirm our results, the reaction was repeated several times and characterised by solid NMR (Figure A. 7). And to find out in which step the triurea is formed we analysed the fibres treated in BHCl-U (solvation step) before reaction with DMC. Figure 10 shows the spectra of three trials of the reaction carried out at 120°C compared to the spectrum of the fibres solvated in BHCl-U at 100°C (before reaction with DMC).

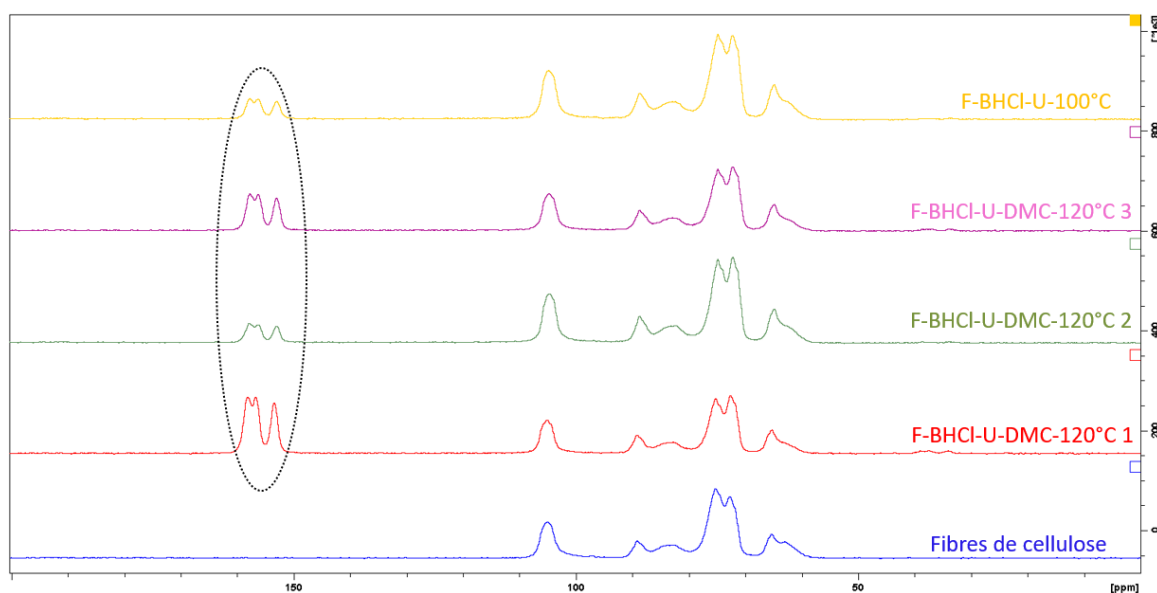


Figure A. 7. ^{13}C solid-state NMR spectra of treated eucalyptus fibres with DMC in BHCl-U at 120°C and treated in BHCl-U at 100°C

Conclusion

In this section, the modification of cellulose using DMC was conducted in DES in order to reach higher DS. The results were not clear and the presence of carbonate group was suggested. The modification of the methyl- α -glucopyranoside using the same conditions was not possible due to the solubilisation of the monomer and DES in water and most of organic solvents.

The presence of triurea on cellulose fibres detected after BHCl-U treatment is due to the side reaction of DES. Since triurea is soluble in hot water, the fibres purification will be performed by excessive washing with hot water followed by cold water.

Based on these results, the strategy used in this PhD project was changed. The new strategy selected is the use of DES as a direct pre-treatment for cellulose microfibrillation. The DES systems, BHCl-U and CC-U which are characterised by acidic and neutral pH, respectively were used as green and soft pre-treatment. Moreover, an alkaline DES was suggested which is choline chloride-monoethanolamine to study the influence of the pH on cellulose fibres pre-treatment. In addition, the MCC presents some limits due to the fact that MCC has been treated by acidic hydrolysis which may decrease its accessibility. The comparison between eucalyptus fibres and MCC will be delicate because the first specie represents a cellulosic

biomass while MCC is considered as cellulose with microstructure. Subsequently, MCC was replaced by cotton fibres as model.

References

- Khiari, R., Brochier-Salon, M.-C., Mhenni, M.F., Mauret, E., Belgacem, M.N., 2016. A New Way to Produce Cellobiose Carbonates Using Green Chemistry. *ChemSusChem* 9, 2143–2148. <https://doi.org/10.1002/cssc.201600430>
- Khiari, R., Brochier-Salon, M.-C., Mhenni, M.F., Mauret, E., Belgacem, M.N., 2017. Synthesis and characterization of cellulose carbonate using greenchemistry: Surface modification of Avicel. *Carbohydrate Polymers* 163, 254–260. <https://doi.org/10.1016/j.carbpol.2017.01.037>
- Khiari, R., Rol, F., Brochier Salon, M.-C., Bras, J., Belgacem, M.N., 2019. Efficiency of Cellulose Carbonates to Produce Cellulose Nanofibers. *ACS Sustainable Chem. Eng.* 7, 8155–8167. <https://doi.org/10.1021/acssuschemeng.8b06039>
- Labafzadeh, S.R., Helminen, K.J., Kilpeläinen, I., King, A.W.T., 2015. Synthesis of Cellulose Methylcarbonate in Ionic Liquids using Dimethylcarbonate. *ChemSusChem* 8, 77–81. <https://doi.org/10.1002/cssc.201402794>
- Sharma, M., Mukesh, C., Mondal, D., Prasad, K., 2013. Dissolution of α -chitin in deep eutectic solvents. *RSC Advances* 3, 18149–18155. <https://doi.org/10.1039/C3RA43404D>

English abstract

Currently the development of “green” chemistry is one of the promising solutions to deal with environmental problems. This chemistry is particularly based on the use of non-toxic solvents and reagents. In this context, Deep Eutectic Solvents (DES) were selected due to their interesting properties such as non or low toxicity, biodegradability, recyclability... In this context, this PhD thesis aims at studying DES as green pre-treatment to produce microfibrillated cellulose MFC. First, the effects of DES pre-treatment on cellulose fibres and paper properties were investigated using several characterisation techniques. It has been demonstrated that DES treatment acts as a green and soft chemical refining with similar effects of internal and external fibrillation of the fibres. The MFC production from DES-treated fibres was then investigated using ultrafine grinding, which results in high quality MFC obtained with a comparable energy consumption to the enzymatic pre-treatment. Finally, the production of MFC at high solid contents was tested by using a twin-screw extruder.

Keywords: *Cellulose fibres, deep eutectic solvents, green chemical refining, microfibrillated cellulose, ultra-fine friction grinder, twin-screw extruder.*

Résumé en français

Actuellement, le développement de la chimie "verte" est une solution pour faire face aux problèmes environnementaux. Cette chimie est notamment basée sur l'utilisation de solvants et de réactifs non toxiques. Dans ce contexte, les solvants eutectiques profonds (DES) ont de nombreux atouts en raison de leur faible toxicité, leur biodégradabilité, leur recyclabilité... Cette thèse vise donc à étudier les DES pour un prétraitement « vert » de fibres végétales en vue de la production de microfibrilles de cellulose. Tout d'abord, les effets des DES sur les fibres de cellulose et sur les propriétés du papier ont été évalués en utilisant plusieurs techniques de caractérisation. Les résultats obtenus montrent que les traitements aux DES s'apparentent à un « raffinage chimique » grâce à leurs effets de fibrillation interne et externe des fibres. La production de MFC à partir de fibres traitées a ensuite été étudiée en utilisant un broyage ultrafin, ce qui permet d'obtenir des MFC de haute qualité avec une consommation d'énergie comparable à celle d'un prétraitement enzymatique conventionnel. Enfin, la production de MFC à haute concentration a été testée en utilisant une extrudeuse bi-vis.

Mots-clés : *Fibres de cellulose, solvants eutectiques profonds raffinage chimique vert, microfibrilles de cellulose, broyeur ultrafin, extrudeuse bi- vis.*